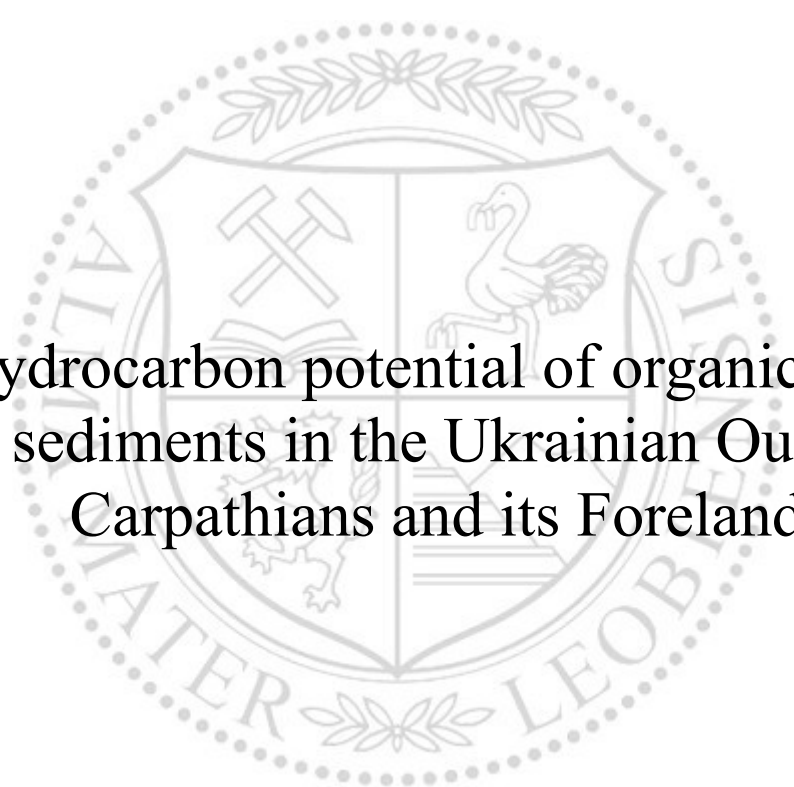




Chair of Petroleum Geology

Doctoral Thesis



Hydrocarbon potential of organic-rich
sediments in the Ukrainian Outer
Carpathians and its Foreland

Johannes Rauball

July 2020



AFFIDAVIT

I declare on oath that I wrote this thesis independently, did not use other than the specified sources and aids, and did not otherwise use any unauthorized aids.

I declare that I have read, understood, and complied with the guidelines of the senate of the Montanuniversität Leoben for "Good Scientific Practice".

Furthermore, I declare that the electronic and printed version of the submitted thesis are identical, both, formally and with regard to content.

Date 01.07.2020

Signature Author

Johannes Rauball

Danksagung

An dieser Stelle möchte ich mich ganz herzlich bei meinem Doktorvater Herrn Prof. Reinhard F. Sachsenhofer dafür bedanken, dass er es mir als Quereinsteiger ermöglicht hat, in Leoben zu promovieren. Ich bedanke mich auch für die Unterstützung und Betreuung in den letzten Jahren, auf die ich mich immer verlassen konnte.

Ein ganz besonderer Dank gilt auch Doris Groß und Achim Bechtel, die mir mit ihrer wissenschaftlichen Expertise immer wieder eine wertvolle Hilfe waren.

Des Weiteren bedanke ich mich bei Dr. Yuriy Koltun für die Unterstützung bei der Probenahme. Durch seine Betreuung und Kooperation wurde die Durchführung dieses Projekts ermöglicht.

Darüber hinaus möchte ich mich bei meiner Bürokollegin Magdalena Pupp bedanken, die mir stets unterstützend zur Seite stand.

Für die organisatorischen und administrativen Tätigkeiten sowie für die aufmunternden Worte möchte ich mich von ganzem Herzen bei Frau Schmid bedanken.

Zu guter Letzt bedanke ich mich bei meiner Familie, die immer für mich da ist und an meiner Seite steht – ohne sie wäre ich nie so weit gekommen.

Abstract

Organic-rich rocks with widely varying ages occur throughout many parts of the Ukrainian Carpathians, some of which are proven hydrocarbon source rocks. For this study, two organic-rich successions in the Outer Carpathians, as well as one potential source rock horizon and three oil samples from the Mesozoic basement of the Carpathian Foredeep, were chosen for a detailed analysis.

Within the Ukrainian Outer Carpathians, the Lower Cretaceous Shypot Formation and the Oligocene-Lower Miocene Menilite Formation contain significant source rock potential. The latter, approximately 1800 m thick in the studied section, is considered to be the primary source rock interval of the region. The Menilite Formation contains thermally immature (vitrinite reflectance: 0.24-0.34 %Rr; T_{\max} : 419-425°C), organic-matter-rich sediments (frequently up to 24 wt.% TOC) that can generate up to 74.5 t of hydrocarbons per m², which is a significantly higher generation potential than other source rocks in the entire Paratethys realm. The studied rocks are dominated by a marine (Type II) organic matter input mixed with varying amounts of land-plant derived material, which is supported by maceral and biomarker data. In addition, varying redox and salinity conditions during deposition are supported by varying dibenzothiophene/phenanthrene (DBT/Phen) and pristane/phytane (Pr/Ph) ratios. In contrast, the Shypot Formation, roughly 400 m thick in the study area, is rich in organic-matter (average TOC: 2.83 wt.%), but the hydrogen index (88 mgHC/gTOC) and the remaining source potential (2 tHC/m²) are low, partly due to the advanced maturity (vitrinite reflectance: 0.82 %Rr; T_{\max} : 456°C) of the succession. The higher maturities observed in the Shypot Formation imply that some hydrocarbons must have already been generated. However, it is argued that these accumulations were likely lost during major uplift and/or erosion. Preservation of the organic matter was supported by an oxygen-deficient environment, but strictly anoxic conditions were rare, which is supported by low DBT/Phen ratios, moderate Pr/Ph ratios and relatively high TOC/S ratios.

The Middle Jurassic rocks, which occur in the Mesozoic basement of the Ukrainian Carpathian Foredeep, display elevated amounts of organic-matter (4.19 wt.%; max 14.98 wt.%). However, HI values (max: 242 mgHC/gTOC) are low, and organic-matter is dominated by gas-prone, Type III kerogen (with rare transitions into type II kerogen), which is supported by a strong predominance of terrestrial macerals. The petroleum potential, classifies the succession as a fair source rock, with only few intervals displaying a good source rock potential. Maturity parameters (vitrinite reflectance: 0.69-0.90 %Rr; T_{\max} : 434°C-448°C) indicate a marginally mature to peak oil window maturity, suggesting that major hydrocarbon generation may be restricted to the more mature sediments.

An oil-source rock correlation was performed on Middle Jurassic rocks to investigate a possible genetic link with oils in the overlying Upper Jurassic reservoirs. However, biomarker analysis identified significant differences in DBT/Phen ratios, Pr/Ph ratios, sterane distributions and in isotopic signatures. As a result, an alternative source was investigated, and the new data collected on the oils was compared to published data on Upper Jurassic rocks in the Mesozoic basement, which presented a better fit and revealed the likely source of these oil accumulations.

Zusammenfassung

In vielen Teilen der ukrainischen Karpaten existieren Gesteine unterschiedlichen Alters mit hohem Gehalten an organischem Kohlenstoff (TOC), von denen einige als potentielle Muttergesteine gelten. Zwei Formationen der äußeren Karpaten, sowie ein potentielles Muttergestein und drei Erdölproben aus dem mesozoischen Untergrund des Karpatenvorlandes wurden im Detail analysiert.

Innerhalb der äußeren ukrainischen Karpaten bilden die Shypot-Formation und die Menilit-Formation potentielle Muttergesteine, die während der Kreidezeit, dem Oligozän und dem frühen Miozän abgelagert wurden. Die Menilit-Formation, die im untersuchten Gebiet eine Mächtigkeit von 1800 m aufweist, gilt als primäres Muttergestein der Region. Die Gesteine sind thermisch unreif (Vitrinitreflexion: 0.24-0.34 % Rr; T_{\max} : 419-425°C) und enthalten viel organisches Material (bis zu 24 wt.% TOC), welches bis zu 74.5 t Kohlenwasserstoffe pro m² erzeugen kann und somit ein höheres Erzeugungspotential besitzt als alle anderen Muttergesteine des gesamten Paratethys-Raumes. Die untersuchten Proben werden von mariner organischer Substanz (Kerogen Typ II) dominiert und enthalten unterschiedliche Mengen von Landpflanzenmaterial, was durch Mazeral- und Biomarkerdaten bestätigt wird. Zusätzlich wurden unterschiedliche Redox und Salzgehaltbedingungen während der Ablagerung der Sedimente durch variierenden Verhältnisse von Dibenzothiophen/Phenanthren (DBT/Phen) und Pristan/Phytan (Pr/Ph) bestätigt. Im Vergleich zur Menilit-Formation, beinhaltet die im Untersuchungsgebiet etwa 400 m mächtige Shypot-Formation geringere Mengen an organischem Material (durchschnittlicher TOC: 2,83 wt.%), welches aufgrund der fortgeschrittenen Reife (Vitrinitreflexion: 0,82% Rr; T_{\max} : 456°C) einen niedrigen Wasserstoffindex (88 mgHC/gTOC) und ein geringes verbleibendes Erzeugungspotential (2 tHC/m²) aufweist. Der höhere Reifegrad impliziert, dass einige Kohlenwasserstoffe bereits erzeugt wurden. Es kann jedoch vermutet werden, dass diese während tektonischer Deformationsphasen und/oder durch Erosion verloren gegangen sind. Sauerstoffarme Verhältnisse halfen bei der Erhaltung des organischen Materials, jedoch waren streng anoxische Bedingungen selten, was durch niedrige DBT/Phen Verhältnisse, moderate Pr/Ph Verhältnisse und hohe TOC/S Verhältnisse bestätigt wird.

Die Gesteine des mittleren Jura im mesozoischen Untergrund des ukrainischen Karpatenvorlandes enthalten erhöhte Mengen an organischem Material (4,19 wt.%; max: 14,98 wt.%). Der HI (max: 242 mgHC/gTOC) ist jedoch niedrig und das organische Material wird von einem Kerogen Typ III (mit seltenen Übergängen in Kerogen Typ II) dominiert, was durch eine Dominanz terrestrischer Mazerale belegt wird. Das Erdölpotential (S_1+S_2 der Rock-Eval Pyrolysis) klassifiziert das Muttergestein als „fair“, wobei nur wenige Intervalle ein „gutes“ Erdölpotential aufweisen. Reifeparameter (Vitrinitreflexion: 0,69-0,90% Rr; T_{\max} : 434°C-448°C) weisen auf eine geringe Reife bis zu einer maximalen Ölfensterreife hin, woraus geschlossen werden kann, dass die Kohlenwasserstoffherzeugung nur auf die reiferen Sedimente beschränkt ist.

Für eine Erdöl-Muttergesteinskorrelation wurden Gesteinsextrakte von Proben aus dem mittleren Jura mit Erdölproben aus den darüber liegenden Oberjura-Lagerstätten verglichen. Die Biomarker Analyse identifizierte jedoch signifikante Unterschiede in den DBT/Phen und Pr/Ph Verhältnissen, Steranverteilungen und in den Isotopensignaturen. Daraufhin wurde ein alternatives Muttergestein gesucht, wobei die Daten der Erdölproben mit veröffentlichten Daten von Gesteinen des Oberjura verglichen wurden, welche Ähnlichkeiten aufweisen und somit die Erdöle in den gleichalten Lagerstättenhorizonten generiert haben.

Table of Content

1. Introduction	8
1.1. Study aim	8
1.2. History of the Petroleum Industry	10
1.3. History of the Petroleum Industry in Western Ukraine.....	11
1.4. Conventional and unconventional hydrocarbons	12
1.5. Unconventional hydrocarbons in the Ukraine.....	13
1.6. Oil to source correlations in conventional plays	14
2. Geological overview of the Carpathians	15
2.1. Geology of the Carpathians.....	15
2.2. Geology of the Ukrainian Outer Carpathians.....	17
2.3. Geology of the Ukrainian Carpathian Foredeep	22
3. Samples and Methods	26
4. Summary of publications and innovative aspects of the presented result	30
4.1. Publication I: The Oligocene-Miocene Menilite Formation in the Ukrainian Carpathians: a world-class source rock.....	30
4.2. Publication II: Hydrocarbon potential of the Lower Cretaceous (Barremian-Albian) Shypot Formation in the Chornohora nappe, Ukraine.....	33
4.3. Publication III: Petroleum potential of Middle Jurassic rocks in the basement of the Carpathian Foredeep (Ukraine) and oil-to-source correlation with oil in Upper Jurassic	34
4.4. List of conference contributions related to this thesis	36
5. General conclusions and outlook	37
6. References	38
7. Oligocene-Miocene Menilite Formation in the Ukrainian Carpathians: a world-class source rock	44
8. Hydrocarbon potential of the Lower Cretaceous (Barremian-Albian) Shypot Formation in the Chornohora nappe, Ukraine	90
9. Petroleum potential of Middle Jurassic rocks in the basement of the Carpathian Foredeep (Ukraine) and oil-to-source correlation with oil in Upper Jurassic reservoirs	118
10. Appendix	152
10.1. Appendix I – Author contributions to the publications in this thesis	152
10.2. Appendix II – Oligocene – Miocene Menilite Formation.....	154
10.3. Appendix III – Lower Cretaceous Shypot Formation.....	170
10.4. Appendix IV – Middle Jurassic strata.....	180
10.5. Appendix V – Oil samples from Upper Jurassic reservoirs	185
10.6. Appendix VI – Poster Presentations.....	186

General part of the PhD thesis

1. Introduction

1.1. Study aim

Since Ukraine is not yet energy-self-sufficient, it still relies on oil and gas imports, particularly from Russia, to meet demands (Van de Graaf and Colgan, 2016). Great hopes were put into unconventional hydrocarbons, including shale oil and shale gas. However, it turned out that shale oil and shale gas in the Dniepr-Donets Basin and western Ukraine are hardly economic (e.g. Misch et al., 2016; Radkovets et al., 2017). As a result, conventional hydrocarbons have become increasingly important for Ukraine's economy, as Ukraine strives to become energy-independent. Apart from the Dniepr-Donets Basin (DDB), which hosts more than 220 oil and gas fields (e.g. Tari, 2010; Misch et al., 2015), the Ukrainian Carpathians (Fig. 1) constitute one of the oldest oil and gas provinces in the world.



Fig. 1 General overview of the Carpathians and adjacent areas with the locations of the main divisions of the Carpathians (after Hrušecký et al., 2006).

The Ukrainian Carpathians form the NE part of the Carpathian orogenic belt, which stretches for approximately 1300 km, from Vienna to the Iron Gate on the River Danube in Romania (Fig. 1). Being a mature oil-producing province, the Ukrainian Carpathians have been explored significantly, due to the high drilling intensity in these regions, and the most important source rock horizons have been identified (e.g. Sachsenhofer and Koltun, 2012). However, past studies have failed to determine the vertical variability of these intervals, and important organic geochemical data are often lacking or missing entirely. An improved understanding of the petroleum generation properties of these source rocks may add to the understanding of new prospects. Therefore, the following successions were chosen for a detailed analysis:

Oligocene – Miocene Menilite Formation - The Menilite Formation is the primary source rock interval in the Ukrainian Carpathians (Köster et al., 1998; Kotarba et al., 2006; 2007; Kosakowski et al., 2018). The most important hydrocarbon accumulations are found within the Boryslav-Pokuttya petroleum system, which hosts more than forty oil and condensate accumulations, with total recoverable reserves estimated at 2249 MMboe (Boote et al., 2018). Smaller oil and gas fields in the Skole-Skyba and Silesian-Krosno petroleum systems (most of them located in Poland), with estimated total recoverable reserves of 200 MMboe, are also sourced by the Menilite Formation, but are economically less relevant. Since a detailed study on the Menilite Formation in the Ukrainian Carpathians has not yet been published, an investigation on this source rock seems worthwhile.

Lower Cretaceous Shypot Formation - The Shypot Formation (Barremian to Albian) is considered as a potential source rock of the Outer Carpathians (Kotarba and Koltun, 2006). Generally, only few data are available and all economic hydrocarbon accumulations in the Ukrainian Carpathians are correlated to the Menilite Formation (Boote et al., 2018; Kotarba et al., 2019). However, possible petroleum contributions from this source rock should not be overlooked and will be investigated in the frame of this study.

Middle Jurassic succession and oils in Upper Jurassic reservoirs - Apart from gas, small oil fields, such as the Kokhanivka and the Orkhovychi oil fields in the Ukrainian part of the Carpathian Foredeep, provide evidence for another petroleum system (Boote et al., 2018). Despite the moderate petroleum potential of the Middle Jurassic succession in the Mesozoic basement of the Carpathian Foredeep (Kosakowski et al., 2012), geological and geochemical data are limited, and no attempt has been made at correlating this interval with oils from

overlying Upper Jurassic reservoirs. The current study attempts to correlate these oils using new geochemical data, and determine their source.

1.2. History of the Petroleum Industry

The petroleum industry looks back at a long-lasting history, starting with the discovery of natural asphalt, a highly viscous liquid or semi-solid form of petroleum, which was used in the construction of the walls of Babylon, four thousand years ago. Approximately 400 BC, petroleum was first used as a fuel in China, and the earliest documented wells were drilled using bamboo poles in 347 AD, at depths of ~250 m (Vogel, 1993).



Fig. 2 Illustration of the first modern well near Titusville, Pennsylvania (1859) privately owned by Edwin Drake (Brice and Black, 2013).

The modern history of the petroleum industry began in the 19th century, with the discovery of Edwin Drake's well, near Titusville, Pennsylvania in 1859 (Fig. 2). The well was drilled to a depth of 21 m, and yielded 25 barrels per day. By the end of the year, crude production in the US reached a total of 2,000 barrels (Vassilliou, 2018). The creation of the oil well

fundamentally altered the course of the 20th century. Other wells, which were either dug or drilled around the same time as Edwin Drake's well, contributed towards this total. Local wells, like those in Pennsylvania, were quickly outpaced by demand, as the industry grew, driven particularly by the demand for kerosene and oil lamps (Vassilliou, 2018)

Today, petroleum is used extensively in modern-day life, and has even become a major factor in military conflicts around the world. Crude oil accounts for 33% of the global energy consumption, whereas natural gas accounts for roughly 24% (Jia et al., 2016). It is predicted that the future global energy supply will mainly come from shale gas, tight oil and oil sands, which will make up approximately 75% of the global energy supply by 2030 (Jia et al., 2016).

1.3. History of the Petroleum Industry in Western Ukraine

The Ukrainian Carpathians constitute one of the oldest and largest petroleum-producing provinces in the Europe; with reserves of 1.6 bn tons of oil and gas condensates and 7,254 billion m³ of gas (Boote et al., 2018; Naftogaz Group, 2020). The first documented data on oil production in Western Ukraine can be dated back to the 14th century; however, commercial production did not start until 1854, with the discovery of the Boryslav oil field, which has become one of the largest onshore oilfields in Europe (Boote et al., 2018). The discovery marked the rise of extensive petroleum exploration in the Ukrainian Carpathians and at the time, resulted in the region becoming the largest oil producing region in Europe. In addition, Ukraine began to export significant amounts of petroleum, and became the first country in the world to distribute natural gas to other countries (Naftogaz Group, 2020).

After World War II, the oil and gas industry in Ukraine developed significantly due to the discovery of large reserves, not only in the Carpathians, but also in the Dnieper-Donets basin and the Black Sea region. In 1972, the Ukrainian oil and gas industry reached the peak level of oil and gas condensate production (14.4 million tons), whereas the peak level of natural gas (68.7 bcm) was reached in 1975.

1.4. Conventional and unconventional hydrocarbons

Conventional hydrocarbons are sources of crude oil, condensates and natural gas that can be extracted using traditional methods. These resources accumulate within a reservoir rock, which is sealed by an impermeable seal that keeps hydrocarbons in place (Fig. 3). In contrast, unconventional hydrocarbons cannot be extracted using conventional operating practices as the porosity and the permeability are often extremely low, restricting the flow of oil and gas. In unconventional hydrocarbon deposits, the source and the reservoir rock often coexist, and traps and seal rocks are generally not needed to keep hydrocarbons in place (Arthur and Cole, 2014).

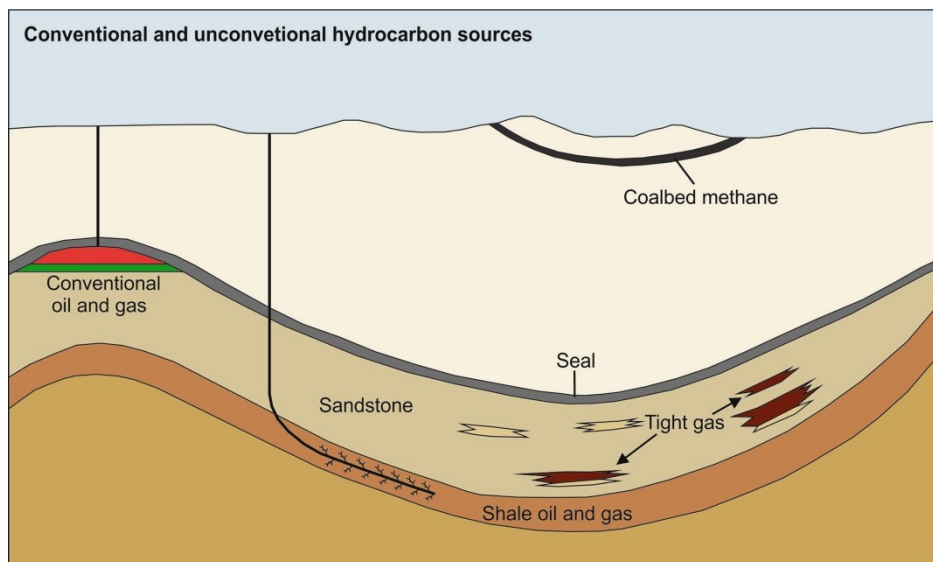


Fig. 3 Schematic sketch of different conventional and unconventional hydrocarbon deposits after Andrleit et al. (2010). The green and red layers indicate oil and gas accumulations in the sandstone reservoir.

Global petroleum exploration is currently undergoing a strategic shift from conventional to unconventional hydrocarbon resources, as a result of technological advances and progress in drilling and development techniques in the recovery of unconventional hydrocarbon resources (Schulz et al., 2010; Jia et al., 2016). As a result, unconventional hydrocarbons have become an increasingly important part of the world energy consumption (Zou, 2015), and different branches of unconventional production have benefited from this in recent years, including some of the following unconventional resources:

- (i) Coal bed methane (CBM) – Coal beds, which contain methane that was generated either through bacterial processes or by thermal decomposition of organic matter (e.g. Moore, 2012).
- (ii) Oil/Tar sands – Shallow, unconsolidated sand bodies, where conventional crude oil has become degraded (through evaporation, biodegradation and water washing) to produce a viscous heavy-oil residue (Arthur and Cole, 2014).
- (iii) Oil shales – Thermally immature organic rich (>5 wt.% TOC) source rocks where hydrocarbons are produced artificially through pyrolytic processes (Symington et al, 2010).
- (iv) Shale oil/gas – Mature to over mature source rocks, where hydrocarbons have been generated but not expelled (Curtis, 2002). Production of hydrocarbons is achieved through hydraulic fracturing.
- (v) Tight oil/gas – Sandstone reservoirs containing hydrocarbons which are trapped within a reservoir rock with extremely low porosity and permeability. Hydrocarbons can only be produced through hydraulic fracturing (Zou, 2015).

1.5. Unconventional hydrocarbons in the Ukraine

Ukraine has a significant potential for developing unconventional hydrocarbons, such as shale gas and coal-bed methane (CBM). However, in many regions, further explorations are needed to identify potential prospects. The most prospective regions for unconventional hydrocarbon exploration are observed in the Dniepr-Donets Basin (DDB) in eastern Ukraine, and within the Lubin basin in western Ukraine.

Western Ukraine

Thick Silurian black shales within the Lubin Basin have attracted much interested for shale gas exploration in the past. These deposits are the continuation of coeval deposits in Poland, and form an approximately 200 km wide NNW–SSE trending belt between the Ukrainian shield and the western margin of the East European Platform. However, recent studies (Kotarba and Koltun, 2006; Radkovets et al., 2017) have yielded disappointing results, which have led to a decline in interest for shale gas exploration in recent years. Nonetheless, a potential for sweet spots, which may be productive, remains.

Eastern Ukraine

The Dniepr Donets Basin is a major coal-mining district in eastern Ukraine. The DDB, which is approximately 650 km long, is a Late Devonian rift-basin located within the East-European Platform (Sachsenhofer and Koltun, 2012). Apart from organic-rich black shales, Carboniferous (Upper Visean “Rudov Beds”) successions contain major coal reserves, which are intensively mined. High methane content in the coals from the DDB present a high potential for coal bed methane projects (Kuznetsov, 1963).

Thick organic-rich black shales, which occur within the Rudov Beds, are an additional prospect for unconventional hydrocarbon exploration, as these sediments hold a slight shale gas potential (Schulz et al., 2010; Sachsenhofer and Koltun, 2012). However, their economic potential remains questionable due to disadvantageous mineralogy and insufficient maturity at reasonable drilling depths (Misch et al., 2016).

1.6. Oil to source correlations in conventional plays

Oil to source correlations determine the genetic relationship between a petroleum source rock and a crude oil, which can be of great interest for scientific and economic reasons (Curiale, 1993). The most critical piece of information for petroleum explorationists is the confirmation that the targeted sedimentary basin has generated oil or gas. The second most important information is determining its source. To conduct such a correlation, oil samples from producing wells, seeps, abandoned wells etc. are compared with their counterparts extracted from the potential source rock. Each crude oil has a specific composition that can be determined using biomarker ratios or by compound specific isotope analysis (CSIA). Biomarkers are complex molecular fossils that occur in crude oils and extracts of petroleum source rocks (Misselwitz et al., 2013), which can provide important information on the organic matter, the environmental conditions during deposition and burial (diagenesis), the thermal maturity experienced by rock or oil (catagenesis), the degree of biodegradation, some aspects of source rock mineralogy (lithology), and age (Peters et al., 2005). The use of CSIA, allows us to determine and compare compound specific isotope patterns, which are generally unique for each source rock and oil sample.

2. Geological overview of the Carpathians

2.1. Geology of the Carpathians

The Carpathians are an approximately 1300 km long and 50-150 km wide arced shaped mountain chain that formed in response to the subduction and continental collision between the European and Apulian plates and related micro-plates, which resulted in the closure of the Tethys Sea (Sandulescu, 1988). To the west, the Carpathians are bordered by the Eastern Alps (Fig. 1), whereas to the southeast, the Carpathians grade into the Balkan mountain chain (Golonka et al. 2006). The Carpathians can be separated geographically into three longitudinal segments: 1) the Western Carpathians, 2) the Eastern Carpathians and 3) the Southern Carpathians.

Western Carpathians

The Western Carpathians stretch from Austria and southeastern Czech Republic into Slovakia, northern Hungary and southern Poland, and can be sub-divided into an older (Inner Carpathians) and a younger (Outer Carpathians) range. The Outer and Inner Carpathians are separated by a narrow (up to 20 km wide), 600 km long strongly tectonized zone known as the Pieniny Klippen Belt (Slaczka et al., 2006; Golonka et al., 2015; Fig. 1). The Pieniny Klippen Belt, which emerges in the west from beneath the Neogene sediments of the Vienna basin, stretches into Poland, Slovakia and the Ukraine (Chorowicz, 2016; Fig. 1).

The Western Outer Carpathians form the SW-NE trending segment of the Outer Carpathians and comprise the Silesian-Sub-Silesian (Krosno) nappe in the north, and the Magura nappe in the south. Similar to other parts of the Outer Carpathians, the nappes of the Western Outer Carpathians consist primarily of siliclastic sediments, Jurassic to Early Miocene in age, which reach maximum thicknesses of up to several thousands of metres (Slaczka et al., 2006; Plasienska et al., 1997). However, it should be noted that the majority of sediments in the Western Outer Carpathians typically range between Late Cretaceous to Early Miocene in age (Chlupac et al., 2002). The Inner Western Carpathians, which lie to the south of the Western Outer Carpathians, are typically covered by thick Tertiary sedimentary and volcanic complexes related to the Pannonian back-arc basin system (Plasienska et al., 1997).

Eastern Carpathians

The Eastern Carpathians are the continuation of the southeastern part of the Western Carpathian segment and stretch from southeast Poland and Slovakia, through western Ukraine and into Romania (Fig. 1). The Outer Eastern Carpathians, which comprise a series of structurally complex nappes, formed on top of the East European Platform margin during Eocene-Pliocene subduction (Sandulescu, 1988). In general, each nappe corresponds to a separate or partly separate sedimentary sub-basin containing different lithostratigraphy and tectonic structures (Slaczka et al. 2006). Sedimentation in these nappes spans between Late Jurassic to Early Miocene in age, and may locally exceed thicknesses of up to 6 km (Slaczka et al. 2006). The Inner Eastern Carpathians, which make up a prolongation of the Northern Calcareous Alps and are related to the Apulia plate (Picha, 1996), formed during the Mid-Cretaceous period and comprises a Precambrian and/or Paleozoic crystalline basement with a Mesozoic sedimentary cover (Sandulescu, 1988).

The Ukrainian Carpathians make up the middle segment of the Eastern Carpathians, which is divided into the Outer and the Inner Carpathians (including the Transcarpathians; Golonka et al., 2015; Fig. 4b). In Ukraine, magmatic formations (e.g. Vyhorlat Huta; Sarmatian-Pannonian) are distributed within the basement of the Transcarpathians, and are observed at the surface of the southern slope of the Ukrainian Outer Carpathians (Pavlyuk et al., 2013; Fig. 5a).

Southern Carpathians

The Southern Carpathians, which are commonly known as the Transylvanian Alps, comprise an E-W and an N-S orientated section (Duchesne et al., 2007; Fig. 4b). The Southern Carpathians are viewed as a Cretaceous nappe pile (Iancu et al., 2005), which are made up of the following structural and paleogeographic sections: the Danubian nappes, the Severin nappe, the Getic and the Supergetic nappes (Burchfiel and Bleahu, 1976). With the exception of the Severin nappe, which is related to a basin with oceanic crust, all the tectonic sections comprise a metamorphic basement that contains Precambrian and Paleozoic rocks as well as a sedimentary cover (Sandulescu and Dimitrescu, 2004). Folds in the youngest rocks continue westward, until all surface expression disappears before reaching the Danube River (Burchfiel and Royden, 1982).

2.2. Geology of the Ukrainian Outer Carpathians

The Ukrainian Outer Carpathians comprise nappes that were thrust northeast-ward over the autothonomous Miocene strata of the Carpathian Foredeep and onto the southwestern margin of the East European Plate during late Oligocene-Early Miocene tectonism (Slaczka et al., 2006). In the Ukrainian Outer Carpathians, the following nappes are distinguished from the northeast (i.e. the most external part of the thrust-belt) to the southwest (most internal part): Sambir, Boryslav-Pokuttya, Skyba, Krosno, Dukla-Chornohora, Porkulec and Marmarosh (Fig. 4b). The position of the Chornohora nappe is not completely clear (see Slaczka et al., 2006), and it has therefore been suggested by Nakapelyukh et al. (2018) that the Chornohora nappe corresponds to the Dukla nappe. As a result, the Chornohora nappe is often referred to as the Dukla-Chornohora nappe (see Fig. 4b, 5a, b).

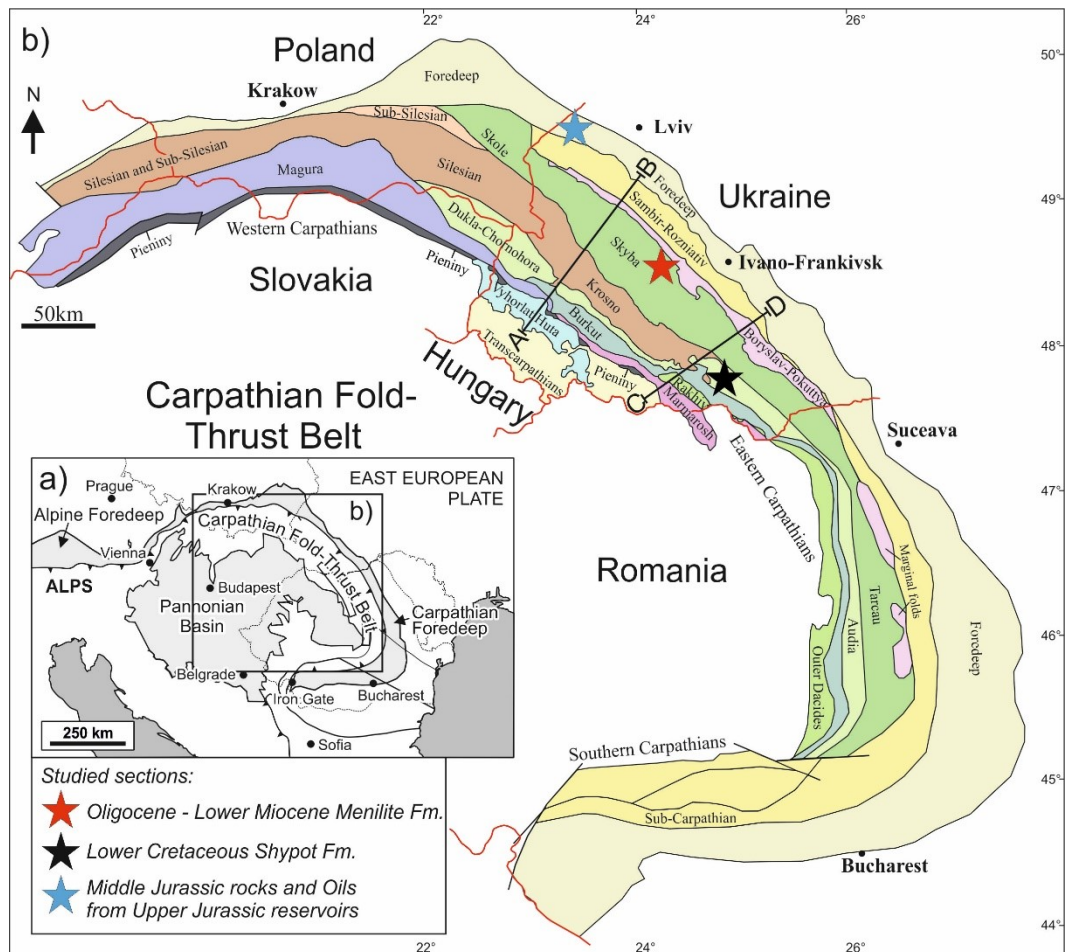


Fig. 4 (a) Outline map of central-eastern Europe (b) Structural map of the Carpathian Fold-Thrust Belt and the locations of the studied sections, which are investigated within the frame of this thesis (after Nakapelyukh et al., 2018; Oszczytko et al., 2006; Slaczka et al., 2006).

The Boryslav-Pokuttya nappe, which is known as the Marginal folds in Romania, is located in the north-eastern part of the Outer Carpathians and comprises Cretaceous-Miocene flysch sediments as well as Early Miocene molasse, and is therefore commonly classified as part of the Carpathian Foredeep (Kruglov et al., 1985; Kotarba et al., 2008). In general, the external part of the Boryslav-Pokuttya nappe and the Skyba nappe are often described together as they show similar sedimentary sequences. The only differentiation between the two nappes is based primarily on their tectonic position and the presence of Molasse sediments in the Boryslav-Pokuttya nappe (Slaczka et al., 2006; Fig. 5a, b).

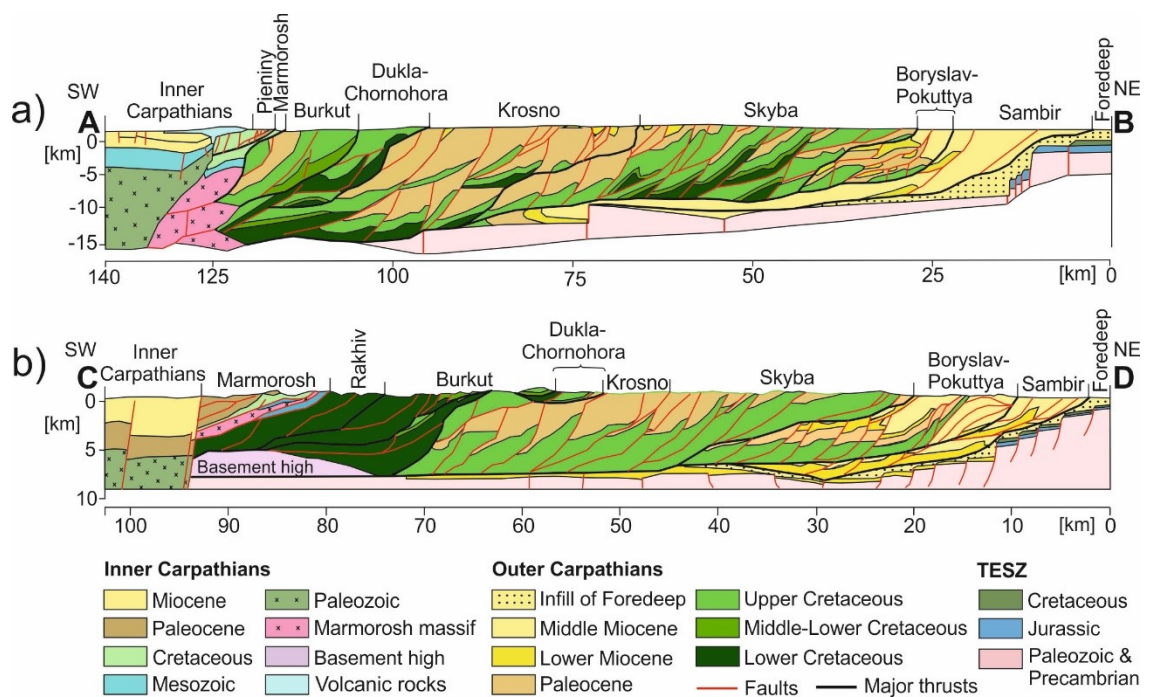


Fig. 5 Cross-sections A-B (a) and C-D (b) of the Ukrainian Carpathians. The locations of the cross-sections are displayed in Fig. 4b (modified after Shlapinskyi, 2015; Nakapelyukh et al., 2018).

The Skyba nappe forms a large portion of the eastern part of the Eastern Carpathians and constitutes the largest tectonic unit in the Outer Carpathians, as it stretches from Poland (where it is known as the Skole nappe) into Romania (Tarcau nappe). The Skyba nappe can be subdivided further into six individual thrust-folds (also referred to as sub-nappes; Slaczka et al., 2006), which can reach maximum widths of up to 12 km for each individual sub-nappe. The maximum recorded width for this nappe is observed in the central part of the Ukrainian Outer Carpathians where the tectonic unit reaches approximately 40 km (Slaczka et al., 2006).

Towards the northwest, the nappe decreases in size, and is eventually thrust beneath the Sub-Silesian nappe (Fig. 4b)

Flysch-type sediments in the Outer Carpathians range from Early Cretaceous to Early Miocene in age and may locally reach thicknesses of up to 6 km (Slaczka et al., 2006; Fig. 6a). As a result of uprooting, generally only the central parts of the basins are preserved (Slaczka et al., 2006). The sediments are bordered to the northeast by a molasses-filled foredeep and to the southeast by the Pienniny Klippen belt (Kotarba et al., 2007).

The Menilite Formation, which forms the upper part of the sedimentary succession of the Ukrainian Outer Carpathians (Fig. 6a), is the primary source rock of the region and occurs in almost all nappes (Sachsenhofer and Koltun, 2012). The formation is dominated by organic-rich shales which were deposited in oxygen-depleted marine conditions during the partial isolation of the Paratethys (including the Carpathian basins) from the Mediterranean and the World Ocean during Oligocene time (Popov et al., 2004). Basin isolation was a result of both tectonic deformations during the Alpine Orogeny and a fall in eustatic sea level (Schulz et al., 2005). The Menilite Formation comprises of shales, siltstones and sandstones, and can reach a maximum thickness of approximately 2050 m in some regions of the Ukrainian Outer Carpathians (Koltun et al., 1998).

Early Cretaceous anoxic black shales, which are commonly interbedded by laminated siltstones and minor sandstone beds, make up the base of the flysch belt (Fig. 6a). These sediments were deposited in oxygen-depleted marine conditions, which partly coincide with a global anoxic event during Barremian to Albian times (OAE-1; Schlanger and Jenkyns, 1976; Jenkyns, 1980). Depending on the tectonic position of these sediments, the successions are assigned to either the Shypot or the Spas Formation. The Spas Formation, which is entirely confined to the Skole-Skyba nappe, crops out locally in the northwestern part of the nappe (Vialov et al., 1988), whereas the Shypot Formation crops out frequently in the more internal nappes (Krosno, Dukla-Chornohora and Burkut) of the Outer Carpathians.

The Shypot and Spas formations are both primarily composed of organic-rich black shales with minor siltstones and sandstones in their lower part and by thick-bedded sandstones in their upper part. The Spas Formation, which reaches a total thickness of approximately 200 m in its lower part, is thinner than the Shypot Formation (300 m; Slaczka et al., 2006). In addition, the upper part of the Shypot Formation comprises a 200 m thick interval comprising

of dark, quartzitic sandstone with black shale intercalations (Albian in age), which is not encountered in the Spas Formation (Slaczka et al., 2006).

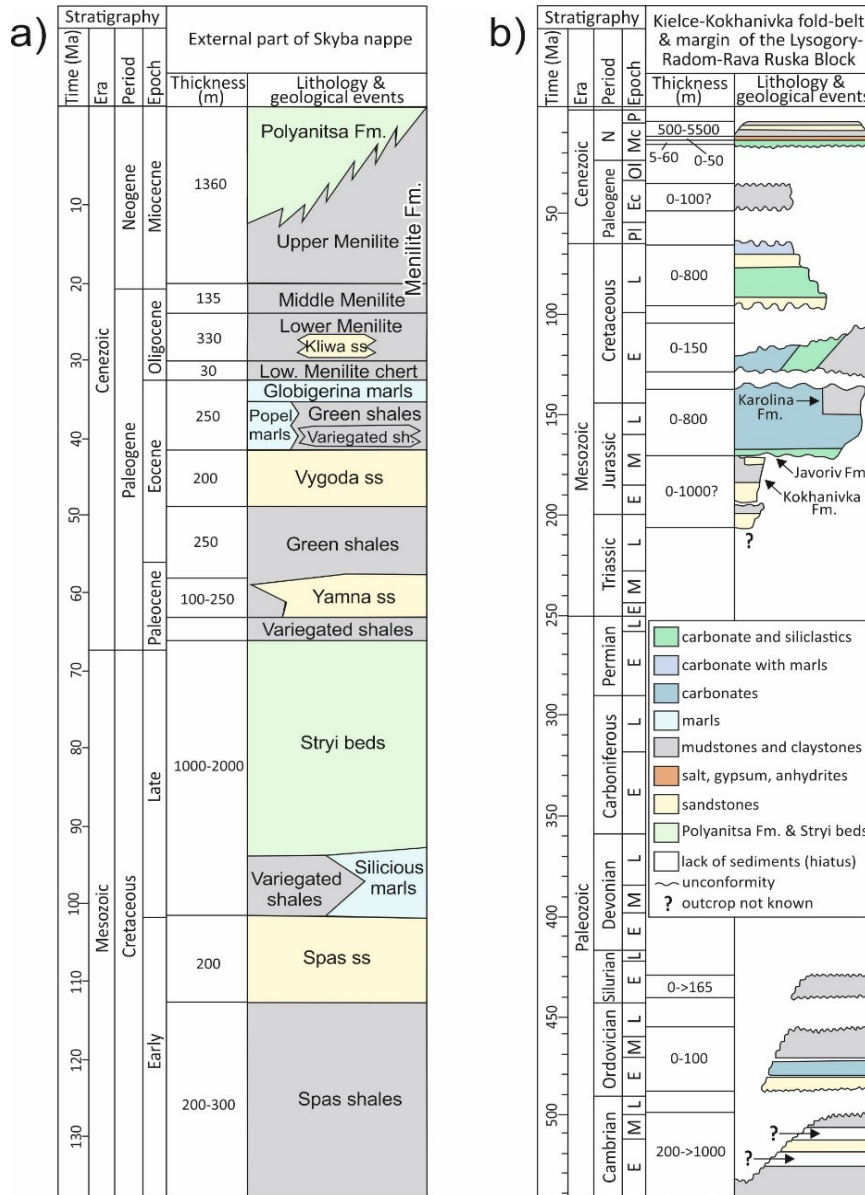


Fig. 6 Stratigraphic column of the (a) Cretaceous to Miocene succession in the external part of the Skyba nappe in the Outer Carpathians, and the b) pre-Miocene basement of the Carpathian Foredeep (after Kotarba and Koltun, 2006; Kotarba et al., 2011).

Petroleum habitat - The Ukrainian Outer Carpathians constitute one the largest petroleum provinces in Central Europe. More than 80 small oil and gas fields, which are mostly located on Polish territory, are hosted by Upper Cretaceous-Paleocene, Eocene and Oligocene sandstones within complex, faulted antiformal structures. The main oil-bearing region is the

Boryslav-Pokuttya petroleum system, which hosts more than forty oil and condensate accumulations with total recoverable reserves estimated at 2249 MM boe (Boote et al., 2018). The Skole-Skyba (Fig. 4a) as well as the Silesian-Krosno petroleum system extend from Poland into western Ukraine, are economically less relevant, and contain total recoverable reserves of approximately 200 MMboe (Boote et al., 2018).

Source rocks - Two organic-rich intervals are found within the Ukrainian Outer Carpathians: the Oligocene - Lower Miocene Menilite Formation and the Lower Cretaceous Shypot and Spas Formations (Sachsenhofer and Koltun, 2012). Both formations have a basin-wide extent, with significant source rock potential.

The Menilite Formation is traditionally divided into Lower (Lower Oligocene), Middle (Upper Oligocene) and Upper (Lower Miocene) members (Koltun, 1992). The Menilite Formation is dominated by oil-prone source rocks which formed under euxinic conditions (Koltun et al., 1998). The thermal maturity varies significantly, both vertically in relation to burial depth, and laterally in the different tectonic units, but generally increases from the outer (external) to the inner (internal) parts of the orogenic belt (Kosakowski et al., 2018). The average TOC content for these rocks ranges between 4-8 wt.% (max: up to 26 wt.%) and the HI values average between 292-344 HC/gTOC (max: 900 HC/gTOC) in the Boryslav-Pokuttya, Skyba, Krosno, Dukla and Porkulets nappes (Kosakowski et al., 2018).

The Shypot Formation is significantly less well understood, and data is limited. However, the formation is considered as an additional potential source rock horizon in the Outer Carpathians (Kotarba and Koltun, 2006). Sediments are organic-matter-rich and TOC content exceeds 2 wt.% frequently and reaches up to 8 wt.% in some parts of the succession. The petroleum potential is considered as fair (S_2 values up to 9.38 mgHC/gRock), but HI values are low, and generally do not exceed 200 mgHC/gTOC often, indicating a dominance of type III kerogen, or II/III kerogen. This is also supported by the presence of high percentages of vitrinite in all samples (Kruge et al., 1996).

Reservoir rocks – In the Boryslav-Pokuttya petroleum system (sensu Boote et al., 2018), Structural traps consist of stacked duplexes; Paleogene and Miocene deep-water reservoir sandstones are sealed by the overlying Miocene molasse. Whereas, in the Skole-Skyba and Silesian-Krosno petroleum systems, petroleum accumulations are hosted by Upper Cretaceous-Paleocene, Eocene and Oligocene sandstones within complex, faulted antiformal structures (Kotarba and Koltun, 2006).

2.3. Geology of the Ukrainian Carpathian Foredeep

The Polish and Ukrainian Carpathian Foredeep developed as a peripheral foreland basin in front of the advancing Carpathian orogenic wedge during early and middle Miocene times. In Ukraine and Poland, the East Carpathian Foredeep overlies the western margin of the East European Platform, and is partly over-thrust by the Eastern Carpathians (Oszczypko et al., 2006). In the Carpathian Foredeep, clastic marine sediments (Miocene in age; Kosakowski et al., 2013), typically make up a significant portion of the sedimentary cover, and can reach thicknesses of up to 6 km (Kurovets et al., 2004; Oszczypko et al., 2006; Fig. 5b). The remaining sedimentary cover comprises of a discontinuous, locally developed, Permian-Mesozoic sedimentary succession, which overlies Precambrian and/or Palaeozoic (from the Cambrian-Carboniferous) sediments that occur in the basement of the Outer Carpathians (Oszczypko et al., 1989; Oszczypko et al., 2006;).

In Ukraine, the basement complex of the Carpathian Foredeep is traditionally known as the Kokhanivka and the Rava Ruska Zones (Fig. 7b), whereas in Poland, it is referred to as the Kielce Fold Belt and the Lysogory-Radom Block (Buła & Habryn 2011). The boundary between the Kokhanivka and the Rava Ruska Zones as well as the Kielce Fold Belt and the Lysogory-Radom Block is marked by the Holy Cross Fault, which stretches from Poland into Ukrainian territory (Fig. 7b), whereas the southwestern margin of the Kokhanivka Zone is formed by the Krakovets Dislocation (Fig. 7b).

Jurassic aged rocks, which make up part of the sedimentary succession of the basement complex in the Carpathians Foredeep (Fig. 6b), comprise of Lower-Middle Jurassic (Hettangian-Callovian) and Upper Jurassic-Lower Cretaceous (Oxfordian-Valanginian) sediments (Kotarba et al., 2011). Due to deformations and tectonic repetition of sedimentary sequences in this region, the true thickness of the successions is difficult to estimate and the identification of the Mesozoic succession and its boundaries with the underlying sediments remains problematic (Kosakowski et al., 2013). Nonetheless, it has been estimated that the Middle Jurassic strata reaches thicknesses of up to 1000 m in the basement complex of the Ukrainian Foredeep, which is significantly higher compared to southeastern Poland, where age-equivalent sediments vary from dozens to several hundreds of metres and only exceed 100 m in a few regions (Moryc, 2004).

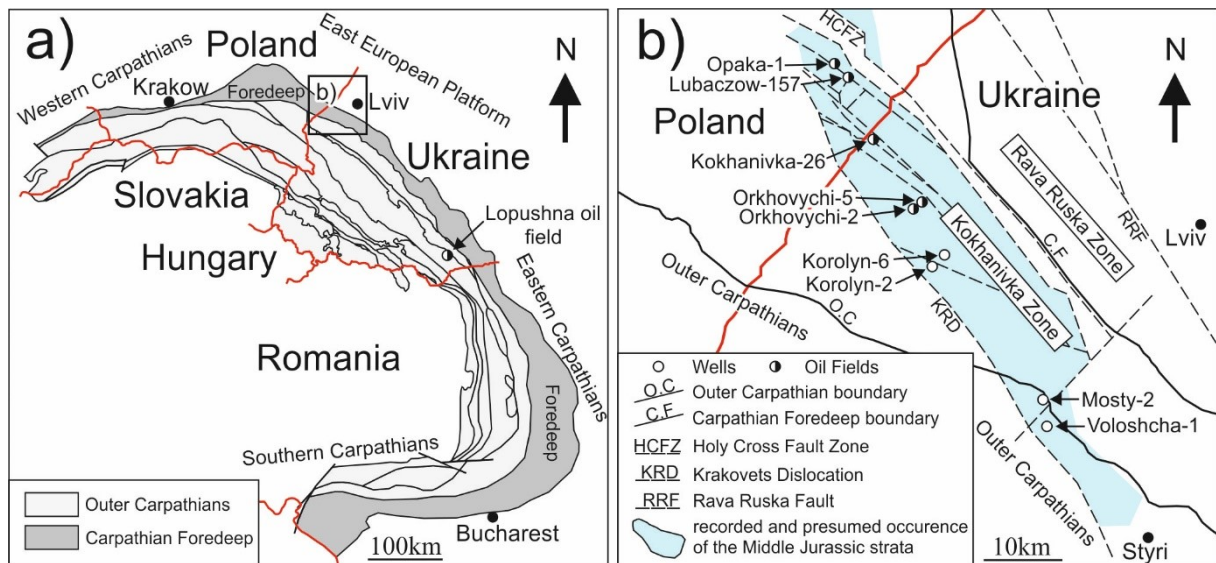


Fig. 7: (a) Structural map of the Carpathian Fold-Thrust Belt and its foredeep basin (after Nakapelyukh et al., 2018; Oszczypko et al., 2006; Slaczka et al., 2006) (b) Sub-crop map of the Middle Jurassic strata and the locations of the discussed oil wells in the northern part of the Ukrainian Carpathians (after Kosakowski et al., 2012a).

In Ukraine, Middle Jurassic rocks (also known as the Kokhanivka Formation) range in age from Aalenian to Bathonian (Pieńkowski et al., 2008), and represent the depositional systems varying from estuary/foreshore (lower part) to dysoxic shelf sediments. Callovian sediments are regarded to represent a shallow carbonate-siliciclastic shelf (Pieńkowski et al., 2008), whereas Oxfordian-lower Kimmeridgian strata were formed by a carbonate ramp grading upwards into a rimmed platform (upper Kimmeridgian-Valanginian). A generalized lithostratigraphic column of the Paleozoic and Mesozoic basement of the Carpathian Foredeep for the eastern part of Poland as well as the northern section of the Ukrainian Carpathian Foredeep is provided in Fig. 4.

Petroleum habitat – The Carpathian Foredeep hosts at least two petroleum systems: a microbial gas system and a thermogenic oil system. To date, more than 40 gas fields and several small oil fields have been detected in the Ukrainian sector the Carpathian Foredeep (Boote et al., 2018). Of those, eleven deposits were found within the Mesozoic basement of the Carpathian Foredeep (Kotarba et al., 2011). Three of them are small heavy oil fields; the Kokhanivka and Orkhovychi fields (Fig. 5a), which occur near the Polish-Ukrainian border, and the Lopushna oil field (Fig. 5a) in the southeastern part of the Carpathian Foredeep.

Source rocks – In the upper part of the Ukrainian Carpathian Foredeep, large quantities of microbial gas are sourced from immature Neogene shales (Kotarba, 1992; Kosakowski et al., 2013), and additional thermogenic gas and condensate are sourced from mature Neogene depo-centers (Kotarba and Koltun, 2011). In the Paleozoic-Mesozoic basement of the Carpathian Foredeep, Cambrian, Ordovician, Silurian, Middle Jurassic siliclastics (Kokhanivka Formation) and Upper Jurassic deep-water carbonate mudstones are regarded as potential source rocks (Kosakowski et al., 2012; Kosakowski et al., 2013; Kotarba et al., 2011; Wieclaw et al., 2011). Cambrian and Ordovician successions display moderately low TOC content (< 1.0 wt.%), whereas Silurian rocks can reach up to 2.6 wt.% TOC in some regions (Wieclaw et al., 2011). However, it should be noted that data for some of these intervals is extremely limited and results are based on only a few samples. Nonetheless, the best source rocks properties are found within the Middle and Upper Jurassic strata.

The Middle Jurassic strata are organic-matter-rich and reach a maximum TOC content of up to 25.9 wt.% in Ukrainian territory (Kosakowski et al., 2013). Generally, samples from the Polish part of the basement complex display a higher median TOC value compared to rocks in the Ukrainian part of the basement (Kosakowski et al., 2012). However, HI values for both territories are low, and only range from 13-289 mgHC/gTOC, with a median of only 57 mgHC/gTOC, indicating a dominance of type III kerogen, with only minor local inputs of type II kerogen. Maturity parameters such as T_{max} values (approximately 430; Kosakowski et al., 2012) and vitrinite reflectance measurements (0.51-0.65 wt.%; Kosakowski et al., 2012) indicate an early phase oil window maturity, particularly for the Ukrainian sediments, suggesting that hydrocarbons may have been generated in intervals with good petroleum potential (Kosakowski et al., 2012).

Data on Upper Jurassic rocks are scarce, but data indicate a fair to good hydrocarbon potential for narrow intervals within the Upper Jurassic succession. TOC content is moderate (max. 1.5 wt.%), but HI values are very high (max: 557 mgHC/gTOC). Sulphur content in these samples is generally elevated, indicating the presence of type IIS kerogen, which typically enables petroleum generation below the normal limits of the oil window (Kosakowski et al., 2012)

Reservoir rocks – In general, Lower Palaeozoic reservoir rocks in the Ukrainian Carpathians contain weak reservoir features due to their limited porosity (Karnkowski, 1999; Kurovets et al. 2011). In contrast, intervals within the Middle Jurassic strata and the Upper Jurassic-Lower Cretaceous carbonates (Kosakowski et al., 2012; Kosakowski et al., 2013) host heavy oil deposits (Glushko, 1968; Vul et al., 1998; Kurovets et al., 2011). These reservoir rocks are provided by carbonate buildups and inner platform sediments (Kotarba et al., 2011). Kurovets et al. (2011) distinguished three main types of reservoir rocks: (i) Fractured low-permeable limestones with small inter-granular porosity; (ii) Organo-detrital limestones with high porosity (15-20%) and permeability (up to $100 \cdot 10^{-3} \mu\text{m}^2$); (iii) Fractured pseudo-oolitic limestones with high porosity (20–30%), but low permeability. The reservoir rocks are sealed by autochthonous Miocene strata, which in some areas reach thicknesses of up to 5000 m (Krajewski et al., 2011). In addition, microbial gas, sourced by Neogene shales, is trapped in karstified Jurassic and Cretaceous carbonate and sandstone reservoirs, as well as in overlying Miocene (Sarmatian) sandstones (Boote et al., 2018).

3. Samples and Methods

Oligocene - Miocene Menilite Formation - 233 outcrop samples were collected from outcrops near the village of Spas, approximately 50 km west of Ivano-Frankivsk; 153 samples of the Lower Menilite Member from a profile location to the SW of Spas in the Oriv sub-nappe (base of section: 48°51'27" N 24°02'50" E); six samples of the Middle Menilite Member from a location to the west of Spas (48°54'17" N 24°02'23" E); and 74 samples of the Upper Menilite Member, which includes four samples of the overlying Polyanytsya Formation from a location to the north of Spas (base of section: 48°54'00" N 24°03'33" E).

Lower Cretaceous Shypot Formation - 94 outcrop samples were collected from the lower part of the Shypot Formation from an outcrop along a small tributary of the river Bystrets, west of the village Bystrets (base of section: 48°07'18" N 24°38'27" E), Ivano-Frankivsk, Ukraine. The study area is located in the south-eastern part of the Ukrainian Outer Carpathians, in the Chornohora Nappe.

Middle Jurassic succession and oils in Upper Jurassic reservoirs - 89 core samples from the Mosty-2 (2361 - 2560 m), Korolyn-6 (3418 - 3523 m) and Korolyn-2 (3642-3652; 3696-3712; 3870-3996 m) boreholes, as well as three oil samples from Upper Jurassic reservoirs in the Kokhanivka-26, Orkhovychi-2 and Orkhovychi-5 boreholes, were collected for analysis.

It should be noted that not all methods were applied to all samples, and only a subset of samples were used for some methods. All analytical methods are described in detail below.

Bulk parameter measurements

All rock samples were analysed for their total carbon (TC), total sulphur (TS) and total organic carbon content (TOC) using an ELTRA Elemental Analyser. Samples measured for TOC were treated twice with 50% phosphoric acid to remove inorganic carbon. Results are based on the averages of at least two corresponding measurements of approximately 100 mg of analytical powder, and are given in weight percent (wt.%). The total inorganic carbon (TIC) was determined by subtracting the TC with the TOC. TIC was then used to calculate the calcite equivalent percentages ($= \text{TIC} * 8.333$).

Rock Eval Pyrolysis

Rock-Eval pyrolysis was carried out with approximately 100 mg of analytical power, using a Rock-Eval 6 analyser in order to determine the S_1 , S_2 (mg HC/g rock) and T_{max} for all samples. S_1 determines the amount of hydrocarbons present in the rock, whereas S_2 determines the amount of hydrocarbons formed during pyrolysis. The petroleum potential (S_1+S_2 [mg HC/g rock]), the hydrogen index ($HI=S_2/TOC*100$ [mg HC/g TOC]) and the Production Index ($S_1/[S_1+S_2]$) were calculated using the S_1 and S_2 measurements. T_{max} is a maturity parameter and indicates the temperature during Rock-Eval pyrolysis at which the maximum amount of hydrocarbons can be generated (Espitalié et al., 1984). S_1 , S_2 and T_{max} results are based on at least two corresponding measurements.

Organic petrography and vitrinite reflectance

Polished blocks were prepared for semi-quantitative maceral analysis and vitrinite reflectance (% Rr) measurements. Maceral composition was determined using white light and fluorescence light. The macerals included in the study were vitrinite (higher plants), liptinite (sporinite, telalginite, lamalginite) and inertinite (charred plant material). In addition, the volume percentages for the mineral matrix, pyrite and glauconite were determined in order to calculate the total maceral amounts in comparison to the mineral matter. For their maturity assessment, vitrinite reflectance was measured in nonpolarized light using a Leice DM4P microscope equipped with Hilgers FOSSIL MOT, with a 50x oil objective, following established procedures (after Taylor et al., 1998).

Geochemical biomarker analysis

Based on the HI and TOC results, samples were selected at similarly spaced intervals for biomarker analyses. Samples were extracted in a Dionex ASE 200 accelerated solvent extractor using dichloromethane at 75° C and 50 bar for approximately 1 hour. Asphaltenes were precipitated from the solution using a hexane-dichloromethane solution (80:1) and then separated by centrifugation. The hexane-soluble fractions were separated into NSO compounds, saturated hydrocarbons and aromatic hydrocarbons using medium pressure liquid chromatography (MPLC) with a Köhnen-Willsch instrument (Radke et al., 1980). The saturated and aromatic hydrocarbon fractions were analysed by a gas chromatograph equipped with a 30 m DB-5MS fused silica column (i.d. 0.25 mm; 0.25 mm film thickness), coupled to a ThermoFischer ISQ Dual-quadrupole mass spectrometer. Using helium as the carrier gas,

the oven temperature was set to increase from 70°C to 300°C at 4°C min⁻¹, which was followed by an isothermal period of 15 min. With the injector temperature set to 275°C, the sample was then injected with a split ratio of 10. The spectrometer was operated in EI (electron ionization) mode over a scan range from *m/z* 50 to 650 (0.7 s total scan time). Data was processed using an Xcalibur data system where individual compounds were identified on the basis of retention time in the total ion current (TIC) chromatogram and by comparison of the mass spectra with published data. Percentages and absolute concentrations of various compound groups in the saturated and aromatic hydrocarbon fractions were calculated using peak areas from the gas chromatograms and their relations to the internal standards (deuterated *n*-tetracosane and 1,1'-binaphthyl, respectively). Concentrations were normalized to TOC.

Isotopy

Stable carbon and oxygen isotope ratios of carbonate phases were measured. The powdered samples were treated with 100 % H₃PO₄ at 70 °C in an online system (Gasbench II) and the released CO₂ analyzed by a ThermoFisher DELTA-V ir-MS. The values were normalized to the V-PDB standard for both δ¹³C and δ¹⁸O and have a standard deviation of 0.8 ‰ for δ¹³C and 0.1 ‰ for δ¹⁸O.

The study of compound specific isotope analysis (CSIA) was performed by Martin Sweda at the Montanuniversitaet Leoben, following established procedures (Bechtel et al., 2013). The *n*-alkanes were separated from branched/cyclic hydrocarbons by an improved 5 Å molecular sieve method for the analysis of stable carbon and hydrogen isotope ratios on individual *n*-alkanes and isoprenoids. Stable C and H isotope measurements were made using a Trace GC-ultra gas chromatograph attached to the ThermoFisher Delta-V isotope ratio mass spectrometer (irMS) via a combustion and high temperature reduction interface, respectively (GC Isolink, ThermoFisher). The GC coupled to the irMS was equipped with a 30 m DB-5MS fused silica capillary column (i.d. 0.25 mm; 0.25 μm film thickness). The oven temperature was programmed from 70–300 °C at a rate of 4 °C/min followed by an isothermal period of 15 min. Helium was used as carrier gas. The sample was not split and was injected at 275 °C. For calibration, a CO₂ or H₂ standard gas was injected at the beginning and at the end of each analysis. Isotopic compositions are reported in the δ notation relative to the PDB (for C) and SMOW (for H) standards. Analytical reproducibility (0.2‰ for δ¹³C; 2–3‰ for δD) was controlled by repeated measurements of *n*-alkane standard mixes.

Nannoplankton determination

The study of calcareous nannofossils was conducted by Stepan Coric at the Geological Survey of Austria (GBA) in Vienna, in order to determine the age of the investigated intervals. Smear slides for the study of calcareous nannofossils were prepared for selected samples using standard procedures described by Perch-Nielsen (1985) and were examined under a light microscope LEICA DMLP (cross and parallel nicols) with 1000x magnification. For biostratigraphic attribution, the nannofossil zonation of Martini (1971) was applied.

Mineralogy - XRD

Preparation of the studied samples for X-ray diffraction (XRD) measurements with a X'Pert³ Powder Diffractometer built by Panalytical, included hand-milling to a grain size of ~10 µm. For determination of the bulk mineralogy, the semi-quantitative mineral analysis with nearly random particle-orientation were used. Quantitative interpretation was done according to Schultz (1964). All mineral amounts are given as wt.%.

Biogenic Silica analysis

Diatoms were detected in samples in the Menilite Formation. In order to quantify the amount of biogenic silica, samples were treated using a modified version of the process described by Zolitschka (1988). However, none of the samples yielded statistically relevant concentrations, and are therefore not discussed in the current study.

4. Summary of publications

4.1. Publication I: **The Oligocene-Miocene Menilite Formation in the Ukrainian Carpathians: a world-class source rock**

This study investigates the petroleum potential of the Oligocene-Miocene Menilite Formation, the primary source rock of the Ukrainian Carpathians. Despite extensive research, detailed studies on the vertical variability on the source rock properties of the Menilite Formation in the Ukrainian Carpathians are still missing. Within the frame of this study, more than 200 rock samples were investigated for their bulk parameters (TOC, Rock Eval), whereas a subset of these samples underwent additional biomarker, mineralogical (XRD) and petrographical (maceral percentages, vitrinite reflectance) analysis. The studied section is located 50 km west of Ivano-Frankivsk, along the Chechva River, and comprises an almost complete succession, approximately 1800 m thick, which can be subdivided into the Lower, Middle and Upper Menilite Members.

The Eocene-Oligocene transition represents an important step in the geodynamic evolution of the Tethyan realm, as the reorganization of the European-Asian and African plates heavily influenced the isolation of the Paratethys, a marine sector separated from the rest of the Tethys (Miclaus et al., 2007). This resulted in anoxic conditions and the deposition of the organic-rich Oligocene-Lower Miocene Menilite shales, which are found throughout many parts of the Outer Carpathians and have become of great importance due to their high petroleum-generation potential.

Lower Menilite Member

The Lower Oligocene Lower Menilite Member is approximately 330 m thick in the studied section of the outer part of the Skyba nappe, and comprises a chert horizon at its base, an overlying sandstone-rich interval and a sandstone-poor upper part.

The chert horizon, which is interpreted as diagenetically altered diatomites, was deposited during the nanoplankton zone NP22. Black shales with very high TOC content (up to 21 wt.%) and HI values (600-800 mgHC/gTOC) are observed in this section. This is due to elevated concentrations of algal-derived lam- and telalginite, which indicates excellent preservation of mainly algal material. Oxygen depleted conditions are indicated by low Pr/Ph ratios (1.0-1.7), and a moderately enhanced DBT/Phen ratio suggests that small amounts of free H₂S were available. TOC/S ratios are often elevated (3-7), most likely due to very high

organic-matter-content and the limited diffusion of sulphate from the water column, inferring a sulphate-limited environment.

The overlying interval (between 310-195 m from the top of the Lower Menilite Member), contains frequent beds of Kliwa sandstones, and is referred to in this thesis as the “sandstone-rich interval”. These sandstones are considered to be deep-marine deposits and represent the transition from a deep-marine channel fill to a depositional fan lobe. TOC content of interbedded black shales are high (>8 wt.%) and exceed 20 wt.% in its upper part, indicating that organic matter accumulation was high shortly before and after the deposition of channel fill sediments. HI values for the black shales are slightly lower compared to rocks within the underlying chert horizon, and typically range between 400-650 mgHC/gTOC. Higher land-plant input is observed through higher concentrations of land-plant derived biomarkers. C₂₅ HBIs, which occur in significant concentrations in some samples, may indicate an input of diatom-derived material. Pr/Ph ratios, which vary significantly, were mainly controlled by the landplant input rather than by the redox conditions and therefore should be taken with caution. TOC/S ratios in samples below 276 m (from the top of the member) are consistent with marine, reduced-oxygen conditions and high ratios are likely the result of higher TOC contents in these samples.

The sandstone-poor upper part (127-0 m from the top of the member), contains a lower proportion of turbiditic sandstones, which suggests a change from a deep-marine channel to a pelitic distal lobe setting. TOC content of the Menilite shales are very high (up to 20 wt.%) and display a decreasing upwards trend. HI values typically range between 350 to 400 mgHC/gTOC, and are generally lower than in the underlying sediments, likely due to a decrease in alginite concentrations and a higher contribution of land-plant derived macerals (vitrinite, inertinite, sporinite). High concentrations of land-plant derived biomarkers support this assumption. Pr/Ph ratios suggest an upward decrease in oxygen availability. However, a positive correlation with CPI ($r^2 = 0.58$) indicates that Pr/Ph ratios may be influenced not only by redox conditions but also by the input of detrital land plants. Samples surrounding the “streaky limestones” (Jaslo Limestone), near the top of the sandstone-poor upper part, are characterized by relatively high DBT/Phen ratios, which suggests the presence of minor amounts of free H₂S in the water column. In addition, this interval is also characterized by the lowest recorded Pr/Ph ratios and MTTC ratios vary slightly, but are consistent with normal marine conditions.

Middle Menilite Member

The Upper Oligocene Middle Menilite Member was considered previously to be of Late Oligocene age and was not studied in detail; however, new nannoplankton data suggests an Early Miocene age (NN2) for this section. If the age dating and the stratigraphic position are correct, the Upper Oligocene succession is either missing or very thin at the locations studied. Nevertheless, organic matter for this section varies depending on the lithology, and TOC contents as well as HI values in the grey shales are lower (0.80-0.96 wt.% TOC; 77-135 mgHC/gTOC) compared to those observed in the black shales (3.19-8.80 wt.%; 311-360 mgHC/gTOC).

Upper Menilite Member

The Lower Miocene Upper Menilite Member, which makes up the upper section of the Menilite Formation, comprises an approximately 10 m thick chert horizon at its base, and a very thick (1300 m) overlying black shale succession with minor thin sandstone beds, which are interpreted to have been deposited in a basin-plain setting. Black shale accumulations were interrupted by a major volcanic event, which resulted in the deposition of a 70 m thick tuff interval in its upper part.

TOC contents for all samples are moderately high (2-7 wt.%), and reach a maximum near the base of the succession (up to 23 wt.%). Relatively low TOC contents (1-2 wt%) are observed in the samples near the transition to the Polyanytsa Formation towards the top of the section. This is also observed in the recorded HI values, which are typically around 400 mgHC/gTOC for all samples, and decrease near the top (200 to 300 mgHC/gTOC), due to lower contributions of algal material. Land-plant derived biomarkers occur in minor concentrations, although high amounts of oleanane in the uppermost sample indicates a higher contribution of angiosperm material. Diatoms occur sporadically, but concentrations of C₂₅ HBIs are low for all samples. Pr/Ph ratios in samples from the Upper Menilite Member are generally lower than in samples from the Lower Member, and infer strongly oxygen-deficient conditions. MTTC ratios suggest normal marine conditions with minor salinity variations and DBT/Phen ratios reach maximum values in the middle part of the succession, which probably suggests the presence of free H₂S.

As a result of the immense thickness as well as the moderately high TOC content, the Source Potential Index (SPI) for the Upper Member is significantly higher (57.9 tHC/m²) compared to the Lower Member (16.6 (tHC/ m²), despite a significantly higher average TOC Content.

4.2. Publication II: **Hydrocarbon potential of the Lower Cretaceous (Barremian-Albian) Shypot Formation in the Chornohora nappe, Ukraine.**

Lower Cretaceous rocks have long been regarded as a potential hydrocarbon source rock of the Ukrainian Outer Carpathians (Kruge et al., 1996). However, the only available study on the Shypot Formation (Barremian-Albian) in the Chornohora nappe by Koltun et al. (1998) failed to address the vertical variability of the source rock properties and did not conduct biomarker analysis. As a result, 94 rock samples were investigated within the frame of this study in order to determine the hydrocarbon potential of the Shypot Formation. The studied section comprised a 405 m thick succession near Bystrets, in the Chornohora Nappe.

The Formation comprises organic-rich shales, which are frequently interbedded with siltstones and sandstones. TOC content for these rocks exceeds 9 wt.% locally in the lower part of the succession and averages 2.83 wt.% for the entire section. Maceral analysis indicates high percentages in terrestrial organic matter (vitrinite: 34-60 vol.%; inertinite: 0-12 vol.%; sporinite: 15-34 vol.%) as well as moderate percentages of aquatic macerals (alginite: 18-32 vol.%), suggesting an oil to gas-prone type III (and II) kerogen. This is supported by very low HI values, which are encountered throughout the entire succession (average 88 mgHC/gTOC). Vitrinite reflectance measurements as well as T_{\max} values indicate peak oil window maturity (vitrinite reflectance: 0.82 %Rr; T_{\max} : 456°C). Lower Pr/Ph ratios (1.0-2.3) indicate an oxygen-deficient environment, with rare intervals <1.0 restricted to the lower part of the studied succession. This is also supported by high TOC/S ratios, which argue against strict anoxic conditions. Very low DBT/Phen ratios, partly due to lower DBT concentrations, indicate that free H₂S was not available in the water column, thus providing an additional argument against anoxic conditions. Oxygen-depleted conditions observed in the Shypot Formation may be related to the late Barremian to Albian global anoxic event (OAE 1; Schlanger and Jenkyns, 1976; Jenkyns, 1980).

According to the petroleum potential, the formation is considered to be a poor to good source rock, despite very high TOC contents. Due to the higher maturities, it is likely that hydrocarbons have already been generated, and the petroleum potential and the HI values can therefore not be considered as the original amount. As a result, the remaining SPI indicates that 1.8 tHC/ m² can be generated, whereas the original SPI, which is a rough estimate based on the marginal mature outcrop samples from previous data collected by Koltun et al. (1998) on the Shypot Formation in the Chornohora nappe, yields an SPI in the order of 4 tHC/m², implying that approximately 2 tHC/m² have already been generated.

4.3. Publication III: **Petroleum potential of Middle Jurassic rocks in the basement of the Carpathian Foredeep (Ukraine) and oil-to-source correlation with oil in Upper Jurassic reservoirs.**

Middle Jurassic succession

Middle Jurassic rocks are regarded as a potential source rock interval of the Ukrainian Carpathian Foredeep as they contain moderately high TOC contents (Kosakowski et al., 2012). However, data on these rocks are limited and further analysis was needed. As a result, 89 core samples representing Middle Jurassic strata, were studied from the Mosty-2 (2361 to 2560 m), Korolyn-6 (3418 and 3523 m) and Korolyn-2 (3642-3652; 3696-3712; 3870-3996 m) boreholes, in order to determine their petroleum potential. In general, Middle Jurassic rocks display very high organic-matter-content (average TOC: 4.19 wt.; max.: 14.98 wt.%) and are considered to be very good source rocks. However, the petroleum potential is fairly low, classifying these rocks only as fair source rocks, with only a few intervals containing good source rock potential. Thermal maturity of these rocks is mainly controlled by the present-day depth and strata in Mosty-2 are marginally mature, whereas sediments in Korolyn-6 and Korolyn-2 reach peak oil window maturity.

The organic matter is dominated by terrestrial macerals, resulting in low HI values (max: 242 mgHC/gTOC), and therefore classifying the organic matter primarily as a gas-prone type III kerogen (with rare intervals containing type II kerogen). As a result of the high terrestrial input, Pr/Ph ratios are often high (max: 2.84) as well. In addition, DBT/Phen ratios are generally low, suggesting that free H₂S was not available in the water column.

Upper Jurassic Oil-source correlation

To our knowledge, no attempt has been made to correlate oils from Upper Jurassic reservoirs in the Carpathian Foredeep with Middle Jurassic strata or age-equivalent rocks. As a result, two oil samples from the Orkhovychi well and one sample from the Kokhanivka borehole, both located close to the Polish-Ukrainian border, were studied for their genetic relationship with Middle and Upper Jurassic sediments in the Mesozoic basement of the Ukrainian Carpathian Foredeep. In addition, two oil samples (Lubaczow-157; Opaka-1) from the same oil family as the studied oils, located on Polish territory, are included for comparison studies and were previously studied by Curtis et al. (2004) and Wieclaw (2011).

The main arguments against a genetic link between the accumulated oils and Middle Jurassic rocks can be made using biomarker data. DBT/Phenanthrene ratios are very high for all the oil samples (>2.70) compared to the ratios observed in the analysed Middle Jurassic rocks (<0.50). In addition, differences in pristane/phytane ratios, which are typically high in the Middle Jurassic strata and low in the analysed oils, agree with this assumption. C_{27} - C_{28} - C_{29} sterane distributions, which infer a genetic relationship if data plot in close proximity, indicate different depositional environments for both the Middle Jurassic strata and the oils. This is also supported by compound specific isotope analysis (CSIA), which determined that there was no genetic link among the oil samples from the Upper Jurassic reservoirs and the Middle Jurassic rocks.

Since the analysed Middle Jurassic strata were not the source for these oils, an alternative source was investigated. Published biomarker data on organic-rich Upper Jurassic rocks by Kosakowski et al. (2012), was compared to the new data collected from the Orkhovychi and Kokhanivka oil fields. Considering their maturity, and the fact that the Upper Jurassic rocks are compatible with the high DBT/Phen ratios and display similar sterane distributions as detected in the oils, it was concluded that it is very likely that these rocks are the source for these oils.

4.4. List of contributions related to this thesis

Rauball, J., Sachsenhofer, R.F., Bechtel, A., Coric, S., Gratzner, R. (2017). Hydrocarbon Potential of the Menilite Formation in Western Ukraine (Poster Presentation). AAPG/SEG International Conference and Exhibition, London, UK.

Rauball, J., Sachsenhofer, R.F., Bechtel, A., Coric, S., Gratzner, R. (2019). Hydrocarbon Potential of the Oligocene – Lower Miocene Menilite Formation and the Cretaceous Shypot Formation in the Ukrainian Outer Carpathians (Poster Presentation). 78th EAGE Conference & Exhibition, Vienna, Austria.

Rauball, J., Sachsenhofer, R.F., Bechtel, A., Coric, S., Gratzner, R. (2019). The Oligocene-Miocene Menilite Formation in the Ukrainian Carpathians: A world-class source rock. *Journal of Petroleum Geology*, 42, 393-415.

Rauball, J., Sachsenhofer, R.F., Bechtel, A., (2020). Hydrocarbon potential of the Lower Cretaceous (Barremian-Albian) Shypot Formation in the Chornohora nappe, Ukraine. *Geologica Carpathica* (in press)

Rauball, J., Sachsenhofer, R.F., Bechtel, A., (2020). Petroleum potential of Middle Jurassic rocks in the basement of the Carpathian Foredeep (Ukraine) and oil-to-source correlation with oil in Upper Jurassic reservoirs. *Geologica Carpathica* (in press)

*The poster presentations are displayed in the Appendix VI.

5. General conclusion and outlook

Within the frame of this thesis, the petroleum generation properties of the most significant source rock intervals in the Ukrainian Carpathians as well as important aspects of their petroleum systems were discussed in detail, which may contribute to future exploration, particularly in the internal parts of the Outer Carpathians, where large areas remain relatively unexplored. The study investigates the importance of the Oligocene-Lower Miocene Menilite Formation, which contributes towards the majority of the petroleum accumulations in the Ukrainian Carpathians, and discusses the possibility of a potential Lower Cretaceous source rock, the Shypot Formation, which is generally ignored and overlooked in terms of its petroleum generation. To date, no Cretaceous-sourced oil and gas has been identified, even though the author of this thesis provides evidence that hydrocarbons have likely already been generated by the Shypot Formation.

The current study has answered many important questions. However, more data and investigations are needed, in particular in regards to the organic-rich Middle Jurassic succession, which has been ruled out as a potential source rock for Upper Jurassic oil accumulations in the Mesozoic basement of the Ukrainian Carpathians. As a result, organic-rich Upper Jurassic rocks are regarded as the likely source, but available data on this interval are extremely scarce and more data are needed to conduct a more accurate and thorough oil-source correlation. In addition, only recently, new data presented by Radkovets et al. (2016), on the petroleum accumulations from the south-eastern part of the Ukrainian foreland autochthon in the Lopushna oil field, where oil occurs in Upper Jurassic, Cretaceous and Paleogene reservoirs, have been published and correlated to the Menilite Formation, but uncertainty still remains.

Clearly, future work needs to focus on further oil to source correlations in the Ukrainian Carpathians, with a particular focus on unidentified potential source rocks such as the Lower Cretaceous Shypot Formation and the organic-rich Upper Jurassic succession. Many parts of the Ukrainian Carpathians are still unexplored and further exploration in these regions is not out of the question.

6. Reference

- Arthur, M., Cole, D., 2014. Unconventional Hydrocarbon Resources: Prospects and Problems. *Elements*, 4, 257-264.
- Andruleit, H., Babies, H.G., Cramer, B., Messner, J., Rempel, H., Schlömer, S., Schmidt, S., 2010. Nicht-konventionelles Erdgas: Weltweit Ressourcen und Entwicklungen eines „Hoffnungsträgers“ unter den fossilen Energierohstoffe. *Erdöl, Erdgas, Kohle*, 126, 277-282.
- Bechtel, A., Gratzer, R., Linzer, H., Sachsenhofer, R., 2013. Influence of migration distance, maturity and facies on the stable isotopic composition of alkanes and on carbonate distributions in oils and source rocks of the Alpine Foreland Basin of Austria. *Organic Geochemistry*, 62, 74-85
- Boote, D.R.D., Sachsenhofer, R.F., Tari, G., Arbouille, D., 2018. Petroleum provinces of the Paratethyan region. *Journal of Petroleum Geology*, 41, 247-298.
- Brice, W.R., Black, M., 2013. 150 Years of producing oil - McClintock Well Number 1 (1861-2011). *Oil-industry History*, 12, 155-158.
- Burchfiel B.C., Royden, L., 1982. Carpathian Foreland Fold and Thrust Belt and its Relation to Pannonian and other Basins. *AAPG Bulletin*, 66, 1179-1195.
- Chorowicz, J., 2016. Genesis of the Pieniny Klippen Belt in the Carpathians: Possible effects of a major paleotransform fault in the Neo-Tethyan domain. *Comptes Rendus Geoscience*, 348, 15-22.
- Chlupac, I., Brzobohaty, R., Kovanda, J., Stranik, Z., 2002. Geological History of the Czech Republic. Academia, Prague. (in Czech).
- Curiale, A.J., 1993. Oil to Source Rock Correlation. Concepts and Case Studies. *Organic Geochemistry*, 11, 473-490.
- Curtis, J., 2002. Fractured shale-gas systems. *American Association of Petroleum Geologists Bulletin*, 86, 1921-1938.
- Curtis, J., Kotarba, M.J., Lewan, M.D., Wiêclaw, D., 2004. Oil/source rock correlations in the Polish Flysch Carpathians and Mesozoic basement and organic facies of the Oligocene Menilite Shales: insights from hydrous pyrolysis experiments. *Organic Geochemistry*, 35, 1573–1596.
- Duchesne, J.C., Iancu, V., Tatu, M., Liegeois, J.P., Berza, T., Matukov, D.I., Sergeev, A.S., 2007. Post-collisional melting of crustal sources: constraints from geochronology, petrology and Sr, Nd isotope geochemistry of the Variscan Sichevita and Poniasca granitoid plutons (South Carpathians, Romania). *International Journal of Earth Sciences*, 97, 705-723.
- Golonka, J., Krobicki, A., Waskowska, M., 2015. Olistostromes of the Pieniny Klippen Belt, northern Carpathians. *Geol. Mag.*, 152, 269-286.
- Glushko, V.V., 1968. Tektonika i neftegazonosnost Karpatiprile-gayuschikh progibov. (In Russian). Nedra, Moscow, 264.
- Hrušecký, I., Plašienka, D., Pospíšil, L., 2006. Identification of the North European Platform below the Eastern Part of the Western Carpathian Flysch Belt. In: Golonka, J. and Picha, F.J. (Eds), *The Carpathians and their foreland: Geology and hydrocarbon resources*. American Association of Petroleum Geologists, 84, 717-728.

- Iancu, V., Berza, T., Seghedi, A., Gheuca, I., Hann, H.P., 2005. Alpine polyphase tectono-metamorphic evolution of the South Carpathians: a new overview. *Tectonophysics*, 410, 337-365.
- Jenkyns, H.C., 1980. Cretaceous anoxic events: from continents to oceans. *Journal Geological Society London*, 137, 171-188.
- Jia, C., Zheng, M., Zhang, Y., 2016. Some key issues on the unconventional petroleum systems. *Petroleum Research*, 1, 113-122.
- Karnkowski, P., 1999. Oil and gas deposits in Poland. The Geosynoptics Society "Geos" and University of Mining and Metallurgy, Krakow, 380.
- Koltun, Y.V., 1992. Organic matter in Oligocene Menilite formation rocks of the Ukrainian Carpathians: palaeoenvironment and geochemical evolution. *Organic Geochemistry*, 18, 423-430.
- Koltun, Y.V., Espitalie, J., Kotarba, M., Roure, F., Ellouz, N., Kosakowski, P., 1998. Petroleum Generation in the Ukrainian External Carpathians and the adjacent Foreland. *Journal of Petroleum Geology*, 21, 265-288.
- Kosakowski, P., Wieclaw, D., Kowalski, A., Koltun, Y., 2012. Assessment of hydrocarbon potential of Jurassic and Cretaceous source rocks in the Tarnograd-Stryi area (SE Poland and W Ukraine). *Geologica Carpathica*, 63, 319-333.
- Kosakowski, P., Koltun, Y., Machowski, G., Poprawa, P., Papiernik, B., 2018. Geochemical characterization of the Oligocene Menilite Formation in the Polish and Ukrainian Carpathians. *Journal of Petroleum Geology*, 41, 319-336.
- Köster, J., Kotarba, M., Lafargue, E., Kosakowski, P., 1998. Source rock habitat and hydrocarbon potential of Oligocene Menilite Formation (Flysch Carpathians, Southeast Poland): An organic geochemical and isotope approach. *Organic Geochemistry*, 29, 543-558.
- Kotarba, M.J., Koltun, Y.V., 2006. The origin and habitat of hydrocarbons of the Polish and Ukrainian parts of the Carpathian Province. In: Golonka, J. and Picha, F.J. (Eds.), *The Carpathians and their foreland: Geology and hydrocarbon resources*, 84, 395-442.
- Kotarba, M.J., Koltun, Y.V., 2011. Origin of natural gas in the autochthonous Miocene strata of the Ukrainian Carpathian Foredeep and its Mesozoic basement. *Annales Societatis Geologorum Poloniae*, 81, 425-441.
- Kotarba, M. J., Nagao, K., 2008. Composition and origin of natural gases accumulated in the Polish and Ukrainian parts of the Carpathian region: Gaseous hydrocarbons, noble gases, carbon dioxide and nitrogen. *Chemical Geology*, 255, 426-438.
- Kotarba, M., Wieclaw, D., Koltun, Y., Marynowski, L., Kusmierk, J., Dudok, I., 2007. Organic geochemical study and genetic correlation of natural gas, oil and Menilite source rocks in the area between San and Stryi rivers (Polish and Ukrainian Carpathians). *Organic Geochemistry*, 38, 1431-1456.
- Kotarba, M., Więclaw, D., Radkovets, N.Y., Koltun, Y.V., Kmieciak, N., Romanowski, T., Kowalski, A., 2019. Origin and migration of oil and natural gas in the western part of the Ukrainian Outer Carpathians: Geochemical and geological approach. *Marine and Petroleum Geology*, 103, 596-619.
- Kovac, M., Hudackova, N., Halasova, E., Kovacova, M., Holcova, K., Oszczytko-Clowes, M., Baldi, K., Less, G., Nagymarosy, A., Ruman, A., Kluciar, T., Jamrich, M., 2017.

- The Central Paratethys palaeoceanography: a water circulation model based on microfossil proxies, climate, and changes of depositional environment. *Acta Geologica Slovaca*, 9, 75-114.
- Krajewski, M., Król, K., Olszewska, B., Felisiak, I., Skwarczek, M., 2011. Facies of the Upper Jurassic–Lower Cretaceous sediments at the basement of the Carpathian Foredeep (western Ukraine). *Annales Societatis Geologorum Poloniae*, 81, 291-307.
- Kruger, M.A., Mastalerz, Maria, Solecki, Andrzej, Stankiewicz, B.A., 1996, Organic geochemistry and petrology of oil source rocks, Carpathian Overthrust region, southeastern Poland—Implications for petroleum generation: *Organic Geochemistry*, 24, 897-912.
- Kruglov, S.S., Smirnov, S.E., Spitkovskaya, S.M., Flishtynski, L.E., Hizhniakov, A.V., 1985. Geodynamics of the Carpathians (in Russian). *Nauka dumka*, 135.
- Kurovets, I., Prytulka, H., Shyra, A., Shuflyak, Y., Peryt, T.M., 2011. Petrophysical properties of pre-Miocene rocks of the outer zone of the Ukrainian Carpathian Foredeep. *Annales Societatis Geologorum Poloniae*, 81, 363-373.
- Kuznetsov, I.A., 1963. Geology of Coal and Oil Shale Deposits of the USSR. In: I.A. Kuznetsov (Ed.), *Coal Basins and Deposits in the Southern European Part of the USSR*, 1 -1170-1210.
- Magoon, L.B., Dow, W.G., 1994. The Petroleum System. In Magoon, L.B., Dow, W.G (Eds.), *The Petroleum System - from source to trap*. AAPG Memoir 60, 3-24.
- Masselnitz M., Cochran, J., English, C., Burger, B., 2013. Fingerprinting Crude Oils and Tarballs using Biomarkers and Comprehensive two-dimensional gas Chromatography. *Environmental Applications*, 4, 135-142.
- Miclaus, C., Loiacono, F., Moretti, E., Puglisi, D., Koltun, Y., 2007. A petro-sedimentary record of Eocene-Oligocene Palaeogeographic changes connected with the separation of the central Paratethys (Romanian and Ukrainian Carpathians). *Bulletin of the Tethys Geological Society*, 2, 117-126.
- Misch, D., Sachsenhofer, R.F., Bechtel, A, Gratzner, R., Gross, D., Makogon, V., 2015. Oil/gas-source rock correlations in the Dniepr-Donets Basin (Ukraine): New insights into the petroleum system. *Marine and Petroleum Geology*, 67, 720-742.
- Misch, D., Gross, D., Mahlstedt, N., Makogon, V., Sachsenhofer, R. (2016): Shale gas/shale oil potential of Upper Viséan Black Shales in the Dniepr-Donets Basin (Ukraine). - *Marine and Petroleum Geology*, 75, 203-219.
- Moore, T., 2012. Coalbed methane: a review. *International Journal of Coal Geology*, 101, 36-81.
- Naftogaz Group, 2020. History of oil and gas industry. Retrieved April 26, 2020 from: <http://www.naftogaz.com/www/3/nakweben.nsf/0/69CDD708EEFC16B4C22570D8003432CC>
- Nakapelukh, M., Bubniak, I., Yegorova, T., Murovskaya, A., Gintov, O., Shlapinski, V., Vikhot, Y., 2017. Balanced geological cross-section of the Outer Ukrainian carpathians along the pancake profile. *Journal of Geodynamics*, 108, 13-25.
- Nakapelyukh, M., Bubniak, I., Bubniak, A., Jonckheere, R., Ratschbacher, L., 2018, Cenozoic structural evolution, thermal history, and erosion of the Ukrainian Carpathians fold-thrust belt. *Tectonophysics*, 722, 197-209.

- Oszczypko, N., 2006. Late Jurassic-Miocene evolution of the Outer Carpathian fold-and-thrust belt and its foredeep basin (Western Carpathians, Poland). *Geological Quarterly*, 50, 169-194.
- Pavlyuk, M.I., Liashevych, Z.M., Medvedev, A.P., 2013. Ukrainian Carpathians in the structure of pancardi (magmatism and geodynamics). *Geodynamics*, 14, 45-60.
- Peters, K.E., Walter, C.C., Moldowan, J.M., 2005. *The Biomarker Guide: Biomarkers and Isotopes in the Environment and Human History*. Cambridge University Press, 2, 700
- Plasienska, D., Grecula, P., Putis, M., Kovac, M., Hovorka, D., 1997. Evolution and structure of the Western Carpathians: an overview. In: Grecula, P., Hovorka, D., Puns, M., (Eds.), *Geological Evolution of the Western Carpathians*. Monograph, Mineralia Solvaca, 2, 1-24.
- Popov, S.V., Rögl, F., Raznov, A.Y., Steininger, F.F., Shcherba, I.G., Kovac, M., 2004. Lithological Paleogeographic maps of Paratethys. *Courier Forschungsinstitut Senckenberg*, 250, 340-348.
- Radkovets, N.Y., Kotarba, M., Koltun, Y., Kowalski, A., Kosakowski, P., Więclaw, D., 2016. Origin and migration of oil from the Ukrainian Outer Carpathians to their Mesozoic basement: a case of Lopushna traps. *Geological Quarterly*, 60, 133-148.
- Radkovets, N.Y., Rauball, J., Iarechuk, I., 2017. Silurian black shales of Western Ukraine: petrography and mineralogy. *Estonian Journal of Earth Sciences*, 66, 161-173.
- Roure, F., Roca, E., Sassi, W., 1993. The Neogene evolution of the Outer Carpathian flysch units (Poland, Ukraine and Romania): kinematics of a foreland/fold-and-thrust belt system. *Sedimentary Geology*, 86, 177-201.
- Sachsenhofer, R.F., Koltun, Y., 2012. Black shales in Ukraine – A review. *Marine and Petroleum Geology*, 31, 125-136.
- Sachsenhofer, R.F., Popov, S.V., Bechtel, A., Coric, S., Francu, J., Gratzner, R., Grunert, P., Kotarba, M., Mayer, J., Pupp, M., Ruprecht, B.J., Vincent, S.J., 2018a. Oligocene and Lower Miocene source rocks in the Paratethys: Palaeogeographical and stratigraphic controls. In: Simmons, M. (Ed): *Geological Society London Special Publication*, 464, 267-306.
- Sachsenhofer, R.F., Popov, S.V., Coric, S., Mayer, J., Misch, D., Morton, M.T., Pupp, M., Rauball, J., Tari, G., 2018b. Paratethyan petroleum source rocks: an overview. *Journal of Petroleum Geology*, 41, 219-245.
- Sandulescu, M., 1988. Cenozoic tectonic history of the Carpathians. In: Royden, L. and Hovarth, F. (Eds.), *The Pannonian Basin: a study in basin evolution*. AAPG Memoir, 45, 17-25.
- Sandulescu, M., Dimitrescu, R., 2004. Geological structure of the Romanian Carpathians. *International Geological Congress*, 1, 1-15.
- Schlanger, S.O., Jenkyns, H.C., 1976. Cretaceous oceanic anoxic events: causes and consequences. *Geologie en Mijnb.*, 55, 179-184.
- Shlapinskyi, V., 2015. *The Geological Architecture of the Skyba, Krosno, Duklya-Chornogora Nappes of the Ukrainian Carpathians and Prospects of Oil and Gas* (in Ukrainian; unpublished doctoral thesis). Institute of Geology and Geochemistry of Combustible Minerals, Lviv.

- Schulz, H.M., Bechtel, A., Sachsenhofer R.F., 2005. The birth of the Paratethys during the early Oligocene: from Tethys to an ancient Black Sea analogue? *Global and Planetary Change*, 49, 163-176.
- Schulz, H.M., Horsefield, B., Sachsenhofer, R.F., 2010. Shale gas in Europe: a regional overview and current research activities. In: Vining, B.A. and Pickering, S.C. (Eds.), *Petroleum Geology: From Mature Basins to New Frontiers-Proceedings of the 7th Petroleum Geology Conference*. Geological Society, London, 7, 1079-1085.
- Slaczka, A., Kruglov, S., Golonka, J., Oszczytko, N., Popadyuk, I., 2006. *Geology and Hydrocarbon Resources of the Outer Carpathians, Poland, Slovakia, and Ukraine: General Geology. The Carpathians and Their Foreland: Geology and Hydrocarbon Researches: AAPG Memoir*, 84, 221-258.
- Symington, W.A., Kaminsky, R.D., Meurer, W.P., Otten, G.A., T.C., Thomas, M.M., Yeakel, J.D., 2010. ExxonMobil's Electrofrac Process for In Situ Oil Shale Conversion. *American Chemical Society*, 10, 185-216.
- Tari, G., 2010. Exploration Country Focus: Ukraine. In: *AAPG European Region Newsletter*, 5, 4-6.
- Taylor, G.H., Teichmüller, M., Davis, A., Diessel, C.F.K., Littke, R., Robert, P., 1998. *Organic Petrology*. Gebrüder Bontaege, Berlin, 655-704.
- Van de Graaf, T., Colgan, J., 2016. Global energy governance: a review and research agenda. *Palgrave Communications*, 2, 15-47.
- Vassiliou, M., 2018. *Historical Dictionary of the Petroleum Industry*. Lanham MD: Rowman and Littlefield-Scarecrow Press, 2, 599-621.
- Vetö, I., 1987. An Oligocene sink for organic carbon: Upwelling in the Paratethys? *Palaeogeography, Palaeoclimatology, Palaeoecology*, 60, 143-153.
- Vogel, H.U., 1993. Great Well of China. *Scientific American*, 268, 116-121.
- Vul, M.Y., Denega, B.I., Krupsky, Y.Z., Nimets, M.V., Svyry-denko, V.G., Fedyshyn, V.O., 1998. Western oil and gas-bearing region. In: Ivanyuta, M.M. and Fedyshyn, V.O., (Eds.), *Atlas of oil and gas fields of Ukraine in six volumes*. Ukrainian Oil and Gas Academy, 4, 328-333.
- Wiêclaw, D., 2011. Origin of Liquid Hydrocarbons accumulated in the Miocene strata of the Polish Carpathian Foredeep and its Palaeozoic-Mesozoic Basement. *Annales Societatis Geologorum Poloniae*, 81, 443-458.
- Zou, C., Zhai, G., Zhang, G., 2015. Formation, distribution, potential and prediction of global conventional and unconventional hydrocarbon resources. *Petrol Exploration Dev.*, 42, 13-25.

Journal Publications

The Menilite Formation in the Ukrainian Carpathians – a world-class source rock

J. F. Rauball^{a,*}, R. F. Sachsenhofer^a, A. BechtelZ, S. Coric^b, R. Gratzner^a

^a Chair of Petroleum Geology, Montanuniversitaet Leoben, 8700 Leoben, Austria.

^b Geological Survey of Austria, Neulinggasse 38, 1030 Vienna, Austria.

Published in:

Journal of Petroleum Geology 42 (2019), 393-416

doi: [10.1111/jpg.12743](https://doi.org/10.1111/jpg.12743)

* Corresponding author. johannes.rauball@gmail.com

Address: Chair of Petroleum Geology, Montanuniversitaet Leoben, Peter-Tuner Straße 5, A-8700 Leoben

Key words: Menilite Formation, source rocks, hydrocarbons, Oligocene, Miocene, Ukrainian Carpathians, Chechva River, organic geochemistry, biomarkers, maturity.

Research Highlights:

The Menilite Formation contains rocks with excellent source rock potential

The total Source Potential Index for the Menilite Formation is 75 tHC/m²

Organic matter is thermally immature

Organic matter dominated by oil-prone Type II kerogen

Abstract

This study investigates the hydrocarbon potential of Oligocene–Miocene shales in the Menilite Formation, the main source rock in the Ukrainian Carpathians. The study is based on the analysis of 233 samples collected from outcrops along the Chechva River in western Ukraine in order to analyse bulk parameters (TOC, Rock-Eval), biomarkers and maceral composition.

In Ukraine, the Menilite Formation is conventionally divided into Lower (Lower Oligocene), Middle (Upper Oligocene) and Upper (Lower Miocene) Members. The Early Oligocene and Early Miocene ages of the lower and upper members are confirmed by new nannoplankton data. The Lower Menilite Member is approximately 330 m thick in the study area and contains numerous chert beds and turbidite sandstones in its lower part together with organic-rich black shales. The shales have a high content of silica which was probably derived from siliceous micro-organisms. The TOC content of the shales frequently exceeds 20 wt.% and averages 9.76 wt.%. HI values range between 600 and 300 mgHC/gTOC (max. 800 mgHC/gTOC). The Middle Member contains thin black shale intervals but was not studied in detail. The Upper Member is about 1300 m thick in the study area and is composed mainly of organic-rich shales. Chert layers are present near the base of the Member, and a prominent tuff horizon in the upper part represents a volcanic phase during shale deposition. The member grades into overlying molasse sediments. The average TOC content of the Upper Menilite succession is 5.17 wt.% but exceeds 20 wt.% near its base.

Low T_{\max} and vitrinite reflectance measurements for the Lower (419°C and 0.24–0.34 %Rr, respectively) and Upper (425°C and 0.26–0.32 %Rr, respectively) Menilite Member successions indicate thermal immaturity. Biomarker and maceral data suggest a dominantly marine (Type II) organic matter input mixed with varying amounts of land-plant derived material, and indicate varying redox and salinity conditions during deposition.

Determination of the Source Potential Index (SPI) shows that the Menilite Formation in the study area has the potential to generate up to 74.5 tons of hydrocarbons per m². The Chechva River outcrops therefore appear to have a significantly higher generation potential than other source rocks in the Paratethys realm. These very high SPI values for the Menilite Formation may explain why a relatively small area in Ukraine hosts about 70% of the known hydrocarbon reserves in the northern and eastern Carpathian fold-thrust belt.

Table of Content

1. Introduction	47
2. Geological setting	49
3. Petroleum Systems	51
4. Samples and Methods	52
5. Results	55
5.1. Lithology and Stratigraphy	55
5.2. Bulk parameters of organic matter and maceral composition	60
5.3. Molecular composition of sample extracts.....	63
6. Discussion	72
6.1. Maturity.....	72
6.2. Stratigraphy.....	73
6.3. Depositional environments.....	74
6.4. Source rock potential.....	79
7. Conclusion	82
8. References	84

1. Introduction

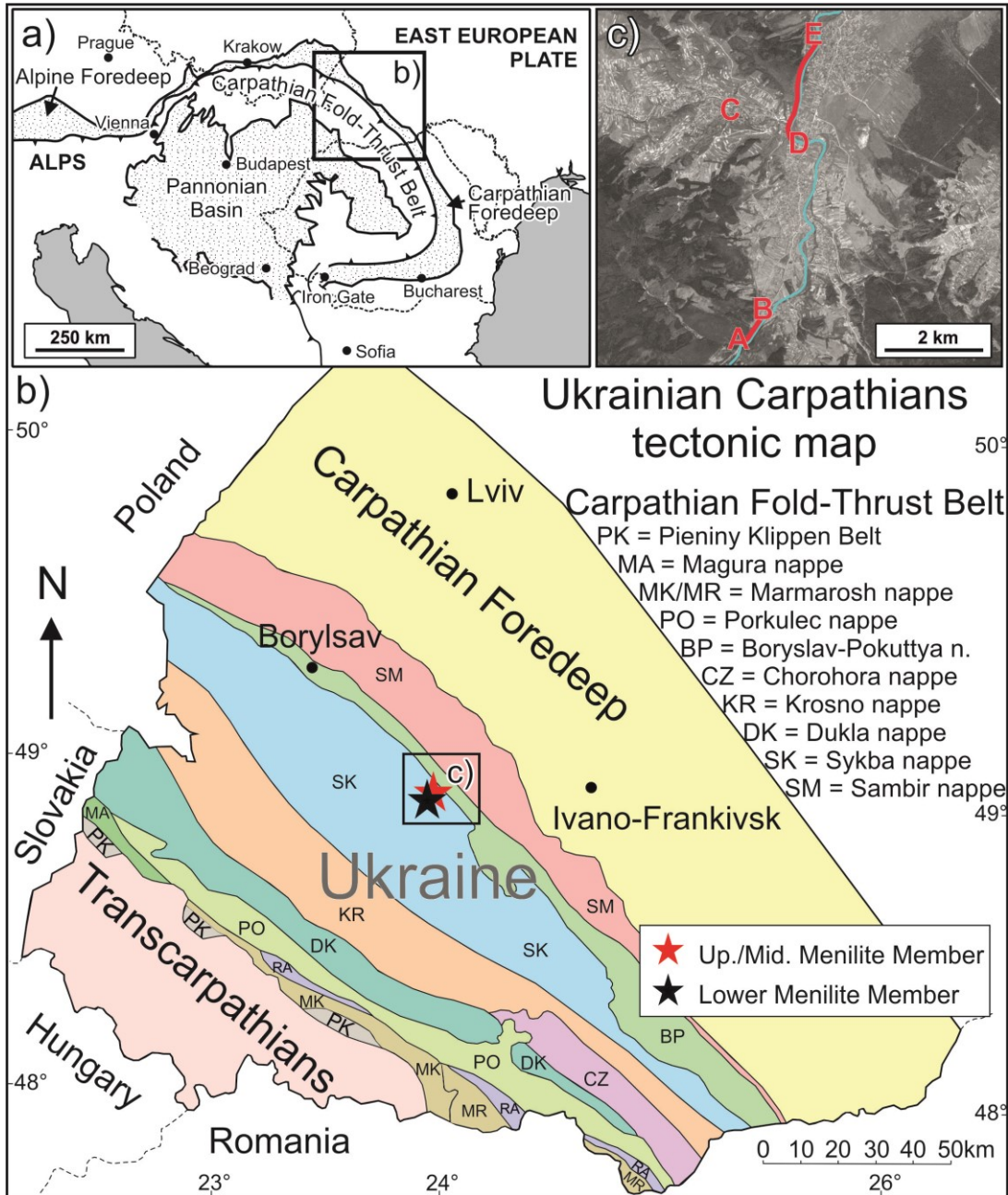


Fig. 1. (a) Outline map of central-eastern Europe showing the location of the study area in the western Ukrainian segment of the Carpathian fold-thrust belt. (b) Structural map of the Ukrainian Carpathians (after Slaczka et al., 2006; Radkovets et al., 2017) showing the sample locations in the Skyba nappe, about 50 km west of the town of Ivano-Frankivsk (red and black stars). (c) Samples of the Lower (A-B), Middle (C) and Upper (D-E) Members of the Menilite Formation were collected from locations along the Chechva River.

The Ukrainian Carpathians are one of the oldest petroleum-producing provinces in the world (Boote et al., 2018). Petroleum production began in 1854 with the discovery of the Boryslav oil field, one of the largest onshore oilfields in Europe (Kotarba et al., 2007). The Lower Oligocene – Lower Miocene Menilite Formation is the primary source rock interval in this region (Köster et al., 1998; Kotarba et al., 2006; 2007; Kosakowski et al., 2018). Age-equivalent “Maikopian” source rocks are important elsewhere in the Paratethys realm including the Alpine Foreland Basin, Caucasus foredeep, Kura Basin and South Caspian Basin (Sachsenhofer et al., 2018a, 2018b).

The Ukrainian Carpathians form the NE part of the Alpine–Carpathian orogenic belt which stretches for approximately 1300 km from Vienna to the Iron Gate on the River Danube in Romania (Slaczka et al., 2006) (Fig. 1a). The study area in western Ukraine is located within the Outer Carpathians which consists of a series of structurally complex, NE-verging nappes (Fig. 1b). The nappes are composed of rocks which range in age from Early Cretaceous to Early Miocene (Slaczka et al., 2006). The Outer Carpathians are bordered to the NE by a molasses-filled foredeep and to the SW by the Pienniny Klippen belt (Kotarba et al., 2007).

The Ukrainian Outer Carpathians are a mature oil-producing province, and the source rock potential of the Menilite Formation has been investigated in detail in previous studies (Koltun, 1992; Krüge et al., 1996; Koltun et al., 1998; Köster et al., 1998). However large areas remain relatively unexplored, particularly in internal parts of the foldbelt. An improved understanding of the petroleum generation properties of the Menilite shales and of the petroleum system may contribute to future exploration in this area. Therefore, the primary objective of this study was to investigate the source rock potential of the Menilite shales in the study area and to interpret the shales’ depositional environment.

2. Geological setting

The Outer Carpathians comprise a series of nappes which were thrust NE-ward during Early Miocene tectonism onto the SW margin of the East European Plate (Fig. 1b). In Ukraine, the following thrust sheets are distinguished from NE (i.e. the most external part of the thrust belt) to the SW (most internal): Sambir, Boryslav-Pokuttya, Skyba, Krosno, Chornohora, Dukla, Porkulec and Marmarosh (Kotarba et al., 2008). The Sambir and Boryslav-Pokuttya nappes include molasse sediments and are considered as part of the Carpathian Foredeep. The Boryslav-Pokuttya nappe includes flysch sediments similar to those typically found within the Skyba nappe. The Skyba nappe extends from Poland (where it is referred to as the Skole nappe) into Romania (= Tarcau nappe) and is composed of six tectonic slices which are referred to as sub-nappes (Slaczka et al., 2006).

Unit		External part of Skyba nappe
Stratigraphy		Lithostratigraphy
Neogene	Miocene	Polyanitsa Fm. Upper Menilite
	Paleogene	Oligocene
Lower Menilite		
Kliwa ss		
Eocene		Low. Menilite chert
		Globigerina marls
Paleocene	Popel marls	
	Green shales	
	Variegated sh.	
Cretaceous	Upper	Vygoda ss
		Green shales
	Lower	Yamna ss
		Variegated shales
		Stryi beds
Upper	Variegated shales	
	Silicious marls	
Lower	Spas ss	
	Spas shales	

Fig. 2. Stratigraphic column of the Cretaceous to Miocene succession in the external part of the Skyba nappe in western Ukraine (after Kotarba and Koltun, 2006).

Flysch-type sediments in the Outer Carpathians range from Early Cretaceous to Early Miocene in age (Fig. 2) and may locally be more than 6 km thick (Slaczka et al., 2006). In the Outer Carpathians, the Menilite Formation is dominated by organic-rich shales which were deposited in oxygen-depleted marine conditions during partial isolation of the Paratethys (including the Carpathian basins) from the Mediterranean and the World ocean during Oligocene time (Popov et al., 2004). Basin isolation was a result of both tectonic deformation during the Alpine Orogeny and a fall in eustatic sea level (Schulz et al., 2005). The upper boundary of the Menilite Formation is diachronous (NP24–NN3) and is marked by a change to flysch- (“Krosno type”) or molasse-type deposits (e.g. Svabenicka et al., 2007; Kusmierik et al., 2013).

The Menilite Formation is present in most of the nappes in Ukraine but only continues up into the Lower Miocene in the Boryslav-Pokuttya nappe and the external part of the Sykba nappe (see Fig. 2). Samples for this study were collected from the outer part of the Skyba nappe (Fig. 1b) where the Menilite Formation reaches its maximum thickness (Slaczka et al., 2006).

In Ukraine, the Menilite Formation is divided into Lower, Middle and Upper Menilite Members (Andreyeva-Grigorovich et al., 1986). The Lower Oligocene Lower Menilite Member consists primarily of organic-rich black shales and thick turbidite sandstones. The base of the formation corresponds roughly to the Eocene – Oligocene boundary and is marked by the presence of chert intervals. Coccolith limestones (approximately 10 cm thick) are used as stratigraphic markers (Haczewski, 1989). The member ranges in thickness from 250 m to 500 m in the Ukrainian Outer Carpathians (Kotarba et al., 2012).

The Middle Menilite Member is considered to be Late Oligocene in age (Andreyeva-Grigorovich and Gruzman, 1994). The type section in the Spas area, west of Ivano-Frankivsk (Fig. 1b), was described in detail by Vialov et al. (1988). According to these authors, the lower 50 m of the 135 m thick succession are dominated by grey, carbonaceous mudstones but contain intercalations of thin (5-20 cm), black, laminated, carbonate-free mudstones. Rare silty mudstones and thin sandstones intervals (2-25 cm) occur. The upper part consists of intercalations of grey carbonaceous mudstones and fine- to medium-grained sandstones. In the uppermost part, intercalations of black and grey mudstones (4-20 cm) occur together with 0.8-2.5 m thick sandstones. The Middle Menilite Member is generally thought to be poor in organic material (Andreyeva-Grigorovich et al., 1986).

The Upper Menilite Member is primarily composed of organic-rich shales and may reach thicknesses exceeding 1000 m (Andreyeva-Grigorovich et al., 1986). A chert horizon at its base is used to mark the boundary between with the Middle Member, and a prominent tuff interval in the upper part of the succession is also used as a marker. The top of the member transitions into the organic-lean shales and grey molasse sandstones of the Early Miocene (NN23) Polyanitsa Formation, which is up to 600 m thick (Andreyeva-Grigorovich et al., 1997). The Menilite Formation is exposed at the surface within the Boryslav-Pokuttya nappe and the Skyba nappe. Due to the structural complexity of the Outer Carpathians, deep boreholes may penetrate the formation multiple times in the subsurface due to thrust repetition. Although structures become less complex in the more internal units of the Outer Carpathians, the Menilite Formation occurs here at widely-varying depths due to nappe superposition (Kotarba et al., 2008).

3. Petroleum Systems

Two organic-rich intervals are found within the Ukrainian Outer Carpathians: the Lower Cretaceous Shypot and Spas Formations, and the Oligocene-Lower Miocene Menilite Formation (Sachsenhofer and Koltun, 2012). Both formations have a basin-wide extent with significant source rock potential; however, the Menilite Formation is considered to be the primary source rock in the region (Kotarba and Koltun, 2006; Kotarba et al., 2019). The petroleum potential of the Menilite Formation in general decreases from outer (external) to inner (internal) units in the fold-thrust belt (Kotarba et al., 2007).

The Boryslav-Pokuttya petroleum system (sensu Boote et al., 2018) is located within the frontal part of the flysch belt (Fig. 1b) which is the main oil-bearing area in the Ukrainian Carpathians. The area hosts more than forty oil and condensate accumulations with total recoverable reserves estimated at 2249 MM boe (Boote et al., 2018). Structural traps consist of stacked duplexes; Paleogene and Miocene deep-water reservoir sandstones are sealed by the overlying Miocene molasse (Kotarba and Koltun, 2006).

The Skole-Skyba and Silesian-Krosno petroleum systems extend from Poland into western Ukraine. However, with estimated total recoverable reserves of only 200 MMboe (Boote et al., 2018), these systems are economically less important than the Boryslav-Pokuttya petroleum system. More than 80 relatively small oil and gas fields (most of them located in Poland) are hosted by Upper Cretaceous – Paleocene, Eocene and Oligocene sandstones within complex, faulted antiformal structures.

4. Samples and Methods

For this study, samples of the Menilite Formation were collected from outcrops near the village of Spas, about 50 km west of Ivano-Frankivsk (Fig. 1b). All sampled sites are located in the outer part of the Skyba nappe. In total, 233 samples were collected: 153 samples of the Lower Menilite Member from a profile location to the SW of Spas in the Oriv sub-nappe (base of section: 48°51'27"N, 24°02'50"E); six samples of the Middle Menilite Member from a location to the west of Spas (48°54'17"N, 24°02'23"E); and 74 samples of the Upper Menilite Member, which includes four samples of the overlying Polyanitsa Formation, from a location to the north of Spas (base of section: 48°54'00"N, 24°03'33"E). The Middle and Upper Menilite Member are from the Berehova sub-nappe. The Lower and Upper Menilite Member were sampled along the banks of the Chechva River, whereas samples from the Middle Menilite Member were collected from a small tributary to the west (Fig. 1c). Together the three outcrops form the Chechva profile of previous studies (Andreyeva-Grigorovich et al., 1986). In addition, two samples which were of Eocene age were collected from the banks of the River Chechva from locations stratigraphically underlying the Lower Menilite Member outcrop.

All the samples were cleaned, dried and pulverized before laboratory analyses were performed. The samples were then analysed for their total carbon (TC), total sulphur (TS) and total organic carbon content (TOC) using an ELTRA Elemental Analyser. Samples measured for TOC were treated twice with 50% phosphoric acid to remove inorganic carbon. Results are based on the averages of at least two corresponding measurements and are given in weight percent (wt.%). The total inorganic carbon (TIC) was determined by subtracting the TC with the TOC. TIC was then used to calculate the calcite equivalent percentages ($= \text{TIC} \cdot 8.333$).

Rock-Eval pyrolysis was carried out using a RockEval 6 analyser in order to determine the S_1 , S_2 (mg HC/g rock) and T_{max} for all samples. S_1 determines the amount of hydrocarbons present in the rock, and S_2 the amount of hydrocarbons formed during pyrolysis. The petroleum potential ($S_1 + S_2$; mg HC/g rock) and the hydrogen index ($\text{HI} = S_2 / \text{TOC} \cdot 100$; HC/g TOC) were calculated using the S_1 and S_2 measurements. T_{max} is a maturity parameter and indicates the temperature during Rock-Eval pyrolysis at which the maximum amount of hydrocarbons can be generated (Espitalié et al., 1984). S_1 , S_2 and T_{max} results were based on at least two measurements.

Based on the HI and TOC results, a total of 36 samples were selected at similarly spaced intervals across the Lower and Upper Menilite Member successions for biomarker analyses. Samples were extracted in a Dionex ASE 200 accelerated solvent extractor using dichloromethane at 75° C and 50 bar for approximately 1 hour. Asphaltenes were precipitated from the solution using a hexane – dichloromethane solution (80:1) and then separated by centrifugation. The hexane-soluble fractions were separated into NSO compounds, saturated hydrocarbons and aromatic hydrocarbons using medium pressure liquid chromatography (MPLC) with a Köhnen-Willsch instrument (Radke et al., 1980). The saturated and aromatic hydrocarbon fractions were analysed by a gas chromatograph equipped with a 30 m DB-5MS fused silica column (i.d. 0.25 mm; 0.25 mm film thickness), coupled to a ThermoFischer ISQ Dual-quadrupole mass spectrometer. Using helium as the carrier gas, the oven temperature was set to increase from 70 °C to 300 °C at 4° C min⁻¹, which was followed by an isothermal period of 15 min. With the injector temperature set to 275 °C, the sample was then injected with a split ratio of 10. The spectrometer was operated in EI (electron ionization) mode over a scan range from m/z 50 to 650 (0.7 s total scan time). Data was processed using an Xcalibur data system where individual compounds were identified on the basis of retention time in the total ion current (TIC) chromatogram and by comparison of the mass spectra with published data. Percentages and absolute concentrations of various compound groups in the saturated and aromatic hydrocarbon fractions were calculated using peak areas from the gas chromatograms and their relations to the internal standards (deuterated *n*-tetracosane and 1,1'-binaphthyl, respectively). Concentrations were normalized to TOC.

Stable carbon and oxygen isotope ratios of carbonate phases were measured. The powdered samples were treated with 100 % H₃PO₄ at 70 °C in an online system (Gasbench II) and the released CO₂ analyzed by a ThermoFisher DELTA-V ir-MS. The values were normalized to the V-PDB standard for both δ¹³C and δ¹⁸O and have a standard deviation of 0.8 ‰ for δ¹³C and 0.1 ‰ for δ¹⁸O.

A total of 33 polished blocks (24 Lower Oligocene and nine Lower Miocene samples) were prepared for semi-quantitative maceral analysis and vitrinite reflectance (% Rr) measurements. Maceral composition was determined using white light and fluorescence light. Vitrinite reflectance measurements were determined using a Leica microscope and following established procedures (Taylor et al., 1998).

Smear slides for the study of calcareous nannofossils were prepared for selected samples using standard procedures described by Perch-Nielsen (1985) and were examined under a light microscope LEICA DMLP (cross and parallel nicols) with 1000x magnification. For biostratigraphic attribution, the nannofossil zonation of Martini (1971) was applied. In total, 71 samples from the Lower and Upper Menilite Members were investigated for the nannofossil biostratigraphy.

Diatoms were detected in several samples. In order to quantify the amount of biogenic silica, 12 samples were treated using a modified version of the process described by Zolitschka (1988). However, because none of the samples yielded statistically relevant concentrations, the results of this technique are not discussed in the present paper.

The study of calcareous nannofossils was conducted in the Geological Survey of Austria (GBA) in Vienna, whereas the remaining research was performed in the laboratories at Montanuniversitaet Leoben, Austria.

5. Results

5.1. Lithology and Stratigraphy

1. Lower Menilite Member

The Lower Oligocene Lower Menilite Member in general consists of alternating organic-rich black shales and thick turbidite sandstones which typically dip at an angle of about 80° throughout the entire Chechva River profile. The member is approximately 330 m thick in this area although neither the boundary with underlying Globigerina marls nor the upper boundary with the Middle Menilite Member are exposed.

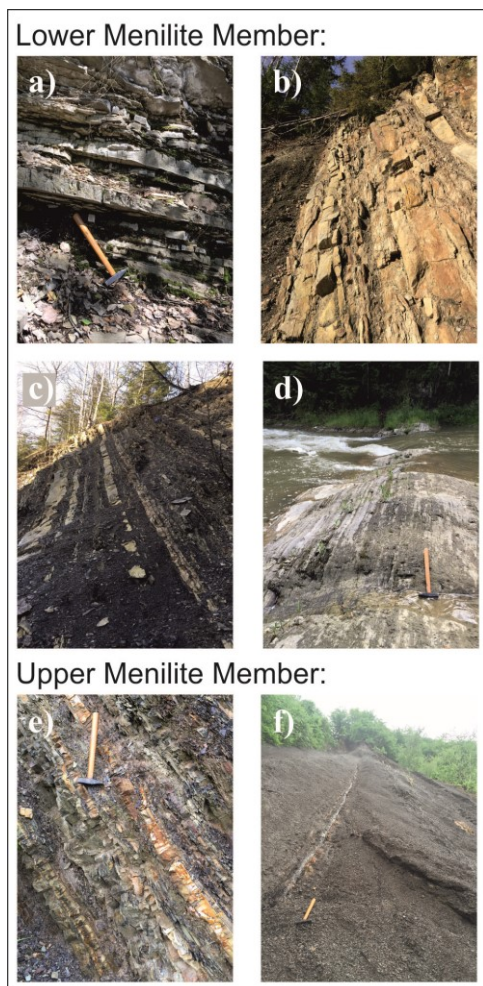


Fig. 3. Outcrop photographs of the Lower and Upper Menilite Members at locations along the Chechva River (Fig. 1c). (a) Thick chert beds in the Lower Menilite Member; (b) transition from the Lower Member shales to the Kliwa sandstones; (c) alternating shales and sandstones in the Lower Member, (d) sandstone-poor interval in the upper part of the Lower Member. (e, f) Upper Menilite Member: (e) thin chert beds within shales; (f) thick black shale succession. Note that not all the photographs show the true stratal dip.

The base of the Lower Menilite Member is marked by a chert-rich interval (329-311 m from the top of the member), which is used as a horizon marker. The interval consists of alternating chert layers, up to 15 cm thick, and thin shales (Fig. 3a). The number and thickness of chert layers decreases upwards. A 30 cm thick sandstone layer occurs near the top of the interval. The overlying sandstone-rich interval of the Lower Menilite Member (310-195 m from the top of the member) is dominated by thick (up to 2 m) sandstone beds (Kliwa Sandstones)

which are interbedded with thin shale layers (Fig. 3b,c). With the exception of a sandstone layer near the base of the unit, the sandstones are typically fine to middle-grained and frequently show irregular bases and wavy tops. Bioturbation was not observed.

The sandstone-poor upper part of the Lower Menilite Member (127 m - 0 m; Fig. 4) is primarily composed of alternating organic-rich shales and thin (typically 5-20 cm) turbidite sandstones (Fig. 3d); the number and thickness of sandstone beds decreases upwards. An interval in the middle part of the Lower Menilite Member, estimated to be approximately 70 m thick, was covered by vegetation and is not exposed. Two thin, laminated marl beds occur near the top of the Lower Menilite Member and in previous studies have been referred to as “streaky limestones”; based on their stratigraphic position in the upper part of the Lower Menilite Member, they have been correlated with the coccolith-rich Jaslo Limestone (Kulchytsky and Sovchyk, 1986; Shlapinski, 2012) which is used as stratigraphic marker in the Oligocene succession throughout the Carpathians (Haczewski, 1989; Melinte-Dobrinescu and Brustur, 2008). Above the “streaky limestones”, a single chert layer (2 cm thick) was observed. The carbonate content of the organic-rich shales in general increases above the “streaky limestones” as organic-lean grey shales become more abundant and the number of organic-rich black shales decreases. The transition to the overlying Middle Menilite Member is not exposed. A number of horizons with dolomite concretions occur within the generally carbonate-lean Lower Menilite Member. Some concretions contain minor amount of ankerite.

Samples from the lowermost, chert-dominated part of the Lower Menilite Member are barren of calcareous nannofossils. However, based on the presence of *Reticulofenestra umbilicus* and the absence of *Coccolithus formosus* in the sample from 316 m depth* relative to the top of the Member, the sample can be attributed to NP22 (lower Rupelian). The sample from 268 m contains well-preserved nannofossils with common *Cyclicargolithus floridanus* and very rare, mostly broken specimens of *Reticulofenestra umbilicus*, which may have been reworked from older sediments. As a result, this part of the section can be assigned to NP22/23 (middle Rupelian).

Samples from the upper part of the Lower Menilite Member (243.5-26.5 m depth*) are generally barren of calcareous nannofossils, but all the studied samples contain detrital terrestrial plant remains. Rare diatoms were observed in samples from depths* of 243.5 m and 125.5 m, whereas samples from 107 m, 97 m, 61 m and 50.5 m contain abundant diatoms. Aragonitic spicules of benthic didemnid ascidians were observed in the sample from 231 m. Most ascidians live in shallow-marine waters but spicules may also occur in turbidite deposits

(Varol and Houghton, 1996 cum lit.; Toledo et al., 2007). Samples from 228 m and 120.5 m contain nannofossils with a bloom of *Cyclicargolithus floridanus*. Melinte-Dobrinescu and Brustur (2008) described similar blooms of *Cyclicargolithus floridanus* in NP24-aged samples from the Eastern Carpathians and NW Transylvania. The common occurrences of *Pontosphaera desueta*, *P. enormis* and *P. multipora* suggest a shallow-marine depositional environment, but transport into deeper-water domains by turbidity currents may also have occurred. Based on the absence of *R. umbilicus* and *C. formosus*, samples from depths of 228 m and 120.5 m can be attributed to nannoplankton Zone NP23/24.

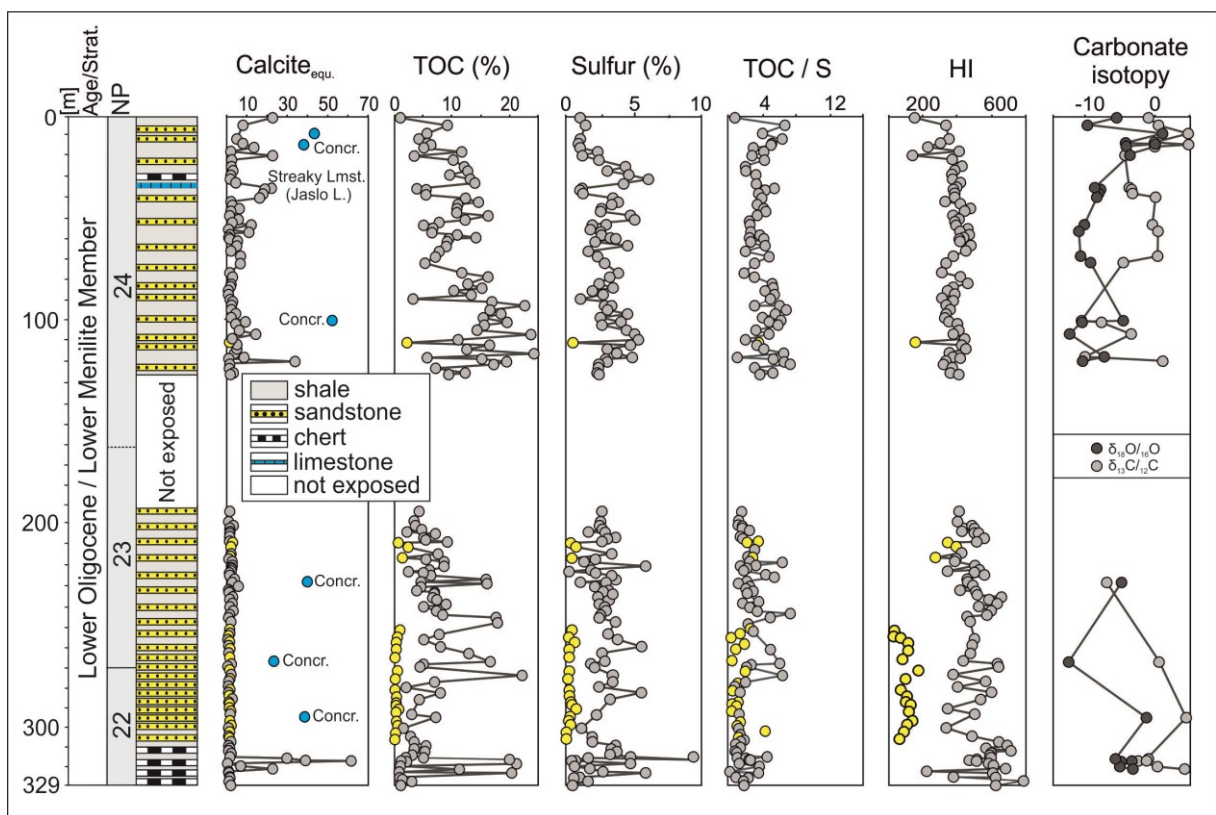


Fig. 4. Bulk geochemical data (after Sachsenhofer et al., 2018b) and total carbonate isotope data for samples of the Lower Menilite Member from the Chechva River profile with nannoplankton zones.

2. Middle Menilite Member

The overlying Middle Menilite Member (Upper Oligocene) was not studied in detail. However, six samples were collected for analyses and comparison from locations along a small river near the village of Lopianka, a few km to the NW of Spas. The exposed section was approximately 7.5 m thick, comprising alternating black shales and organic-lean grey

shales and sandstone beds (approximately 10 cm thick). The carbonate content of the grey shales (22.6 wt.%) was in general higher than that of the black shales (4.2 wt.%). The lithology of the studied section suggested that it represented the lower part of the Middle Menilite Member. However, samples of grey shale contained *Helicosphaera ampliaperta* which has its first occurrence in the upper NN2 (20.43 Ma) at the base of chron C6An.1r (Lourens et al., 2004), indicating an Early Miocene rather than a Late Oligocene age.

3. Upper Menilite Member

The Upper Menilite Member, which is approximately 1300 m thick in the studied profile along the Chechva River (Fig. 5), is marked by the occurrence of multiple thin chert beds (“Upper Chert”) at its base (Fig. 3e). The overlying sediments are dominated by alternating black and dark grey shales with a varying abundance of sandstone beds (typically 20 to 50 cm thick; max. 3 m). The number of sandstone beds is in general low (Fig. 3f) but is slightly higher in the lower part of the member.

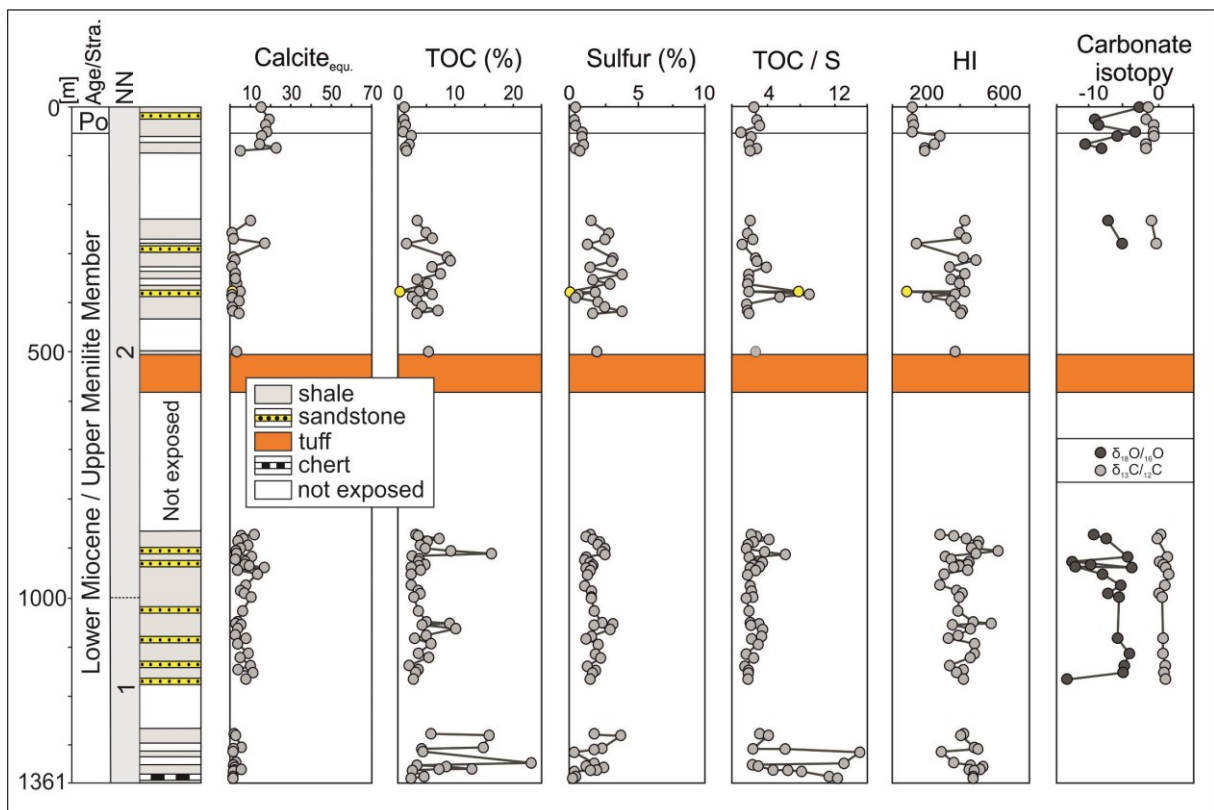


Fig. 5. Bulk geochemical data (after Sachsenhofer et al., 2018b) and total carbonate isotope data for samples of the Upper Menilite Member from the Chechva River profile with nannoplankton zones.

An approximately 70 m thick horizon consisting of dacitic tuffs, tuffites and tuffogenic clays and sandstones (Andreyeva-Grigorovich et al., 1997) near the middle of the member is used as a regional marker. The carbonate content of the black shales increases in the uppermost part of the member near to the transition with the overlying grey shales of the Polyanitsa Formation. Thin, grey sandstone beds are present in the uppermost part of the Upper Menilite Member.

Sediments from the lower part of the member (1343-348 m depth) contain rare and moderately preserved calcareous nannofossils accompanied by detrital terrestrial plant remains. Diatoms occur sporadically in samples from 1106.5 m, 947 m and 933.5 m which contain rare *Reticulofenestra pseudoumbilicus*, indicating an NN1 / lower NN2 (Aquitanian / earliest Burdigalian) age.

The upper part of the profile (278-25 m) contains common and well-preserved nannofossils dominated by *Coccolithus pelagicus*, indicating a shallow- and relatively cold-water marine environment with a high nutrient input, possibly caused by upwelling (Veto, 1987). The occurrence of *Coronosphaera mediterranea*, *Helicosphaera carteri* and *Reticulofenestra pseudoumbilicus* indicate a Miocene age. The sample from 278 m contains *H. ampliapertura* which indicates a depositional age younger than 20.43 Ma (upper NN2; early Burdigalian). In addition, this part of the section is characterized by high percentages of nannofossils which were reworked from the Upper Cretaceous and Eocene. Rare diatoms were observed in a sample from a depth of 51 m.

5.2. Bulk parameters of organic matter and maceral composition

A summary of bulk parameters from the Lower and Upper Menilite Members from samples from the Chechva River profiles was presented in a recent overview paper (Sachsenhofer et al., 2018b) and is shown in Figs 4 and 5.

The TOC content of black shales from the Lower Menilite Member averages 9.76 wt.% (max. 24.25 wt.%). HI values typically range between 400 and 650 mgHC/gTOC in the lower part of the member (max. 800 mgHC/gTOC), and from 300 and 450 mgHC/gTOC in the upper part (max. 475 mgHC/gTOC).

The average HI for the shales in the Lower Menilite Member is 448 mgHC/gTOC. The Kliwa sandstones have lower values of TOC (0.10-0.86 wt.%) and HI (29-165 mgHC/gTOC). TOC contents and HI values for grey shales in the Middle Menilite Member are low (0.80-0.96 wt.% TOC; 77-135 mgHC/gTOC) compared to black shales (3.19-8.80 wt.%; 311-360 mgHC/gTOC).

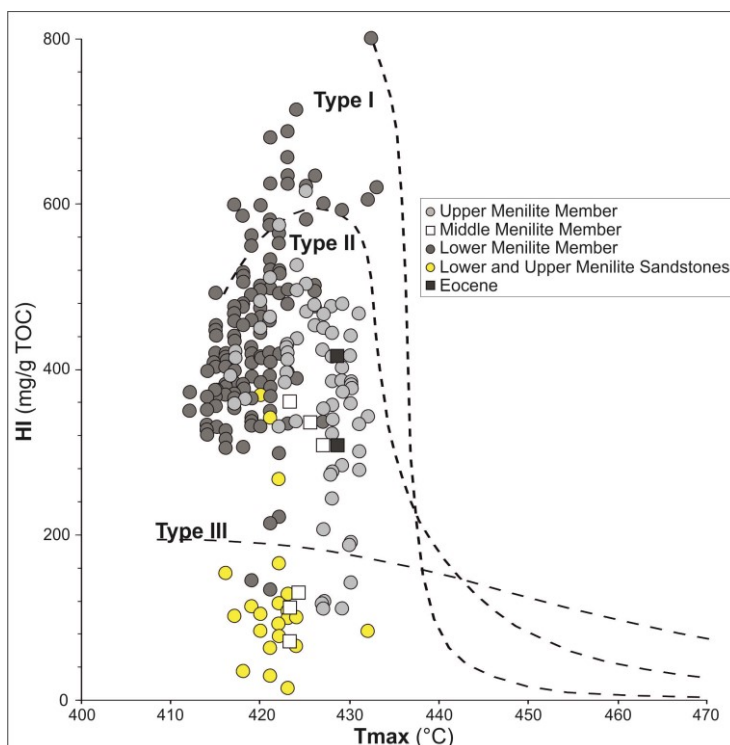


Fig. 6. Cross-plot of HI versus T_{max} (after Espitalié et al., 1984) for shale samples from the Lower, Middle and Upper Menilite Members, and for two Eocene-aged shale samples. The cross-plot also includes samples from sandstones in the Lower and Upper Members.

In the Upper Menilite Member, TOC exceeds 20 wt.% near the base of the unit and ranges from 1.52 to 23.11 wt% (average: 5.17 wt.%). Relatively low TOC contents (1.17-2.18 wt.%) are observed near the top of the member. HI values typically range between 300 and 500 mgHC/gTOC (average: 379 mgHC/gTOC). In four samples from the overlying Polyanitsa Formation, TOC contents (0.87-1.21 wt.%) and HI values (111-119 mgHC/gTOC) are low.

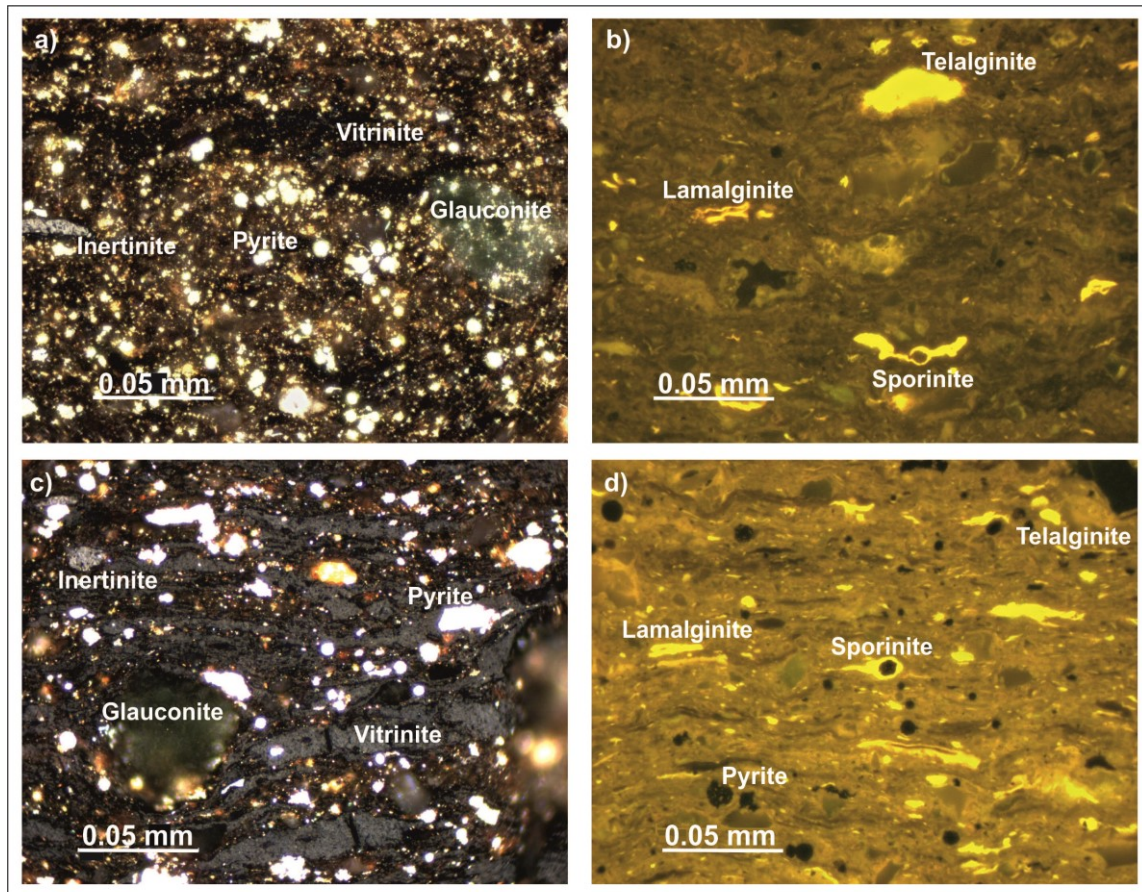


Fig. 7. Photomicrographs of samples from the Upper Menilite Member (a, b; 1299 m) and the Lower Menilite Member (c, d; 107 m) from the Chechva River profile. (a, c) Photomicrographs in white light showing inertinite, glauconite, vitrinite and pyrite; (b, d) Photomicrographs in fluorescence mode illumination showing lamalginite, sporinite, telalginite and pyrite.

Low T_{max} values for samples from the Lower, Middle and Upper Menilite Members (average: 419°C, 425°C and 425°C, respectively) together with vitrinite reflectance measurements for samples from the Lower (0.24-0.34 %Rr) and Upper (0.26-0.32 %Rr) Menilite Members, indicate that the organic matter is thermally immature (Fig. 6, Table 1).

The trend of sulphur content versus depth is similar to the trend of TOC content versus depth (Figs 4 and 5). TOC/S ratios, which are commonly used as a parameter to distinguish between anoxic and oxic conditions as well as between marine and freshwater deposits (Berner and Raiswell, 1984), are 0.23-10.38 wt.% in the Lower Menilite Member, 1.54-8.53wt.% in the Middle Menilite Member, and 0.99-15.14 wt.% in the Upper Menilite Member. High ratios were observed in black shales with very high TOC contents (>10 wt.%).

The maceral composition (Table 1; Fig. 7) for the Lower Menilite Member is characterized by high proportions of vitrinite (15-47 vol.%) and lamalginite (30-43 vol.%); also present are telalginite (10-23 vol.%), sporinite (4-23 vol.%) and inertinite (1-8 vol.%) In the Upper Menilite Member, the maceral composition consists of moderate proportions of vitrinite (16-38 vol.%), lamalginite (13-39 vol.%) and telalginite (16-31 vol.%), with minor sporinite (8-23 vol.%) and inertinite (3-7 vol.%). Lamalginite is in general considered to represent the remains of algae or bacterial mats, whereas telalginite is typically of planktonic derivation (Hutton, 1995).

Glauconite as well as framboidal pyrite was observed frequently in samples from both the Upper and Lower Menilite Members. Fig. 8 shows that there is a strong correlation between the hydrogen index (HI) and the amount of lam- and telalginite.

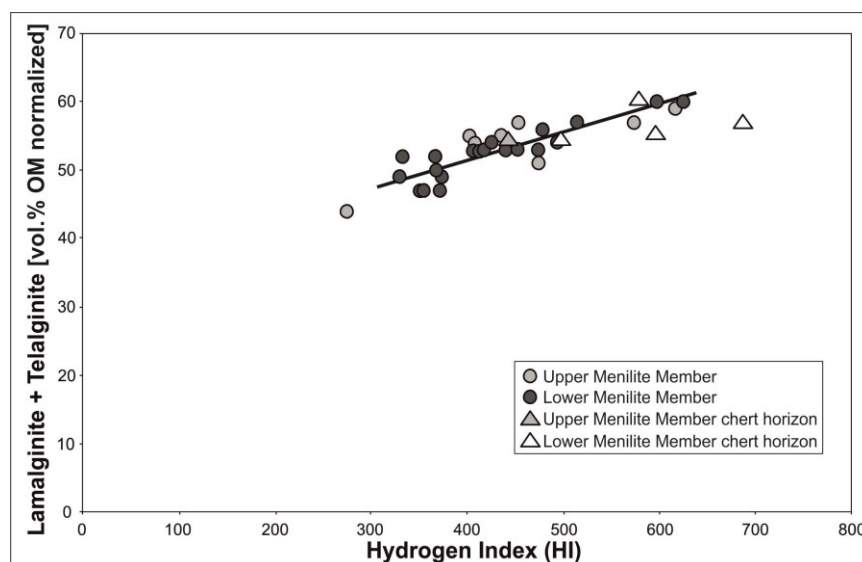


Fig. 8. Cross-plot of alginite percentages versus HI, showing that HI is mainly controlled by the abundances of lam- and telalginite.

5.3. Molecular composition of sample extracts

Geochemical data are listed in Table 2, and the vertical variations of biomarker proxies versus depth are shown in Figs 9 and 10 for the Lower and Upper Menilite Members respectively. Yields of extractable organic matter (EOM) vary between 3.25 and 36.07 mg/g TOC (average 19 mg/g TOC; Table 2). Extracts from all samples are dominated by NSO compounds (48-75% of the EOM). In the Upper Menilite Member, saturated hydrocarbons are often more abundant than aromatic hydrocarbons; but this is not the case in the Lower Menilite Member where saturated hydrocarbons are less abundant than aromatic hydrocarbons. The total relative percentages of saturated and aromatic hydrocarbons vary between 16 and 48 mg/g TOC (average 32 mg/gTOC) which is typical for sediments of low maturity (Tissot and Welte, 1984).

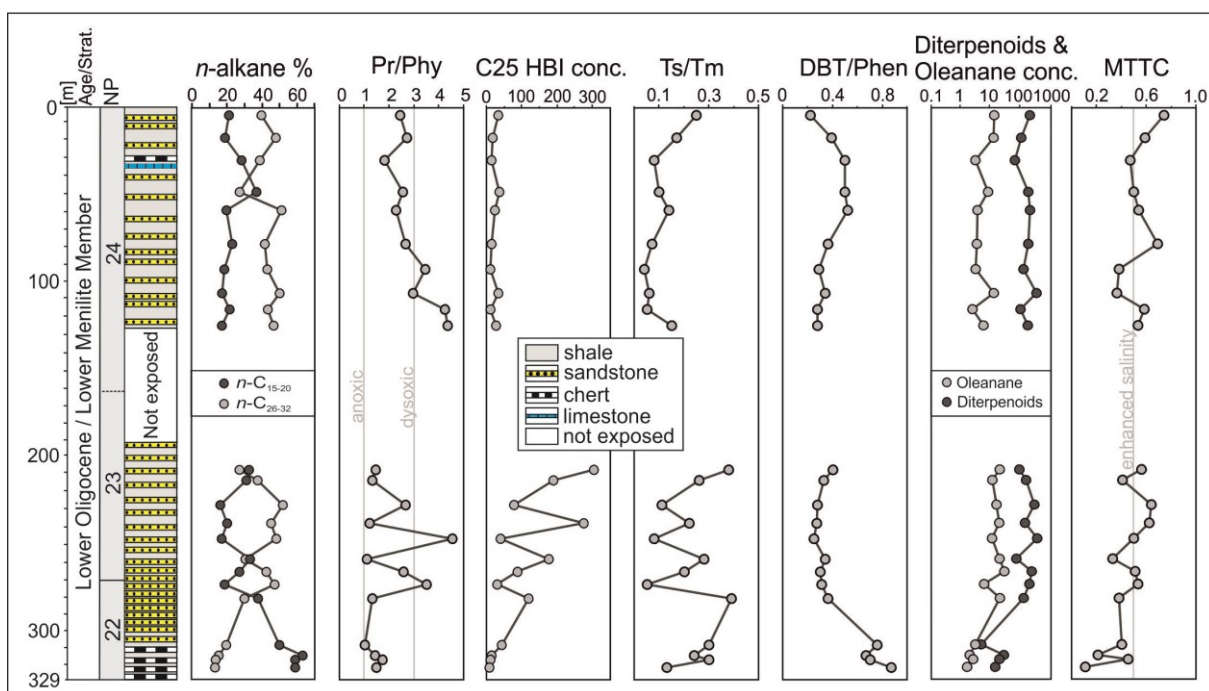


Fig. 9. Profile of biomarker ratios versus depth with nannoplankton zones for samples of the Lower Menilite Member from the Chechva River profile.

n-alkanes and isoprenoids

Extracts of samples from the Lower Menilite Member contain high amounts of long-chain *n*-alkanes (nC_{26-32} : 13-52 %), which is characteristic of higher land plants (Peters et al., 2007); however they are less abundant (13-19 %) in samples from the chert horizon at the base of the unit (323.4-310.0 m) (Table 2). Long-chain *n*-alkanes are in general less abundant in samples from the Upper Menilite Member and range from 17 to 32 %, except for the sample at the top of the succession (59.0 m) in which long-chain *n*-alkanes make up 40% of the total amount of *n*-alkanes.

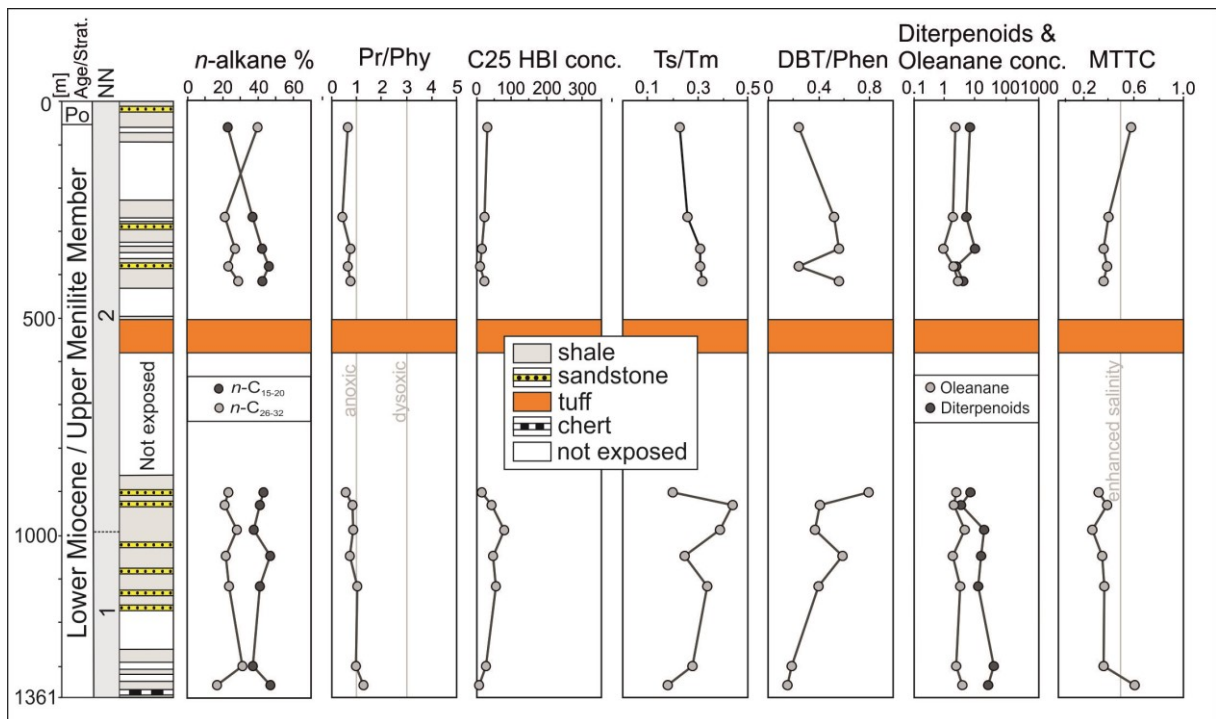


Fig. 10. Profile of biomarker ratios versus depth with nannoplankton zones for samples of the Upper Menilite Member from the Chechva River profile.

Concentrations of short-chain *n*-alkanes, which are derived from microbial organisms or algae (Dinel et al., 1990), show an opposite trend (Figs 9 and 10). They are abundant (50-63 %) in extracts of samples from the chert horizon at the base of the Lower Menilite Member, but present in lower proportions in samples from the overlying part of the Lower Member (16-38 %) and the Upper Member (23-47 %).

Table 1. Maceral composition of the Lower and Upper Menilite Members.

Depth [m]	Unit	TOC	S [wt.%]	Calcite equ. [mg/gTOC]	HI [mg/gTOC]	VR [%Rr]	Vitrinite	Inertinite [%OM normalized]	Sporinite [%OM normalized]	Lamalginitite	Telaginitite	Maceral [vol.%]	Glauconite yes/no
Upper Menilite Member													
59.0		2.18	0.94	13.83	275	*	30	4	22	13	31	4.3	y
413.0		6.88	3.88	0.05	408	0.32	21	4	21	35	19	9.4	y
899.0		9.16	1.64	1.44	617	0.26	26	4	11	36	23	10.9	y
928.0	Black Shale	4.70	1.54	5.95	436	*	16	6	23	39	16	6.1	y
985.0	Succession	3.75	1.54	5.99	403	*	21	3	21	34	21	6.6	y
1045.5		9.03	3.17	1.49	574	0.29	26	6	11	35	22	9.3	y
1115.5		5.38	2.28	3.58	454	*	25	7	11	35	22	6.1	y
1299.0		14.94	2.39	4.26	475	0.26	38	3	8	27	24	15.1	y
1343.0	Up. Chert	12.80	1.94	4.46	445	0.28	31	7	8	30	24	12.7	y
Lower Menilite Member													
4.0		9.21	1.38	6.44	333	*	35	4	9	35	17	11.1	n
17.0		11.58	2.35	0.56	409	0.34	38	2	7	30	23	13.5	y
30.0		13.08	6.03	0.02	367	*	34	1	13	37	15	18.4	n
48.5		16.09	4.66	0.23	374	*	36	1	14	31	18	20.6	y
59.0	Sandstone-	13.97	3.20	0.01	441	*	39	2	6	35	18	14.2	y
78.5	poor	16.22	3.18	1.32	412	*	40	1	6	36	17	20.0	y
93.0	Succession	22.47	3.31	0.65	330	0.29	45	1	5	39	10	28.4	y
107.0		23.67	4.99	13.15	372	0.27	47	2	4	36	11	34.6	y
116.5		24.25	3.74	2.42	351	0.31	46	1	6	35	12	27.2	y
125.5		12.19	2.3	1.43	355	*	42	4	7	35	12	20.6	y
209.0		9.10	2.62	0.30	515	0.27	27	5	11	39	18	13.8	y
215.0		7.46	3.29	0.68	418	*	32	4	11	39	14	11.4	y
229.5		15.84	2.91	1.20	453	*	40	2	5	42	11	21.1	n
240.0		8.83	2.44	1.18	625	0.27	29	3	8	42	18	10.1	y
249.0	Sandstone-	17.73	3.63	0.97	475	0.24	39	2	6	34	19	21.8	n
260.5	rich	7.90	5.54	0.02	479	*	29	2	13	37	19	13.2	y
268.0	Succession	16.54	2.79	21.91	426	0.25	38	2	6	38	16	18.1	y
275.2		21.94	3.43	0.81	369	*	41	2	7	35	15	26.6	y
283.5		7.84	5.48	0.01	598	*	29	3	8	43	17	13.0	y
294.5		2.84	2.24	0.12	494	*	15	8	23	39	15	4.1	y
310.0		5.32	3.64	0.07	687	*	35	3	5	31	26	7.6	y
316.5		19.85	9.28	0.01	501	*	41	1	4	31	23	22.0	n
318.8	Lower Chert	21.11	4.73	0.01	581	*	15	2	23	40	20	21.9	n
323.4		20.36	5.79	0.06	600	+	31	3	11	36	19	20.4	n

CPI values (Bray and Evans, 1961) in general range from 1.3 to 1.9. Values are lower in the chert horizon at the base of the Lower Menilite Member (0.9-1.2) and higher in the upper part of the Upper Menilite Member (2.1-2.4; Table 2).

Pristane (Pr) and phytane (Ph) form preferentially under oxidizing (pristane) and reducing (phytane) conditions respectively, and the Pr/Ph ratio can therefore be used as a redox indicator of the depositional environment (Peters et al., 2007). Pr/Ph ratios below 1.0 reflect a strict anoxic environment, whereas ratios above 1 suggest a suboxic to oxic environment or a high terrigenous input under oxic conditions. The Pr/Ph ratio for samples from the Lower Menilite Member varies widely (1.0-4.5; Table 2). Samples with relatively high Pr/Ph ratios (>3.0) occur irregularly throughout the member (Fig. 9), but decrease upwards in the upper part. Pr/Ph ratios in samples from the Upper Menilite Member (0.4-1.3) are generally lower (Fig. 10) and suggest oxygen-deficient depositional conditions. In common with the Lower Member, values tend to decrease upwards.

C25 highly branched isoprenoids (HBIs) are regarded to be biomarkers for marine diatoms and may form C25 HBI thiophenes due to sulphurization (Nichols et al., 1988; Summons et al., 1993; Volkman et al., 1994). C25 HBIs are present in samples from both the Lower and the Upper Menilite Members (Table 2). Elevated concentrations with an upward-increasing trend are observed in samples from the bottom half of the Lower Menilite Member (5.5-304.0 $\mu\text{g/g}$ TOC), but concentrations in samples from the remaining part of the succession are lower (8.7-33.8 $\mu\text{g/g}$ TOC). Concentrations in samples from the Upper Menilite Member are of the same order of magnitude (3.4-75.0 $\mu\text{g/g}$ TOC).

Steroids

High sterane concentrations, as well as high sterane/ hopane ratios (>1.0), are typical of marine organic matter with major contributions from planktonic and/or benthic algae (Moldowan et al., 1986). In samples from the Lower Menilite Member, sterane concentrations range from 20.23 to 478.95 $\mu\text{g/g}$ TOC. The highest concentrations are found towards the middle of the succession, in samples from between 260.5 m and 209.0 m (Table 2), although there was no clear trend versus depth. In samples from the Upper Menilite Member, sterane concentrations range from 80.47 to 262.48 $\mu\text{g/g}$ TOC (Table 2).

Table 2. Organic geochemical data for samples from the Lower and Upper Menilite Members.

Depth	TOC	HI	EOM	Sat. Aro. NSO Asph.		$n-C_{15-20} / n-C_{15-32}$	$n-C_{21-26} / n-C_{15-32}$	$n-C_{26-32} / n-C_{15-32}$	Pr/Ph	τ_5/τ_m	DBT/ MITC	CPI	Sterane/ Moretane/ Hopanes	22S/(S+R)	C ₂₅ HBI	Diterpenoids	Oleanane	Steranes				
				HC	HC														Phen ratio	Hopanes	C ₃₂ hopanes	conc.
[m]	[wt.%]	[mg/gTOC]	[ug/gTOC]	[mg/gTOC]	[mg/gTOC]													(ug/g TOC)				
Upper Menilite Member																						
59.0	2.18	275	3.25	12	13	65	10	0.23	0.37	0.40	0.63	0.23	0.25	0.58	2.40	2.64	0.53	0.22	29.38	8.24	3.04	80.47
265.0	5.94	429	7.22	14	10	67	9	0.37	0.42	0.21	0.41	0.26	0.53	0.40	2.27	2.13	0.19	0.27	21.80	6.41	2.40	127.34
339.0	7.39	423	8.14	15	11	69	5	0.42	0.31	0.27	0.73	0.31	0.57	0.36	2.25	2.80	0.23	0.29	13.20	10.07	0.96	97.98
379.0	5.82	361	7.39	14	9	73	4	0.46	0.31	0.23	0.63	0.31	0.25	0.39	2.14	3.27	0.20	0.33	9.67	3.55	3.02	150.52
413.0	6.88	408	8.23	15	11	68	6	0.42	0.29	0.29	0.75	0.32	0.57	0.36	2.08	2.76	0.23	0.33	19.84	5.33	3.42	262.48
899.0	9.16	617	17.95	9	7	74	10	0.43	0.33	0.24	0.56	0.20	0.81	0.32	1.50	3.92	0.15	0.32	11.78	8.85	3.06	185.09
928.0	4.70	436	8.24	16	11	69	4	0.41	0.37	0.22	0.82	0.44	0.42	0.39	1.67	2.76	0.18	0.30	39.04	5.15	3.38	210.17
985.0	3.75	403	7.26	18	10	65	7	0.39	0.33	0.28	0.84	0.39	0.38	0.27	1.58	1.70	0.19	0.34	74.99	16.62	6.83	188.28
1045.5	9.03	574	19.01	12	9	69	10	0.47	0.31	0.22	0.72	0.25	0.60	0.15	1.66	2.42	0.16	0.30	43.97	13.58	2.97	125.58
1115.5	5.38	454	7.41	18	14	58	10	0.41	0.35	0.24	1.01	0.34	0.41	0.37	1.64	2.16	0.20	0.30	51.57	11.37	4.51	157.22
1299.0	14.94	475	31.07	15	19	56	9	0.37	0.31	0.32	0.96	0.28	0.19	0.36	1.62	3.03	0.21	0.35	24.95	58.55	4.15	158.86
1343.0	12.80	445	23.19	8	14	65	13	0.47	0.36	0.17	1.27	0.18	0.16	0.61	1.70	1.64	0.18	0.26	3.37	37.74	6.50	107.45
Lower Menilite Member																						
4.0	9.21	333	12.63	19	19	51	11	0.21	0.40	0.39	2.45	0.25	0.22	0.74	1.65	1.73	0.24	0.32	32.42	212.53	11.40	107.99
17.0	11.58	409	21.04	16	19	50	15	0.19	0.33	0.48	2.71	0.17	0.39	0.59	1.65	1.04	0.34	0.38	16.39	106.60	11.32	76.12
30.0	13.08	367	19.30	12	18	56	14	0.28	0.33	0.39	1.81	0.08	0.50	0.47	1.55	0.87	0.35	0.32	13.28	85.39	5.21	47.12
48.5	16.09	374	27.85	10	23	58	9	0.37	0.36	0.27	2.54	0.10	0.50	0.50	1.59	1.63	0.33	0.39	33.77	183.33	9.27	116.26
59.0	13.97	441	19.68	15	20	50	15	0.20	0.30	0.50	2.27	0.14	0.52	0.54	1.48	1.50	0.31	0.34	23.47	213.36	6.61	68.23
78.5	16.22	412	23.53	15	23	54	8	0.23	0.35	0.42	2.66	0.07	0.36	0.69	1.77	1.10	0.38	0.32	14.39	175.30	6.07	43.78
93.0	22.47	330	15.10	12	24	57	7	0.18	0.39	0.43	3.46	0.04	0.29	0.38	1.71	0.57	0.44	0.37	8.70	152.38	5.22	22.58
107.0	23.67	372	36.07	15	26	50	9	0.17	0.32	0.51	2.96	0.06	0.34	0.36	1.68	0.90	0.44	0.39	32.16	480.02	10.92	39.04
116.5	24.25	351	25.27	8	22	60	10	0.21	0.36	0.43	4.24	0.05	0.28	0.58	1.92	0.82	0.42	0.36	10.63	103.84	4.77	20.23
125.5	12.19	355	19.01	14	20	52	14	0.17	0.37	0.46	4.33	0.15	0.28	0.53	1.71	0.95	0.36	0.37	26.41	250.44	7.24	51.82
209.0	9.10	515	17.17	19	18	57	6	0.32	0.41	0.27	1.46	0.38	0.40	0.56	1.39	2.56	0.26	0.35	303.97	98.21	35.14	392.50
215.0	7.46	418	13.96	24	18	54	4	0.31	0.32	0.37	1.31	0.26	0.33	0.41	1.42	2.31	0.26	0.35	186.93	108.11	11.93	219.03
229.5	15.84	453	24.88	19	27	49	5	0.16	0.32	0.52	2.65	0.11	0.28	0.64	1.80	1.10	0.47	0.36	76.34	356.11	16.26	75.00
240.0	8.83	625	22.37	17	18	57	8	0.20	0.35	0.45	1.22	0.22	0.27	0.62	1.42	3.11	0.31	0.35	273.08	120.09	21.29	402.73
249.0	17.73	475	26.92	17	31	48	4	0.17	0.35	0.48	4.53	0.08	0.25	0.50	1.87	0.51	0.54	0.35	39.04	415.30	11.71	35.32
260.5	7.90	479	19.03	17	18	57	8	0.32	0.37	0.31	1.09	0.28	0.34	0.33	1.44	3.36	0.28	0.38	173.89	95.77	28.68	478.95
268.0	16.54	426	35.36	14	20	58	8	0.27	0.30	0.43	2.56	0.20	0.30	0.51	1.83	1.18	0.37	0.34	86.41	335.52	49.06	195.35
275.2	21.94	369	29.05	13	27	51	9	0.19	0.34	0.47	3.50	0.05	0.31	0.53	1.76	1.12	0.47	0.35	29.30	280.71	7.55	59.27
283.5	7.84	598	18.91	19	16	62	3	0.38	0.31	0.31	1.20	0.39	0.36	0.38	1.33	2.91	0.24	0.33	117.40	140.66	17.16	266.56
310.0	5.32	687	7.74	11	17	69	3	0.50	0.31	0.19	1.01	0.30	0.76	0.40	1.55	4.10	0.22	0.34	42.40	7.63	5.08	196.61
316.5	19.85	501	25.90	8	14	68	10	0.63	0.22	0.15	1.42	0.24	0.67	0.21	0.89	1.63	0.26	0.32	13.38	27.47	2.49	62.35
318.8	21.11	581	26.76	10	15	70	5	0.59	0.28	0.13	1.74	0.30	0.70	0.45	1.18	4.62	0.27	0.35	9.63	22.81	3.04	132.73
323.4	20.36	600	26.87	8	13	74	5	0.59	0.28	0.13	1.48	0.13	0.87	0.11	1.10	0.86	0.35	0.32	5.55	15.57	1.81	51.71

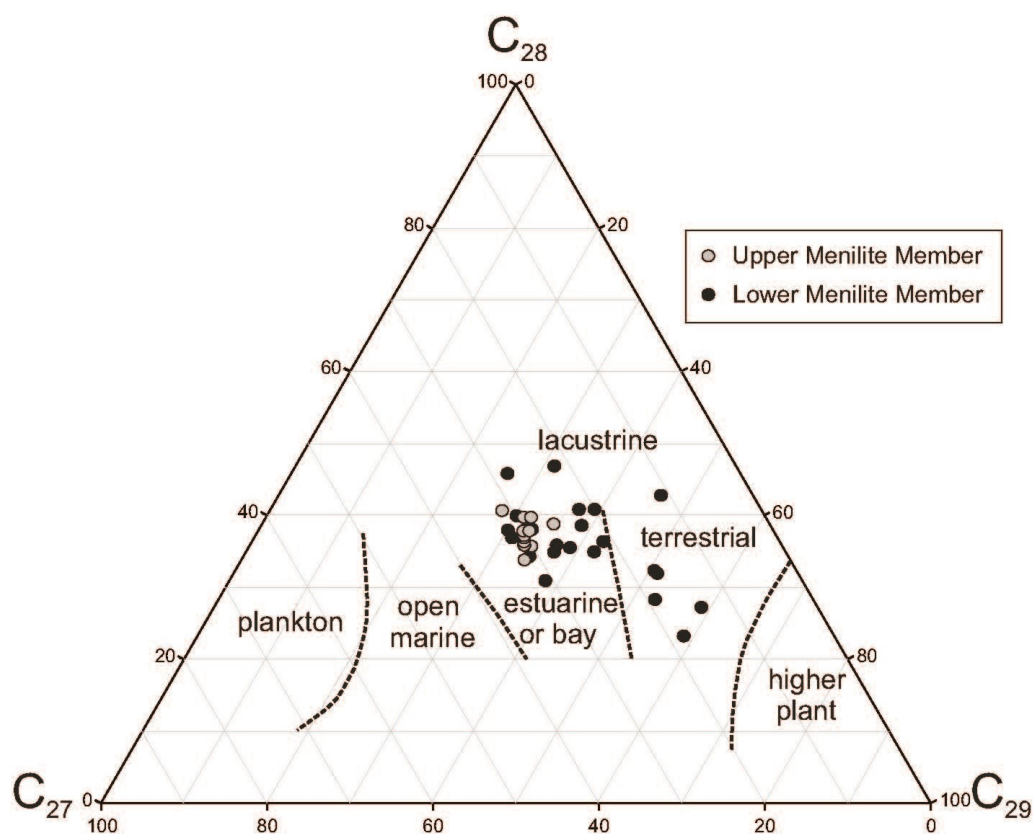


Fig. 11. Triangular diagram for C_{27} , C_{28} and C_{29} steranes for samples of the Lower and Upper Menilite Members.

The relative proportions of C_{27} , C_{28} and C_{29} steranes in a sample (Fig. 11) may provide palaeoenvironmental information (Huang and Meinschein, 1979). For samples from the Lower Menilite Member, C_{28} and C_{29} steranes (23-47 %; 26-58 %) are slightly elevated compared to C_{27} steranes (11-32 %). For the Upper Menilite Member, C_{27} , C_{28} and C_{29} steranes are more or less equally abundant for the samples analysed. However, C_{28} (34-41 %) steranes are slightly elevated compared to C_{27} (23-31 %) and C_{29} (28-35 %) steranes. C_{29} steranes correlate roughly with the Pr/ Ph ratio ($r^2 = 0.56$), suggesting that both parameters may be controlled by land-plant input. Elevated concentrations of C_{28} steranes in Cenozoic samples may indicate derivation from diatoms (Peters et al., 2007). However, no correlation between C_{28} steranes and HBI concentrations was observed for the studied samples.

High sterane/hopane ratios for samples from the Lower (0.51–4.62) and Upper Menilite Members (1.64–3.92; Table 2) are consistent with a marine depositional environment. The 20S isomer of the C_{29} sterane occurred in amounts which were not sufficient to be quantified, and the 20S/(20S + 20R) isomer ratio of C_{29} steranes was close to zero.

Terpenoids

Hopanes are non-aromatic cyclic triterpenoids which originate from precursors in bacterial membranes (Ourisson et al., 1979). They were found in all the samples analysed with concentrations ranging from 24.6 to 165.7 mg/g TOC in the Lower Menilite Member and 30.4 to 110.7 mg/g TOC in the Upper Menilite Member. The highest concentrations were in general found in samples from the middle of both members.

Moretane/hopane ratios can be used as a thermal maturity parameter for immature to early oil-window mature source rocks (Peters et al., 2007). Ratios below 0.15 indicate mature source rocks, whereas ratios up to 0.8 occur in source rocks which are considered to be immature (Peters et al., 2007). Moretane/hopane ratios in samples from both the Lower Menilite Member (0.22-0.54) and the Upper Member (0.15-0.53) indicate a low level of thermal maturity. This is in agreement with low 22S/(22S+22R) isomerization ratios of C₃₂ hopanes for samples from both Lower and Upper Members (0.32-0.39 and 0.22-0.35, respectively).

The trisnorneohopane/trisnorhopane (Ts/Tm) ratio is a thermal maturity parameter which can also be influenced by the source of organic matter (Moldowan et al., 1986) and by differences in lithology and in the oxicity of the depositional environment. The Ts/ Tm ratios for samples from the Lower and Upper Menilite Members are low (0.04-0.39 and 0.18-0.44, respectively), indicating their thermal immaturity (Figs 9 and 10).

Dibenzothiophene, phenanthrenes

The dibenzothiophene/phenanthrene (DBT/Phen) ratio reflects the availability of free H₂S in the water column (Hughes et al., 1995). DBT/Phen ratios for samples from the Menilite Formation are generally low (0.16-0.87) but exhibit clear trends versus depth (Figs 9 and 10). Maximum values are observed in samples from the chert horizon at the base of the Lower Menilite Member.

Land-plant related biomarkers

Diterpenoids (e.g. cadalene, retene, simonellite), which are gymnosperm-derived biomarkers (Simoneit, 1986; Alexander et al., 1988; Wakeham et al., 1980), were encountered in higher concentrations (7.63-480.02 µg/g TOC) in samples from the Lower Menilite Member compared to the Upper Member (3.55-58.55 µg/g TOC) (Table 2).

Oleanane was the only angiosperm-derived biomarker (Moldowan et al., 1995) observed in samples from the Menilite Formation (Köster, 1998).

Similar to the diterpenoids, its concentration is higher in samples from the Lower Menilite Member (1.8149.06 $\mu\text{g/g}$ TOC) than in samples from the Upper Member (0.96-6.83 $\mu\text{g/g}$ TOC).

Thus in general, gymnosperm-derived biomarkers are dominant in the samples analysed (>90 %), but angiosperm-derived biomarkers make up 40 % of total land-plant derived biomarkers in some samples from the Upper Menilite Member.

Chromans

Methyltrimethyltridecylchromans (MTTCs) are formed from bacteria or archaea and are used as markers for palaeosalinity (Sinninghe Damsté, 1987). They were observed in all the Lower and Upper Menilite samples analysed. The MTTC ratio is calculated by dividing the trimethyl MTTCs by the sum of the methylated MTTCs (Sinninghe Damsté, 1987). The MTTC ratio for the Lower Menilite Member ranges from 0.11 to 0.74 and increases from base to top. The ratio for the Upper Menilite Member is relatively uniform throughout the middle and upper part of the succession and ranges from 0.15 to 0.61, indicating mesosaline conditions in the water column during deposition.

Stable carbon isotope composition

Carbonate contents are typically low in the Menilite Formation. Therefore, isotope ratios from only a limited sample set (samples containing >5 wt.% calcite equivalent) were used to determine the $\delta^{13}\text{C}$ and $\delta^{18}\text{O}$ isotope compositions.

In the Lower Chert horizon, the bulk carbon isotopic composition is moderately stable and $\delta^{13}\text{C}$ and $\delta^{18}\text{O}$ values range between -3 and +5‰ and from -7 to -5‰, respectively. Since the carbonate content is particularly low in the sandstone-rich part of the Lower Menilite Member, three dolomite concretions were analysed for their isotopic composition. $\delta^{13}\text{C}$ and $\delta^{18}\text{O}$ values range from -7 to +4‰ and from -13 to -2‰, respectively.

The carbonate content in sediments in the sandstone-poor upper part of the member is higher, and isotope ratios for carbonate-rich shales, carbonate concretions and “streaky limestones” were determined. $\delta^{13}\text{C}$ values for carbonate concretions range from -12‰ in the lower part to +5‰ towards the top of the member. A similar trend was recorded for $\delta^{18}\text{O}$ values which range from -11‰ in the lower part to 0‰ and +1‰ towards the top. The “streaky limestone” sample had a $\delta^{13}\text{C}$ value of -4‰ and a $\delta^{18}\text{O}$ value of -9‰.

In the Upper Menilite Member, carbon isotopic composition values are typically more stable compared to the Lower Menilite Member. $\delta^{13}\text{C}$ values range between -2‰ and +1‰, and show little variation for samples near the transition to the Polyanitsa Formation. $\delta^{18}\text{O}$ values reach a minimum of -14‰ towards the bottom of the Upper Member and range from -13‰ to -3‰ for the remaining samples. Similarly, $\delta^{18}\text{O}$ values remain relatively constant near the transition to the Polyanitsa Formation.

6. Discussion

Deposition of organic matter-rich Oligocene to Lower Miocene rocks of the Menilite Formation (and of ageequivalent “Maikopian” sediments) was a consequence of the isolation of Paratethys from the Mediterranean Sea and the World ocean (Vetö, 1978; Popov et al., 2004; Sachsenhofer et al., 2018a; 2018b). Basin isolation resulted in oxygen-depleted conditions and facilitated the development of salinity and thermal stratification (Kovac et al., 2017). Strong subsidence after basin isolation increased water depths in many Paratethyan basins to more than 1000 m, but water depths in the Carpathian Basin remained permanently high from Cretaceous times onwards (Slaczka et al., 2006). Oligocene and Miocene thrusting further increased subsidence in the Outer Carpathians.

The outcrops along the Chechva River form the type section of the Menilite Formation in the Ukrainian Carpathians (Andreyeva-Grigorovich et al., 1986), and an almost complete succession comprising the Lower, Middle and Upper Menilite Members can be studied here. The stratigraphy, depositional environment and source rock potential of the Menilite Formation are discussed in the following section. However, because many organic geochemical proxies are influenced by diagenetic processes, the discussion starts with a brief outline of the thermal maturity of the studied succession.

6.1. Maturity

T_{\max} measurements for samples from the Lower (~415-425 °C), Middle (423-427 °C) and Upper (~420-430 °C) Menilite Members, as well as sterane and hopane isomerisation ratios, T_s/T_m ratios and vitrinite reflectance measurements for the Lower and Upper Members (0.24-0.34 and 0.26-0.32 %Rr, respectively), indicate that the organic matter is immature. T_{\max} measurements for samples of the Middle and Upper Menilite suggest a higher thermal maturity than for Lower Oligocene (Lower Menilite) samples, despite being younger. This may be attributed to a deeper structural position in the lowermost tectonic slice in the Skyba nappe, or to differences in facies; for example, source rocks with a higher sulphur content may display lower T_{\max} values (Vetö et al., 2000). This is noticeable in the Upper Menilite Member. The low thermal maturity for both the Lower and Upper Members is consistent with the light blue fluorescence colour of the liptinite macerals.

6.2. Stratigraphy

In previous studies, the Lower Menilite Member has been considered to be Early Oligocene (AndreyevaGrigorovich et al., 1986), and this age assignment was supported by new nannoplankton data from the basal chert horizon (NP22) and from samples from depths of 268-118 m (relative to the top of the Member) (NP23). The Solenovian event, a carbonate-rich, low salinity marker horizon at the base of NP23 (e.g. Popov et al., 2004), was not recorded; carbonate-rich samples in the lower part of the succession, where the horizon could be expected to occur; were not observed. The “streaky limestones” (Jaslo Limestone) is often taken to mark the boundary between the Lower and Upper Oligocene. Unfortunately however, age-diagnostic nannoplankton were absent from the top part of the Lower Menilite Member.

The Middle Menilite Member has previously been dated as Late Oligocene (Andreyeva-Grigorovich et al., 1986; Kotarba and Koltun, 2006). However, the nannoflora observed in the studied samples, considered to represent the Middle Menilite Member, clearly indicate an Early Miocene (NN2) age. Based on geological position and lithology, the samples appear to belong to the lower part of the Middle Member. Nevertheless, the stratigraphic position of the sediments, exposed in a small isolated outcrop, was not completely clear. If the age dating and the stratigraphic position are correct, the Upper Oligocene succession is either missing or very thin at the locations studied. By contrast, sediment accumulation rates must have been very high during Early Miocene times (NN2) perhaps due to intensive turbidite deposition and an increase in basin subsidence accompanying a phase of increased regional compressional (Slaczka et al., 2006; Nakapelukh et al., 2017).

An Early Miocene age for the Upper Menilite Member was confirmed by the samples analysed (NN2). The 70 m thick tuff horizon in the middle of the member, which is known to occur in the external part of the Skyba nappe and in the Boryslav-Pokuttya nappe, has not to the authors' knowledge yet been dated.

6.3. Depositional environments

The Lower Menilite Member

Lower chert horizon

Deposition of the Lower Menilite Member began during NP22 with the deposition of the lower chert horizon (Figs 3a, 9). Chert intervals are interpreted to be composed of diagenetically altered diatomite. Some chert intervals (samples from ~322 m to 316 m) have high contents of carbonate which is at least partly derived from calcareous nannoplankton. Shalerich sediments between the chert beds are very rich in organic matter (~20 wt.% TOC). The very high HI values (600-800mgHC/gTOC) are a result of the high contents of algal-derived lam- and telalginite (Fig. 8), and indicate excellent preservation of mainly algal material. This is consistent with the low concentrations of land-plant derived biomarkers in samples from the lower chert horizon, which are lower than in any other part of the Lower Member. Surprisingly, the concentration of C₂₅ HBIs, which are often considered as biomarkers for diatoms, is low.

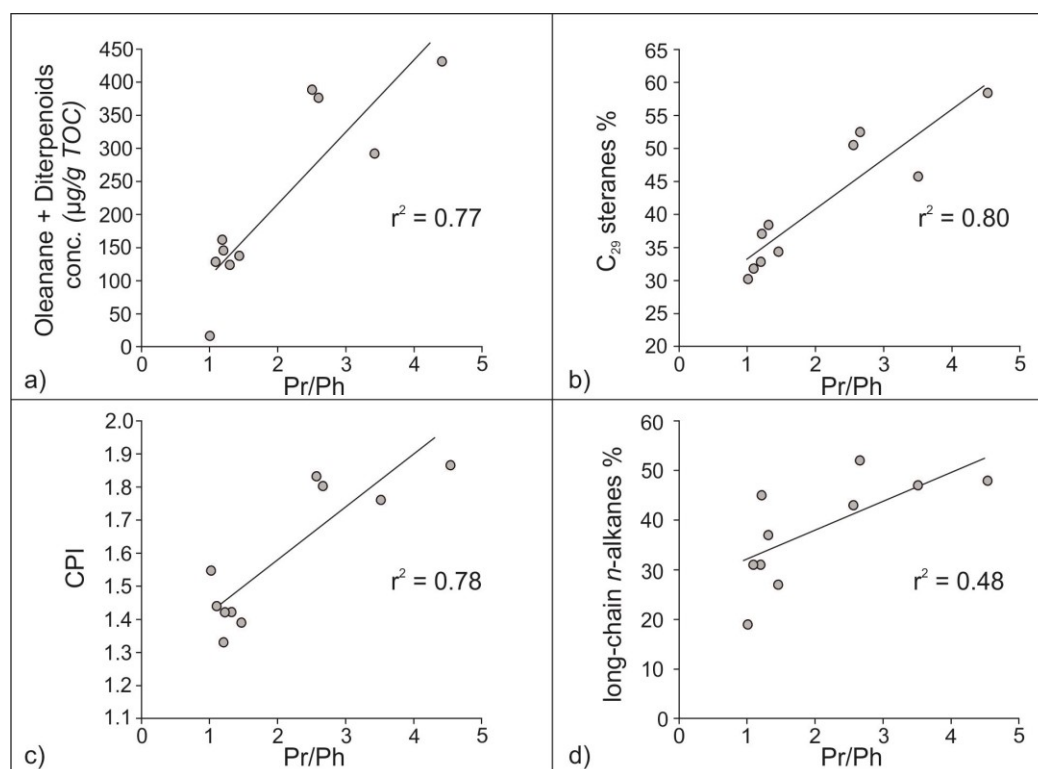


Fig. 12. Cross-plot of Pr/Ph ratios versus (a) oleanane + diterpenoids concentrations, (b) relative percentages of C₂₉ steranes, (c) Carbon Preference Index (CPI) and (d) relative percentages of long-chain *n*-alkanes.

Pr/Ph ratios (1-1.74; Table 2) indicate strongly oxygen-depleted but not strictly anoxic conditions. A moderately enhanced DBT/Phen ratio suggests that small amounts of free H₂S were available. However, the absence of arylisoprenoids shows that photic zone anoxia was not developed during deposition of the chert (or the rest of the Menilite Formation).

On average, MTTC ratios are lower in the lower chert horizon than in the remaining section of the Lower Member, which may indicate slightly elevated salinity. TOC/S ratios are often high (3-7), indicating a sulphate-limited environment (Bernier and Raiswell, 1984). However, high TOC/S ratios are probably a result of the very high organic matter contents and the limited diffusion of sulphate from the water column (Schulz et al., 2002).

Time-equivalent cherts are present throughout the entire Carpathians but are missing in other Paratethyan basins. The cherts have been related to upwelling (e.g. Picha et al., 2006) but, based on trace fossils and fish fauna, Kotlarczyk and Uchman (2012) proposed that they were deposited in oxygen-depleted conditions due to thermal stratification of the water column.

$\delta^{13}\text{C}$ values (-3 to +5 ‰) are within the range typical for marine carbonates, whereas $\delta^{18}\text{O}$ values are low (-7 to -5 ‰). The low $\delta^{18}\text{O}$ values may be due to elevated palaeotemperatures (~50°C, cf. Bojanowski et al., 2018), or to increased freshwater influx or diagenetic overprint. Palaeotemperatures in the order of 50°C are unreasonably high for the Oligocene in the Carpathians (Bojanowski et al., 2018). As calcareous nannofossils are missing in this section, the low $\delta^{18}\text{O}$ values are interpreted probably to reflect a diagenetic overprint.

The sandstone-rich interval in the Lower Menilite Member

The interval between 310 and 195 m contains frequent beds of Kliwa sandstones (Figs 3b, 9). These sandstones are considered to be deep-marine deposits (Kotlarczyk and Uchman, 2012; Miclaus et al., 2009), although Dziadzio et al. (2006, 2016) assumed a shallow-water depositional environment. In the present paper the conventional interpretation was followed, and the thick, laterally continuous sandstone beds were interpreted as deep-water deposits representing the transition from a deep-marine channel fill to a depositional fan lobe (e.g. Miclaus et al., 2009).

The TOC contents of interbedded shale samples from the lower part of the succession are high (up to 8 wt.%) and exceed 20 wt.% in the upper part, indicating that organic matter accumulation was high shortly before and after the deposition of channel fill sediments. HI values are high (~400-650 mgHC/gTOC) but are reduced compared to values for the lower

chert horizon (Table 1) due to decreasing proportions of alginite. A higher land plant input is indicated by higher concentrations of land-plant derived biomarkers (Fig. 9). C25 HBIs occur in significant concentrations and may indicate an input of diatom-derived material; diatoms were also observed in some smear slides.

Pr/Ph ratios for this part of the Lower Member vary widely and correlate positively with the content of land-plant biomarkers (oleanane + diterpenoids; $r^2 = 0.77$), with relative percentages of C₂₉ steranes ($r^2 = 0.80$), with CPI ($r^2 = 0.78$) and with the amount of long-chain *n*-alkanes ($r^2 = 0.48$; Fig. 12). This suggests that Pr/Ph ratios were mainly controlled by the landplant input rather than by redox conditions. Based on the absence of bioturbation in the shales, a continuation of oxygen-depleted depositional conditions is likely.

MTTC ratios suggest normal-marine conditions. TOC/S ratios in samples below 276 m are consistent with marine, reduced-oxygen conditions. Higher values in samples from above this depth are biased due to very high TOC contents.

Carbonate concretions within the sandstone-rich but largely carbonate-free interval of the Lower Menilite Member show strongly varying values of $\delta^{13}\text{C}$ (-7 to +4 ‰) and $\delta^{18}\text{O}$ (-13 to -2 ‰). Varying $\delta^{18}\text{O}$ values may indicate different diagenetic temperatures, whereas low $\delta^{13}\text{C}$ values may indicate the addition of isotopically light, methane-derived carbon. Bojanowski et al. (2012) reported even lower $\delta^{13}\text{C}$ values (-38.7 ‰ to -34.7 ‰) from concretions underlying the Jaslo Limestone in the Polish Carpathians.

The sandstone-poor upper part of the Lower Menilite Member

Compared to the underlying unit, the upper interval of the Lower Menilite Member (127-0 m) contains a lower proportion of turbiditic sandstones, suggesting a change from a deep-marine channel to a pelitic distal lobe setting. TOC contents of shale samples are very high and in general decrease upwards from 20 to 5 wt.%. HI values are in the order of 350 to 400 mgHC/gTOC. The decrease in HI compared to the underlying sediments reflects a decrease in the content of alginite (Fig. 8) and a higher contribution of landplant derived macerals (vitrinite, inertinite, sporinite). High concentrations of land-plant derived biomarkers are consistent with this interpretation.

Pr/Ph ratios suggest an upward decrease in oxygen availability. However, a positive correlation with CPI ($r^2 = 0.58$) shows that Pr/Ph ratios may be influenced not only by redox conditions but also by the input of detrital land plants (see above).

Samples from above and below the stratigraphic level of the “streaky limestones” (Jaslo Limestone) are characterized by relatively high DBT/Phen ratios, suggesting the presence of minor amounts of free H₂S in the water column. This interval is characterized by the lowest Pr/Ph ratios recorded. MTTC ratios vary but are consistent with normal marine conditions.

The sediments above the chert horizon represent deep-water settings, in which deep-marine channels transported (Kliwa-type) sandstones from the European platform into the oxygen-depleted basin (Popdayuk et al., 2006). A deep-water environment is also supported by the observation of a deep-marine benthic-pelagic fish (family Macrouridae) in a sample from above the Jaslo Limestone (Gorbach, 1961 in Kotlarczyk et al., 2006). Kliwa-type sandstones are a common part of the Oligocene succession throughout the Carpathians (e.g. Picha et al., 2006; Slaczka et al., 2006; Sylvester and Lowe, 2004). Age-equivalent sediments in many Paratethyan basins contain elevated organic matter contents due to extensive anoxia. However, TOC contents in the Carpathians are significantly higher than in other basins and this may reflect high bioproductivity and the excellent preservation of organic matter.

$\delta^{13}\text{C}$ (-11 ‰ to +5 ‰) and $\delta^{18}\text{O}$ values (-11‰ to +1 ‰) for dolomite concretions in the sandstone-poor part of the member display similar values to those in the sandstone-rich interval, consistent with the addition of methane-derived carbon and the varying mineralogy.

$\delta^{13}\text{C}$ (-12 to +2) and $\delta^{18}\text{O}$ (-11 to -5) values in calcareous shales vary over a similar wide range. $\delta^{13}\text{C}$ and $\delta^{18}\text{O}$ values for the “streaky limestone” (Jaslo Limestone) are -4 ‰ and -9 ‰, respectively, similar to those in the under- and overlying calcareous shales. These values are lower than average $\delta^{13}\text{C}$ (+1.4±1.4 ‰) and $\delta^{18}\text{O}$ (-4.7±1.1 ‰) isotopic composition data published by Bojanowski et al. (2018) for the Jaslo Limestone.

The Upper Menilite Member

Upper chert horizon

The upper chert horizon, about 10 m thick, is present at the base of the Upper Menilite Member. The chert is interpreted to be composed of diagenetically altered diatomite, suggesting that diatom blooms reoccurred during Early Miocene time. In comparison to the lower chert horizon, TOC/S ratios are higher and the DBT/Phen ratio (of a single sample) and HI values are lower. This indicates that free H₂S was in general absent from the water column and that anoxia was less strict. This result agrees well with the model of Kotlarczyk and Uchmann (2012) who tentatively identified upwelling and less oxygen-depleted conditions during the deposition of the upper chert horizon.

Black shale succession

The upper chert horizon is overlain by a very thick black shale succession with minor thin sandstone beds which is interpreted to have been deposited in a basin-plain setting. Black shale accumulation was interrupted by a major volcanic event which resulted in the deposition of the 70 m thick tuff interval (Fig. 5). Glauconite was observed in all samples and suggests a detrital input from a near-shore setting.

TOC contents are moderately high (2-7 wt.%), but significantly higher values occur near the base of the succession. Relatively low TOC contents (1-2 wt%) are observed in samples near the transition to the Polyanitsa Formation. HI values are approximately 400 mgHC/gTOC, but range between 200 to 300 mgHC/gTOC near the top of the Upper Menilite Member, due to a lower contribution of algal material (Fig. 8). Land-plant derived biomarkers in general occur in minor concentrations, although high amounts of oleanane in the uppermost sample (Fig. 10) indicates a higher contribution of angiosperm material. Diatoms occur sporadically, but concentrations of C₂₅ HBIs are in general low.

Pr/Ph ratios in samples from the Upper Menilite Member are generally lower than in samples from the Lower Member, and suggest strongly oxygen-deficient conditions. MTTC ratios suggest normal marine conditions with minor salinity variations. DBT/Phen ratios reach maximum values in the middle part of the succession which probably suggests the presence of free H₂S.

Carbonate contents are elevated in the uppermost part of the Upper Menilite Member and remain constant into the basal section of the Polyanitsa Formation. For this study, the boundary was defined where TOC contents decrease below 1.2 wt.% and HI decreases significantly from >180 mgHC/gTOC to <120 mgHC/gTOC.

The thick Lower Miocene black shale succession in the studied area is unique in the Carpathians (and in the entire Paratethys; Sachsenhofer et al., 2018a,b). In internal units of the Outer Carpathians, the Lower Miocene succession is dominated by (Krosno-type) sandstones transported from the thrust front into the deep-marine basin (Slaczka et al., 2006; Kotlarczyk et al., 2006). Hence, black shales are restricted to the most external units, but even there, their thickness is in general significantly lower (e.g. Sachsenhofer et al., 2015). This may be because significant thicknesses of the Upper Menilite Member had been eroded before deposition of the Polyanitsa Formation (AndreyevaGrigorovich et al., 1997; Popadyuk et al., 2006). Also, subsidence rates must have been high in the study area in order to allow the

accumulation of sediments about 1300 m thick (Upper Menilite Member) or even 1450 m thick (Middle and Upper Menilite Members) during less than 5 million years (NN2).

$\delta^{13}\text{C}$ (-2 ‰ to +1 ‰) ratios for the black shale succession are fairly uniform and are consistent with a marine environment. $\delta^{18}\text{O}$ values are very low (-14 ‰ to -3 ‰) and may indicate a diagenetic overprint and/or a freshwater influx (Bojanowski et al., 2018).

6.4. Source rock potential

Two samples of Eocene age were collected from an outcrop along the Chechva River stratigraphically below the Menilite Formation, and had low TOC contents (0.88-1.32 wt.%) and moderate HI values (311-428 mgHC/gTOC).

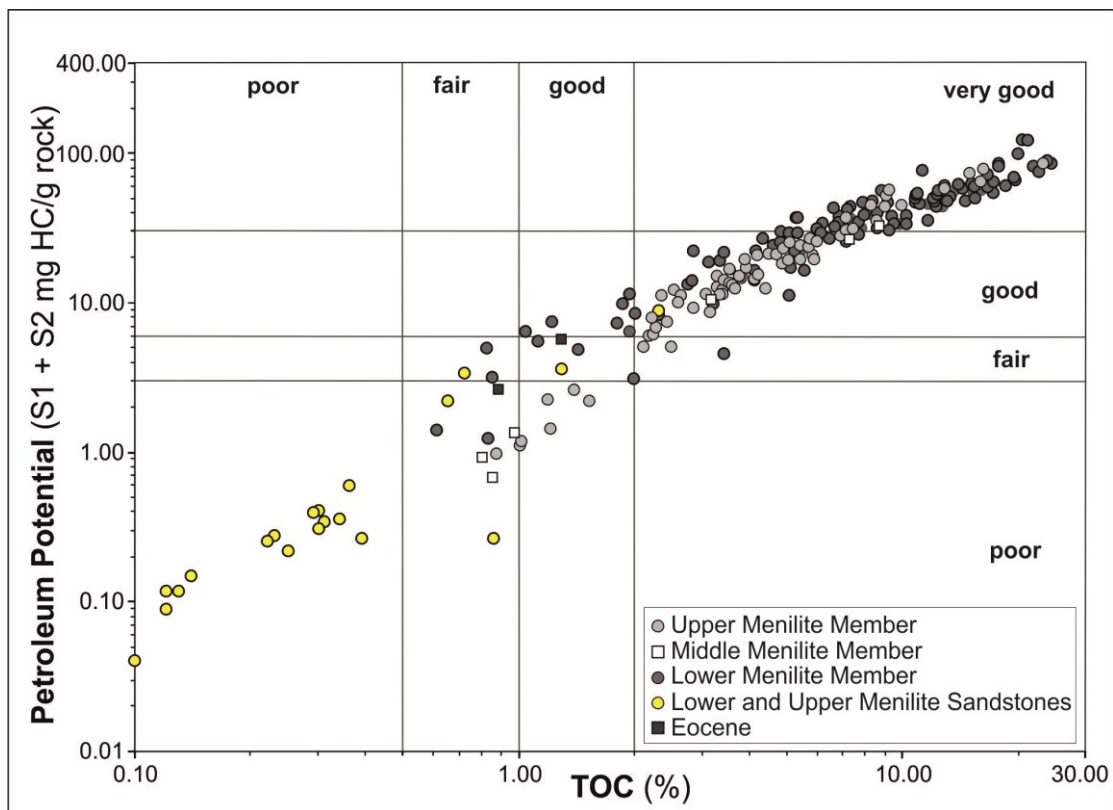


Fig. 13. Cross-plot of petroleum potential versus TOC for samples of the Lower, Middle and Upper Menilite Members and for two Eocene samples from the Chechva River profile. The cross-plot also includes samples from sandstones in the Lower and Upper Menilite Members.

Higher amounts of organic matter occur in the Menilite Formation, in which the average TOC content in shale samples from the Lower and Upper Members is 9.76 wt.% and 5.17 wt.%, respectively. Average HI values are 448 mgHC/gTOC for samples from the Lower Member and 379 mgHC/gTOC for samples from the Upper Member, indicating the dominance of oil-prone Type II kerogen. Grey and black shales within the Middle Member have poor source rock potential (0.80-0.96 wt.% TOC; 77-135 mgHC/gTOC) and good to very good potential (3.19-8.80 wt.%; 311-360 mgHC/gTOC), respectively.

A cross-plot of Rock-Eval $S_1 + S_2$ (petroleum potential) versus TOC (Fig. 13) indicates the excellent source rock potential of both the Lower and Upper Members. The Source Potential Index ($SPI = \text{thickness} * [S_1 + S_2] * \text{bulk density}/1000$; Demaison and Huizinga, 1994), which was calculated using the data from Table 3, indicates SPI values of 16.6 tons of hydrocarbons per square metre surface area (tHC/ m²) for the Lower Member, and 57.9 tHC/m² for the Upper Member. Estimates for unexposed sections in the measured outcrop profiles were included in these calculations, and the true SPI values for black shale intervals may therefore be higher.

Even if hydrocarbons generated from the Middle Member are neglected, the cumulative SPI of the Menilite Formation exposed at outcrop along the Chechva River (75 tHC/m²) is higher than that of any other source rock unit known to the authors (cf. Demaison and Huizinga, 1994). Source rocks elsewhere in the Paratethys area, including the Carpathians, have significantly lower SPI values, reaching 10 tHC/m² only in a local area in the Polish part of the Silesian-Krosno nappe (Sachsenhofer et al. 2018a,b). The SPI of the Lower Oligocene Lower Menilite succession is higher (16 tHC/m²) than that of time-equivalent rocks in the Polish and Romanian Carpathians (up to 10 tHC/m²). Even though the 330 m thick organic-rich sequence of the Lower Menilite Member itself represents an important source-rock level, the exceptionally high SPI of the Chechva River section is mainly a result of the great thickness (>1000 m) of organic-matter rich Lower Miocene shales in the Upper Menilite Member. The SPI of this section is also enhanced because of the comparative rarity of turbidite sandstones in the succession; these sandstones are common in time-equivalent sections in other parts of the Carpathians.

Age	Net thickness [m]	S1 + S2 [mg HC/g rock]	Density [ρ]	SPI [tHC/m ²]
L. Miocene	1225	22,52	2.1	57,9
L. Oligocene	190	41,7	2.1	16,6

Table 3. Calculation of the source potential index (SPI) for samples of the Lower and Upper Menilite Members from the Chechva River profile.

Nearly 70 % of the proven reserves in the North and East Carpathian fold-thrust belt (2249 of 3279 MM boe; Boote et al., 2018) are concentrated in the Boryslav-Pokuttya nappe of Ukraine, where the Upper Menilite Member has a similar thickness to that in the external part of the Skyba nappe (e.g. Vialov et al., 1988; Kosakowski et al., 2018). It can therefore be proposed that the prolific nature of the Boryslav-Pokuttya petroleum system is mainly related to the large thickness of the Menilite Formation, the exceptional high SPI in this region, and the occurrence of these source rocks within the oil window. In addition, the Boryslav-Pokuttya petroleum system may have retained most of its hydrocarbons with less evidence of leakage (surface seeps) than in the SkoleSkyba and Silesian-Krosno petroleum systems (Boote et al., 2018).

7. Conclusions

The Lower Oligocene to Lower Miocene Menilite Formation at outcrop along the Chechva River in western Ukraine is approximately 1800 m thick and can be divided into Lower, Middle and Upper Members. The generally organic-matter lean Middle Member was considered previously to be of Late Oligocene age and was not studied in detail, but new nannoplankton data suggest an Early Miocene age for the unit. By contrast, the Early Oligocene and Early Miocene ages for the Lower and Upper Menilite Members were confirmed by the biostratigraphic data in this study.

The Lower Oligocene Lower Menilite Member is approximately 330 m thick, and contains chert beds (“lower chert horizon”) at its base and thin coccolith limestones in its upper part. The frequent sandstone beds, in particular in the lower part of the member (above the lower chert horizon), are interpreted as turbidite deposits. The total organic carbon (TOC) content of interbedded shale samples frequently exceeds 20 wt.% and averages 9.76 wt.%. HI values are up to 800 mgHC/gTOC and more typically range between 300 and 600 mgHC/gTOC in the rest of the section. Pr/Ph ratios >1.0 tend to refute a strictly anoxic setting and may suggest a suboxic to oxic environment or a high terrigenous input under oxic conditions. The high TOC contents are due to the abundant input of land-plant derived material, consistent with relatively low HI values (<400 mgHC/gTOC), very high Pr/Ph ratios (up to 5) and the presence of land-plant derived biomarkers. Biomarkers for diatoms are abundant in samples with high HI.

The Lower Miocene Upper Menilite Member is ~1300 m thick in the study area. However this thickness is limited to the external parts of the Skyba nappe and the neighbouring Boryslav-Pokuttya nappe. The member grades into the overlying molasse sediments of the Polyanitsa Formation. The average TOC content of shale samples from the member is 5.17 wt.%, and exceeds 20 wt.% in samples from near the base. Pr/Ph ratios decrease upwards and are in general lower (0.4 -1.3) than in the Lower Member.

Organic matter in both Lower and Upper Members is thermally immature and is dominated by oil-prone Type II kerogen. Differences in HI are controlled by varying proportions of land-plant and algal-derived organic matter. Although TOC contents and HI values are on average higher for the Lower Member than for the Middle and Upper Members, shales from the entire formation have a good to very good potential to generate oil. The Source Potential Index (SPI) for the Lower and Upper Members was calculated to be 16.6 and 57.9 tons of

hydrocarbons per m², respectively. These SPI values are higher than for any other profile in the Paratethys realm. The Menilite Formation in the neighbouring Boryslav-Pokuttya nappe, which has a similar thickness and a similar stratigraphic extent and which is in the oil window, probably also has similarly high SPI values. This may explain why approximately 70% of the proven hydrocarbon reserves in the northern and eastern Carpathian fold-thrust belt are found in the Boryslav-Pokuttya nappe.

ACKNOWLEDGEMENTS

The authors would like to thank Drs Yuriy Koltun and V. E. Shlapinski for their insights and expertise in the field. Reviews of a previous version by Alexander Kitchka, István Veto and an anonymous referee are acknowledged with thanks and improved the paper.

8. References

- ALEXANDER, R., KAGI, R. I., TOH, E. and VAN BRONSWIJK, W., 1988. The use of aromatic hydrocarbons for assessment of thermal histories in sediments. In: Purcell, P. G., Purcell, R. R. (Eds.): *The North West Shelf, Australia: Proceedings of the Petroleum Exploration Society of Australia*, Perth. Petroleum Exploration Society of Australia, Perth, Australia, 62-559.
- ANDREYEVA-GRIGOROVICH, A.S., GRUZMAN, A.D., REJFMAN, L.M. and SMIRNOV, S.E., 1986. Biostratigraphic characteristic of the Menilite suite standard section along the river Chechva (Ukrainian Carpathians). *Paleontol. Sbor.* 23, 83-89 (in Russian).
- ANDREYEVA-GRIGOROVICH, A.S. and GRUZMAN, A.D., 1994. The biostratigraphic basis of the Paleogene–Neogene boundary in the Central (Ukrainian Carpathians) and Eastern (Black Sea Depression, Northern Caucasus – Paratethys. *Geologica Carpathica*, 45, 333-342.
- ANDREYEVA-GRIGOROVICH, A.S., KULCHYSKY, Y.O., GRUZMAN, A.D., LOZYNIAK, P.Y., PETRASHKEVICH, M.I., PORTNYGINA, L.O., IVANINA, A.V., SMIRNOV, S.E., TRIFOMOVICH, N.A., SAVITSKAYA, N.A. and SHVAREVA, N.J., 1997. Regional stratigraphic scheme of Neogene formations of the Central Paratethys in the Ukraine. *Geologica Carpathica*, 48, 123-136.
- BEMIS, B.E., SPERO, H.J., BIJMA, J., and LEA, D.W., 1998. Reevaluation of the oxygen isotopic composition of planktonic foraminifers: Experimental results and revised paleotemperature equations. *Paleoceanography* 13, 2, 150-160.
- BERNER, R.A. and RAISWELL, R., 1984. C/S method for distinguishing freshwater from marine sedimentary rocks. *Geology*, 12, 365–368.
- BOJANOWSKI, M.J., CIUREJ, A., HACZEWSKI, G., and JOKUBAUKAS, P., 2018. The Central Paratethys during Oligocene as an ancient counterpart of the present-day Black Sea: Unique records from the coccolith limestones. *Marine Geology*. 403, 301-328.
- BOOTE, D.R.D., SACHSENHOFER, R.F., TARI, G. and ARBOUILLE, D., 2018. Petroleum provinces of the Paratethyan region. *Journal of Petroleum Geology*, 41, 247-298.
- BRAY, E.E. and EVANS, E.D., 1961. Distribution of n-paraffins as a clue to recognition of source beds. *Geochimica et Cosmochimica Acta*, 22, 2-15.
- DEMAISON, G. and HUIZINGA, B.J., 1994. Genetic classification of petroleum systems using three factors: charge, migration and entrapment. In: Magoon, L.B., Dow, W.G. (Eds.): *The Petroleum System, from Source to Trap*. AAPG Memoir, 60, 73-89.
- DINEL, H., SCHNITZER, M. and MEHUYS, G.R., 1990. Soil lipids: origin, nature, contents, decomposition and effect on soil physical properties. *Soil Biochemistry*, 12, 397-427.
- DZIADZIO, P., BORYS, Z., KUK, S. and PIETRUSIAK, M., 2006. Hydrocarbon Resources of the Polish Outer Carpathians—Reservoir Parameters, Trap Types, and Selected Hydrocarbon Fields: A Stratigraphic Review. *The Carpathians and Their Foreland: Geology and Hydrocarbon Researches*.
- DZIADZIO, P.S., MATYASIK, I., GARECKA, M. and SZYDLO, A., 2016. Lower Oligocene Menilite Beds, Polish Outer Carpathians: supposed deep-sea flysch locally

- reinterpreted as shelfal, based on new sedimentological, micropalaeontological and organic-geochemical data. *Prace Naukowe Instytutu Nafty i Gazu - Państwowy Instytut Badawczy*, 213, 1-120.
- ESPITALIÉ, J., MARQUIS, F. and BARSONY, I., 1984. Geochemical logging. In: Voorhess, K..J. (Ed.): *Analytical Pyrolysis*. Butterworths, Boston, 53-79.
- FRIEDMAN, I., and O'NEIL, J.R., 1977. Compilation of stable isotope fractionation factors of geochemical interest. In: M. Fleischer (ed.). *Data of Geochemistry*. US Geological Survey the Professional Paper, 6, 440-456.
- HACZEWSKI, G., 1989. Cocolith limestone horizons in the Menilite-Krosno series (Oligocene, Carpathians) – identification, correlation and origin. *Annales Societatis Geologorum Poloniae*, 59, 435-523 (in Polish with English abstract).
- HUANG W.Y. and MEINSCHEN W.G., 1979. Sterols as ecological indicators. *Geochimica et Cosmochimica Acta*, 43, 739-745
- HUGHES, W.B., HOLBA, A.G. and DZOU, L.I.P., 1995. The ratios of dibenzothiophene to phenanthrene and pristane to phytan as indicators of depositional environment and lithology of petroleum source rocks. *Geochimica et Cosmochimica Acta*, 59, 3581-3598.
- IRWIN, H., CURTIS, C.D., and COLEMAN, M., 1977. Isotopic evidence for source of diagenetic carbonates formed during burial of organic-rich sediments. *Nature*, 269, 209-213.
- KOLTUN, Y.V., 1992. Organic matter in Oligocene Menilite formation rocks of the Ukrainian Carpathians: palaeoenvironment and geochemical evolution. *Organic Geochemistry*, 18, 423-430.
- KOLTUN, Y.V., ESPITALIE, J., KOT, M., ESPITALIE J., KOTARBA, M., ROURE, F., ELLOUZ, N. and KOSAKOWSKI, P., 1998. Petroleum Generation in the Ukrainian External Carpathians and the adjacent Foreland. *Journal of Petroleum Geology*, 21, 265-288.
- KOSAKOWSKI, P., KOLTUN, Y., MACHOWSKI, G., POPRAWA, P. and PAPIERNIK, B., 2018. Geochemical characterization of the Oligocene Menilite Formation in the Polish and Ukrainian Carpathians. *Journal of Petroleum Geology*, 41, 319-336.
- KÖSTER, J., KOTARBA, M., LAFARGUE, E. and KOSAKOWSKI, P., 1998. Source rock habitat and hydrocarbon potential of Oligocene Menilite Formation (Flysch Carpathians, Southeast Poland): An organic geochemical and isotope approach. *Org. Geochemistry*, 29, 543-558.
- KOTARBA, M.J. and KOLTUN, Y.V., 2006. The origin and habitat of hydrocarbons of the Polish and Ukrainian parts of the Carpathian Province. In: Golonka, J, Picha, F. J. (Eds): *The Carpathians and their foreland: Geology and hydrocarbon resources*. 84, 395-442.
- KOTARBA, M., WIECLAW, D., KOLTUN, Y., MARYNOWSKI, L., KUSMIEREK, J. and DUDOK, I., 2007. Organic geochemical study and genetic correlation of natural gas, oil and Menilite source rocks in the area between San and Stryi rivers (Polish and Ukrainian Carpathians). *Organic Geochemistry*, 38, 1431-1456.
- KOTARBA, M. J. and NAGAO, K., 2008. Composition and origin of natural gases accumulated in the Polish and Ukrainian parts of the Carpathian region: Gaseous

- hydrocarbons, noble gases, carbon dioxide and nitrogen. *Chemical Geology*, 255, 426-438.
- KOTARBA, M., WIECLAW, D., KOSAKOWSKI, P., WROBEL, M., MATYSZKIEWICZ, J., BULA, Z., KRAJEWSKI, M., KOLTUN, Y. and TARKOWSKI, J., 2012. Petroleum systems in the Palaeozoic-Mesozoic basement of the Polish and Ukrainian parts of the Carpathian Foredeep. *Annales Societatis Geologorum Poloniae*, 81, 487-522.
- KOTARBA, M., WIECLAW, D., BILKIEWICZ, E., RADKOVETS, N.Y., KOLTUN, Y.V., KMIECIK, N., ROMANOWSKI, and T., KOWALSKI, A., 2019. Origin and migration of oil and natural gas in the western part of the Ukrainian Outer Carpathians: Geochemical and geological approach. *Marine and Petroleum Geology*, 103, 596-619.
- KOTLARCZYK, J. and UCHMAN, A., 2012. Integrated ichnology and ichthyology of the Oligocene Menilite Formation, Skole and Subsilesian nappes, Polish Carpathians: A proxy to oxygenation history. *Palaeogeography, Palaeoclimatology, Palaeoecology*, 331-332, 104-118.
- KOTLARCZYK, J., JERZMANSKA, A., SWIDNICKA, E. and WISZNIOWSKA, T., 2006. A framework of ichtyofaunal ecostratigraphy of the Oligocene-Early Miocene strata of the Polish Outer Carpathian Basin. *Annales Societatis Geologorum Poloniae*, 76, 1-111.
- KOVAC, M., Hudáčková, N., Halásová, E., Kováčová, M., Holcová, K., Oszczypko-Clowes, M., Báldi, K., Less, G., 5, NAGYMAROSY, A., Ruman, A., Klučiar, T. and Jamrich, M., 2017. The Central Paratethys palaeoceanography: a water circulation model based on microfossil proxies, climate, and changes of depositional environment. *Acta Geologica Slovaca*, 9, 75-114.
- KRUGE, M., MASTALERZ, M., SOLECKI, A. and STANKIEWICZ, B., 1996. Organic geochemistry and petrology of oil source rocks, Carpathian Overthrust region, southeastern Poland – implications for petroleum generation. *Organic Geochemistry*, 24, 897-912.
- KULCHYTSKY, Y.O., and SOVCHYK, Y.V., 1986. To the problem of Paleogene-Neogene border in Carpathians. *Paleontologicheskii sbornik* 23, 89-99. (in Russian with English abstract).
- KUSMIEREK, J., BARAN, U. and GOLONKA, J., 2013. Tectonic and geological characteristic of the eastern part of the Polish Carpathians and transborder zone with Ukraine. In: Gorecki, W. (ed.) *Geothermal atlas of the Eastern Carpathians*. AGH University of Science and Technology, Kraków, 74-102.
- LOURENS, L., HILGEN, F., SHACKLETON, N.J., LASCAR, J. and WILSON, J., 2004. Orbital tuning calibrations and conversions for the Neogene Period. In: Gradstein, F., Ogg, J., Smith, A. (Eds.): *A Geologic Time Scale 2004*, Cambridge University Press, 469-484.
- Martini E., 1971: Standard Tertiary and Quaternary calcareous nannoplankton zonation. *Proceedings of the II Planktonic Conference*. Tecnoscienza, Roma, 739-785.
- MELINTE-DOBRINESCU, M. and BRUSTUR, T., 2008. Oligocene – Lower Miocene events in Romania. *Acta Palaeontologica Romaniaae*, 6, 203-215.

- MICLAUS, C., LOIACONO, F., PUGLISI, D. and BACIU, D.S., 2009. Eocene-Oligocene sedimentation in the external areas of the Moldavide Basin (Marginal Folds Nappe, Eastern Carpathians, Romania): sedimentological, paleontological and petrographical approaches. *Geologica Carpathica*, 60, 397-417
- MOLDOWAN, J.M. and FAGO, F.J., 1986. Structure and significance of a novel rearranged monoaromatic steroid hydrocarbon in petroleum. *Geochimica et Cosmochimica Acta*, 50, 343–51.
- MOLDOWAN J. M., DAHL J., HUIZINGA B. J., FAGO F. J., HICKEY L. J., PEAKMAN T. M. and TAYLOR D. W., 1995. The molecular fossil record of oleanane and its relation to angiosperms. *Science*, 265, 768-777.
- Nakapelukh, M., Bubniak, I., Yegorova, T., Murovskaya, A., Gintov, O., Shlapinskyi, V. and Vikhot, Yu., 2017. Balanced geological cross-section of the outer ukrainian carpathians along the pancake profile. *Journal of Geodynamics*, 108, 13-25.
- NICHOLS, P.D., VOLKMAN, J.K., PALMISANO, A.C., SMITH, G.A. and WHITE, D.C., 1988. Occurrence of an isoprenoid C₂₅ diunsaturated alkene and a high neutral lipid content in Antarctic Sea-Ice diatom communities. *Journal of Phycology*, 24, 90-96.
- OURISSON, G., ALBRECHT, P. and ROHMER, M., 1979. The hopanoids: palaeo-chemistry and biochemistry of a group of natural products. *Pure Applied Chemistry*, 51, 709-729.
- PERCH-NIELSEN K., 1985. Cenozoic calcareous nannofossils. In: Bolli, H.M., Saunders, J.B. & Perch-Nielsen, K. (Eds.): *Plankton stratigraphy*. Cambridge University Press, 427-554.
- PETERS, K.E., WALTER, C.C. and MOLDOWAN, J.M., 2007. Biomarkers and Isotopes in Petroleum Systems and Earth History. *The Biomarker Guide 2*, 499-502.
- PICHA, F.J., STRANIK, Z. and KREJCI, O., 2006, Geology and hydrocarbon resources of the Outer Western Carpathians and their foreland, Czech Republic. In: Golonka, J., Picha, F. J. (Eds): *The Carpathians and Their Foreland: Geology and Hydrocarbon Researches: AAPG Memoir*, 84, 221-258.
- Popadyuk, I., Vul, M., Ladyzhensky, G. and Shpak, P., 2006, Petroleum geology of the Boryslav – Pokuttya zone, the Ukrainian Carpathians. In: Golonka, J., Picha, F. J. (Eds): *The Carpathians and Their Foreland: Geology and Hydrocarbon Researches: AAPG Memoir*, 84, 455-466.
- POPOV, S.V., RÖGL, F., RAZNOV, A.Y, STEININGER, F.F., SHCHERBA, I.G. and KOVAC, M., 2004. Lithological Paleogeographic maps of Paratethys. 10 Maps Late Eocene to Pliocene, volume 250. Courier Forschungsinstitut Senckenberg.
- RADKE, M. WILLISCH, H. and WELTE, D.H., 1980. Preparative hydrocarbon group type determination by automated medium liquid pressure chromatography. *Anal. Chem.* 52, 406-411.
- RADKOVETS, N., RAUBALL, J. and IAREMCHUK, I., 2017. Silurian black shales of Western Ukraine: petrography and mineralogy. *Estonian Journal of Earth Sciences*, 66, 161–173.
- SACHSENHOFER, R.F. and KOLTUN, Y.V., 2012. Black shales in Ukraine - A review. *Marine and Petroleum Geology*, 31, 125-136.

- SACHSENHOFER, R.F., POPOV, S.V., BECHTEL, A., CORIC, S., FRANCU, J., GRATZER, R., GRUNERT, P., KOTARBA, M., MAYER, J., PUPP, M., RUPPRECHT, B.J. and VINCENT, S.J., 2018a. Oligocene and Lower Miocene source rocks in the Paratethys: Palaeogeographical and stratigraphic controls. In: Simmons, M. et al. (Eds): Geological Society London Special Publication, 464.
- SACHSENHOFER, R.F., POPOV, S.V., CORIC, S., MAYER, J., MISCH, D., MORTON, M.T., PUPP, M., RAUBALL, J. and TARI, G., 2018b. Paratethyan petroleum source rocks: an overview. *Journal of Petroleum Geology*, 41, 219-245.
- SCHULZ, H.M., SACHSENHOFER, BECHTEL, A., POLESNY, H. and WAGNER, L., 2002. The origin of hydrocarbon source rocks in the Austrian Molasse Basin (Eocene–Oligocene transition). *Marine and Petroleum Geology*, 19, 683-709.
- SCHULZ, H.M., BECHTEL, A. and SACHSENHOFER R.F., 2005. The birth of the Paratethys during the early Oligocene: from Tethys to an ancient Black Sea analogue? *Global and Planetary Change*, 49, 163-176.
- SHLAPINSKI, V.E., 2012. About the detailed subdivision of the Oligocene deposits of Skyba and Krosno nappes. Proceedings of the XXXIV session of the Paleontologic Society of NAS of Ukraine. Kyiv: Institute of Geological Sciences. 86-88 (In Ukrainian).
- SIMONEIT, B.R.T., 1986. Cyclic terpenoids of the geosphere. In: Johns, R. B. (Ed.): *Biological Markers in the Sedimentary Record* Elsevier, New York, 43–99.
- SINNINGHE DAMST'E, J.S., KOCK-VAN DALEN, A.C., DE LEEUW, J.W., SCHENCK, P.A., GUOYING, S. and BRASSELL, S.C., 1987. The identification of mono-, di- and trimethyl 2-methyl-2 (4,8,12-trimethyltridecyl) chromans and their occurrence in the geosphere. *Geochimica et Cosmochimica Acta*, 51, 2393-2400.
- SLACZKA, A., KRUGLOV, S., GOLONKA, J., OSZCZYPKO, N. and POPADYUK, I., 2006. Geology and Hydrocarbon Resources of the Outer Carpathians, Poland, Slovakia, and Ukraine: General Geology. In: Golonka, J., Picha, F. J. (Eds): *The Carpathians and Their Foreland: Geology and Hydrocarbon Researches: AAPG Memoir*, 84, 221-258.
- SUMMONS, R. E., BARROW, R. A., CAPTON, R. J. and HOPE, J. M., 1993. The structure of a new C25 isoprenoid alkene biomarker from diatomaceous microbial communities. *Australian Journal of Chemistry*, 46, 407-413.
- SVABENICKA, L., BUBIK, M. and STRANIK, Z. 2007. Biostratigraphy and paleoenvironmental changes on the transition from the Menilite to Krosno lithofacies (Western Carpathians, Czech Republic). *Geologica Carpathica*, 58, 237–262.
- Sylvester, Z. and Lowe D.R., 2004. Textural trends in turbidites and slurry beds from the Oligocene flysch of the East Carpathians, Romania. *Sedimentology*, 51, 945-972.
- TAYLOR, G.H., TEICHMÜLLER, M., DAVIS, A., DIESSEL, C.F.K., LITTKER, R. and ROBERT, P., 1998. *Organic Petrology*. Gebrüder Bontaege, Berlin, 655-704.
- TOLEDO, A.L.F., CACHAO, M., COSTA, B.K. and PIVEL, G.A.M., 2007. Planktonic foraminifera, calcareous nannoplankton and ascidian variations during the last 25 kyr in the Southwestern Atlantic: A paleoproductivity signature? *Marine Micropaleontology*, 64, 67–79.
- VAROL, O. and HOUGHTON, S.D., 1996. A review and classification of fossil didemnid ascidian spicules. *Journal of Micropalaeontology*, 15, 135-149.

- VETÖ, I., HETENYI, M., HAMOR-VIDO, M., HUFNAGEL, and H., HAAS, J., 2000. Anaerobic degradation of organic matter controlled by productivity variation in a restricted late Triassic basin. *Organic Geochemistry*, 31, 439-452.
- VETÖ, I., 1987. An Oligocene sink for organic carbon: Upwelling in the Paratethys? *Palaeogeography, Palaeoclimatology, Palaeoecology*, 60, 143-153.
- VIALOV, O.S., GAVURA, S.P., DANYSH, V.V., LEMISHKO, O.D., LESHCHUKH, R.Y., PONOMARIOVA, L.P., ROMANIV, A.M., SMIRNOV, S.E., SMOLINSKA, N.I. and TSARNENKO, P.N., 1988. Stratotypes of the Cretaceous and Paleogene deposits of the Ukrainian Carpathians (in Russian). Nauka dumka, Kiev. 204 pp.
- VOLKMAN, J. K., BARRETT, S. M. and DUNSTAN, G. A., 1994. C25 and C30 highly branched isoprenoids in laboratory cultures of two marine diatoms. *Organic Geochemistry*, 21, 407-414.
- WAKEHAM, S. G., SCHAFFNER, C. and GIGER, W., 1980. Polycyclic aromatic hydrocarbons in recent lake sediments – II. Compounds derived from biogenic precursors during early diagenesis. *Geochimica et Cosmochimica Acta*, 44, 415–29.
- ZOLITSCHKA, B., 1988. Spätquartäre Sedimentationsgeschichte des Meerfelder Maares (Westeifel).—Mikrostratigraphie jahreszeitlich geschichteter Seesedimente. *Quaternary Science Journal*, 381, 1988-01-01.

Hydrocarbon potential of the Lower Cretaceous (Barremian-Albian) Shypot Formation in the Chornohora nappe, Ukraine

J. F. Rauball^{a*}, R. F. Sachsenhofer^a, A. Bechtel^a

^aChair of Petroleum Geology, Montanuniversitaet Leoben, 8700 Leoben, Austria.

Published in:

Accepted for publication in *Geologica Carpathica*

* Corresponding author. johannes.rauball@gmail.com

Address: Chair of Petroleum Geology, Montanuniversitaet Leoben, Peter-Tuner Straße 5, A-8700 Leoben

Keywords: Carpathians, Lower Cretaceous, source rocks, organic geochemistry, Rock-Eval, kerogen type, organic matter, maturity

Research Highlights:

The Shypot Formation contains an average total organic carbon content of 2.8 wt.%

Organic matter indicates peak oil maturity (~0.85%Rr)

Average HI values and the remaining petroleum potential are low due to higher maturities

It is estimated that approximately 2 tHC/m² have been generated during deep burial

Abstract

Organic matter-rich rocks occur in the Carpathians, both in Lower Cretaceous and Oligocene. Whereas, the Oligocene Menilite Formation has been intensely studied, the hydrocarbon potential of Lower Cretaceous rocks is less well understood. In the present paper a 405 m thick succession of the lower part of the Shypot Formation in the Chornohora nappe (Ukraine) is studied using 94 outcrop samples.

Maturity parameters for the Lower Cretaceous rocks indicate peak oil maturity ($\sim 0.85\%R_r$) and organic carbon content averages 2.8 wt.% for all samples. As a result of the enhanced maturity, the hydrogen index (88 mgHC/gTOC) and the remaining petroleum potential (2 tHC/m²) are low. Comparisons with coeval rocks from the same tectonic unit, but with lower maturity suggest that the original petroleum potential was significantly higher (4 tHC/m²). Probably about 2 tHC/m² have been generated during deep burial (6 km?), but were lost during uplift and erosion. Macerals analysis reveals a mixed type III-II kerogen, with domination of terrigenous components, which is also supported by HI values of nearby marginal mature samples (~ 200 mgHC/gTOC).

Lower Cretaceous organic matter-rich rocks are found along the entire Carpathian arc. A compilation of published data for age-equivalent rocks across the Carpathian Fold-Thrust Belt shows that HI values are mainly controlled by maturity as well as the moderately high original HI values. Most of these rocks contain predominantly type III-II kerogen, whereas Lower Cretaceous rocks in the Skole-Skyba nappe near the Polish-Ukrainian border contain type (III-) IV kerogen.

Table of Content

1. Introduction	93
2. Geological setting	95
2.1. Stratigraphy and tectonics	95
2.2. Lithology of the Early Cretaceous strata	95
3. Petroleum Systems	96
4. Samples and Methods	97
5. Results	99
5.1. Lithology	99
5.2. Bulk parameters of organic matter and maceral composition	99
5.3. Molecular composition of hydrocarbons	103
6. Discussion	107
6.1. Maturity and burial depth	107
6.2. Remaining and original source rock potential	107
6.3. Organic matter type and depositional environment	109
6.4. Comparison with coeval rocks in the Carpathian Basin	110
7. Conclusion	113
8. References	114

1. Introduction

The Ukrainian Carpathians form the NE part of the Carpathian orogenic belt which stretches for approximately 1300 km from Vienna to the Iron Gate on the River Danube in Romania (Slaczka et al., 2006; Fig. 1a). They host one of the oldest petroleum-producing provinces in the world (Boote et al., 2018). Petroleum production began in 1854 with the discovery of the Boryslav oil field, one of the largest onshore oilfields in Europe (Kotarba et al., 2007). All oil and gas fields are located within the Outer Carpathians, bordered to the NE by a molasse-filled foredeep and to the SW by the Pieniny Klippen belt. Internally, the Outer Carpathians consist of a series of structurally complex, NE-verging nappes which comprise rocks that are Early Cretaceous to Early Miocene in age (Slaczka et al., 2006; Nakapelyukh et al., 2018).

The Lower Oligocene to Lower Miocene Menilite Formation is the primary source rock interval in the Carpathians and has been studied extensively in the past (e.g. Curtis et al., 2004; Kotarba et al., 2007; Kosakowski et al., 2018, Sachsenhofer et al., 2018a,b; Jirman et al., 2019; Jirman and Gerslova, 2019; Rauball et al., 2019 cum lit.). In contrast, information on organic matter-rich Lower Cretaceous rocks is limited (e.g. Kruge et al., 1996; Kotarba and Koltun, 2006; Kotarba et al., 2013, 2014; Slaczka et al., 2014). For example, only few data are available from the Barremian to Albian Shypot and Spas formations in the Ukraine (Koltun et al., 1998), as all economic hydrocarbon accumulations in the Ukrainian Carpathians have been correlated to the Menilite Formation (Kotarba et al., 2019), although the authors state that a contribution of Lower Cretaceous source rocks cannot be excluded.

The main goal of the present contribution is to provide an analysis of the vertical variation of organic matter content and hydrocarbon potential of the Lower Cretaceous Shypot Formation, a potential source rock, several hundred metres thick. For this, we selected a well-exposed outcrop section west of the village Bystrets in the Chornohora nappe (Fig. 1b). The study results are compared to source rock data from other areas in the Carpathian Fold-Thrust Belt and will contribute to a better understanding of the petroleum system, particularly in the internal parts of the fold-belt, which are still relatively unexplored.

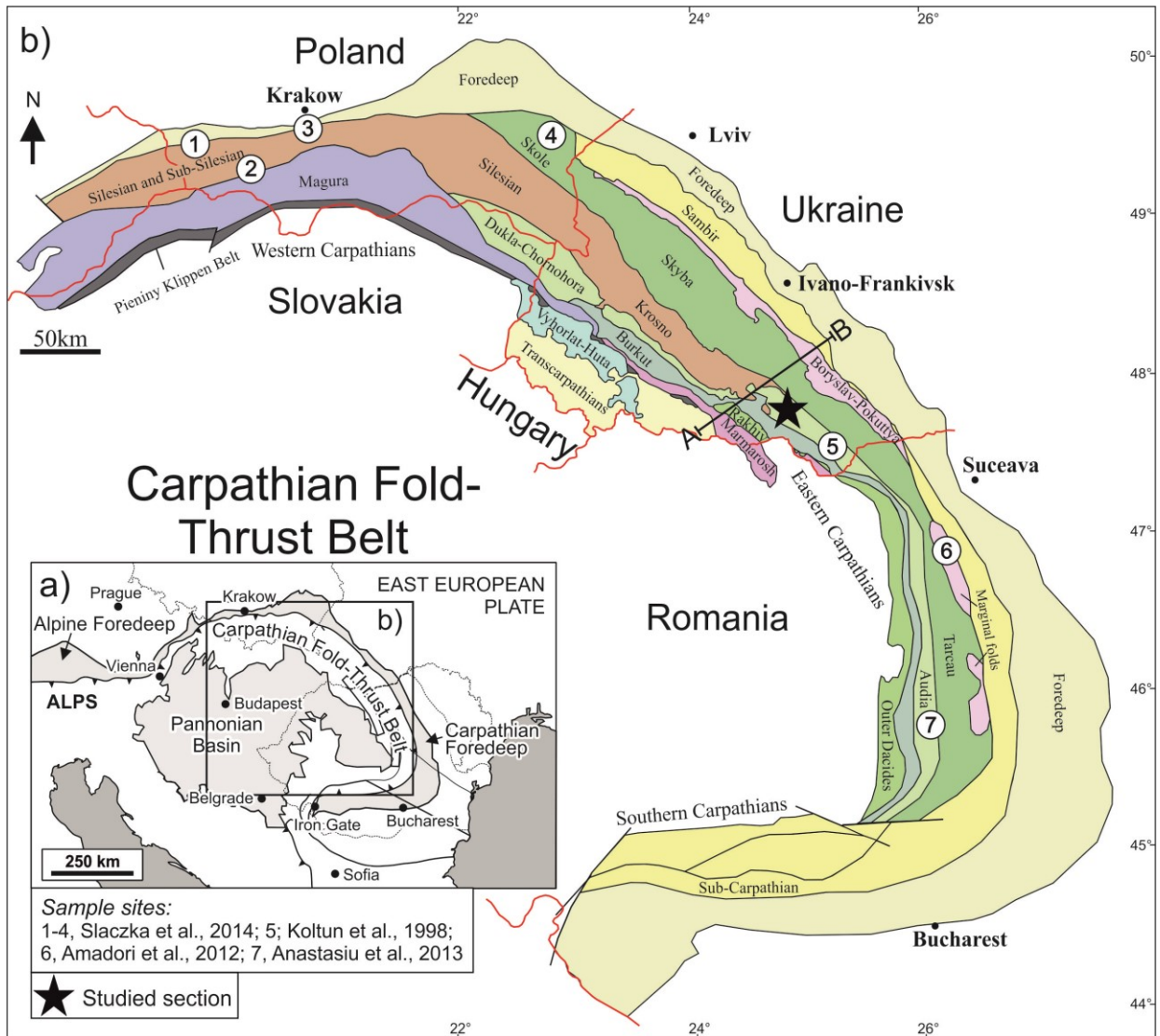


Fig. 1: (a) Outline map of central-eastern Europe showing the location of the study area in the Carpathian orogenic belt. (b) Structural map of the Carpathian Fold-Thrust Belt (after Nakapelyukh et al., 2018; Oszczytko et al., 2006; Slaczka et al., 2006) with the location of the studied section in western Ukraine. Locations of profiles (1-9) with comparative samples are also shown.

2. Geological setting

2.1 Stratigraphy and tectonics

The Outer Carpathians comprise a series of nappes which have been thrust NE-ward, during Early Miocene tectonism, onto the SW margin of the East European Plate (Slaczka et al., 2006). In Ukraine, the following thrust sheets are distinguished from the NE (i.e. the most external part of the thrust-belt) to the SW (most internal): Sambir (Stebnik), Boryslav-Pokuttya, Skyba (Skole), Krosno (Silesian), Dukla-Chornohora, Burkut, Magura, and Rhakiv (Nakapelyukh et al., 2018; Fig. 1b). The tectonic position of the Chornohora nappe is not completely clear (see Slaczka et al., 2006). According to Nakapelyukh et al. (2018), the Chornohora nappe corresponds to the Dukla nappe, and therefore is often regarded as the Dukla-Chornohora nappe.

Each thrust-sheet represents a separate or partly separate sedimentary sub-basin containing different lithostratigraphy and tectonic structures (Golonka et al., 2006). Strata in the Outer Carpathians ranges from Early Cretaceous to Early Miocene in age and may locally exceed thicknesses of 6 km (Slaczka et al., 2006). During overthrusting, the tectonic units became uprooted, and generally only the central parts of the basins are preserved (Slaczka et al., 2006).

2.2 Lithology of the Early Cretaceous strata

Early Cretaceous black shales make up the base of the flysch belt. They were deposited in oxygen-depleted marine conditions, which partly coincide with a global anoxic event during Barremian to Albian times (OAE-1; Schlanger and Jenkyns, 1976; Jenkyns, 1980), and are assigned to either the Shypot or the Spas Formation, depending on their tectonic position. The Spas Formation is confined to the Skole-Skyba Nappe and crops out locally in the NW part of the nappe (Vialov et al., 1988), whereas the Shypot Formation crops out frequently in the internal Krosno, Dukla-Chornohora and Burkut nappes.

Both formations are primarily composed of organic-rich black shales with minor siltstones and sandstones in their lower part and by thick-bedded sandstones in their upper part. The thickness of the organic-rich part of the Spas Formation in the Skyba Nappe (approximately 200 m; Kotlarczyk, 1988) is typically lower than that of the Shypot Formation (up to 300 m; Slaczka et al., 2006). As described by Slaczka et al. (2006), the upper part of the Shypot Formation in the Chronohora nappe comprises 200 m of dark, quartzitic sandstone with black shale intercalations (Albian in age). The studied section is located within the south-eastern

part of the Ukrainian Outer Carpathians where Lower Cretaceous sediments outcrop within the Dukla-Chornohora nappe (Fig. 2).

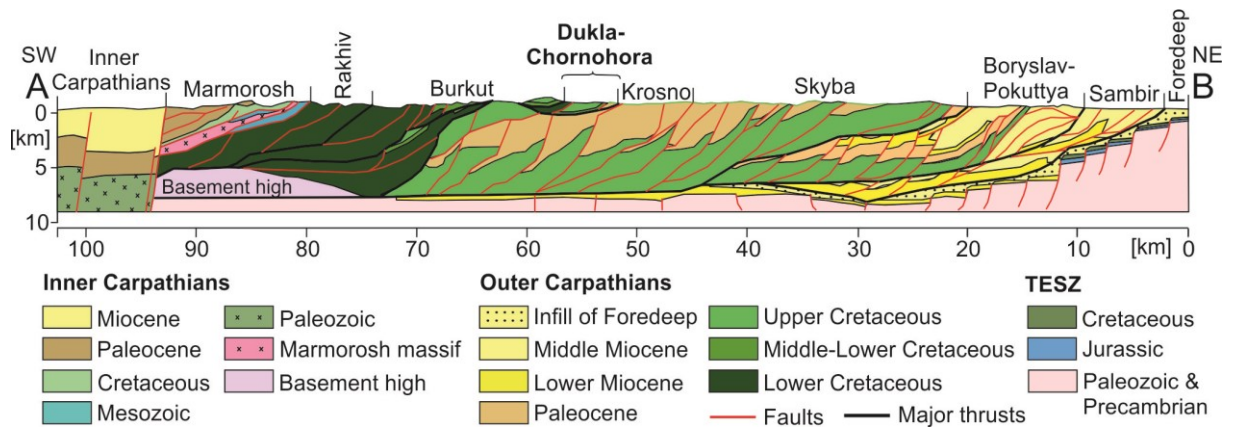


Fig. 2: Cross-section (A-B) of the Ukrainian Carpathians (modified after Shlapinskyi, 2015; Nakapelyukh et al., 2018)

3. Petroleum Systems

The Ukrainian Outer Carpathians host two organic rich horizons: the Lower Cretaceous (Barremian-Albian) Shypot and Spas Formations and the Oligocene-Lower Miocene Menilite Formation (e.g. Sachsenhofer and Koltun, 2012). The genetic potential of the source rocks increases from the Jurassic to the Oligocene-Lower Miocene Menilite Formation in the Outer Carpathians (Francu et al., 1996). The Menilite Formation is the primary source rock interval of the region (Kotarba and Koltun, 2006) and contains very high TOC contents (locally exceeding 20 wt.%) with HI values up to 800 mgHC/gTOC (Rauball et al., 2019 cum lit.)

The Shypot and Spas formations are considered as additional potential source rocks (Kotarba and Koltun, 2006). Their TOC is generally greater than 2 wt.% and may reach as much as 8 wt.%. Rock-Eval data show that the shales contain a type III or II/III kerogen (Sachsenhofer and Koltun, 2012). A type III kerogen is also indicated by the presence of high percentages of vitrinite (Kruge et al., 1996). Despite the occurrence of this potential source rock, no Cretaceous-sourced oil and gas has been identified across Ukrainian territory (Boote et al., 2018; Kotarba et al., 2019). However, according to Więclaw et al. (2020), gaseous hydrocarbons in the eastern part of the Polish Outer Carpathians originated from Upper Cretaceous–Palaeocene Istebna shales or Lower Cretaceous strata (Veřovice, Lgota and Spas shales).

4. Samples and Methods

For this study, 94 samples from the Shypot Formation in the Chornohora nappe were collected from an outcrop along a small tributary of the river Bystrets, west of the village Bystrets (base of section: 48°07'18" N 24°38'27" E), Iwano-Frankiivsk, Ukraine. All samples were cleaned (using water), dried (at 30°C in a drying-cabinet for two days) and pulverized (to a fraction below 0.2 mm; using a stone grinding machine) before laboratory analyses were performed.

The samples were analysed for their total carbon (TC), total sulphur (TS) and total organic carbon content (TOC) using an ELTRA Elemental Analyser and calcium carbonate (12.00 % Carbon) as a standard. Samples measured for TOC were treated twice with 50% phosphoric acid to remove inorganic carbon. Results are based on the averages of at least two corresponding measurements and are given in weight percent (wt.%). The total inorganic carbon (TIC) was determined by subtracting the TC with the TOC. TIC was then used to calculate the calcite equivalent percentages ($=\text{TIC} \times 8.333$ - which is the stoichiometric factor or CaCO_3).

Rock-Eval pyrolysis was carried out using a "Rock-Eval 6" analyser in order to determine the S_1 , S_2 peaks (mgHC/grock) and T_{max} for all samples. The S_1 peak records hydrocarbons volatilized at 300°C and determines the amount of hydrocarbons present in the rock, whereas the S_2 peak is produced during gradual heating from 300 to 650°C, and determines the amount of hydrocarbons formed during pyrolysis. The petroleum potential (S_1+S_2 [mgHC/grock]), the hydrogen index ($\text{HI} = S_2 \times 100 / \text{TOC}$ [mgHC/gTOC]) and the Production Index ($S_1 / [S_1+S_2]$) were calculated. T_{max} is a maturity parameter and indicates the temperature during Rock-Eval pyrolysis at which the maximum amount of hydrocarbons can be generated (Espitalié et al., 1984). S_1 , S_2 and T_{max} results are based on the average of at least two measurements.

Based on the TOC contents and HI values (preferably higher values), a total of 24 samples were selected at similarly spaced intervals across the Shypot Formation for biomarker analyses. Samples were extracted in a Dionex ASE 200 accelerated solvent extractor using dichloromethane at 75° C and 50 bar for approximately 1 hour. Asphaltenes were precipitated from the solution using a hexane–dichloromethane solution (80:1) and then separated by centrifugation (1000 rpm). The hexane-soluble fractions were separated into NSO compounds, saturated hydrocarbons and aromatic hydrocarbons using medium pressure liquid chromatography (MPLC) with a Köhnen-Willsch instrument (Radke et al., 1980). The

saturated and aromatic hydrocarbon fractions were analysed by a gas chromatograph equipped with a 30 m DB-5MS fused silica column (i.d. 0.25 μm ; 0.25 μm film thickness), coupled to a ThermoFisher ISQ Dual-quadrupole mass spectrometer. Using helium as the carrier gas, the oven temperature of the GC was set to increase from 70° C to 300° C at 4° C min⁻¹, which was followed by an isothermal period of 15 min. With the injector temperature set to 275° C, the sample was injected with a split ratio of 10. The spectrometer was operated in the EI (electron ionization) mode over a scan range from m/z 50 to 650 (0.7 s total scan time). Data was processed using an Xcalibur data system where individual compounds were identified on the basis of retention time in the total ion current (TIC) chromatogram and by comparison of the mass spectra with published data (e.g. Peters et al., 2007). Percentages and absolute concentrations of various compound groups in the saturated and aromatic hydrocarbon fractions were calculated using peak areas from the gas chromatograms and their relations to the internal standards (deuterated *n*-tetracosane and 1,1'-binaphthyl, respectively). Concentrations were adjusted according to the TOC content of each sample.

The samples used for biomarker analysis were also selected for organic petrographic investigations (with the exception of one sample, where not enough material was available for further analysis). In total, 23 polished blocks were prepared for semi-quantitative maceral analysis. Maceral composition was determined using white light and fluorescence light. Vitrinite reflectance measurements were determined using a Leica microscope and following established procedures (Taylor et al., 1998).

The Methylphenanthrene Index-1 (MPI-1) was calculated following the equation: $(1.5 \times (2\text{-MP} + 3\text{-MP}) / (\text{Phen} + 9\text{-MP} + 1\text{-MP}))$. The MPI-1 was then used to calculate vitrinite reflectance following the equation ($R_c = 0.60 \text{ MPI-1} + 0.40$) proposed by Radke and Welte (1982) Phen – Phenanthrene, MP – Methylphenanthrene.

5. Results

5.1. Lithology

At the study location in the Chornohora nappe, the lower black shale part of the Shypot Formation is estimated to be about 400 m thick, which is slightly thicker than the 300 m thick lower part of the Shypot Formation analysed by Slaczka et al. (2006). The sandstone-rich upper part of the Shypot Formation (Slaczka et al., 2006) was not encountered and may be missing in this part of the Chornohora nappe. The base of the formation, which is marked by an unconformity, is fault-bound and underlying sediments were not exposed. The studied section is primarily composed of organic-rich black shales with minor siltstone and sandstone beds. Organic-rich shale intervals are represented by brighter and darker shale intervals. Darker shales outnumber the lighter shales significantly throughout the entire section. Surprisingly, the lighter shales analysed at 0 m, 257.5 m, 324 m, 332 m, and 385 m (all positions are relative to the top of the formation) contain a lower carbonate content (average: 3.0 wt.%) than the darker shales (average: 8.0 wt.%). Carbonate content is highest in the middle of the formation (max. 38.5 wt.%) and generally decreases slightly towards the top. Sandstones are typically 30 to 40 cm thick (max. 1.5 m). They are fine- to middle-grained and occur frequently throughout the formation. The percentage of sandy sediments is in the order of approximately 35 %. Sedimentary structures such as dewatering structures are present in some sandstone beds.

5.2. Bulk parameters of organic matter and maceral composition

The TOC content of black shales of the Shypot Formation in the Chornohora nappe averages 2.8 wt.% (Table 1; Fig. 3). Maximum TOC contents (up to 9.4 wt.%; Fig. 3) occur 280 to 325 m below the top of the section. HI values are low (average: 88 mgHC/gTOC; max. 185 mgHC/gTOC; Table 1; Figs. 3, 4) and increase slightly in the upper part of the section. On average, the grey shales contain a lower TOC content (average: 0.86 wt.%) and lower HI values (average: 49 mgHC/gTOC) than the black shales. T_{\max} values (average: 456°C; Table 2) show a general upward decreasing trend. Production Index (PI) values range from 0.06 to 0.26 (average 0.13). The calcite equ. varies considerably (Fig. 3), and reaches a maximum of 38.5 wt.% in the lower part of the section.

Sulphur contents reach a maximum of 2.5 wt.% (Fig. 3). TOC/S ratios (Fig. 3), which are commonly used as a parameter to distinguish between anoxic and oxic conditions, as well as between marine and freshwater deposits (Bernier and Raiswell, 1984), range from 0.7 to 5.2

(average 2.4) in samples with at least 0.3 wt.% TOC. TOC/S ratios generally increase slightly in the upper part of the section.

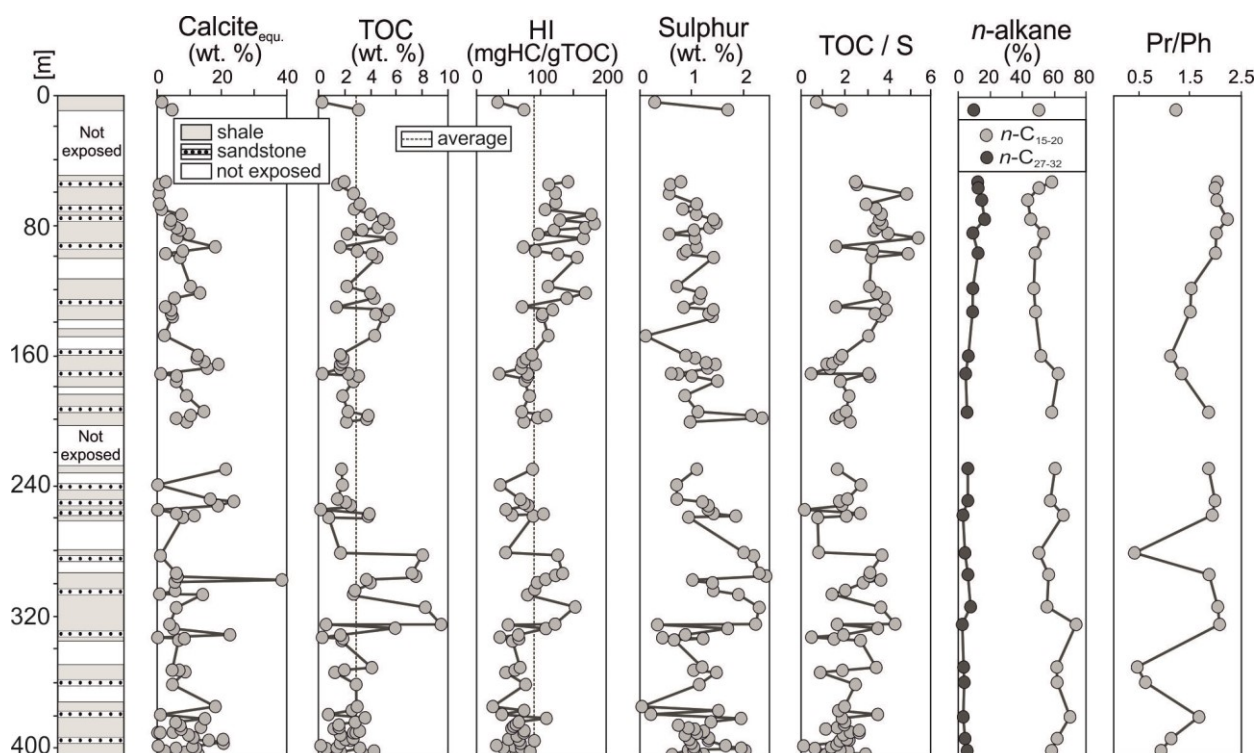


Fig. 3: Geochemical data for the Shypot Formation in the Chornohora nappe. Calcite equ. – calcite equivalents; TOC – total organic carbon; HI – Hydrogen Index; S – Sulphur; Pr/Ph – Pristane/Phytane.

Yields of extractable organic matter (EOM) for a subset of samples from the Shypot Formation vary from 3.70 to 22.78 mg/g TOC (average: 9 mg/g TOC; Table 2). Extracts from all samples are primarily dominated by NSO compounds (31 to 81% of the EOM), with the exception for sample 281 m (from the top of the section) which contains elevated Asphaltene content (80% of the entire EOM).

Maceral composition for the Shypot Formation (Table 1) is characterized by a high abundance of vitrinite (34-60 vol.%; Fig. 5). Moderate amounts of sporinite (15-34 vol.%), lamalginitite (9-19 vol.%) and telalginitite (6-20 vol.%) make up the remaining maceral composition. Inertinite (mainly fusinite) is observed frequently throughout the succession (max. 12 vol.%). Glauconite and authigenic carbonate minerals (Fig. 5) are also frequently present in most samples. Without a noticeable trend in the studied section, vitrinite reflectance ranges from 0.74 to 0.86 % (average: 0.83%; Table 1).

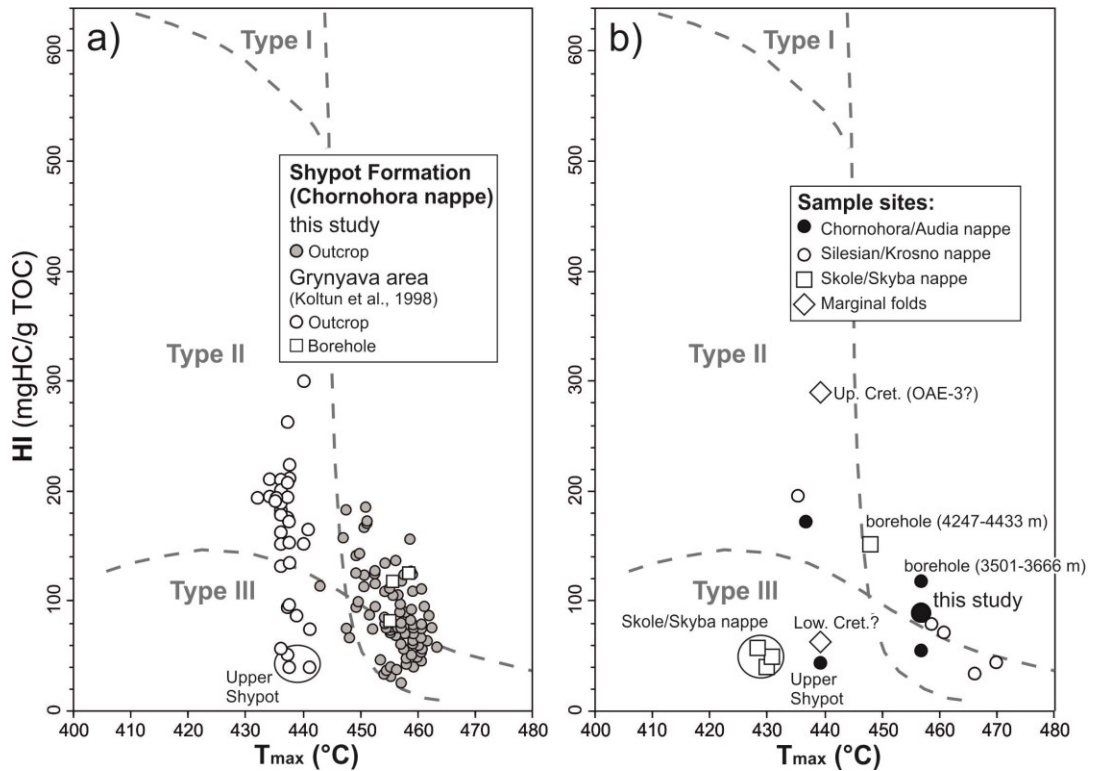


Fig. 4: HI vs. T_{max} (Espitalie et al., 1986). a) Shypot Formation in the Chornohora nappe. Data from additional samples in the Grynnyava area (site 7 in Fig. 1; Koltun et al., 1998) are shown for comparison. b) Mean values of Lower Cretaceous outcrop and borehole samples from different nappes (data are from Koltun et al., 1998; Amadori et al., 2012; Anastasiu et al., 2013; Slaczka et al., 2014).

Position in relation to Top [m]	TOC	S	Calcite equ.	HI	S1+S2	PI	Vitrinite reflectance	n#	Standard Deviation	Vitrinite	Inertinite	Liptinite			Maceral	Glauconite
	[wt.%]			[mgHC/gTOC]	[mgHC/grock]		[%]		[%]	[% OM normalized]			[vol.%]	yes/no		
5.0	3.1	1.7	4.4	75	2.6	0.13	0.85	51	0.12	40	6	30	18	6	5.6	n
49.0	1.9	0.8	2.6	143	3.2	0.13	*	*	*	40	0	30	10	20	1.9	y
56.5	2.6	0.6	0.6	126	3.6	0.10	0.82	32	0.10	39	9	26	17	9	4.3	y
63.0	3.2	1.1	0.0	125	4.4	0.10	0.83	17	0.09	39	3	34	17	7	4.7	y
75.5	5.3	1.5	3.9	185	10.6	0.07	*	*	*	34	6	28	19	13	9.4	y
84.0	5.6	1.1	6.2	168	10.1	0.07	0.83	26	0.09	31	10	26	23	10	6.6	y
96.0	4.5	1.4	7.0	158	7.7	0.08	*	*	*	48	2	26	13	11	7.4	n
118.0	4.0	1.2	12.8	171	7.5	0.09	*	*	*	50	6	22	11	11	3.8	y
133.0	4.9	1.4	4.4	105	5.7	0.09	0.74	39	0.09	36	7	30	17	10	5.9	y
159.0	1.8	1.1	12.0	80	1.7	0.15	*	*	*	52	6	24	12	6	3.1	y
170.0	3.1	1.0	5.7	81	2.9	0.13	*	*	*	45	9	17	13	16	6.2	y
194.0	3.8	2.2	10.3	111	4.7	0.11	0.85	52	0.10	38	6	22	18	16	5.5	y
228.0	1.8	2.1	21.3	90	1.9	0.18	*	*	*	43	7	29	14	7	2.2	y
248.0	2.1	1.2	23.7	74	1.8	0.16	*	*	*	49	6	19	13	13	3.4	y
257.0	3.8	1.9	11.3	89	4.0	0.16	*	*	*	59	7	16	11	7	5.3	y
281.0	8.0	2.2	0.7	127	11.2	0.09	0.8	67	0.11	49	8	16	16	11	7.9	y
294.0	7.5	2.5	6.1	124	10.4	0.11	*	*	*	60	6	14	11	9	7.0	y
313.0	8.2	2.3	5.6	157	14.0	0.09	0.85	43	0.11	37	5	26	19	13	11.3	y
323.8	9.4	2.3	3.8	124	12.8	0.09	*	*	*	47	7	20	15	11	9.6	n
361.0	2.8	1.2	4.8	77	2.5	0.12	0.86	43	0.11	43	7	29	14	7	5.5	y
382.0	3.6	2.0	14.7	110	2.1	0.13	*	*	*	54	5	23	9	9	4.4	y
394.0	2.6	1.3	11.1	66	2.4	0.12	*	*	*	44	4	26	17	9	4.1	y
402.3	4.2	2.1	2.2	86	4.1	0.10	0.86	32	0.09	55	9	15	12	9	7.1	y

Table 1: Selected Bulk and Rock-Eval data, vitrinite reflectance and maceral composition for the Shypot Formation in the Chornohora nappe. TOC – total organic carbon; S – total sulphur; Calcite equ. – calcite equivalent; HI – Hydrogen Index; PI – Production Index; n# –number of measurements; * – not defined.

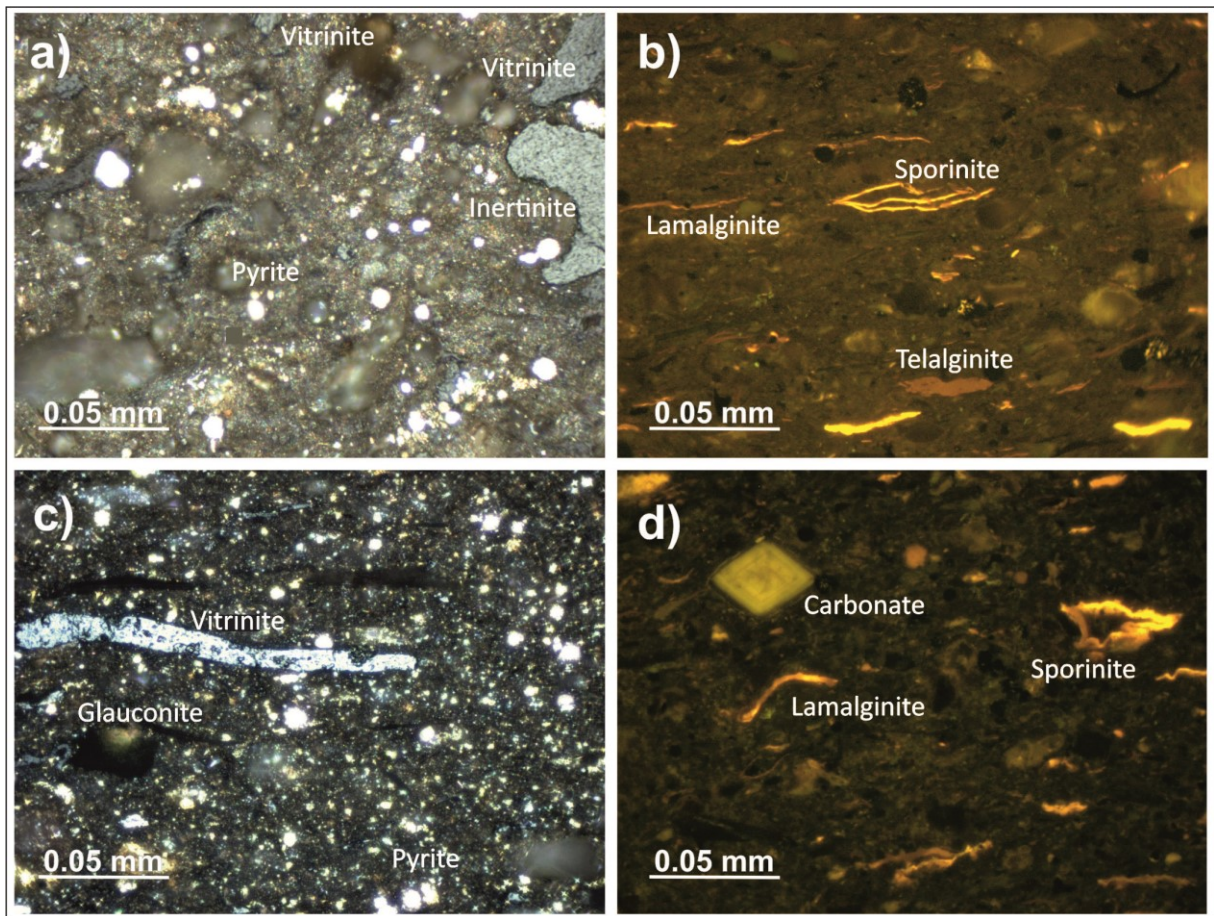


Fig. 5: Photomicrographs of samples from the Shypot Formation in the Chornohora nappe. (a, c) Photomicrographs in white light showing inertinite, vitrinite, glauconite and pyrite; (b, d) Photomicrographs in fluorescence mode illumination showing lamalginate, sporinite, telalginate and carbonate.

5.3. Molecular composition of hydrocarbons

Geochemical data are listed in Table 2, and the vertical variation of important biomarker proxies versus depth are shown in Fig. 3.

***n*-alkanes and isoprenoids** - Samples from the Shypot Formation contain high amounts of short-chain *n*-alkanes (*n*-C₁₅₋₂₀: 43-73%) and very low amounts of long-chain *n*-alkanes (*n*-C₂₆₋₃₂: 2-16 %; Table 2, Fig. 6). The percentage of the long-chain *n*-alkanes slightly increases upwards.

Pristane/*n*-C₁₇ (0.09-1.33) and phytane/*n*-C₁₈ (0.05-0.61) ratios vary significantly and show a positive correlation with the percentage of long-chain *n*-alkanes ($r^2=0.74$ and 0.73 , respectively; Fig. 6). CPI values (Bray and Evans, 1961) range from 1.06 to 1.25 (Table 2), but do not show a clear depth trend.

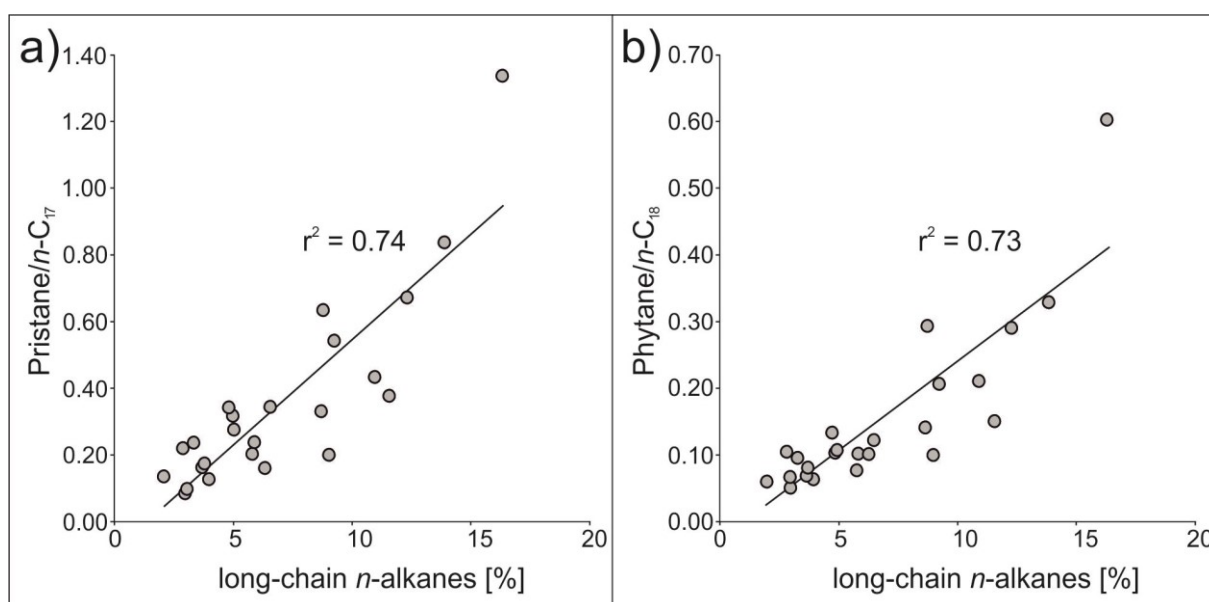


Fig. 6: Cross-plot of relative concentration of long-chain *n*-alkanes versus (a) pristane/*n*-C₁₇ and (b) phytane/*n*-C₁₈ ratios.

Pristane/phytane (Pr/Ph) ratios are commonly used as redox indicator. Ratios < 1.0 are attributed to strictly anoxic environments, whereas ratios above 1 suggest a suboxic (1-3) to oxic (>3) environments (Didyk et al., 1978). Pr/Ph ratios for the Shypot Formation range from 0.41 to 2.23 (average: 1.58; Table 2, Fig. 3). Although suggested to be used with caution, ratios < 1.0 are restricted to the lower part of the succession.

Steroids - Sterane concentrations are very low (0.02-2.32 $\mu\text{g/gTOC}$), likely due to an increased thermal maturity of the rocks (Tissot and Welte, 1984). High steranes/hopanes ratios (1.30-8.54; Table 2), which are prone to maturity (Requejo, 1994; Mißbach et al., 2016), are an indicator of a marine organic matter with major contributions from algae, and can be observed throughout the formation (Moldowan et al., 1986). The highest sterane concentrations, as well as the highest steranes/hopanes ratios, are both found 49 m below the top of the section.

The relative proportions of C_{27} , C_{28} and C_{29} steranes may provide paleoenvironmental information (Huang and Meinschein, 1979). For the Shypot Formation, the relative proportions of C_{27} steranes (33-54 %) are slightly elevated compared to C_{28} (21-35 %) and C_{29} steranes (24-39 %; Fig. 7; Table 2). The ratio of C_{28}/C_{29} steranes in marine source rocks increases during geological history (Grantham and Wakefield, 1988). In the Shypot Formation, the C_{28}/C_{29} steranes ratio varies widely (0.64-1.27; Table 2), but the average ratio of 0.90 agrees with the Early Cretaceous age of the rocks.

Terpenoids - Hopanes originate from precursors in bacterial membranes (Ourisson et al., 1979). Similar to sterane concentrations, hopane concentrations range from 0.01 to 0.29 ($\mu\text{g/g TOC}$; Table 2), whereas the 22S/(22S+22R) isomerization ratio of C_{31} hopanes varies between 0.40 to 0.85 (average: 0.63; Table 2).

Moretane/hopane and trisnorneohopane/trisnorhopane (Ts/Tm) ratios are thermal maturity parameters, but are also influenced by different source of organic matter and depositional environment (Moldowan et al., 1986; Peters et al., 2007). The moretane/hopane ratio varies from 0.07 to 0.32 (average: 0.15), whereas the Ts/Tm ratio ranges between 0.45 to 4.17 (average: 2.31).

Considering the Early Cretaceous age of the Shypot Formation, it is not surprising that oleanane was not detected in any of the studied samples.

Polycyclic aromatic hydrocarbons (PAH) and S-containing compounds

The dibenzothiophene/phenanthrene (DBT/Phen) ratio reflects the availability of free H_2S in the water column (Hughes et al., 1995). DBT/Phen ratios for the Shypot Formation are extremely low (≤ 0.02) as a result of low DBT concentrations which are generally insufficient for quantification.

The Methylphenanthrene Index-1 (MPI-1) is a maturity parameter and can be used to calculate vitrinite reflectance (R_c) of a sample (Radke and Welte, 1983). The calculated R_c for the Shypot Formation ranges from 0.77 to 1.01 % (average: 0.87 %).

Polycyclic aromatic hydrocarbons, including Chrysene, Perylene, which are typically found in coal deposits and may be used as an indicator for forest fires, are found in high concentrations (28.6-186.6 $\mu\text{g/g}$ TOC) throughout the succession.

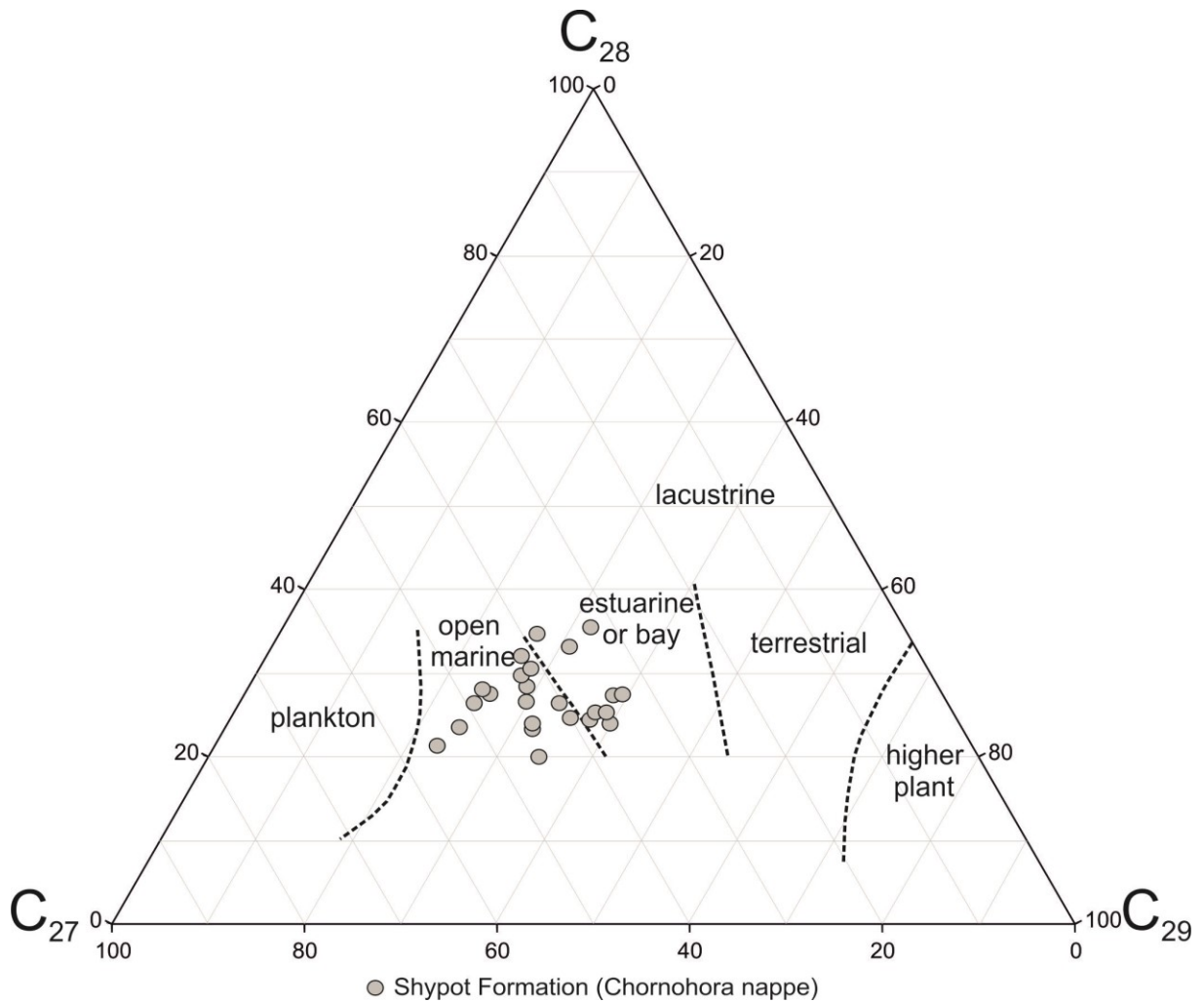


Fig. 7: Triangle diagram of C_{27} , C_{28} and C_{29} regular sterane composition for the Shypot Formation in the Chornohora nappe. Modified after Huang & Meinschein (1979).

Table 2: Organic geochemical data for samples from the Shypot Formation in the Chornohora nappe. EOM – Extractable Organic Matter; Sat. HC – Saturated Hydrocarbons; Aro. HC – Aromatic Hydrocarbons; Asp. – Asphaltene, Pr/Ph – Pristane/Phytane; CPI – Carbon Preference Index; Ts/Tm – Trisnorneohopane/Trisnorhopane; MPI-1 – Methylphenanthrene Index-1; DBT/Phen. – Dibenzothiophene/Phenanthrene; PAH – Polycyclic Aromatic Hydrocarbons; * – not defined.

Position in relation to Top [m]	TOC	HI	EOM	Sat. Aro. NSO Asp. HC	HC	HC	$n-C_{15-20} / n-C_{15-32}$	$n-C_{21-26} / n-C_{15-32}$	$n-C_{27-32} / n-C_{15-32}$	Pr/Ph	CPI	Steranes conc. [µg/gTOC]	%C ₂₇ %C ₂₈ %C ₂₉ Sterane/ Steranes	Hopanes C28/C29	Hopanes conc. [µg/gTOC]	22S/(S+R) C ₃₁ hopanes	Moretane/Hopanes	Ts/Tm	DBT/Phen	MPI-1	PAH conc. [µg/gTOC]				
	[wt.%]	[mg/gTOC]	[mg/gTOC]	[wt.%]	[wt.%]	[wt.%]	[wt.%]	[wt.%]	[wt.%]	[wt.%]	[wt.%]	[µg/gTOC]	[wt.%]	[µg/gTOC]	[wt.%]	[wt.%]	[wt.%]	[wt.%]	[wt.%]	[wt.%]	[wt.%]	[µg/gTOC]			
5.0	3.08	75	5.95	13	11	49	27	0.50	0.41	0.09	1.24	1.19	0.06	0.46	0.28	0.25	3.06	1.11	0.02	0.40	0.08	3.32	0.01	0.89	155.1
49.0	1.94	143	10.79	27	11	40	22	0.58	0.31	0.11	2.03	1.07	2.32	0.42	0.30	0.28	8.54	1.06	0.27	0.72	0.18	2.38	0.00	0.91	88.0
56.5	2.62	126	8.68	24	11	37	28	0.50	0.38	0.12	2.00	1.08	0.67	0.40	0.25	0.35	2.77	1.27	0.24	0.66	0.12	2.08	0.00	0.76	83.9
63.0	3.18	125	9.39	16	9	41	34	0.43	0.43	0.14	2.03	1.12	0.33	0.38	0.34	0.27	2.49	0.69	0.13	0.63	0.07	3.17	0.00	0.74	83.3
75.5	5.33	185	15.08	15	13	34	38	0.45	0.39	0.16	2.23	1.06	0.57	0.38	0.25	0.37	2.38	0.89	0.24	0.68	0.10	1.61	0.01	0.69	125.3
84.0	5.60	168	14.01	7	9	31	53	0.53	0.38	0.09	2.01	1.09	0.27	0.43	0.27	0.30	1.61	0.64	0.17	0.77	0.16	0.67	0.01	0.72	153.9
96.0	4.45	158	11.59	10	10	36	44	0.48	0.40	0.12	2.00	1.08	0.27	0.36	0.25	0.39	1.30	0.69	0.21	0.78	0.20	0.45	0.01	0.73	186.6
118.0	3.99	171	11.72	9	9	*	*	0.47	0.44	0.09	1.53	1.18	0.32	0.36	0.26	0.38	3.72	1.12	0.09	0.49	0.07	4.17	0.00	0.75	124.0
133.0	4.93	105	8.47	9	11	*	*	0.48	0.43	0.09	1.52	1.17	0.18	0.33	0.35	0.32	3.02	1.00	0.06	0.69	0.14	1.34	0.01	0.72	46.8
159.0	1.83	80	4.03	25	13	48	14	0.51	0.43	0.06	1.12	1.17	0.04	0.42	0.29	0.29	4.61	0.74	0.01	0.69	0.27	2.15	0.01	0.84	59.4
170.0	3.07	81	5.48	16	13	48	23	0.62	0.34	0.04	1.34	1.23	0.02	0.34	0.28	0.38	2.60	1.17	0.01	0.63	0.10	1.71	0.01	0.73	28.6
194.0	3.78	111	7.71	15	15	53	17	0.58	0.37	0.05	1.88	1.21	0.09	0.41	0.32	0.27	2.94	0.62	0.03	0.65	0.13	2.62	0.00	0.62	78.3
228.0	1.77	90	6.65	29	11	46	14	0.60	0.35	0.05	1.88	1.19	0.02	0.45	0.21	0.34	5.14	0.82	0.01	0.38	0.16	3.29	0.00	0.75	39.6
248.0	2.05	74	5.40	25	14	50	11	0.57	0.38	0.05	2.00	1.22	0.33	0.40	0.27	0.33	1.57	0.71	0.21	0.85	0.23	1.28	0.00	0.74	36.8
257.0	3.77	89	7.45	17	16	51	16	0.65	0.32	0.03	1.95	1.21	0.06	0.33	0.28	0.39	3.28	0.70	0.02	0.46	0.09	4.05	0.01	0.73	87.8
281.0	7.99	127	10.47	1	3	81	15	0.50	0.46	0.04	0.41	1.19	0.56	0.37	0.26	0.37	5.93	0.99	0.09	0.69	0.15	2.12	0.01	0.80	79.3
294.0	7.51	124	11.80	6	12	33	49	0.56	0.38	0.06	1.88	1.24	0.81	0.51	0.24	0.25	2.83	0.75	0.29	0.48	0.07	3.96	0.02	0.73	114.2
313.0	8.15	157	22.78	3	5	12	80	0.55	0.38	0.07	2.05	1.20	0.63	0.44	0.24	0.32	3.09	0.79	0.20	0.43	0.07	3.56	0.01	0.80	45.4
323.8	9.39	124	13.50	10	18	54	18	0.73	0.25	0.02	2.08	1.24	0.16	0.44	0.25	0.32	4.12	0.88	0.04	0.55	0.07	3.92	0.02	0.68	87.6
350.5	4.04	69	4.49	11	12	54	23	0.61	0.36	0.03	0.47	1.15	0.06	0.54	0.22	0.24	3.47	1.04	0.02	0.79	0.32	1.00	0.01	0.91	51.0
361.0	2.80	77	3.70	13	14	51	22	0.61	0.36	0.03	0.63	1.19	0.06	0.48	0.27	0.25	6.62	1.09	0.01	0.74	0.17	1.46	0.01	1.01	65.2
382.0	3.56	110	7.23	15	15	56	14	0.69	0.28	0.03	1.67	1.18	0.03	0.46	0.28	0.26	3.18	1.07	0.01	0.72	0.32	1.32	0.01	0.78	120.6
394.0	2.64	66	4.88	18	14	55	13	0.61	0.35	0.04	1.14	1.16	0.12	0.41	0.31	0.29	3.77	1.09	0.03	0.70	0.28	1.82	0.01	0.91	65.4
402.3	4.23	86	5.87	8	11	38	43	0.57	0.37	0.06	0.93	1.25	0.23	0.36	0.33	0.31	3.51	0.73	0.07	0.56	0.09	2.06	0.01	0.85	52.0

6. Discussion

6.1 Maturity and burial depth

Vitrinite reflectance values (average: 0.82 %) indicate peak oil window maturity for the Shypot Formation at the study location. T_{\max} values (average: 456°C) and vitrinite reflectance calculated using MPI-1 values (average 0.87 %) agree with a peak oil window maturity. A subtle downward increase in maturity with depth of burial is indicated by T_{\max} values and a downward increase in short-chain *n*-alkanes, which are mainly controlled by the advanced maturity of the studied section. In addition, since pristane/*n*-C₁₇ and phytane/*n*-C₁₈ ratios correlate positively with the percentage of long-chain *n*-alkanes ($r^2=0.74$ and 0.73, respectively), isoprenoid/*n*-alkane ratios and the percentage of long-chain *n*-alkanes are also mainly controlled by maturity. Furthermore, maturity parameters, including CPI (1.06-1.25), hopane isomerization (average 0.63), moretane/hopane ratios (0.07 - 0.32; average: 0.15) and Ts/Tm ratios (average: 2.31), support oil window maturity for rocks at the studied section.

Compared to another outcrop locality in the Chornohora nappe (Gryniava, site 7 in Fig. 1; 433-441°C; Koltun et al., 1998), T_{\max} values in the studied profile are significantly higher and similar T_{\max} values (454-458°C) are observed only at 3.5 km depth (borehole Gryniava-1; Koltun et al., 1998; Fig. 3). Koltun et al. (1998) reconstructed a maximum burial depth of about 6 km for the Lower Cretaceous rocks in the Gryniava-1 well and a similar burial depth has to be assumed for the Shypot Formation exposed at the study location.

6.2. Remaining and original source rock potential

The high maturity of the Shypot Formation implies that hydrocarbons have already been generated (see also PI values exceeding 0.1). Hence, HI values and the petroleum potential (S_1+S_2) cannot be considered original. Consequently, a plot of the petroleum potential vs. TOC provides information on the remaining source rock potential only (Fig. 8). Based on the (remaining) petroleum potential, the Shypot Formation is a poor to good source rock (Fig. 8), despite the very high TOC contents (max. 9.4 wt.%).

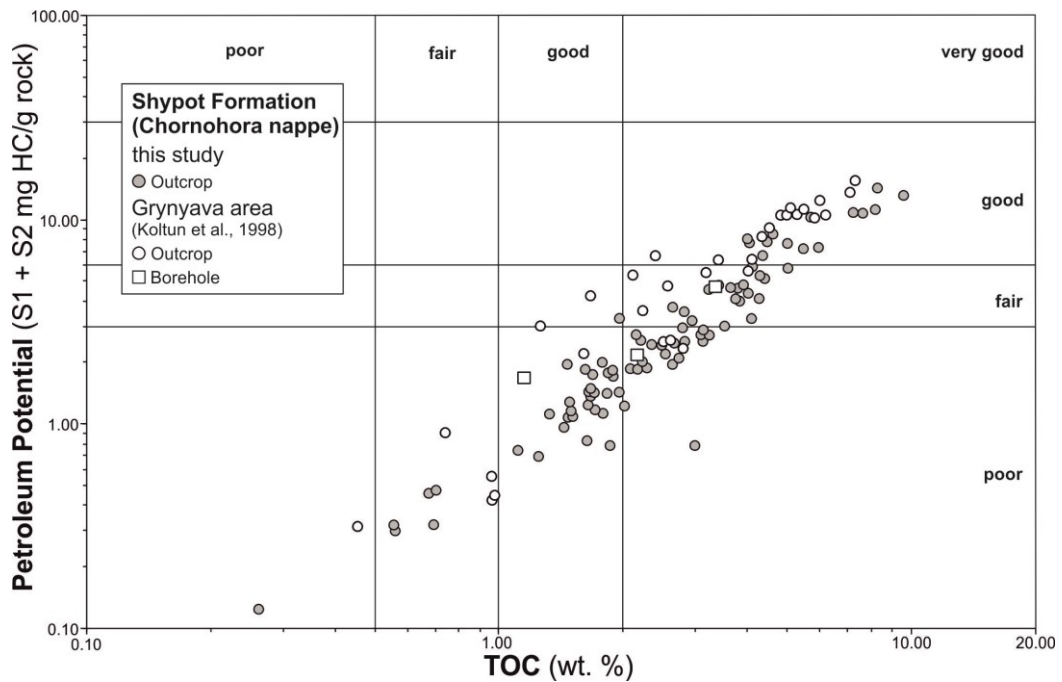


Fig. 8: Petroleum potential vs. TOC for the Shypot Formation in the Chornohora nappe. Data from additional outcrop and borehole samples in the Grynyava area (site 7 in Fig. 1; Koltun et al., 1998) are shown for comparison. Classification after Peters and Cassa (1994).

The remaining source potential of the Shypot Formation was calculated following the equation for the Source Potential Index (SPI) proposed by Demaison and Huizinga (1994) ($SPI = \text{thickness} \cdot [S_1 + S_2] \cdot \text{bulk density} / 1000$). Assuming a net source rock thickness of 263 m (65 % of the total thickness of the studied section), as well as an average remaining petroleum potential of 3.3 mgHC/g rock and an average density of 2.3 t/m³ (Demaison and Huizinga, 1994), an SPI of 2.0 tons of hydrocarbons per square metre surface area can be calculated (tHC/m²).

HI values of the marginal mature outcrop samples at Gryniava (average T_{max} : 437°C; see Fig. 3) may be used for a very rough estimate of the original SPI. At that locality, HI values range from 58 to 300 mgHC/gTOC and the average HI is 172 mgHC/gTOC (Koltun et al., 1998). The average HI at the studied section is 88 mgHC/gTOC, suggesting that about 50 % of the original potential has already been generated during burial and heating. Hence, the original SPI may have been in the order of 4.0 tHC/m², implying that about 2 tHC/m² have been generated and expelled.

If the generated hydrocarbons formed any accumulations, it is reasonable to assume that these accumulations were destroyed during major uplift and erosion. Based on the thermochronological data, major uplift commenced 12 to 10 Ma ago and post-dated nappe stacking and shortening (Nakapelyukh et al., 2018).

6.3. Organic matter type and depositional environment

Maceral analysis (Table 1; Fig. 5) reveals a high percentage in terrestrial organic matter (vitrinite: 34-60 vol.%; inertinite: 0-12 vol.%; sporinite: 15-34 vol.%). However, aquatic macerals (alginite: 18-32 vol.%) also occur in significant amounts. This suggests a mixture of type III and II kerogen, which is also supported by HI values of marginal mature samples (ca. 40-300 mgHC/gTOC) from the Chornohora nappe (Koltun et al., 1998). In contrast, high maturity of the Bystrets section prohibits the use of HI for kerogen classification (Fig. 4).

Relatively high amounts of alginite are reflected by high concentrations of C₂₇ steranes (Fig. 7). Nevertheless, considering the maceral percentages, the content in C₂₉ steranes, characteristic for woody land-plant input, is surprisingly low.

Preservation of the organic matter was supported by an oxygen-deficient environment, indicated by Pr/Ph ratios, which are low and range between 1.0 to 2.3. Pr/Ph ratios below 1 reflect strict anoxic conditions, and are only observed in the lower part of the studied succession. This, together with relatively high TOC/S ratios (Berner and Raiswell, 1984), shows that strictly anoxic conditions were rare. Very low DBT/Phen ratios, partly due to low DBT concentrations, suggest that free H₂S was not available in the water column, providing an additional argument against strict anoxic conditions. Oxygen-depletion may be related to late Barremian to Albian global anoxic event (OAE 1; Jenkyns, 1980).

Glauconite is formed in oxygen-depleted shallow marine environments. Its appearance in most samples (Table 1) suggests detrital input from near-shore environments, which is in line with the high percentages of landplant-derived macerals (esp. vitrinite and sporinite).

Vertical trends show that the environment did not change significantly during deposition of the lower, shaly part of the Shypot Formation.

6.4 Comparison with coeval rocks in the Carpathian Basin

Stratigraphic rocks equivalent to the Shypot Formation are found in different nappes along the entire Carpathian Belt. However, many parts of these rocks are unexplored and therefore only few source rock data are available. The following discussion summarizes bulk geochemical data from Lower Cretaceous rocks according to their tectonic position.

The most external nappe is the **Boryslav-Pokuttya - Marginal Folds nappe**. Lower Cretaceous rocks are absent in the Boryslav-Pokuttya nappe in Ukraine. In contrast, the Sarata Formation in Romania has been traditionally considered as Lower Cretaceous (e.g. Melinte et al., 2007; Roban et al., 2017). However, according to Amadori et al. (2012) and Guerrero et al. (2012), only the lower member of the Sarata Formation may be Lower Cretaceous, whereas the middle and upper member are probably Late Cretaceous (Campanian – Maastrichtian) in age. Silicified black shales occur in the lower and in the middle member and contain on average 1.49 wt.% and 1.37 wt.% TOC, respectively (Fig. 9d; Amadori et al., 2012). Similar TOC contents (0.3-1.5 wt.%) have been reported recently by Roban et al. (2017). Both successions are marginal mature (439°C), but HI values vary considerably (Fig. 4b). Organic matter in the lower member has low HI values (47-111 mgHC/gTOC; average: 76 mgHC/gTOC), whereas the middle member displays relatively high HI values (196-394 mgHC/gTOC; average: 290 mgHC/gTOC; based on four samples only), which is the highest recorded value for all Cretaceous rocks in the entire Carpathian Basin. However, as pointed out by Amadori et al. (2012), these rocks are probably Late Cretaceous in age and may represent the Coniacian to early Campanian OAE 3. Relatively high TOC contents (~3 wt.%) also occur in thin shaly layers within the Cenomanian/Turonian succession (Roban et al., 2017).

Data from the **Skole-Skyba-Tarcau nappe** are available from Poland and Ukraine. In both countries (sites 4 and 5 in Fig. 1) Hauterivian to Aptian aged rocks (Lower Spas Formation) are immature (average T_{max} : 429°C) and contain high amounts of organic matter (Ukraine: 2.02-6.19 wt.% TOC; average 3.30 wt.% TOC; Poland: max. 4.53 wt.% TOC; average: 2.85 wt.%). HI values are very low (~50 mgHC/gTOC) despite of low maturity. Deep borehole samples in Ukraine (~4400 m; site 6 in Fig. 1) are mature (448°C) and contain even higher TOC contents (4.05 wt.%; max. 7.84 wt.%) with an average HI of 153 mgHC/gTOC; max. 235 mgHC/gTOC) (Figs. 4b, 9c). Melinte-Dobrinescu and Roban (2011) report high TOC contents (average: 3.2 wt.%; max. 5.5 wt.%) from the Tarcau nappe in Romanian. Unfortunately, Rock Eval data are not available.

Data from the **Silesian-Krosno nappe** are available from the Polish Carpathians (sites 1-3 in Fig. 1; Slaczka et al., 2014). Only samples from site 2 are immature to marginal mature (T_{\max} : 435°C). They contain high amounts of organic matter (average 2.5 wt.%, max. 3.72 wt.%TOC) with HI values ranging from 92 to 267 mgHC/gTOC (average 196 mgHC/gTOC). Average TOC contents (1.6 wt.%) of mature to overmature samples at sites 1 and 3 are slightly lower, although the maximum content is similar (3.70 wt.%). HI values are low (average 65 mgHC/gTOC), due to advanced maturity. High TOC contents (2.0-3.7 wt.%) were also reported from the western Czech part of the nappe (Pavlus and Skupien, 2014).

Lower Cretaceous rocks in the **Dukla-Chornohora-Audia nappe** have been studied in this paper and by Koltun et al. (1998) in its Ukrainian sector (Chornohora nappe) and by Anastasiu et al. (2013) in its Romanian sector (Audia nappe). The average TOC content in immature to marginal mature outcrops of the Lower Shypot Beds in the Grynyava area (T_{\max} 437°C) is 4.6 wt.% (max. 7.5 wt.%) and the average HI is 177 mgHC/gTOC. Mature outcrop samples in Ukraine (this study) and Romania (site 9 in Fig. 1) and mature samples from a deep borehole are characterized by an average T_{\max} of 456°C. The average TOC (1.3 – 2.8 wt.%) and HI values (56-109 mgHC/gTOC) for these regions varies significantly. According to Melinte-Dobrinescu and Roban (2011), TOC contents in the Audia nappe range from 1.05 to 3.35 wt.%. Marginal mature outcrop samples from the Upper Shypot Beds (439°C) contain low amounts of organic matter (ca. TOC 1.0 wt.%) with very low HI values (ca. 45 mgHC/gTOC).

Overall, the comparison generally shows a strong dependency of HI values from maturity (Fig. 4b). Black shales with a remarkably low potential occur in the northwestern part of the Skole-Skyba nappe and in the upper Shypot Beds (Chornohora nappe). The interpretation of data from the Marginal Folds in Romania is complicated by the uncertain age data. Apart from that, most sections contain TOC-rich samples, but HI values are relatively low even in immature samples, indicating the presence of an original type III-II kerogen. Nevertheless, their hydrocarbon potential should be considered, although the Menilite formation clearly contains source rocks with a better quality (Sachsenhofer et al., 2018a,b).

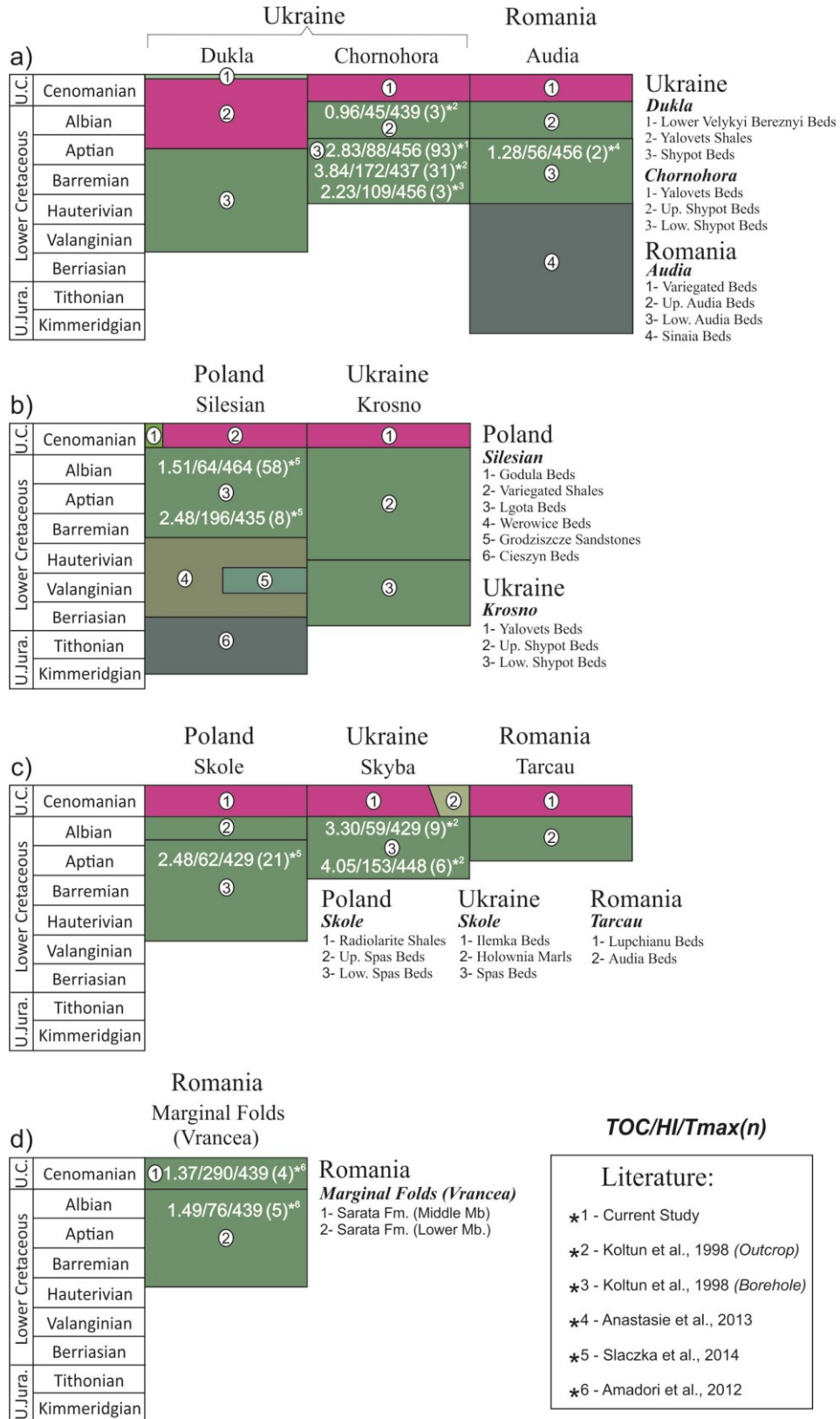


Fig. 9: Lithostratigraphic correlation of age equivalent rocks of the Shypot Formation in the Carpathian Basin (after Jankowski et al., 2012). Bulk parameters and Rock Eval data according to Koltun et al. (1998), Anastasiu et al. (2013), Slaczka et al. (2014) and Amadori et al. (2012).

7. Conclusion

The Shypot Formation in the Chornohora nappe comprises of organic-rich shales with interbedded siltstones and sandstones at the studied section near the village Bystrets. The succession is approximately 405 m thick and is characterized by high organic matter content. TOC content exceeds 9 wt.% in one sample in the lower part of the succession and averages 2.8 wt.% for the entire section. HI values (average 88 mgHC/gTOC), suggest an gas-prone type III kerogen, but increase slightly towards the top of the Formation. The Shypot Formation is thermally mature (average vitrinite reflectance: 0.82 %R_r; T_{max}: 456°C). Pr/Ph ratios (0.41 to 2.23) argue for oxygen-depleted conditions during deposition. Ratios below 1.0 are restricted to the lower part of the succession. Compared to other parts of the Carpathian Basin, the Shypot Formation in the study area is slightly more mature, but displays similar TOC content compared to other coeval rocks.

TOC suggests very good source rock potential, however according to the petroleum potential, the formation is a poor to good source rock. The high maturity of the Shypot Formation implies that hydrocarbons have likely already been generated. Hence, HI values and the petroleum potential (S₁+S₂) cannot be considered as the original amount. The remaining Source Potential Index (SPI) shows that 1.8 tons of hydrocarbons per m² can be generated, whereas the original SPI, which is a rough estimate based on the marginal mature outcrop samples from previous data on the Shypot Formation in the Chornohora nappe, yields an SPI in the order of 4 tHC/m², implying that about 2 tHC/m² have been generated.

Acknowledgments

We would like to thank Drs Yuriy Koltun and V.E. Shlapinsky for their insights and expertise in the field, as well as three anonymous reviewers for their useful comments.

8. References

- Amadori, M.L., Belayouni, H., Guerrero, F., Martin-Martin, M., Martin-Rojas, I., Miclaus, C., Raffaelli, G., 2012. New data on the Vrancea Nappe (Moldavidian Basin, Outer Carpathian Domain, Romania): paleogeographic and geodynamic reconstructions. *International Journal of Earth Sciences*, 101, 1599-1623.
- Anastasiu, N., Rabon, R.D., Popa, M., Seclaman, A., 2013. Black shales facies from Audia Formation (the Eastern Carpathians), a shale gas potential. *Sedimentology. Rom. Acad.*, 15, 51-58.
- Berner, R.A., Raiswell, R., 1984. C/S method for distinguishing freshwater from marine sedimentary rocks. *Geology*, 12, 365–368.
- Boote, D.R.D., Sachsenhofer, R.F., Tari, G., Arbouille, D., 2018. Petroleum provinces of the Paratethyan region. *Journal of Petroleum Geology*. 41, 247-298.
- Bray, E.E., Evans, E.D., 1961. Distribution of n-paraffins as a clue to recognition of source beds. *Geochimica et Cosmochimica Acta*, 22, 2-15.
- Curtis, J., Kotarba, M., Lewan, M., Więclaw, D., 2004. Oil/source rock correlations in the Polish Flysch Carpathians and Mesozoic basement and organic facies of the Oligocene Menilite Shales: insights from hydrous pyrolysis experiments. *Organic Geochemistry*, 35, 1573-1596.
- Demaison, G., Huizinga, B.J., 1994. Genetic classification of petroleum systems using three factors: charge, migration and entrapment. In: Magoon, L.B., Dow, W.G. (Eds.): *The Petroleum System, from Source to Trap*. AAPG Memoir, 60, 73-89.
- Didyk, B.M., Simoneit, B.R.T., Brassell, S.C., Eglinton, G., 1978. Organic geochemical indicators of palaeoenvironmental conditions of sedimentation. *Nature* 272, 216-222.
- Dinel, H., Schnitzer, M., Mehuys, G.R., 1990. Soil lipids: origin, nature, contents, decomposition and effect on soil physical properties. *Soil Biochemistry*, 12, 397-427.
- Eglinton, G., Gonzalez, A.G., Hamilton, R.J., Raphael, R.A., 1962. Hydrocarbon constituents of the wax coatings of plant leaves: A taxonomic survey. *Phytochemistry*, 1, 89-102.
- Espitalié, J., Marquis, F., Barsony, I., 1984. Geochemical logging. In: Voorhess, K..J. (Ed.): *Analytical Pyrolysis*. Butterworths, Boston, 53-79.
- Espitalié, J., Deroo, G., Marquis F., 1986. *Rock-Eval Pyrolysis and Its Applications (Part Three)*. Institut Français du Pétrole, 41, 73-89.
- Francu, J., Radke, M., Schaefer, R.G., Poelchau, H.S., Caslavsky, J., Bohacek, Z., 1996. Oil-oil and oil-source rock correlations in the northern Vienna Basin and adjacent Carpathian Flysch Zone (Czech and Slovak area). *EAGE Special Publications*, 5, 343-353.
- Grantham, P.J., Wakefield, L.L., 1988. Variations in the sterane carbon number distributions of marine source rock derived crude oils through geological time. *Organic Geochemistry*, 12, 61-73.
- Golonka, J., Gahagan, L., Krobicki, M., Marko, F., Oszczytko, N., Slaczka, A., 2006. Plate-tectonic Evolution and Paleogeography of the Circum-Carpathian Region. In: Golonka, J. and Picha, F.J. (Eds), *The Carpathians and their foreland: Geology and hydrocarbon resources*. AAPG Memoir, 84, 11-46.

- Huang W.Y, Meinschein W.G., 1979. Sterols as ecological indicators. *Geochimica et Cosmochimica Acta*, 43, 739-745
- Hughes, W.B., Holba, A.G., Dzou, L.I.P., 1995. The ratios of dibenzothiophene to phenanthrene and pristane to phytane as indicators of depositional environment and lithology of petroleum source rocks. *Geochimica et Cosmochimica Acta*, 59, 3581-3598.
- Jankowski, L.S., Kopciowski, R., Rylko, W., Danysh, V., Tsarnenko, P.N., Hnylko, O., 2012. Lithostratigraphic correlation of the Outer Carpathians borderlands of Poland, Ukraine, Slovakia and Romania. *Panstwowego Instytutu Geologicznego*, 449, 87-98.
- Jenkyns, H.C., 1980. Cretaceous anoxic events: from continents to oceans. *Journal Geological Society London*, 137. 171-188.
- Jirman, P., Gerslova, E., 2019. The source rock potential and thermal maturity of the Menilite Formation: A new insights from the Czech Republic. *Geological Quarterly*, 62, 858-872.
- Jirman, P., Gerslova, E., Bubik, M., Sachsenhofer, R.F., Bechtel, A., Więclaw, D., 2019. Depositional environment and hydrocarbon potential of the Oligocene Menilite Formation in the Western Carpathians: A case study from the Loučka section (Czech Republic). *Marine and Petroleum Geology*, 107, 334-350.
- Koltun, Y.V., Espitalie, J., Kotarba, M., Roure, F., Ellouz, N., Kosakowski, P., 1998. Petroleum Generation in the Ukrainian External Carpathians and the adjacent Foreland. *Journal of Petroleum Geology*, 21, 265-288.
- Kotarba, M.J., Koltun, Y.V., 2006. The origin and habitat of hydrocarbons of the Polish and Ukrainian parts of the Carpathian Province. In: Golonka, J. and Picha, F.J. (Eds), *The Carpathians and their foreland: Geology and hydrocarbon resources*. 84, 395-442.
- Kotarba, M., Więclaw, D., Koltun, Y., Marynowski, L., Kusmierk, J., Dudok, I., 2007. Organic geochemical study and genetic correlation of natural gas, oil and Menilite source rocks in the area between San and Stryi rivers (Polish and Ukrainian Carpathians). *Organic Geochemistry*, 38, 1431-1456.
- Kotarba, M., Więclaw, D., Dziadzio, P., Kowalski, A., Bilikiewicz, E., Kosakowski, P., 2013. Organic geochemical study of source rocks and natural gas and their genetic correlation in the central part of the Polish Outer Carpathians. *Marine and Petroleum Geology*, 45, 106-120.
- Kotarba, M., Więclaw, D., Bilkiewicz, E., Radkovets, N.Y., Koltun, Y.V., Kmiecik, N., Romanowski, T., Kowalski, A., 2019. Origin and migration of oil and natural gas in the western part of the Ukrainian Outer Carpathians: Geochemical and geological approach. *Marine and Petroleum Geology*, 103, 596-619.
- Kosakowski, P., Koltun, Y., Machowski, G., Poprawa, P., Papiernik, B., 2018. Geochemical characterization of the Oligocene Menilite Formation in the Polish and Ukrainian Carpathians. *Journal of Petroleum Geology*, 41, 319-336.
- Kruege, M.A., Mastalerz, Maria, Solecki, Andrzej, and Stankiewicz, B.A., 1996, Organic geochemistry and petrology of oil source rocks, Carpathian Overthrust region, southeastern Poland—Implications for petroleum generation: *Organic Geochemistry*, 24, 897–912.

- Melinte-Dobrinescu, M.C., Roban, R.D., 2011. Cretaceous anoxic–oxic changes in the Moldavids (Carpathians, Romania). *Sedimentary Geology*, 235, 79-90.
- Mißbach, H., Duda, J.P., Lünsdorf, N.K., Schmidt, B.C., Thiel, V., 2016. Testing the preservation of biomarkers during experimental maturation of an immature kerogen. *International Journal of Astrobiology*, 15, 165-175.
- Moldowan, J. M., Fago, F. J., 1986. Structure and significance of a novel rearranged monoaromatic steroid hydrocarbon in petroleum. *Geochimica et Cosmochimica Acta*, 50, 343–51.
- Nakapelyukh, M., Bubniak, I., Bubniak, A., Jonckheere, R., Ratschbacher, L., 2018, Cenozoic structural evolution, thermal history, and erosion of the Ukrainian Carpathians fold-thrust belt. *Tectonophysics*, 722, 197-209.
- Oszczypko, N., 2006. Late Jurassic-Miocene evolution of the Outer Carpathian fold-and-thrust belt and its foredeep basin (Western Carpathians, Poland). *Geological Quarterly*, 169-194.
- Ourisson, G., Albrecht, P., Rohmer, M., 1979. The hopanoids: palaeo-chemistry and biochemistry of a group of natural products. *Pure Applied Chemistry*, 51, 709-729.
- Pavlus, J., Skupien, P., 2014. Lower Cretaceous black shales of the Western Carpathians, Czech Republic: Palynofacies indication of depositional environment and source potential for hydrocarbons. *Marine and Petroleum Geology*, 57, 14-24.
- Peters, K.E., Cassa, M.R., 1994. Applied Source Rock Geochemistry. In: Magoon, L.B. and Dow, W.G. (Eds.) *The Petroleum System-From Source to Trap*. American Association of Petroleum Geologists Memoir, 60, 93-111.
- Peters, K. E., Walter, C. C., Moldowan, J. M., 2007. Biomarkers and Isotopes in Petroleum Systems and Earth History. *The Biomarker Guide 2*, 499-502
- Radke, M. Willisch, H., Welte, D.H., 1980. Preparative hydrocarbon group type determination by automated medium liquid pressure chromatography. *Anal. Chem.* 52, 406-411.
- Rauball, J.F., Sachsenhofer, R.F., Bechtel, A., Coric, S., Gratzer, R., 2019. The Oligocene-Miocene Menilite Formation in the Ukrainian Carpathians: A world-class source rock. *Journal of Petroleum Geology*, 42, 392-416.
- Requejo, A.G., 1994. Maturation of petroleum source rocks—II. Quantitative changes in extractable hydrocarbon content and composition associated with hydrocarbon generation. *Organic Geochemistry*, 21, 91-105.
- Roban, R.D., Krezsek, C., Melinte-Dobrinescu, M.C., 2017. Cretaceous sedimentation in the outer Eastern Carpathians: Implications for the facies model reconstruction of the Moldavide Basin. *Sedimentary Geology*, 354, 24-42.
- Sachsenhofer, R.F., Koltun, Y., 2012. Black shales in Ukraine – A review. *Marine and Petroleum Geology*. 31, 125-136.
- Sachsenhofer, R.F., Popov, S.V., Bechtel, A., Coric, S., Francu, J., Gratzer, R., Grunert, P., Kotarba, M., Mayer, J., Pupp, M., Ruprecht, B.J., Vincent, S.J., 2018a. Oligocene and Lower Miocene source rocks in the Paratethys: Palaeogeographical and stratigraphic controls. In: Simmons, M. et al. (Eds): *Geological Society London Special Publication*, 464, 267-306.

- Sachsenhofer, R.F., Popov, S.V., Coric, S., Mayer, J., Misch, D., Morton, M.T., Pupp, M., Rauball, J., Tari, G., 2018b. Paratethyan petroleum source rocks: an overview. *Journal of Petroleum Geology*, 41, 219-245.
- Schlanger, S.O., Jenkyns, H.C., 1976. Cretaceous oceanic anoxic events: causes and consequences. *Geologie en Mijnb.*, 55, 179-184.
- Shlapinskyi, V., 2015. The Geological Architecture of the Skyba, Krosno, Duklya-Chornogora Nappes of the Ukrainian Carpathians and Prospects of Oil and Gas (in Ukrainian; unpublished doctoral thesis). Institute of Geology and Geochemistry of Combustible Minerals, Lviv.
- Slaczka, A., Kruglov, S., Golonka, J., Oszczytko, N., Popadyuk, I., 2006. Geology and Hydrocarbon Resources of the Outer Carpathians, Poland, Slovakia, and Ukraine: General Geology. *The Carpathians and Their Foreland: Geology and Hydrocarbon Researches: AAPG Memoir*, 84, 221-258.
- Slaczka, A., Golonka, J., Oszczytko, N., Cieszkowski, M., Słomka, T., Matyasik, I., 2014. Occurrence of Upper Jurassic–Lower Cretaceous black organic-rich pelitic sediments as targets for unconventional hydrocarbon exploration in the Outer Carpathians and adjacent part of the Alps. *AAPG Bulletin*, 98, 1967-1994.
- Taylor, G.H., Teichmüller, M., Davis, A., Littke, R., Robert, P., 1998. *Organic Petrology*, Gebrüder Bornträger, 136, 655-704.
- Tissot, B.P., Welte, D.H., 1984. Recent Advances in Petroleum Geochemistry Applied to Hydrocarbon Exploration. *AAPG Bulletin*, 68, 545-563.
- Vialov, O.S., Gavura, S.P., Danysh, V.V., Lemishko, O.D., Leshchukh, R.Y., Ponomariova, L.P., Romaniv, A.M., Smirnov, S.E., Smolinska, N.I., Tsarnenko, P.N., 1988. Stratotypes of the Cretaceous and Paleogene deposits of the Ukrainian Carpathians (in Russian). *Nauka dumka*, Kiev. 204 .
- Więclaw, D., Bilkiewicz, E., Kotarba, M., Lillis, P., Dziadzio, P., Kowalski, A., Kmiecik, N., Romanowski, T., Jurek, K., 2020. Origin and secondary processes in petroleum in the eastern part of the Polish Outer Carpathians. *International Journal of Earth Sciences*, 109, 63-99.

Petroleum potential of Middle Jurassic rocks in the basement of the Carpathian Foredeep (Ukraine) and oil-to-source correlation with oil in Upper Jurassic reservoir

J. F. Rauball^{a*}, R. F. Sachsenhofer^a, A. Bechtel^a

^aChair of Petroleum Geology, Montanuniversitaet Leoben, 8700 Leoben, Austria.

Published in:

Geologica Carpathica 71 (2020), 150-165

doi: 10.31577/GeolCarp.71.2.4

* Corresponding author. johannes.rauball@gmail.com

Address: Chair of Petroleum Geology, Montanuniversitaet Leoben, Peter-Tuner Straße 5, A-8700 Leoben

Keywords: Ukrainian Carpathians, Mesozoic basement, Kokhanivka Zone, oil-source correlation, organic geochemistry, kerogen type, maturity

Research Highlights:

Middle Jurassic rocks are rich in organic matter (average: 4.19 wt.%)

Hydrogen Index values are typically around 100 mg HC/g TOC for Middle Jurassic rocks

Organic matter is marginally mature to mature and thermal maturity increases with depth

New geochemical data suggests a genetic link between Upper Jurassic source rocks and oils from Upper Jurassic reservoirs

Abstract

Organic matter-rich Middle Jurassic rocks occur in the Mesozoic basement of the Carpathian Foredeep in Ukraine. Eighty-nine core samples from the Mosty-2, Korolyn-6 and Korolyn-2 wells as well as three oil samples from the Kokhanivka and Orkhovychi oil fields in the Kokhanivka Zone, were investigated. Bulk geochemical data as well as maceral analysis have been determined, and a subset of these samples, including all oil samples, have been investigated for biomarker composition.

Middle Jurassic strata are rich in organic matter (average: 4.19 wt. %) and reach TOC contents of up to 14.98 wt. %. However, HI values are low, typically around 100 mg HC/g TOC, and only reach a maximum of 242 mg HC/g TOC, indicating dominance of gas-prone, Type III kerogen. T_{\max} values as well as random vitrinite reflectance measurements for the Mosty-2 (434°C; 0.69–0.71% Rr), Korolyn-6 (443°C; 0.78–0.82% Rr) and Korolyn-2 (448 °C; 0.85–0.90 % Rr) wells indicate that thermal maturity increases with depth from marginally mature to mature, suggesting that hydrocarbon generation may have occurred. However, biomarker data suggests no genetic link between these rocks and Upper Jurassic oils, as C_{27} – C_{28} – C_{29} sterane distributions, Pr/Ph ratios, DBT/Phenanthrene ratios and isotope data display significant differences between the two.

New geochemical data, along with published biomarker data on Upper Jurassic rocks and crude oils belonging to the same oil family as the Upper Jurassic oils in the Ukrainian Carpathians, showed that Upper Jurassic rocks from the Korolyn-6 well present a better fit and are the source for the analysed oils.

Table of Content

1. Introduction	121
2. Geological setting	122
3. Petroleum Systems	125
4. Samples and Methods	126
5. Results	128
5.1. Bulk parameters of organic matter and maceral composition	128
5.2. Molecular composition of rock extracts	134
5.3. Oil samples	137
6. Discussion	139
6.1. Middle Jurassic rocks	139
6.1.1 Maturity	139
6.1.2 Hydrocarbon potential	142
6.2. Oil samples: Thermal maturity and implications for source rocks	143
6.3. Oil-source correlation	144
7. Conclusion	146
8. References	147

1. Introduction

The East Carpathian Foredeep overlies the western margin of the East European Platform and is partly overthrust by the Eastern Carpathians (Oszczypko et al. 2006). It hosts about 120 gas fields with total reserves of 2373 MMboe (Boote et al. 2018). The gas is mainly of microbial origin (Kotarba & Koltun 2011), sourced from immature Neogene shales (Kosakowski et al. 2013), which accumulated in Miocene sandstones and in Mesozoic carbonate and sandstone reservoirs (Popadyuk et al. 2006; Boote et al. 2018).

Apart from a microbial gas system, small oil fields (e.g., Kokhanivka, Orkhovychi; see Fig. 1b for location) in the Ukrainian sector of the foredeep (Glushko 1968; Vul et al. 1998; Kurovets et al. 2011) provide evidence for another petroleum system. The oil is reservoided in Upper Jurassic and Upper Cretaceous carbonate rocks. A Middle Jurassic source rock (Kokhanivka Fm.) is tentatively assumed as the source for the above accumulations (e.g., Koltun et al. 1998; Kotarba & Koltun 2006). Alternatively, thin intervals within the Upper Jurassic succession may have generated the sulphur-rich oil (Kotarba et al. 2011; Kosakowski et al. 2012).

In Ukraine, geological and geochemical data regarding potential source rock intervals in the Mesozoic basement of the Carpathian Foredeep are limited (Koltun et al. 1998; Kotarba & Koltun 2006; Kosakowski et al. 2012; Sachsenhofer & Koltun 2012). Additional information on the petroleum generation potential of these intervals and their petroleum systems may contribute to further exploration success in this area. Therefore, the primary objective of the present study is to determine the vertical and lateral variability of the hydrocarbon potential of the Middle Jurassic succession, and to analyse the genetic relationship between the Middle Jurassic rocks and the oil accumulations in the Upper Jurassic reservoirs.

Additional data from Upper Jurassic source rocks from the Voloshcha-1 and Korolyn-6 wells in Ukraine (Kosakowski et al. 2012) as well as for oil samples from the Opaka-1 (Więclaw 2011) and Lubaczow-157 (Curtis et al. 2004) wells were taken into consideration for oil-to-source correlation.

2. Geological setting

The Carpathian Foredeep developed as a peripheral foreland basin in front of the advancing Carpathian orogenic wedge during early and middle Miocene times (Oszczypko 2006; Oszczypko et al. 2006). A generalized lithostratigraphic column of the Paleozoic and Mesozoic basement of the Carpathian Foredeep in eastern Poland and Ukraine is provided in Fig. 2.

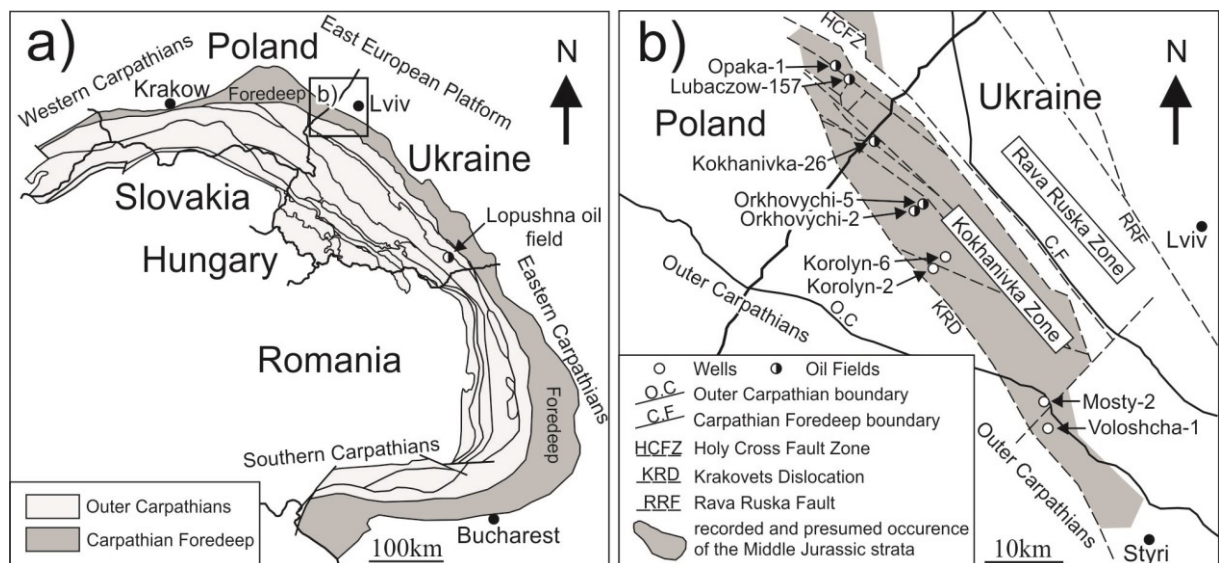


Fig. 1. a) Structural map of the Carpathian Fold-Thrust Belt and its foredeep basin (after Oszczypko et al. 2006; Slaczka et al. 2006; Nakapelyukh et al. 2018) showing the location of the study area in western Ukraine; b) Subcrop map of Middle Jurassic strata in the study area and the locations of the discussed wells (after Kosakowski et al. 2012).

The basement complex is traditionally referred to as the Kokhanivka and the Rava Ruska Zones in Ukraine (Fig. 1b), and as the Kielce Fold Belt and the Lysogory–Radom Block in Poland (Buła & Habryn 2011). The boundary between the Kokhanivka and the Rava Ruska Zones is formed by the Holy Cross Fault Zone. The south-western margin of the Kokhanivka Zone is formed by the Krakovets Dislocation (Fig. 1b). The Paleozoic strata include Cambrian, Ordovician and Silurian rocks (Drygant 2000; Buła & Habryn 2011; Jachowicz-Zdanowska 2011), partly with high TOC contents (e.g., Kotarba et al. 2011).

Jurassic rocks overlie the Paleozoic (Cambrian to Silurian) succession and comprise Lower–Middle Jurassic (Hettangian–Callovian) and Upper Jurassic–Lower Cretaceous (Oxfordian–

Valanginian) sedimentary complexes (Kotarba et al. 2011). Lower Jurassic rocks are quartz arenite and mudstones with coal intercalations (Kurovets et al. 2011). The Middle Jurassic strata display variable thicknesses. In Poland Middle Jurassic sediments vary from dozens to several hundreds of metres, exceeding 100 m only in a few wells (Moryc 2004). In Ukraine, the Middle Jurassic complex in the Kokhanivka Zone shows a greater thickness and a more complete stratigraphic succession, as Middle Jurassic sediments reach up to 1000 m in thickness, likely due to deformations and tectonic repetition of sedimentary sequences. As a result, the true thickness of this sequence may only be in the order of hundreds of metres (Dulub et al. 1986, 2003; Moryc 2004; Swidrowska et al. 2008).

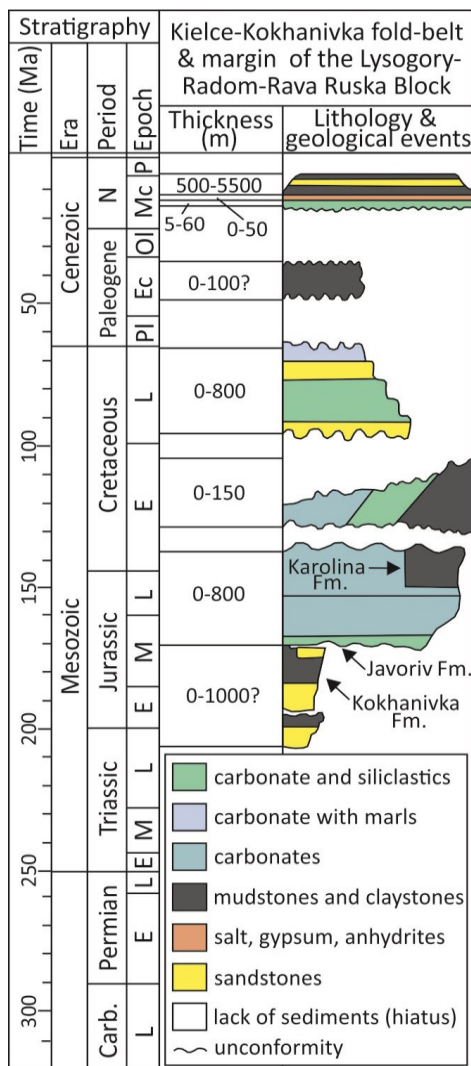


Fig. 2. Lithostratigraphic column of the pre-Miocene basement of the Carpathian Foredeep in the Ukrainian-Polish border region (after Kotarba et al. 2011).

Middle Jurassic strata in the study area start with a sandstone-rich unit (e.g., Kurovets et al. 2011) grading upwards into organic matter-rich claystones and siltstones with scarce intercalations of sandstones (Fig. 2). This succession has been termed Kokhanivka Formation and ranges in age from Aalenian to Bathonian (Pieńkowski et al. 2008). The Kokhanivka Formation represents depositional systems varying from estuary/foreshore (lower part) to dysoxic shelf sediments. Sediments of a shallow carbonate–siliciclastic shelf accumulated during Callovian time (Javoriv Fm.; Pieńkowski et al. 2008) and have a much wider aerial extension than the underlying rocks. Dolomites and limestone with fossil remains, up to several centimetres thick, can be observed (Dulub et al. 2003). The facies distribution during Late Jurassic/Early Cretaceous times has been described in detail by Gutowski et al. (2005a,b) and Krajewski et al. (2011). According to these authors, the south-western margin of the East European Platform was formed by a carbonate ramp (Oxfordian, lower Kimmeridgian) grading upwards into a rimmed platform (upper Kimmeridgian to Valanginian). Deep-water (marly) limestones overlain by a platform slope facies (Karolina Fm.) prevailed along the south-western margin of the Kokhanivka Zone near the Krakovets Fault (Anikeyeva & Zhabina 2002; Gutowski et al. 2005a; Krajewski et al. 2011). Carbonate buildups (Gutowski et al. 2005a,b) grading north-eastwards into an inner platform facies formed the platform margin facies. These shallow marine carbonates provide reservoir rocks for oil and gas fields in Ukraine (e.g., Kokhanivka, Orkhovychi) and Poland (e.g., Lubaczow) (Kotarba et al. 2011; Kurovets et al. 2011).

Lower and Upper Cretaceous rocks comprising siliciclastic and carbonate successions conclude the Mesozoic succession, but are often missing due to erosion. Miocene molasse-type sediments follow above the major erosional unconformity. Partly the platform was overridden by the Outer Carpathians (Fig. 1b).

3. Petroleum Systems

The East Carpathian Foredeep is mainly a gas province and hosts a microbial gas system and a thermogenic oil system.

More than 40 gas fields have been detected in the Ukrainian sector of the Carpathian Foredeep (Boote et al. 2018). The microbial gas, sourced from immature Neogene shales (Kosakowski et al. 2013) is trapped both in karstified Jurassic and Cretaceous carbonate and sandstone reservoirs, as well as in the overlying Miocene (Sarmatian and Badenian) sandstones (Boote et al. 2018). Minor thermogenic gas and condensate is sourced from mature Neogene depocenters (Kotarba & Koltun 2011).

The thermogenic petroleum system produced small fields with heavy oil (Kokhanivka and Orkhovychi) near the Polish– Ukrainian border. The oil is reservoired in Upper Jurassic and Cretaceous carbonates (Glushko 1968; Vul et al. 1998; Kurovets et al. 2011). Reservoir rocks in Ukraine (e.g., Kokhanivka, Orkhchivy) and Poland (e.g., Opaka, Lubaczow) are provided by carbonate buildups and inner platform sediments (Kotarba et al. 2011). Kurovets et al. (2011) distinguished three main types of reservoir rocks: (i) Fractured low-permeable limestones with small inter-granular porosity; (ii) Organodetrital limestones with high porosity (15–20 %) and permeability (up to $100 \cdot 10^{-3} \mu\text{m}^2$); (iii) Fractured pseudo-oolitic limestones with high porosity (20–30 %), but low permeability. The reservoir rocks are sealed by Miocene shales. Potential source rocks include black shales in the middle Jurassic Kokhanivka Formation (e.g., Koltun et al. 1998; Kotarba & Koltun 2006) or deep-water carbonate mudstones within the Upper Jurassic Karolina Formation (Kotarba et al. 2011; Kosakowski et al. 2012).

Although located outside the study area, the Lopushna oil field (Popadyuk et al. 2006) in the south-eastern part of the Ukrainian foreland autochthon, beneath the Carpathian flysch nappes (for location see Fig. 1a) deserves mention. Here oil occurs in Upper Jurassic, Cretaceous and Paleogene reservoirs. Jurassic source rocks are not present in the area. Therefore, and based on the presence of oleanane, Koltun et al. (1998) and Kotarba & Koltun (2006) assumed that the oil was generated from the Oligocene Menilite shales from the Carpathian flysch sequence (Radkovets et al. 2016).

4. Samples and Methods

For this study, a total of eighty-nine core samples from the Mosty-2, Korolyn-6 and Korolyn-2 wells, as well as three oil samples from the Kokhanivka-26, Orkhovychi-2 and Orkhovychi-5 wells, were collected for analyses. Core samples from the Mosty-2, Korolyn-6 and Korolyn-2 wells were taken at similarly spaced intervals (where possible), spanning from the uppermost part of the available core, to its base. The studied sections only represent a portion of the Middle Jurassic succession as overlying and underlying core samples from the selected wells were not available or do not exist. Before laboratory analyses, all core samples were cleaned, dried and pulverized.

The core samples were analysed for their total carbon (TC), total sulphur (TS) and total organic carbon content (TOC) using an ELTRA Elemental Analyser. Samples measured for TOC were treated twice with 50 % phosphoric acid to remove inorganic carbon. Results are based on the averages of at least two corresponding measurements and are given in weight percent (wt. %). The total inorganic carbon (TIC) was determined by subtracting the TOC from the TC. TIC was then used to calculate the calcite equivalent percentages ($=\text{TIC} \times 8.333$).

Rock-Eval pyrolysis was carried out using a Rock-Eval 6 analyser in order to determine the S_1 , S_2 (mgHC/grock) and T_{max} for all core samples. S_1 determines the amount of hydrocarbons present in the rock, whereas S_2 determines the amount of hydrocarbons formed during pyrolysis. The petroleum potential ($S_1 + S_2$ [mg HC/g rock]), the hydrogen index ($\text{HI} = S_2 / \text{TOC} \times 100$ [mgHC/gTOC]) and the Production Index ($S_1 / [S_1 + S_2]$) were calculated using the S_1 and S_2 measurements. T_{max} is a maturity parameter and indicates the temperature during Rock-Eval pyrolysis, at which the maximum amount of hydrocarbons can be generated (Espitalié et al. 1984). S_1 , S_2 and T_{max} results are based on at least two measurements.

Based on the TOC contents and HI values, a total of 10 core samples were selected at similarly spaced intervals across the different wells, for biomarker analyses together with three oil samples. Rock samples were extracted in a Dionex ASE 200 accelerated solvent extractor using dichloromethane at 75°C and 50 bar for approximately 1 hour. Asphaltenes were precipitated from the solution using a hexane–dichloromethane solution (80:1) and then separated by centrifugation. The hexane-soluble fractions were separated into NSO compounds, saturated hydrocarbons and aromatic hydrocarbons using medium pressure liquid chromatography (MPLC) with a Köhnen–Willsch instrument (Radke et al. 1980). The saturated and aromatic hydrocarbon fractions were analysed by a gas chromatograph equipped

with a 30 m DB-5MS fused silica column (i.d. 0.25 mm; 0.25 mm film thickness), coupled to a ThermoFischer ISQ Dual-quadrupole mass spectrometer. Using helium as the carrier gas, the oven temperature was set to increase from 70°C to 300°C at 4°C·min⁻¹, which was followed by an isothermal period of 15 min. With the injector temperature set to 275°C, the sample was then injected with a split ratio of 10. The spectrometer was operated in the EI (electron ionization) mode over a scan range from m/z 50 to 650 (0.7 s total scan time). Data was processed using an Xcalibur data system where individual compounds were identified on the basis of retention time in the total ion current (TIC) chromatogram and by comparison of the mass spectra with published data. Percentages and absolute concentrations of various compound groups in the saturated and aromatic hydrocarbon fractions were calculated using peak areas from the gas chromatograms and their relations to the internal standards (deuterated n-tetracosane and 1,1'-binaphthyl, respectively). Concentrations were normalized to TOC.

The samples used for biomarker analysis were also selected for organic petrographic investigations (with the exception of two samples, where not enough material was available for further analysis). Some additional samples have been selected based on their TOC content. In total, 14 polished rock blocks were chosen and analysed using a single-scan method on approximately 1500 random distributed points per sample in white light and fluorescence (UV) mode (after Taylor et al. 1998). Depending on their origin, the macerals are divided into groups outlined by the International Committee for Coal Petrology (ICCP System 1998, 2001). For their maturity assessment, random vitrinite reflectance was measured in non-polarized light using a Leice DM4P microscope equipped with Hilgers FOSSIL MOT, with a 50× oil objective, following established procedures (after Taylor et al. 1998).

The MPI-1 was used to calculate vitrinite reflectance following the equation ($R_c = 0.60 \text{ MPI-1} + 0.40$) proposed by Radke et al. (1982).

5. Results

5.1. Bulk parameters of organic matter and maceral composition

A summary of bulk parameters for the rocks from the Mosty-2, Korolyn-6 and Korolyn-2 wells are displayed in Fig. 3.

Plots of hydrogen index (HI) versus T_{\max} are shown in Fig. 4. The Middle Jurassic section in well Mosty-2 ranges from 2268 to 2559 m. The studied samples cover the depth interval from 2361 to 2560 m. Carbonate contents are typically low (<2 wt.%), but reach 43 wt. % in marly sediments at 2512 and 2513 m depth. TOC contents range between 1.16 and 14.98 wt.% (average: 3.93 wt.%) and are especially high between 2512 and 2525 m depth. HI values (36–242 mgHC/gTOC) are low and reach a maximum at 2518 m depth. T_{\max} (432–440°C; average 434°C), and low Production Index (PI: 0.01–0.05) values show that the organic matter is immature, whereas vitrinite reflectance (0.69–0.71% Rr; Table 1) measurements indicate early oil window maturity. Sulphur contents are low (≤ 1.0 wt.%). TOC/S ratios typical for marine sediments (~2.8; Berner & Raiswell 1984) are observed in shallow samples (2361–2364 m), but TOC/S ratios are often significantly higher (max. 69.2) in the organic matter rich interval.

In well Korolyn-6, the Middle Jurassic succession ranges from 3037 to 4060 m. The studied samples represent the depth interval between 3418 and 3642 m. In this interval carbonate contents vary between 0.6 and 32.2 wt. % and are slightly higher than in Mosty-2. Even though the Mosty-2 and Korolyn-6 wells both contain an interval with significantly higher carbonate content (>30 wt. %) than the remaining samples, it is unlikely that these intervals can be correlated, considering their distance. The rocks contain high amounts of organic matter (TOC: 2.68–5.75 wt. %; average: 4.18 wt. %) with low HI values (average: 105 mg HC/g TOC). Whereas TOC contents show little vertical variation, HI values are especially low between 3430 and 3437 m depth, an interval characterized by silty plant-bearing, carbonate-free sediments. T_{\max} (432–440 °C; average 434 °C), vitrinite reflectance (0.78–0.82 % Rr; Table 1) and PI values (0.15–0.23) are higher than in Mosty-2 and indicate early oil window maturity. Sulphur contents are moderately high (0.20–3.08 wt. %) and TOC/S ratios typically range from 1.3 to 6.6, but are higher (max: 29.4) in some samples near the base and in the middle part of the studied section.

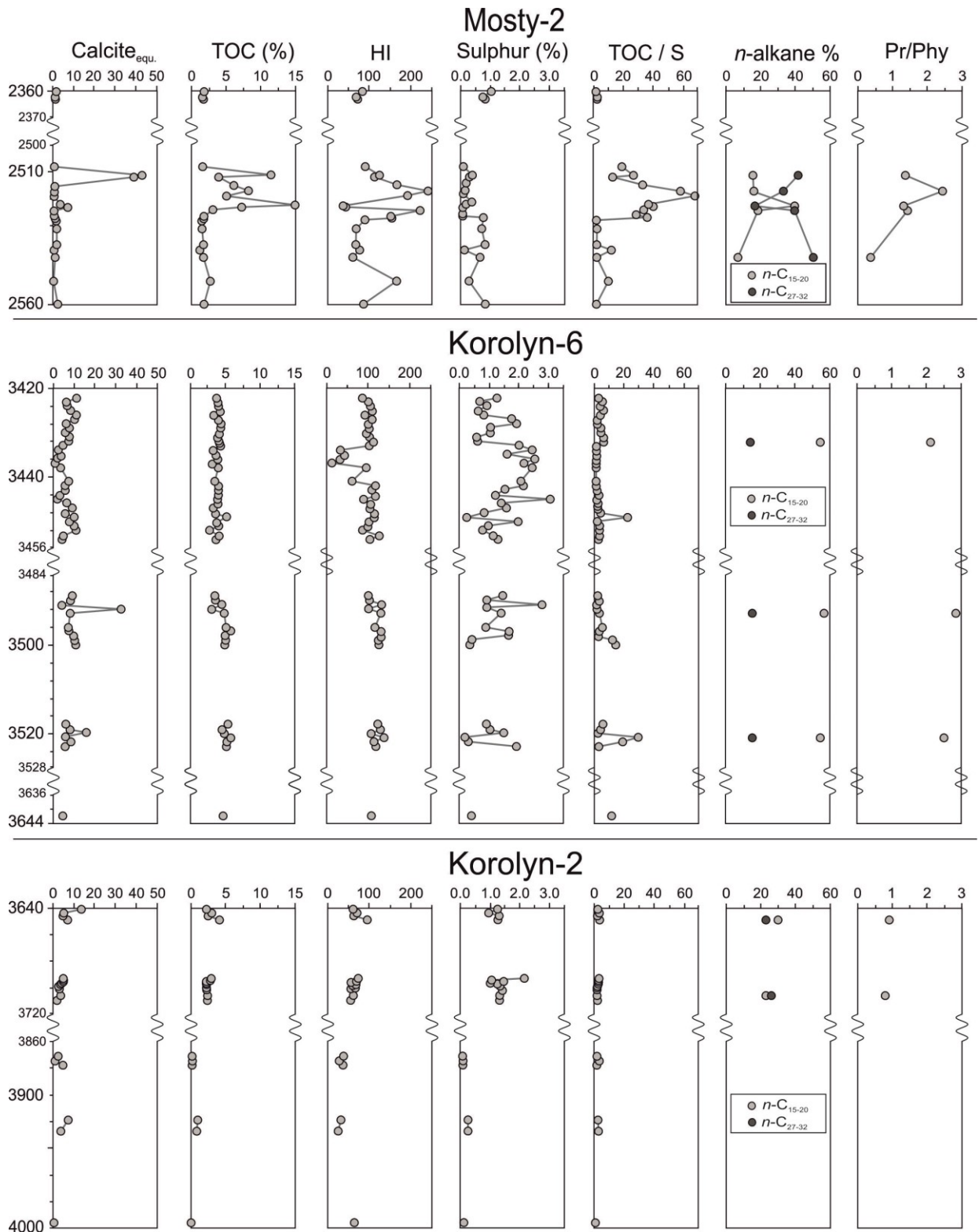


Fig. 3. Bulk geochemical data and important biomarker proxies versus depth for rocks from the Mosty-2, Korolyn-6 and Korolyn-2 wells.

In well Korolyn-2, the Middle Jurassic strata was drilled between 3590 and 4212 m depth. Three depth intervals (3642–3652; 3696–3712; 3870–3996 m) were studied and contain rocks with low carbonate contents (0.6–13.9 wt. %). TOC contents are high (2.13–4.05 wt. %; average: 2.62 wt. %) in the upper intervals, but low (~0.1 wt. %) in the bright coloured deepest interval. HI values range from 55 to 105 mg HC/g TOC in the organic-rich intervals. T_{\max} values (445–450 °C; average 448 °C) as well as vitrinite reflectance (0.85–0.90 % Rr) indicate that the organic matter is mature. PI values (0.11–0.36) increase downwards and support oil window maturity.

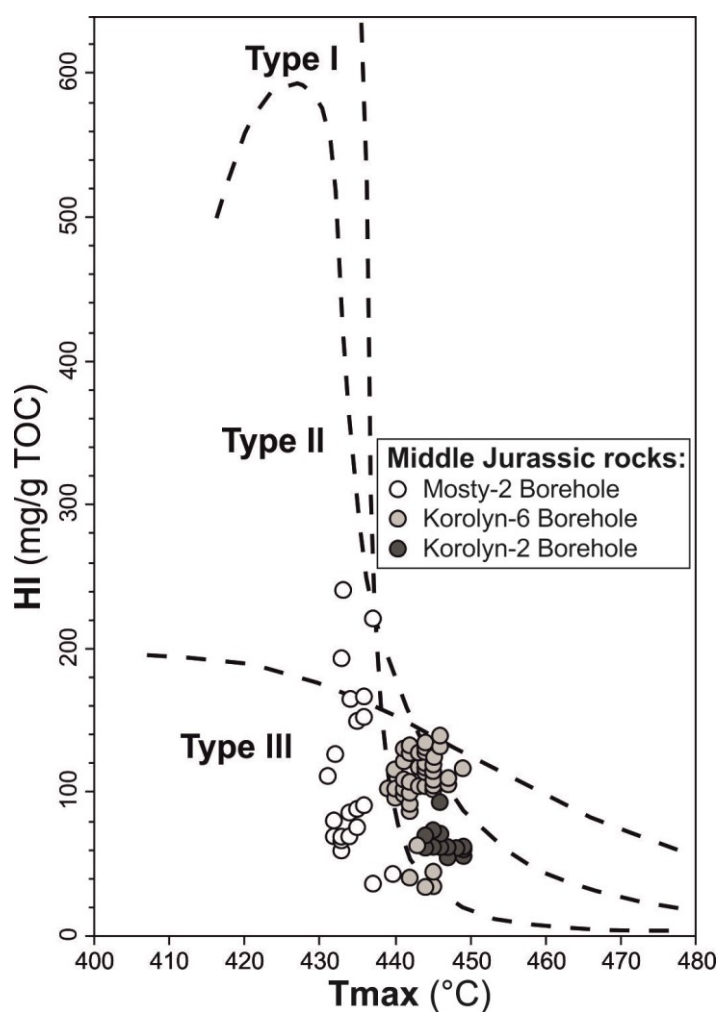


Fig. 4. Cross-plot of HI versus T_{\max} (after Espitalié et al. 1984) for the rocks from the Mosty-2, Korolyn-6 and Korolyn-2 wells.

Maceral assemblages (Table 1; Fig. 5) are similar in all studied samples and show a predominance of terrigenous maceral groups (detrovitrinite: 15–50 vol. %; inertinite: 7–49 vol. %; sporinite: 7–37 vol. %), whereas aquatic macerals (alginite: 14–46 vol. %) occur in variable amounts. Overall, slight differences are observed in the fluorescence colouring between the individual wells as the more mature rocks in Korolyn-6 and Korolyn-2 display

darker and more red coloured liptinites, compared to the studied samples in Mosty-2 (Fig. 5). Despite the small sample-set, an attempt was made to correlate the HI values with the vitrinite and liptinite populations of the selected samples. However, these yielded inconclusive results as the data do not correlate.

The standard deviation for the random vitrinite reflectance measurements ranges from 0.07–0.13 and macerals were standardized to 100 % organic matter (% OM normalized; Table 1). In addition, the volume percentage of the mineral matrix (darker regions in the photomicrographs under white light; Fig. 5) and pyrite was determined, which allowed the calculation of the total maceral amount in comparison to the mineral matter (vol. %; Table 1).

Depth [m]	TOC	S [wt.%]	Calcite equ.	HI [mg/gTOC]	Vitrinite [%Rr]	Standard Deviation	Vitrinite	Inertinite	Sporinite	Lamalginites	Telalginites	Maceral [vol.%]	
					n#		[% OM normalized]						
Mosty-2													
2361	1.74	1.02	1.69	81	0.69	47	0.07	50	7	7	14	21	2.7
2512	11.57	0.42	42.68	126	*	*	*	19	49	16	10	5	15.7
2518	8.17	0.14	0.00	242	*	*	*	15	33	30	18	5	9.5
2525	3.25	0.09	0.07	221	*	*	*	30	8	33	23	8	5.5
2529	1.55	0.74	1.37	91	0.71	42	0.07	47	7	20	13	13	2.9
Korolyn-6													
3421	4.39	0.66	8.05	112	0.80	73	0.12	24	22	27	20	7	7.3
3428	4.07	0.63	7.40	116	*	*	*	27	8	37	19	10	7.3
3434	3.97	2.48	2.85	96	*	*	*	26	17	31	11	14	5.9
3445	5.20	0.24	9.62	117	0.82	68	0.13	27	19	24	14	16	6.6
3493	4.87	1.40	8.12	133	*	*	*	19	8	27	27	19	8.3
3521	5.75	0.20	6.23	141	0.78	74	0.13	26	14	26	17	17	7.7
Korolyn-2													
3652	4.05	1.25	7.34	93	0.85	70	0.11	33	25	21	13	8	4.2
3698	3.00	1.47	4.03	74	0.88	52	0.12	44	17	11	17	11	3.4
3708	2.48	1.30	3.41	61	0.90	50	0.11	26	21	21	11	21	3.4

Table 1: TOC, S, Calcite equ., HI, mean random vitrinite reflectance measurements and maceral composition for rocks from the Mosty-2, Korolyn-6 and Korolyn-2 wells. Depth - measured depth; TOC - total organic carbon; S - total sulphur; Calcite equ. - calcite equivalents; HI - Hydrogen Index; n# - measurements.

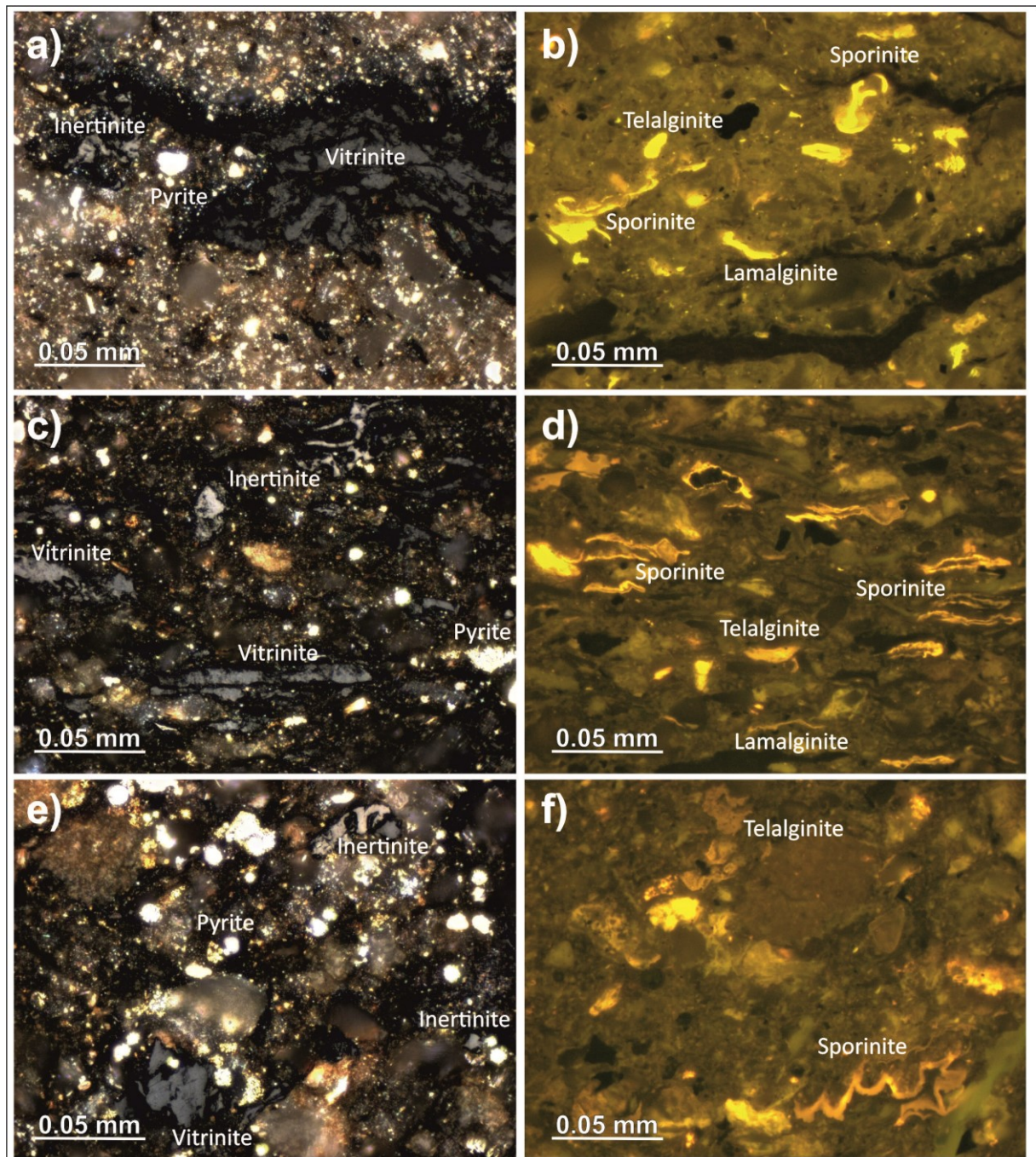


Fig. 5. Photomicrographs of samples from the Mosty-2 (a, b), Korolyn-6 (c, d) and Korolyn-2 (e, f) wells. a, c, e - Photomicrographs in white light showing inertinite, vitrinite and pyrite; b, d, f - photomicrographs in fluorescence mode illumination showing sporinite, lamalginite and telalginite.

5.2. Molecular composition of rock extracts

Geochemical data for Middle Jurassic rocks from the Mosty-2, Korolyn-6 and Korolyn-2 wells are listed in Table 2 and plotted versus depth in Fig. 3.

Yields of extractable organic matter (EOM) vary between 1.07–7.63 mg/g TOC. NSO compounds (29–59 % of the EOM) dominate in all samples, but asphaltene contents are elevated in parts of the Mosty-2 well and both samples from the Korolyn-2 well.

***n*-alkanes and isoprenoids:** The carbon preference index (CPI) values (Bray & Evans 1961) are high in the Mosty-2 well (1.44–2.36), reflecting enhanced terrestrial input and low thermal maturity. CPI values for the deeper rocks (Korolyn-6: 1.20–1.27; Korolyn-2: 1.19–1.22) are lower. The relative amount of short-chain *n*-alkanes ($n\text{-C}_{15-20}$), which are typically derived from microbial organisms (Peters et al. 2007), depends on organic matter input and increases also with maturity. Hence, it is surprising that the highest relative amounts are present in the Korolyn-6 ($n\text{-C}_{15-20}$: 54–56 %) samples compared to the shallower Mosty-2 ($n\text{-C}_{15-20}$: 6–40 %) and the deep Korolyn-2 ($n\text{-C}_{15-20}$: 23–30 %) samples. Conversely, long-chain *n*-alkanes, which are characteristic of higher land plants (Peters et al. 2007), are higher in the Mosty-2 ($n\text{-C}_{26-32}$: 17–50 %) and the Korolyn-2 ($n\text{-C}_{26-32}$: 23–26 %) rocks compared to the Korolyn-6 samples.

The Pristane/phytane (Pr/Ph) ratio is commonly used as redox parameter (Peters et al. 2007). Pr/Ph ratio is elevated in the Mosty-2 (1.33–2.46) and Korolyn-6 (2.12–2.84) wells, except for one sample in Mosty-2 at 2542 m with a Pr/Ph ratio of 0.30. The ratios for the Korolyn-2 (0.83–0.94) samples is lower. Highly-branched isoprenoid (HBI) alkanes were not detected in quantifiable concentrations in any of the rocks.

Steroids: With one exception (Korolyn-6; 3428 m: 2.7 $\mu\text{g/g}$ TOC), sterane concentrations are typically very low (<0.6 $\mu\text{g/g}$ TOC; Table 2). Diasteranes/steranes ratio range from 0.13 to 0.44 and steranes/hopanes ratio ranges from 0.08 to 0.59.

The relative abundances of C_{27} – C_{28} – C_{29} steranes are dominated by the source input (Fig. 6). The ratio does not change significantly throughout the oil-generative window, so it is possible to distinguish crude oils from different source rocks (Huang & Meinschein 1979). The relative proportions of C_{29} steranes are dominant (32–60 %) over the C_{28} (17–34 %) and C_{27} steranes (17–34 %; Fig. 6).

The $20S/(20S+20R)$ C_{29} -sterane isomerization ratio and the $C_{29}\beta\beta/(\beta\beta+\alpha\alpha)$ ratio can be used as a thermal maturity parameter, as the ratios rise with increasing maturity (Seifert & Moldowan 1986). $20S/(20S+20R)$ C_{29} -sterane isomerization ratios for the Mosty-2 (0.16–0.29) and Korolyn-6 (0.08–0.12) wells are lower, compared to the Korolyn-2 well (0.39–43). $20S/(20S+20R)$ C_{29} -sterane isomerization ratios observed in Korolyn-6 indicate thermal immaturity, which correspond to an approximately 0.5 % Ro (Callejon et al. 2003), which is lower than the measured vitrinite reflectance (ca. 0.8 % Rr). A similar trend is observed for the $C_{29}\beta\beta/(\beta\beta+\alpha\alpha)$ ratio (Mosty-2: 0.30–0.41; Korolyn-6: 0.30–0.38; Korolyn-2: 0.58–0.63).

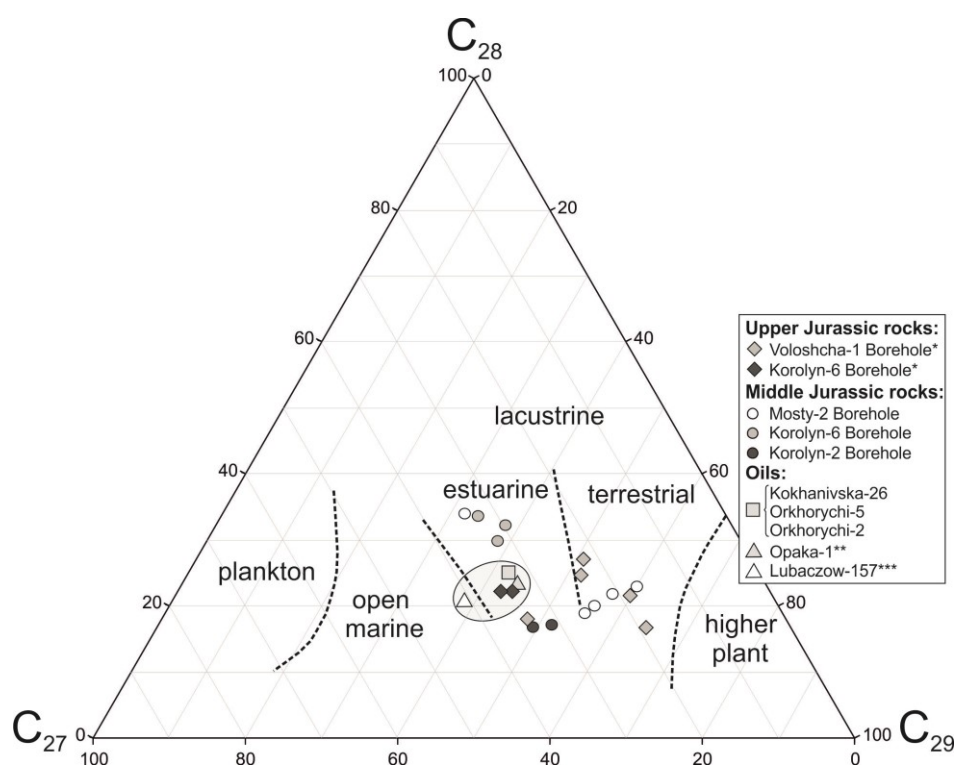


Fig. 6. Ternary diagram of regular steranes (C_{27} – C_{29}) showing the relationship between sterane compositions for rocks from the Voloshcha-1, Korolyn-6, Mosty-2, Korolyn-6 and Korolyn-2 wells, as well as oils from Kokhanivka-26, Orkhovychi-5, Orkhovychi-2, Opaka-1 and Lubaczow-157 wells (*after Kosakowski et al. 2012; **after Więclaw 2011; ***after Curtis et al. 2004).

Terpenoids: Hopanes are non-aromatic cyclic triterpenoids, which originate from precursors in bacterial membranes (Ourisson et al. 1979). Similar to sterane concentrations, concentrations are low in the rock extracts (0.36–5.00 $\mu\text{g/g}$ TOC; Table 2).

The trisnorneohopane/trisnorhopane (Ts/Tm) is a thermal maturity parameter, which can be lithology and facies dependent and decreases in carbonate environments (Moldowan & Fago 1986; Peters et al. 2007). For Middle Jurassic rocks, the Ts/Tm ratios are extremely low (0.01–0.11). However, since Ts/Tm ratios are extremely vulnerable and are heavily influenced by the source of the organic matter and the lithology, this parameter should be taken with caution.

The moretane/hopane ratio can also be used as a thermal maturity parameter as the ratio of moretane to their corresponding hopanes decreases with increasing thermal maturity, from approximately 0.8 in immature sediments, to about 0.15–0.05 in mature source rocks (Mackenzie et al. 1980; Seifert & Moldowan 1980). Moretane/hopane ratios for Mosty-2 samples (0.28–0.55) are higher than in deeper samples (Korolyn-6: 0.18–0.24; Korolyn-2: 0.16–0.21; Table 2).

A widely used maturity parameter is the $C_{31} 22S/(22S+22R)$ homohopane ratio. The ratio increases from 0 to 0.6 at equilibrium during maturation (Seifert & Moldowan, 1980). Most of the samples yield values near the equilibrium (0.54–0.61; Peters et al. 2007).

The **dibenzothiophene/phenanthrene** (DBT/ Phen) ratio reflects the availability of free H₂S in the water column (Hughes et al. 1995). DBT/ Phen ratios for the rocks are low (≤ 0.41 ; Table 2).

The **Methylphenanthrene Index** (MPI-1) is a maturity parameter and can be used to calculate vitrinite reflectance (% Rc; Radke et al. 1980). The calculated % Rc values for the Mosty-2 (0.66–0.79 % Rc), Korolyn-6 (0.62–0.68 % Rc) and Korolyn-2 (0.73–0.90 % Rc) rocks suggest early to peak oil window maturity.

Land-plant related biomarkers: Diterpenoids (e.g., cadalene, retene), which are gymnosperm- derived biomarkers (Wakeham et al. 1980; Simoneit 1986; Alexander et al. 1988), were encountered in all rocks (3.36 to 37.51 $\mu\text{g/g}$ TOC; Table 2). Considering their Jurassic age, it is not surprising that pentacyclic non-hopanoid triterpenoids (incl. oleanane) were not detected in any of the studied samples.

Compound specific isotope analysis (CSIA) of individual *n*-alkanes can be used as a tool to determine oil-source correlations, as the depositional setting of the source rock influences the shape of the *n*-alkane isotopic signature (Bechtel et al. 2012). Carbon isotope ratios of *n*-alkanes derived from Mosty-2 and Korolyn-6 samples range from -29 to -26 ‰. There is no distinct trend with chain length visible (Fig. 7).

5.3 Oil samples

Geochemical data for the oil samples from the Kokhanivka-26, Orkhovychi-2 and the Orkhovychi-5 wells are listed in Table 2. NSO compounds (50–57 %) dominate in all oil samples. Biodegradation was not observed in any of the studied samples (Fig. 8).

***n*-alkanes and isoprenoids:** Oil samples are dominated by short-chain (44–48 %; Fig. 8) and mid-chain *n*-alkanes (29–31 %). Long-chain *n*-alkanes are rare (11–12 %) and show CPI values (Bray & Evans 1961) near unity. Pr/Ph ratios are very low (0.29–0.54). HBI alkanes were not detected in quantifiable concentrations.

Steroids: Sterane concentrations range from 300 to 350 $\mu\text{g/g}$ oil; Table 2). Steranes/hopanes ratios are rather uniform (0.50–0.56) and diasteranes/steranes ratios are extremely low (0.01). C_{29} steranes (38–48 %) are slightly more abundant than C_{27} (33–41 %) and C_{28} (21–27 %; Fig. 6) steranes. $20\text{S}/(20\text{S}+20\text{R})$ sterane isomerization ratios (0.44–0.47) and the $\text{C}_{29}\beta\beta/(\beta\beta+\alpha\alpha)$ ratio (0.67–0.69) agree with oil window maturity.

Terpenoids: Concentrations of hopanes in oil samples ranges from 550–720 $\mu\text{g/g}$ oil; Table 2. The T_s/T_m is extremely low for the oil samples (0.07–0.16). The moretane/hopane ratios of oil samples are close to the equilibrium values of 0.6 (Seifert & Moldowan 1980).

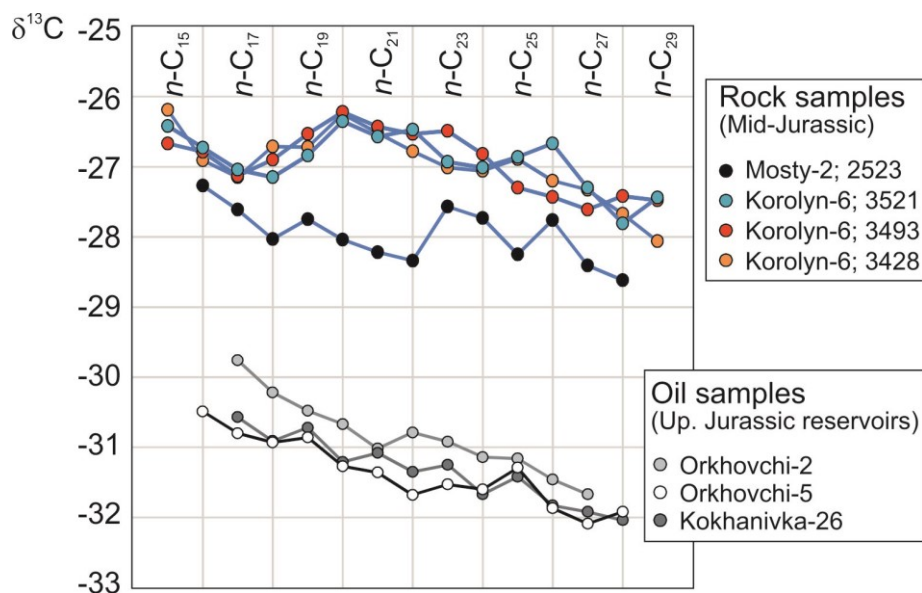


Fig. 7. Carbon isotopic composition of individual *n*-alkanes and acyclic isoprenoids in rock extracts and oil samples.

The DBT/Phen ratios of oil samples are significantly higher (2.76–3.70) compared to the studied rock samples. Based on MPI-1, the oil samples were generated at oil window maturity (Kokhanivka-26: 0.68 % Rc; Orkhovychi-5: 0.71 % Rc; Orkhovychi-2: 0.71 % Rc).

Land-plant related biomarkers: Gymnosperm-derived diterpenoids (Wakeham et al. 1980, Simoneit 1986; Alexander et al. 1988), were encountered in significant concentrations (4.58 to 7.11 µg/g TOC; Table 2), whereas oleanane was not detected (Fig. 8).

CSIA: $\delta^{13}\text{C}$ values of *n*-alkanes range from –31.9 to –29.8 ‰, showing that oil samples are isotopically lighter than the studied rock samples (Fig. 7).

6. Discussion

6.1 Middle Jurassic rocks

6.1.1 Maturity

T_{\max} values as well as vitrinite reflectance measurements (% Rr) indicate that thermal maturity in the studied Middle Jurassic sample-set increases with depth of burial from immature to peak oil window maturity (Fig. 9). PI values also increase with depth and reach a value of 0.1, which is often considered as the top of the oil generating zone (e.g., Peters 1986), at approximately 3500 m depth.

In general, the fluorescence colouring of the liptinite (sporinite, lamalginite and telalginite) macerals differs between the individual wells, and is consistent with their maturities. The more mature rocks in Korolyn-6 and Korolyn-2 typically display darker and more red coloured liptinites (sporinite, lamalginite and telalginite), compared to the rocks observed in Mosty-2, suggesting higher maturities (Fig. 5).

It should be noted that in some cases the re-working of sediments may influence colouring, however, to our knowledge, this was not the case for any of the analysed samples. Biomarker ratios are in general agreement with the thermal maturity trend suggested by Rock-Eval data. For example, average CPI values decrease from 1.89 in Mosty-2 to 1.24 in Korolyn-6 and 1.21 in Korolyn-2. Moretane/hopane ratios decrease in the same direction from 0.45 (Mosty-2) to 0.21 (Korolyn-6) and 0.18 (Korolyn-2). However, plots of $20S/(20S+20R)$ versus T_s/T_m and $\beta\beta/(\beta\beta+\alpha\alpha)$ for the C_{29} steranes (Fig. 10), shows that sterane-based maturity parameters pretend a lower maturity for Korolyn-6 samples compared to the shallower, immature Mosty-2 samples. Probably this discrepancy reflects a facies influence on sterane proxies. Within this context, it is worth noting that rocks from the Korolyn-6 well typically contain higher sulphur contents than those from Mosty-2 and Korolyn-2. However, low DBT/Phen ratios show that organic sulphur contents are probably low.

C_{31} $22S/(22S+22R)$ homohopane ratios are similar and near the equilibrium value and do not contribute to the maturity assessment. MPI-1 ratios and calculated Rc values for the Mosty-2 (average: 0.71 %Rc; Table 2) and Korolyn-2 (average: 0.82 %Rc; Table 2) are in line or slightly below the vitrinite reflectance measurements for these wells (0.69–0.71 %Rr and 0.85–0.90 %Rr, respectively). In contrast, similar to sterane isomerization, the MPI-derived vitrinite reflectance value in Korolyn-6 (average: 0.66 %Rc; Table 2) is significantly lower than the measured value (ca. 0.80 % Rr).

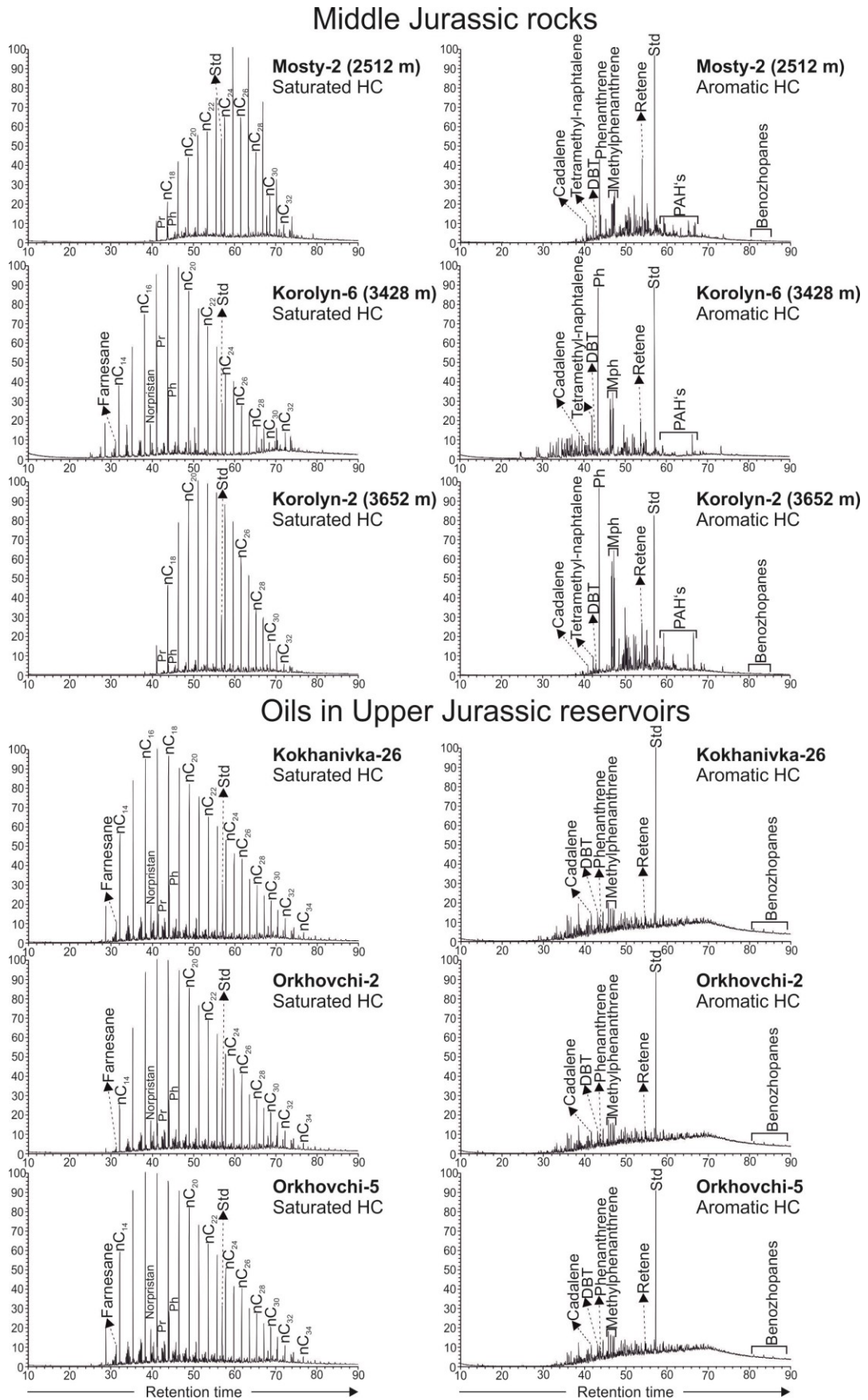


Fig. 8. Ion traces of saturated and aromatic hydrocarbons of the studied Upper Jurassic Oils and Middle Jurassic rocks.

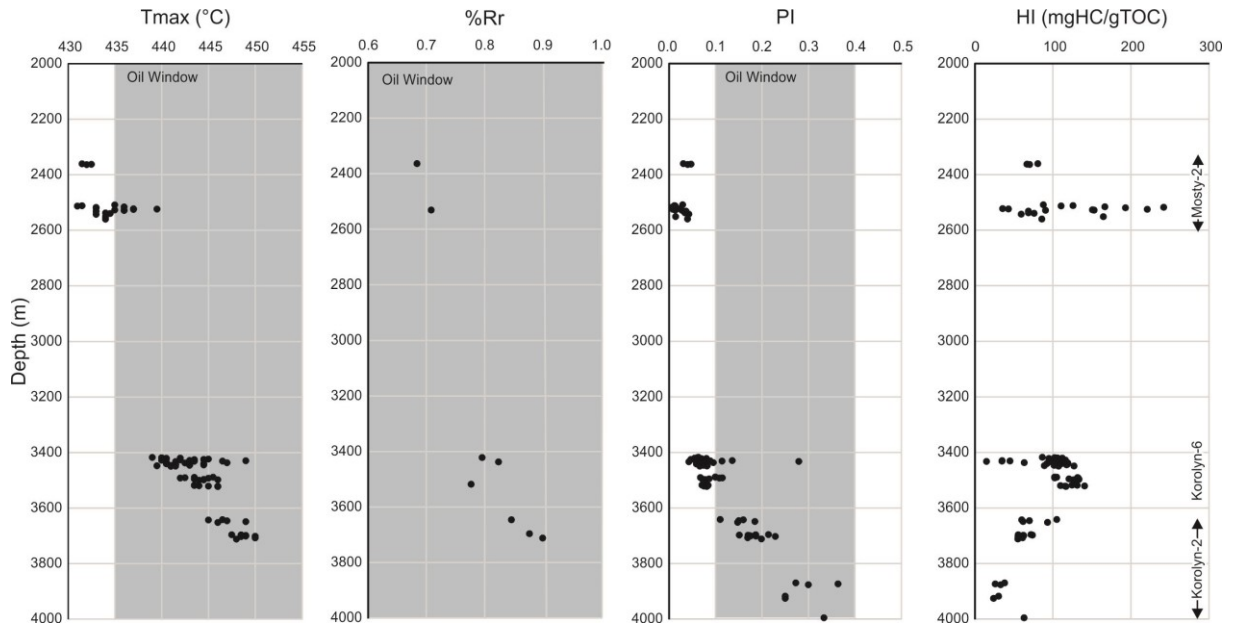


Fig. 9. Depth plot of T_{max} , Production Index (PI), Hydrogen Index (HI) and Vitrinite reflectance (% Rr) measurements for Middle Jurassic rocks in Mosty-2, Korolyn-6 and Korolyn-2 wells.

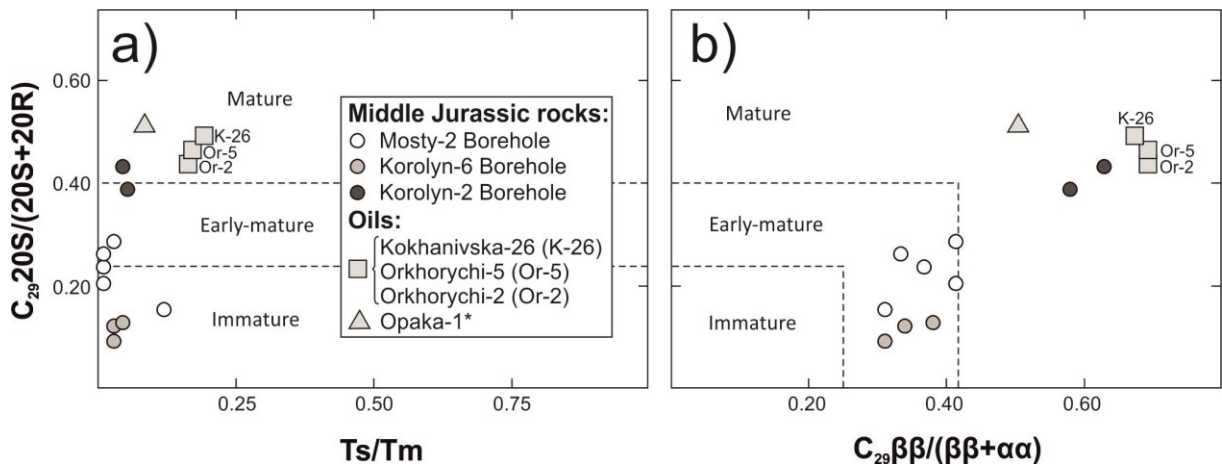


Fig. 10. Plots of Sterane $C_{29} 20S/(20S+20R)$ versus Ts/Tm and $\beta\beta/(\beta\beta+\alpha\alpha)$ (after Peters et al. 2007) for Middle Jurassic rocks and oil samples from Upper Jurassic carbonate reservoirs.

6.1.2 Hydrocarbon potential

Differences in thermal maturity have to be considered when assessing the hydrocarbon potential. The original potential can be determined for Mosty-2 samples, whereas the hydrocarbon potential of Korolyn-6 rocks may be slightly lower, and that of Korolyn-2 rocks significantly reduced due to advanced maturity. A decrease in HI for Korolyn-2 rocks is clearly evident in Fig. 9. However, a downward increase in HI is observed in the lowermost sample (3996 m), likely due to extremely low TOC and S_2 values. Hence only a remaining petroleum potential can be determined for Korolyn-2.

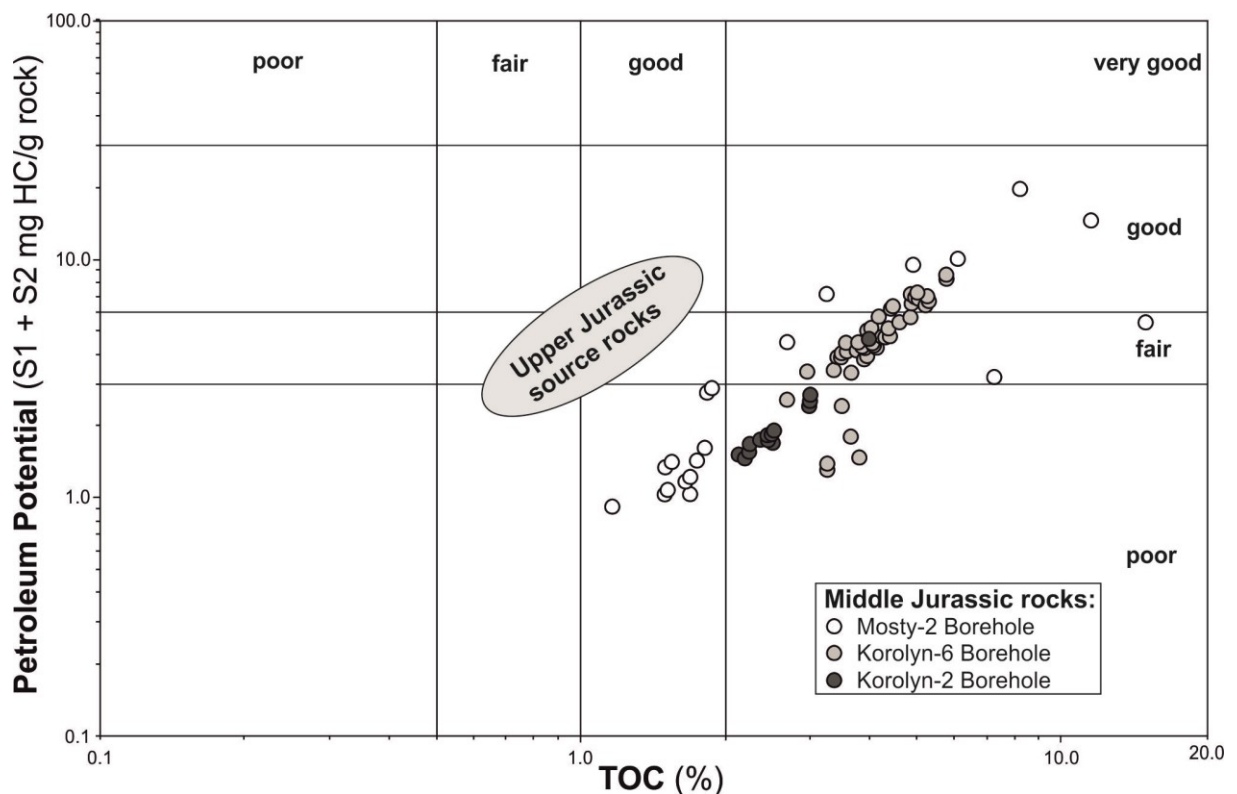


Fig. 11. Petroleum potential vs. TOC for the rocks from the Mosty-2, Korolyn-6 and Korolyn-2 wells. Grey field represents Upper Jurassic source rocks after Kosakowski et al. (2012).

Irrespective of maturity, TOC contents for the Mosty-2, Korolyn-6 and Korolyn-2 rocks are high (Fig. 3) and average 3.93, 4.17, and 2.75 wt. %, respectively. Low TOC contents are observed only in Middle Jurassic rocks between 3870 and 3996 m depth in Korolyn-2 (max. 0.13 wt. %). HI values of immature to marginally mature samples in the Mosty-2 (average 112; max. 242 mg HC/g TOC) and Korolyn-6 (average 105 mg HC/g TOC) wells show the presence of type III kerogen, which is also supported by a strong predominance of terrigenous macerals.

A cross-plot of Rock-Eval S_1+S_2 (petroleum potential) versus TOC (Fig. 11) indicates strongly varying source potential for Mosty-2 samples ranging from poor to good. A fair to good source potential is also visible for Korolyn-6 samples, however, the original potential of rocks from this well may have been slightly higher. In contrast, the poor (remaining) potential of the Korolyn-2 samples is clearly a result of their higher maturity.

6.2 Oil samples: Thermal maturity and implications for source rocks

The three studied oil samples are from Upper Jurassic reservoirs in the Kokhanivka Zone in Ukraine. Two nearby oil samples from the extension of this zone in Poland (Lubaczow-157; Opaka-1) have been studied by Curtis et al. (2004) and Więclaw (2011) and are included in this discussion. Well locations are shown in Fig. 1b and available data is listed in Table 2.

The MPI-1 (Table 2) values for the Kokhanivka-26 (0.68 % Rc), Orkhovychi-2 (0.71 % Rc), Orkhovychi-5 (0.71 % Rc) and Opaka-1 (0.78 % Rc) wells indicate early oil window maturity. In contrast, moretane/hopane ratios (0.07–0.08), C31 22S/(22S+22R) homohopane ratios (~0.6), CPI values (0.94–0.96) as well as the 20S/(20S+20R) versus $\beta\beta/(\beta\beta+\alpha\alpha)$ for the C₂₉ steranes and Ts/Tm (Fig. 10) suggest peak oil maturity.

Pr/Ph ratios are very low (0.29–0.54; Table 2) indicating strongly oxygen-depleted conditions during deposition of the rocks. Very high DBT/Phen ratios (Table 2) indicate that free H₂S was elevated in the water column. On a cross-plot of Pr/Ph vs. DBT/Phen (Fig. 12b; Hughes et al. 1995), the studied oils plot in Zone 1 (A and B sub-zones), which denotes a marine carbonate depositional environment. This is further supported by very low diasteranes/steranes ratios observed in the oil samples, as well as the low CPI (<1). In addition, distributions of *n*-alkanes in the crude oil samples display a maximum in short-chain hydrocarbons (Table 2), reflecting hydrocarbons generated from marine organic matter (Peters et al. 2007), which was deposited in a carbonate-rich environment. Since oleanane was not detected in any of the oils, the age of the source rock most probably is Jurassic or older. However, it is important to consider that the absence of oleanane does not always necessarily indicate pre-Cretaceous source rocks.

Elevated asphaltene content (Table 2) in the analysed oil samples, generally around 20 wt. % (max: 33 wt. %), is higher than in oils from the Outer Carpathians (Boryslaw–Pokuttya Unit; Więclaw et al. 2012). Więclaw et al. (2012) used this fact as an indication for short-distance migration and postulated that the source rock is in close proximity to the reservoir rocks.

6.3 Oil-source correlation

An important aspect of the study was to correlate oils within Upper Jurassic reservoirs with the potential Middle Jurassic source rocks (Kokhanivka Fm.). However, because biomarker and isotope data are not compatible with a genetic link between the oils and the Middle Jurassic rocks (see below), data from Upper Jurassic source rocks (Kosakowski et al. 2012) are also taken into account.

The main arguments against a genetic link between accumulated oils and the Middle Jurassic rocks are derived from plots of DBT/Phenanthrene ratios versus pristane/phytane ratios (Fig. 12b). DBT/Phenanthrene ratios are very high for the oil samples compared to the Middle Jurassic rocks. The mismatch is also evident in plots of pristane/ nC_{17} vs. phytane/ nC_{18} ratios (Fig. 12a), isotopic signatures (Fig. 7) and in differing sterane distributions (Fig. 6).

This shows that the studied section of the Middle Jurassic Kokhanivka Formation is not the source rock for the accumulated oil. Hence an alternative solution has to be found. According to Kosakowski et al. (2012), the TOC contents in Upper Jurassic rocks from the study area are usually low (median: 0.08 wt. %), but samples from the Voloshcha-1 and Korolyn-6 (for location see Fig. 1b; for selected data, see Table 2) wells contain high amounts of organic matter. TOC values in samples between 2650 and 3300 m depth from the Voloshcha-1 well displayed average TOC content of over 1 wt. % (max: 12.1 wt. %), but low HI values (~100 mg HC/g TOC), indicating the presence of type III kerogen, which is also supported by maceral data and high CPI values (Kosakowski et al. 2012).

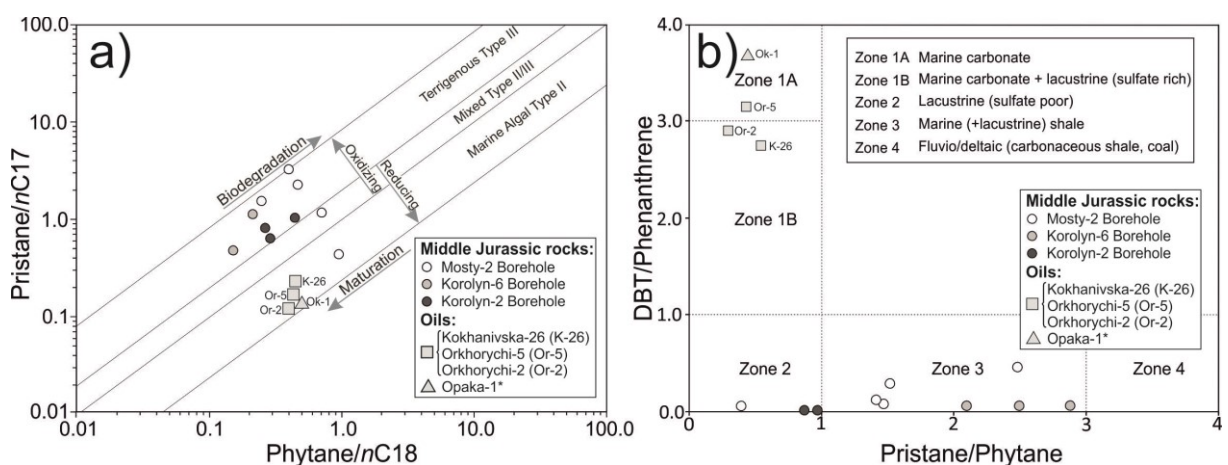


Fig. 12. a) Pristane/ nC_{17} versus phytane/ nC_{18} for rocks and oil samples after Peters et al. 2007. b) A cross-plot of the dibenzothiophene (DBT)/ phenanthrene ratio versus the

pristane/phytane ratio. Classification of source kerogen sedimentation conditions after Hughes et al. 1995. Data from Opaka-1 according to Więclaw 2011.

In contrast, Upper Jurassic rocks from the Korolyn-6 well (1973–3037 m depth) contain layers with very high HI (max: 557 mg HC/g TOC), but moderately high TOC (max. 1.5 wt. %; Kosakowski et al. 2012) in the depth interval between 2140 and 2500 m, which can be considered as having a fair to good hydrocarbon potential (Fig. 11). High organic sulphur contents classify the kerogen as type IIS (Kosakowski et al. 2012), which may generate hydrocarbons below the typical limits of the oil window. The potential source rocks are also compatible with the high DBT/Phenanthrene ratios detected in oil samples. Furthermore, two Upper Jurassic samples from the Korolyn-6 well yield the best fit in the steranes triangular diagram with the oil samples (Fig. 6). Hence, it is very likely that the oil was generated from platform slope deposits preserved in the south-western part of the Kokhanivka Zone in a narrow strip along the Krakovets Fault (Fig. 1b; Krajewski et al. 2011). This study, therefore, confirms earlier models published by Kotarba et al. (2011) and Kosakowski et al. (2012).

7. Conclusion:

The investigation of 89 samples representing the Middle Jurassic Kokhanivka Formation in the basement of the Ukrainian Carpathian Foredeep and of three oil samples from Upper Jurassic reservoirs yielded important insights into the petroleum system:

- Middle Jurassic rocks contain high organic matter contents (average TOC: 4.19 wt.; max.: 14.98 wt.%). The organic matter is dominated by terrigenous macerals from a nearby hinterland. Therefore, HI values are generally low (max: 242 mgHC/gTOC), classifying the organic matter a gas-prone type III kerogen (with rare transitions to type II kerogen).
- Despite the high TOC contents, Middle Jurassic rocks can be considered “fair” source rocks. Based on the total petroleum potential (Rock-Eval S_1+S_2), only few horizons display “good” source rock potential.
- As a consequence of the high terrestrial input, Pr/Ph ratios are often high (max: 2.84). DBT/Phen ratios for these rocks are generally low, arguing for an absence of salinity stratification of the water column.
- Thermal maturity of the Middle Jurassic rocks is mainly controlled by depth of burial. Mosty-2 samples (2361-2560 m depth) are marginally mature, whereas Korolyn-6 (3418-3523 m) and Korolyn-2 samples (3642-3996 m) reach peak oil window maturity. Major hydrocarbon generation started at about 3500 m depth.
- Oil samples derived from Upper Jurassic reservoir rocks are sulphur-rich and show very high DBT/Phen ratios. In contrast, Pr/Ph (<0.6) and diasterane/sterane (0.01) ratios are very low.
- Major differences in DBT/Phen ratios, Pr/Ph ratios and carbon isotope ratios between oil and rock samples clearly show that the oils have not been charged from Middle Jurassic rocks.
- A comparison with published data from Upper Jurassic rocks (Kosakowski et al., 2011a) suggests that the oils have been generated from platform slope deposits preserved in a narrow stripe along the southwestern part of the Kokhanivvka Zone.

Acknowledgements

The authors would like to thank Drs Yuriy Koltun and V. E. Shlapinski for their contributions to the current study and for their insights and expertise in the field.

References:

- Alexander, R., Kagi, R.I., Toh, E., and Van Bronswijk, W., 1988. The use of aromatic hydrocarbons for assessment of thermal histories in sediments. In: Purcell, P. G., Purcell, R. R., (Eds.), *The North West Shelf, Australia: Proceedings of the Petroleum Exploration Society of Australia, Perth*. Petroleum Exploration Society of Australia, 62-559.
- Anikeyeva, O., and Zhabina, N., 2002. Facies of Late Jurassic source rocks: Ukrainian Carpathian Foredeep. In: *New methods and technologies in petroleum geology, drilling, and reservoir engineering*. Akademia Gurniczno-Hutnicza, 1, 23-27.
- Bechtel, A., Jia, J., Strobl, S.A.I., Sachsenhofer, R.F., Liu, Z., Gratzner, R., and Püttmann, W., 2012. Palaeoenvironmental conditions during deposition of the Upper Cretaceous oil shale sequences in the Songliao Basin (NE China): Implications from geochemical analysis. *Organic Geochemistry*, 46, 76-95.
- Berner, R.A., and Raiswell, R., 1984. C/S method for distinguishing freshwater from marine sedimentary rocks. *Geology*, 12, 365-368.
- Bray, E.E., and Evans, E.D., 1961. Distribution of n-paraffins as a clue to recognition of source beds. *Geochimica et Cosmochimica Acta*, 22, 2-15.
- Boote, D.R.D., Sachsenhofer, R.F., Tari, G., and Arbouille, D., 2018. Petroleum provinces of the Paratethyan region. *Journal of Petroleum Geology*, 41, 247-298.
- Buła, Z., and Habryn, R., 2011. Precambrian and Palaeozoic basement of the Carpathian Foredeep and the adjacent Outer Carpathians (SE Poland and western Ukraine). *Annales Societatis Geologorum Poloniae*, 81, 221-239.
- Callejon, A.F., Briceno, H., Ostos, M., Talkukdar, S., Yoris, F., and Lander, R., 2003. Petroleum Systems in the Rubio and Burgua Depressions, Venezuela. In: Bartolini, R. T., Buffler, and Blickwede, J., (Eds.), *The Circum-Gulf of Mexico and the Caribbean: Hydrocarbon habitats, basin formation, and plate tectonics: AAPG Memoir*, 79, 937-960.
- Curtis, J.B., Kotarba, M.J., Lewan, M.D., and Więclaw, D., 2004. Oil/source rock correlations in the Polish Flysch Carpathians and Mesozoic basement and organic facies of the Oligocene Menilite Shales: insights from hydrous pyrolysis experiments. *Organic Geochemistry*, 35, 1573-1596.
- Drygant, D., 2000. Lower and Middle Palaeozoic of the Volyn–Podollya margin of the East-European Platform and Carpathian Foredeep. (In Ukrainian, English summary). *Naukovizapiski Derzhavnogo prirodoznavechego muzeyu*, 15, 24-130.
- Dulub, V.G., Burova, M.I., Burov, V.S., and Vishniakov, I.B., 1986. Explanatory Note to the Regional Stratigraphic Scheme of the Jurassic Deposits of the Carpathian Foredeep and Volyn-Podolian Margin of the East-European Platform (In Russian). Leningrad, 58 pp.
- Dulub, W.G., Zhabina, N.M., Ohorodnik, M.E., and Smirnov, S.E., 2003. The explanatory note to the stratigraphy of Jurassic deposits of Ukrainian Carpathian foreland; Stryj Jurassic basin (In Ukrainian). Ukrainian State Geological Research Institute, 30 pp.
- Espitalie, J., Marquis, F., and Barsony, I., 1984. Geochemical logging. In: Voorhess, K. J. (Ed), *Analytical Pyrolysis*, 53-79.

- Glushko, V.V., 1968. Tektonika i neftegazonosnost Karpatiprile-gayuschikh progibov. (In Russian). Nedra, Moscow, 264-267.
- Gutowski, J., Popadyuk, I.V., and Olszewska, B., 2005a. Late Jurassic-earliest Cretaceous evolution of the epicontinental sedimentary basin of southeastern Poland and Western Ukraine. *Geological Quarterly*, 49, 31-44.
- Gutowski, J., Popadyuk, I.V., Olszewska, B., 2005b. Stratigraphy and facies development of the upper Tithonian-lower Berriasian Nizniów Formation along the Dnister River (Western Ukraine). *Geological Quarterly*, 49, 45-52.
- Huang, W.Y., and Meinschein, W.G., 1979. Sterols as ecological indicators. *Geochimica et Cosmochimica Acta*, 43, 739-745.
- Hughes, W.B., Holba, A.G., and Dzou, L.I.P., 1995. The ratios of dibenzothiophene to phenanthrene and pristan to phytane as indicators of depositional environment and lithology of petroleum source rocks. *Geochimica et Cosmochimica Acta*, 59, 3581-3598.
- International Committee for Coal and Organic Petrology (ICCP), 1998. The new vitrinite classification (ICCP System 1994). *Fuel*, 77, 349-358.
- International Committee for Coal and Organic Petrology (ICCP), 2001. The new inertinite classification (ICCP System 1994). *Fuel*, 80, 459-471.
- Jachowicz-Zdanowska, M., 2011. Cambrian organic microfossils at the border area of the East- and West-European platforms (SE Poland and west Ukraine). *Annales Societatis Geologorum Poloniae*, 81, 241-267.
- Karnkowski, P., 1999. Oil and gas deposits in Poland. The Geosynoptics Society "Geos" and University of Mining and Metallurgy, 380.
- Koltun, Y., Espitalié, J., Kotarba, M., Roure, F., Ellouz, N., and Kosakowski, P., 1998. Petroleum generation in the Ukrainian External Carpathians and the adjacent foreland. *Journal of Petroleum Geology*, 21, 265-288.
- Kosakowski, P., Więclaw, D., Kowalski, A., and Koltun, Y., 2012a. Assessment of hydrocarbon potential of Jurassic and Cretaceous source rocks in the Tarnograd-Stryi area (SE Poland and W Ukraine). *Geologica Carpathica*, 63, 319-333.
- Kosakowski, P., Więclaw, D., Kotarba, M.J., and Kowalski, A., 2012b. Habitat and hydrocarbon potential of the Mesozoic strata in the Kraków-Rzeszów area (SE Poland). *Geol. Quart.*, 56, 139-152.
- Kosakowski, P., Wrobel, M., and Krzywiec, P., 2013. Modelling hydrocarbon generation in the Palaeozoic and Mesozoic successions in SE Poland and West Ukraine. *Journal of Petroleum Geology*, 36, 139-162.
- Kotarba, M.J., and Koltun, Y.V., 2006. The origin and habitat of hydrocarbons of the Polish and Ukrainian parts of the Carpathian Province. In: Golonka, J. and Picha, F.J. (Eds), *The Carpathians and their foreland: Geology and hydrocarbon resources*. 84, 395-442.
- Kotarba, M.J., and Koltun, Y.V., 2011. Origin of natural gas in the autochthonous Miocene strata of the Ukrainian Carpathian Foredeep and its Mesozoic basement. *Annales Societatis Geologorum Poloniae*. 81, 425-441.
- Kotarba, M., Więclaw, D., Kosakowski, P., Wrobel, M., Matyszkiewicz, J., Bula, Z., Krajewski, M., Koltun, Y., and Tarkowski, J., 2011. Petroleum systems in the

- Palaeozoic-Mesozoic basement of the Polish and Ukrainian parts of the Carpathian Foredeep. *Annales Societatis Geologorum Poloniae*, 81, 487-522.
- Kotarba, M., Więclaw, D., Koltun, Y., Marynowski, L., Kusmierk, J., and Dudok, I., 2007. Organic geochemical study and genetic correlation of natural gas, oil and Menilite source rocks in the area between San and Stryi rivers (Polish and Ukrainian Carpathians). *Organic Geochemistry*, 38, 1431-1456.
- Krajewski, M., Krol, K., Olszewska, B., Felisiak, I., Skwarczek, M., 2011. Facies of the Upper Jurassic-Lower Cretaceous sediments in the basement of the Carpathian Foredeep (western Ukraine). *Annales Societatis Geologorum Poloniae*, 81, 291-307.
- Kurovets, I., Prytulka, H., Shyra, A., Shuflyak, Y. and Peryt, T. M., 2011. Petrophysical properties of pre-Miocene rocks of the outer zone of the Ukrainian Carpathian Foredeep. *Annales Societatis Geologorum Poloniae*, 81, 363-373.
- Mackenzie, A.S., Patience, R.L., Maxwell, J.R., Vandenbroucke, M. and Durand, B., 1980. Molecular parameters of maturation in the Toarcian shales, Paris Basin, France - I. Changes in the configuration of acyclic isoprenoid alkanes, steranes, and triterpanes. *Geochimica et Cosmochimica Acta*, 44, 1709-21.
- Mello, M.R., Telnaes, N., and Gaglianone, P.C., 1988. Organic geochemical characterization of depositional paleo-environments in Brazilian marginal basins. *Organic Geochemistry*, 13, 31-46.
- Moldowan, J.M., and Fago, F.J., 1986. Structure and significance of a novel rearranged monoaromatic steroid hydrocarbon in petroleum. *Geochimica et Cosmochimica Acta*, 50, 343-51.
- Moryc, W., 2004. Middle and Lower Jurassic deposits in the Księżpol-Lubaczów area (SE Poland). (In Polish, English summary). *Biuletyn Państwowego Instytutu Geologicznego*, 408, 5-71
- Nakapelyukh, M., Bubniak, I., Bubniak, A., Jonckheere, R., and Ratschbacher, L., 2018, Cenozoic structural evolution, thermal history, and erosion of the Ukrainian Carpathians fold-thrust belt. *Tectonophysics*, 722, 197-209.
- Oszczypko, N., 2006. Late Jurassic-Miocene evolution of the Outer Carpathian fold-and-thrust belt and its foredeep basin (Western Carpathians, Poland). *Geological Quarterly*, 169-194.
- Oszczypko, N., Krzywiec, P., Popadyuk, I., and Peryt, T., 2006. Carpathian Foredeep Basin (Poland and Ukraine): Its Sedimentary, Structural, and Geodynamic Evolution. In: J. Golonka and Frank J. Puicha, (Eds.), *The Carpathians and Their Foreland: Geology and Hydrocarbon Researches: AAPG Memoir*, 84, 261-318.
- Ourisson, G., Albrecht, P., and Rohmer, M., 1979. The hopanoids: palaeo-chemistry and biochemistry of a group of natural products. *Pure Applied Chemistry*, 51, 709-729.
- Peters, K.E., 1986. Guidelines for Evaluating Petroleum Source Rock Using Programmed Pyrolysis. *AAPG Bulletin*, 70, 318-329.
- Peters, K.E., Walter, C.C., and Moldowan, J.M., 2007. Biomarkers and Isotopes in Petroleum Systems and Earth History. *The Biomarker Guide* 2, 499-502.
- Pieńkowski, G., Schudack, M.E., Bosák, P., Enay, R., Feldman-Olszewska, A., Golonka, J. Gutowski, J., Hengreen, G.F.W., Jordan, P., Krobicki, M., Lathuiliere, B., Leinfelder, R.R., Michalík, J., Mönnig, E., Noe-Nygaard, N., Pálffy, J., Pint, A., Rasser, M.W.,

- Reisdorf, A.G., Schmid, D.U., Schweigert, G., Surlyk, F., Wetzel, A., and Wong, T.E., 2008. Jurassic. In: T. McCann, (Ed.), *Geology of Central Europe, Volume 2: Mesozoic and Cenozoic*, Geological Society of London, 823-922.
- Popadyuk, I., Vul, M., Ladyzhensky, G., Shpak, P., 2006. The Petroleum Geology of the Ukrainian Carpathian Foredeep. In: J. Golonka and Frank J. Picha, (Eds.), *The Carpathians and Their Foreland: Geology and Hydrocarbon Researches: AAPG Memoir*, 84, 443-454.
- Radke, M., Welte, D. H. and Willsch, H. (1982) Geochemical study on a well in the Western Canada Basin: relation of the aromatic distribution pattern to maturity of organic matter. *Geochimica et Cosmochimica Acta*, 46, 1–10.
- Radke, M., Willisch, H., and Welte, D.H., 1980. Preparative hydrocarbon group type determination by automated medium liquid pressure chromatography. *Anal. Chem.* 52, 406-411.
- Radkovets N., Kotarba M., Koltun Y., Kowalski A., Kosakowski P., and Więclaw D., 2016. Origin and migration of oil from the Ukrainian Outer Carpathians to their Mesozoic basement: a case of Lopushna traps. *Geological Quarterly*, 60, 88 -103.
- Rauball, J.F., Sachsenhofer, R.F., Bechtel, A., Coric, S., and Gratzner, R., 2019. The Oligocene-Miocene Menilite Formation in the Ukrainian Carpathians: A world-class source rock. *Journal of Petroleum Geology*, 42, 392-416.
- Sachsenhofer, R.F., and Koltun, Y., 2012. Black shales in Ukraine - A review. *Marine and Petroleum Geology*. 31, 125-136.
- Slaczka, A., Kruglov, S., Golonka, J., Oszczytko, N., and Popadyuk, I., 2006. Geology and Hydrocarbon Resources of the Outer Carpathians, Poland, Slovakia, and Ukraine: General Geology. J. Golonka and Frank J. Picha, (Eds.), *The Carpathians and Their Foreland: Geology and Hydrocarbon Researches: AAPG Memoir*, 84, 221-258.
- Seifert, W. K., and Moldowan, J. M., 1986. Use of biological markers in petroleum exploration. In: Johns, R.B., (Eds), *Methods in Geochemistry and Geophysics*, 261–90.
- Seifert, W. K., and Moldowan, J. M., 1980. The effect of thermal stress on source-rock quality as measured by hopane stereochemistry. *Physics and Chemistry of the Earth*, 12, 229-37.
- Simoneit, B.R.T., 1986. Cyclic terpenoids of the geosphere. In: Johns, R. B., (Ed.), *Biological Markers in the Sedimentary Record*, 43-99.
- Swidrowska, J., Hakenberg, M., Poluhtovia, B., Seghedi, A., and Višnikov, I., 2008. Evolution of the Mesozoic Basins on the southwestern edge of the East European Craton (Poland, Ukraine, Moldova, Romania). *Studia Geologica Polonica*, 130, 3-130.
- Taylor, G.H., Teichmüller, M., Davis, A., Diessel, C.F.K., Littke, R., and Robert, P., 1998. *Organic Petrology*, 655-704.
- Wakeham, S.G., Schaffner, C., and Giger, W., 1980. Polycyclic aromatic hydrocarbons in recent lake sediments - II. Compounds derived from biogenic precursors during early diagenesis. *Geochimica et Cosmochimica Acta*, 44, 415-29.
- Więclaw, D., Kosakowski, P., Kotarba, M. J., Kowalski, A., and Koltun, Y. V., 2012. Assessment of hydrocarbon potential of the Lower Palaeozoic strata in the Tarnogród-Stryi area (SE Poland and western Ukraine). *Geological Quarterly*, 56, 153-168.

- Więclaw, D., 2011. Origin of Liquid Hydrocarbons accumulated in the Miocene strata of the Polish Carpathian Foredeep and its Palaeozoic-Mesozoic Basement. *Annales Societatis Geologorum Poloniae*, 81, 443-458.
- Vul, M.Y., Denega, B.I., Krupsky, Y.Z., Nimets, M.V., Svyry-denko, V.G. and Fedyshyn, V.O., 1998. Western oil and gas-bearing region. In: Ivanyuta, M. M., Fedyshyn, V. O. et al., (Eds), *Atlas of oil and gas fields of Ukraine in six volumes*. Ukrainian Oil and Gas Academy, 4, 328.

10.1 **Appendix I** – Author contributions to the publications included in this thesis.

Publication I:

The Oligocene-Miocene Menilite Formation in the Ukrainian Carpathians: A world-class source rock. Journal of Petroleum Geology (2019), 42, 393-415.

Rauball, J., Sachsenhofer, R.F., Bechtel, A., Coric, S., Gratzner, R.

Contributions:

Johannes Rauball did the sampling of the Menilite Fm. in the Skyba nappe in Ukraine, together with Y. Koltun, who provided additional regional information. Johannes Rauball did the sample preparation as well as all the analytical work and data interpretation. A. Bechtel and R. Gratzner were helpful with the execution of biomarker and isotope geochemical analysis. R. Sachsenhofer helped with the interpretation of the geochemical parameters and gave a thorough proofread of several versions of the manuscript. The study of calcareous nanofossils was conducted in the Geological Survey of Austria (GBA) in Vienna by S. Coric.

A majority of the work necessary for this paper (approximately 90 %) was conducted by Johannes Rauball.

Publication II:

Hydrocarbon potential of the Lower Cretaceous (Barremian-Albian) Shypot Formation in the Chornohora nappe, Ukraine. Geologica Carpathica. Accepted for publication in Geologica Carpathica (2020).

Rauball, J., Sachsenhofer, R.F., Bechtel, A.

Contributions:

Johannes Rauball did the sampling of the Shypot Fm. in the Chornohora nappe in Ukraine, together with R.F. Sachsenhofer and Y. Koltun as well as V.E. Shlapinsky, who provided additional regional information. Johannes Rauball did the sample preparation as well as all the analytical work and data interpretation. A. Bechtel was helpful with the execution of biomarker and isotope geochemical analysis. R. Sachsenhofer helped with the interpretation of the geochemical parameters and gave a thorough proofread of several versions of the manuscript.

A majority of the work necessary for this paper (approximately 90 %) was conducted by Johannes Rauball.

Publication III:

Petroleum potential of Middle Jurassic rocks in the basement of the Carpathian Foredeep (Ukraine) and oil-to-source correlation with oil in Upper Jurassic reservoirs. Geologica Carpathica (2020), 71, 150-165.

Rauball, J., Sachsenhofer, R.F., Bechtel, A.

Contributions:

Y. Koltun did the sampling of the Middle Jurassic strata as well as the oil samples from the Upper Jurassic reservoirs in Ukraine. Johannes Rauball did all the analytical work and data interpretation. A. Bechtel was helpful with the execution of biomarker and isotope geochemical analysis. R. Sachsenhofer helped with the interpretation of the geochemical parameters and gave a thorough proofread of several versions of the manuscript.

A majority of the work necessary for this paper (approximately 95 %) was conducted by Johannes Rauball.

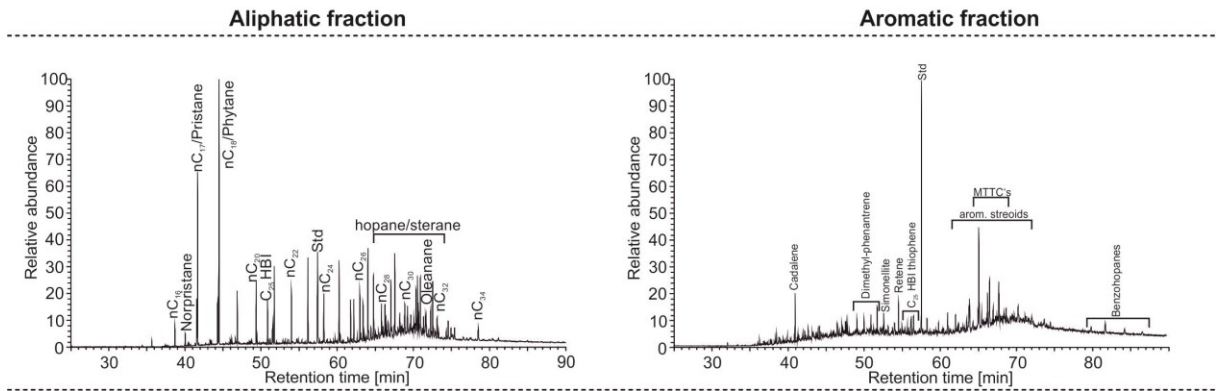
Appendix abbreviations:

C	Total carbon content
Calc. Equiv.	Calcite Equivalent
Fm.	Formation
HI	Hydrogen Index
NP	Nannoplankton Zone
S	Sulphur content
TIC	Total inorganic carbon
TOC	Total organic carbon
TOC/S	TOC/S ratio

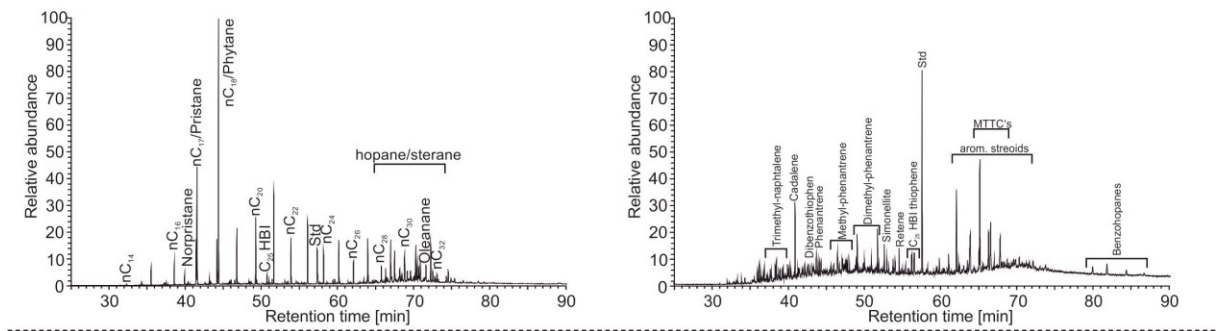
10.2 Appendix II – Oligocene – Lower Miocene Menilite Formation

NP	Depth [m]	S ₁ [mgHC/gRock]	S ₂	T _{max} [°C]	TOC [%]	S [%]	TOC/S [-]	HI [mgHC/gTOC]	TIC [%]	Calc. Equiv. [%]	Isotopy δ13C δ18O	Biomarker
Lower Miocene Upper Menilite Member												
NN2	0	0.01	1.19	427	1.01	0.38	2.64	117	1.69	14.06	-1.98 -3.24	
NN2	25	0.02	1.11	427	1.00	0.35	2.90	111	2.20	18.36	-2.04 -9.67	
NN2	37	0.01	1.44	427	1.21	0.37	3.24	119	1.93	16.11	-0.78 -9.05	
NN2	51	0.01	0.98	429	0.87	0.89	0.99	111	2.02	16.82	-0.86 -4.01	
NN2	59	0.05	6.00	428	2.18	0.94	2.31	275	1.66	13.83	-0.85 -5.87	x
NN2	75	0.04	5.14	428	2.10	1.01	2.08	244	1.61	13.42	-2.13 -12.44	
NN2	83	0.03	2.24	430	1.19	0.43	2.76	188	2.60	21.70	-2.13 -8.84	
	89	0.04	2.63	430	1.39	0.65	2.15	189	0.47	3.95		
NN2	230	0.14	14.27	427	3.36	1.59	2.12	424	1.05	8.75	-1.67 -7.87	
	256	0.34	19.13	420	4.97	2.88	1.73	385	0.00	0.00		
	265	0.61	25.49	423	5.94	2.51	2.37	429	0.03	0.27		x
NN2	278	0.07	2.17	430	1.52	1.27	1.20	142	1.92	15.99	-1.01 -5.20	
	304	0.49	35.38	417	8.52	3.17	2.69	415	0.03	0.22		
	311	0.90	43.51	419	8.94	3.05	2.93	487	0.19	1.59		
	324	0.22	19.40	422	5.86	1.45	4.03	331	0.00	0.00		
	339	0.47	31.34	417	7.40	3.80	1.95	423	0.13	1.12		x
	348	0.18	11.31	428	3.33	1.68	1.98	339	0.18	1.53		
	356	0.25	19.38	423	5.01	2.93	1.71	387	0.23	1.95		
	373	0.01	0.21	432	0.25	0.03	7.78	144	0.00	0.00		
	375	0.16	15.56	423	3.71	1.89	1.96	420	0.42	3.49		
	379	0.19	21.02	423	5.82	0.63	9.19	361	0.00	0.06		x
	386	0.05	5.13	427	2.49	0.44	5.65	206	0.00	0.00		
	393	0.15	11.38	424	3.37	2.06	1.63	338	0.37	3.11		
	403	0.24	15.22	418	4.18	2.59	1.61	364	0.00	0.00		
	413	0.46	28.07	416	6.88	3.88	1.77	408	0.01	0.05		x
	418	0.15	12.87	423	3.26	1.65	1.98	395	0.37	3.06		
	495	0.21	19.69	421	5.39	1.97	2.73	365	0.20	1.70		
NN2	865	0.10	8.70	428	3.15	1.46	2.16	276	1.27	10.59	-1.67 -10.41	
	870	0.12	12.15	430	3.39	1.20	2.82	359	0.52	4.36		
NN2	875	0.30	30.60	423	7.10	1.70	4.19	431	0.68	5.69	-1.87 -9.21	
	880	0.28	25.30	425	5.03	2.12	2.37	503	0.31	2.62		
NN2	888	0.48	19.17	424	3.87	2.08	1.86	496	0.92	7.67	0.54 -5.10	
	894	0.31	21.71	421	4.68	2.55	1.83	464	0.45	3.79		
	899	0.75	56.57	425	9.16	2.40	3.82	617	0.17	1.44		x
	906	1.30	78.38	420	16.19	2.58	6.27	484	0.23	1.89		
NN2	911	0.10	7.46	427	2.43	1.19	2.05	307	1.15	9.55	-1.34 -13.78	
	916	0.15	12.49	432	3.64	1.09	3.34	343	0.14	1.18		
NN2	922	0.18	15.78	428	3.57	1.45	2.46	442	0.72	6.01	-1.20 -10.76	
	928	0.28	20.49	424	4.70	1.64	2.86	436	0.71	4.80		x
	930.5	0.20	13.34	428	3.46	1.62	2.13	386	0.97	3.76		
NN2	933.5	0.11	7.93	428	2.22	1.19	1.86	357	1.89	15.76	-1.11 -4.45	

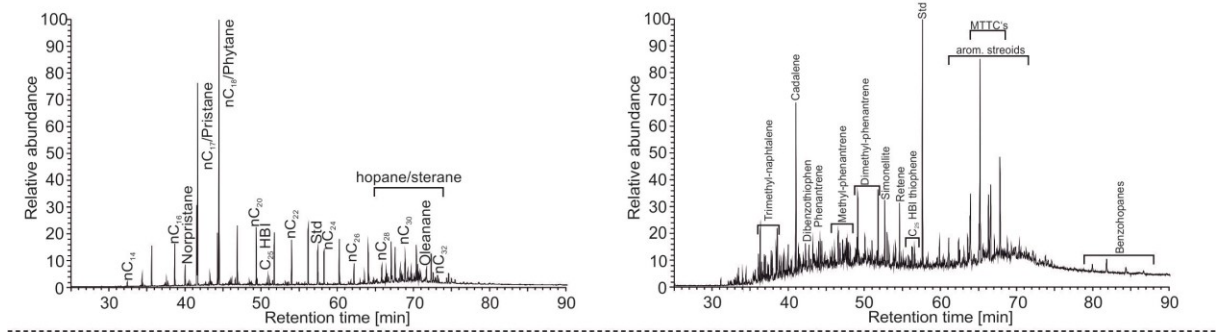
NP	Depth [m]	S ₁ [mgHC/gRock]	S ₂	T _{max} [°C]	TOC [%]	S [%]	TOC/S [-]	HI [mgHC/gTOC]	TIC [%]	Calc. Equiv. [%]	Isotopy δ13C δ18O		Biomarker
Lower Miocene Upper Menilite Member													
	939.5	0.21	17.21	430	3.91	1.44	2.72	441	0.29	2.40			
NN2	947	0.10	6.79	431	2.26	1.29	1.75	301	1.48	12.36	-0.56	-13.43	
NN2	970	0.09	6.19	431	2.23	1.05	2.12	278	0.76	6.34	-0.98	-8.00	
	979	0.21	13.40	430	3.57	1.53	2.33	376	0.44	3.70			
NN2	985	0.19	15.11	429	3.75	1.54	2.43	403	0.72	5.99	-1.77	-6.12	x
NN2	993	0.13	10.01	429	2.59	1.56	1.65	387	1.11	9.28	-1.02	-7.23	
NN2	1020	0.17	13.51	430	3.52	1.81	1.94	383	0.59	4.95	-1.00	-6.34	
	1042	0.29	22.91	425	4.88	2.38	2.05	470	0.30	2.49			
	1045.5	0.83	51.82	422	9.03	3.17	2.85	574	0.18	1.49			x
	1048	0.15	14.36	427	4.08	1.82	2.24	352	0.54	4.51			
	1056	0.46	44.58	420	9.90	2.99	3.32	450	0.29	2.45			
	1071	0.18	18.32	430	4.84	1.54	3.14	379	0.20	1.65			
NN2	1077	0.14	9.18	428	2.85	1.23	2.31	322	0.77	6.41	-0.96	-6.55	
	1089	0.35	27.03	428	5.70	2.03	2.80	475	0.27	2.29			
NN2	1106.5	0.23	16.91	426	3.53	1.91	1.84	479	0.94	7.79	-0.54	-5.88	
	1115.5	0.29	24.39	426	5.38	2.28	2.36	454	0.43	3.58			x
NN1	1132	0.09	6.45	431	1.93	1.31	1.47	334	1.03	8.61	-0.44	-6.01	
	1139.5	0.18	14.12	428	3.40	1.92	1.77	416	0.33	2.78			
NN1	1146	0.16	11.40	429	3.06	1.66	1.84	373	1.21	10.09	-0.65	-6.07	
NN1	1159	0.25	10.98	430	2.64	1.48	1.78	416	0.82	6.83	-0.65	-14.12	
	1270	0.63	23.43	423	5.69	1.77	3.21	412	0.06	0.53			
	1274	2.82	63.24	417	15.95	3.77	4.23	396	0.19	1.60			
	1299	3.71	70.89	417	14.94	2.39	6.25	475	0.51	4.26			x
	1301	0.54	20.72	423	4.18	1.76	2.38	495	0.04	0.31			
	1306	0.08	12.41	429	4.37	0.29	15.14	284	0.01	0.12			
	1327	3.73	82.87	417	23.11	1.74	13.29	359	0.14	1.14			
	1333	0.53	14.69	427	3.26	1.21	2.70	450	0.03	0.22			
	1338	1.84	43.63	424	8.27	2.46	3.36	527	0.11	0.94			
	1341	1.44	36.25	421	7.08	1.44	4.92	512	0.08	0.63			
	1343	2.12	56.91	420	12.80	1.94	6.60	445	0.54	4.46			x
	1346	0.26	12.10	429	2.52	0.31	8.13	480	0.04	0.32			
	1350	0.03	0.54	433	0.34	0.18	1.91	159	0.06	0.47			
	1355	0.91	20.75	427	4.44	0.38	11.56	468	0.03	0.27			
	1360	0.31	10.92	431	2.34	0.19	12.45	467	0.01	0.12			



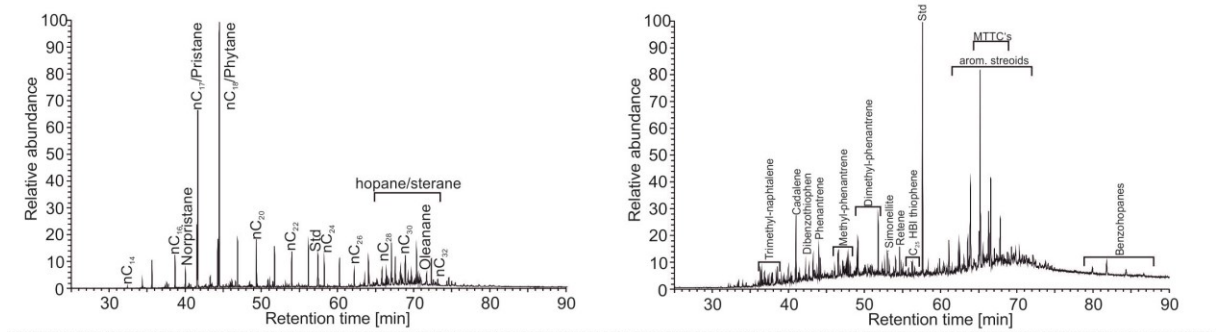
Menilite Formation/ Miocene/ Skyba nappe/ 59 m



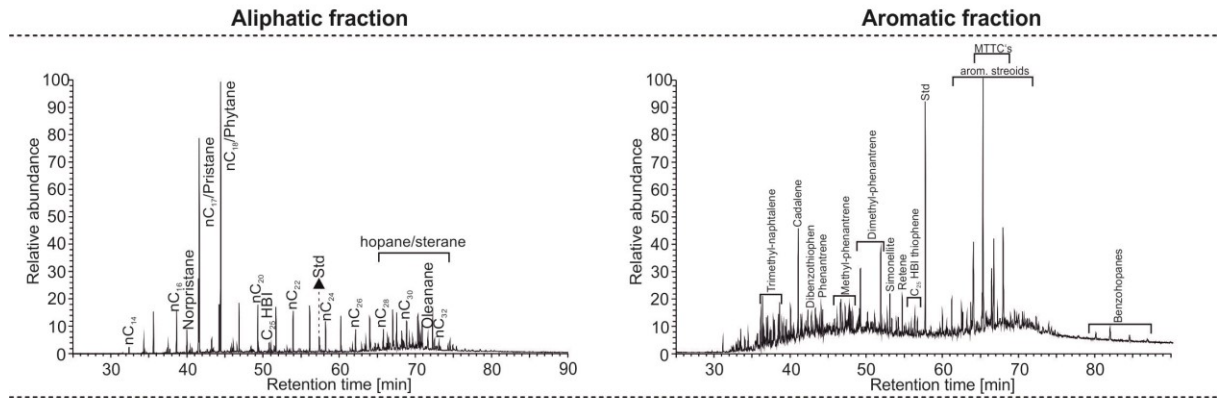
Menilite Formation/ Miocene/ Skyba nappe/ 265 m



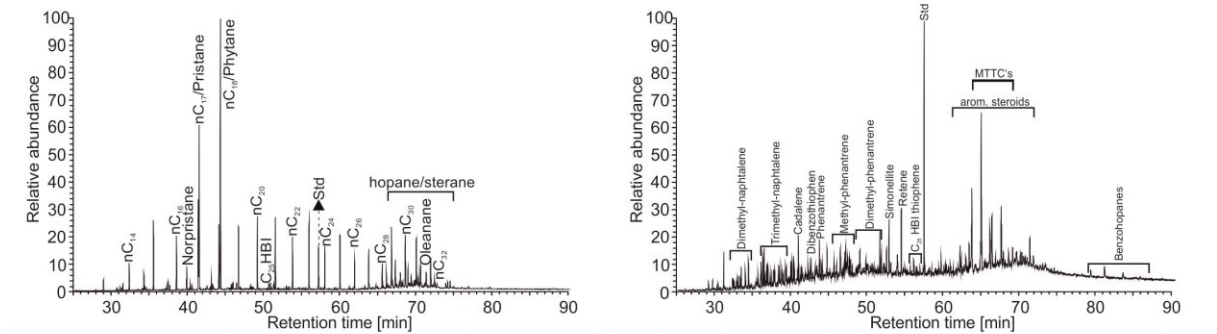
Menilite Formation/ Miocene/ Skyba nappe/ 339 m



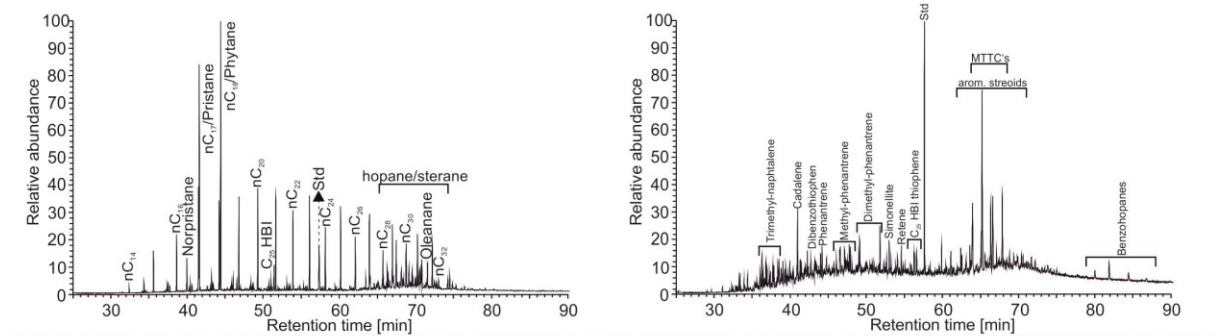
Menilite Formation/ Miocene/ Skyba nappe/ 379 m



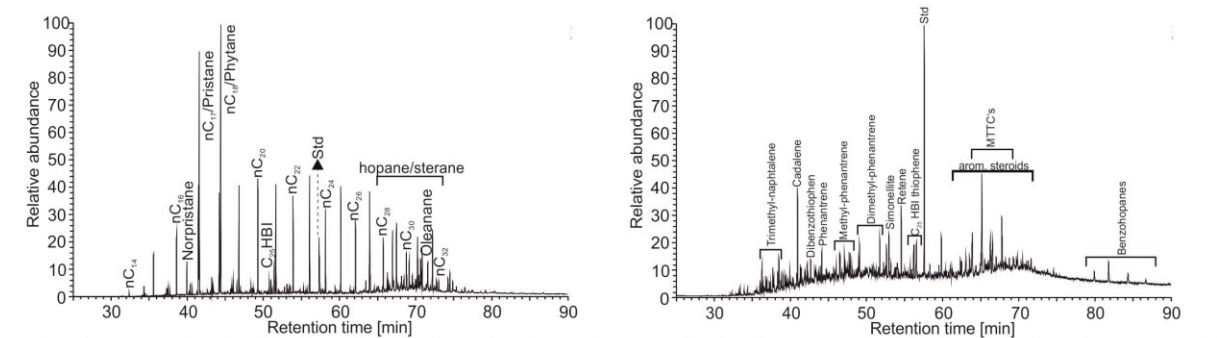
Menilite Formation/ Miocene/ Skyba nappe/ 413 m



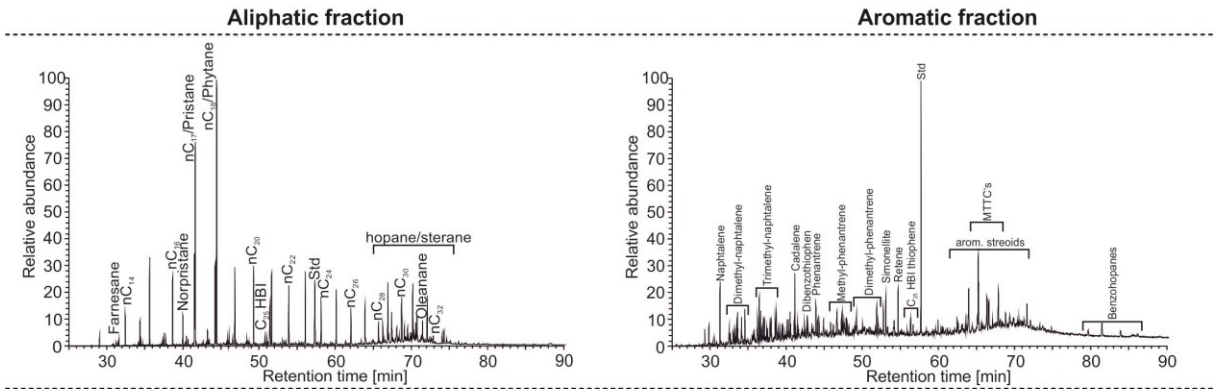
Menilite Formation/ Miocene/ Skyba nappe/ 899 m



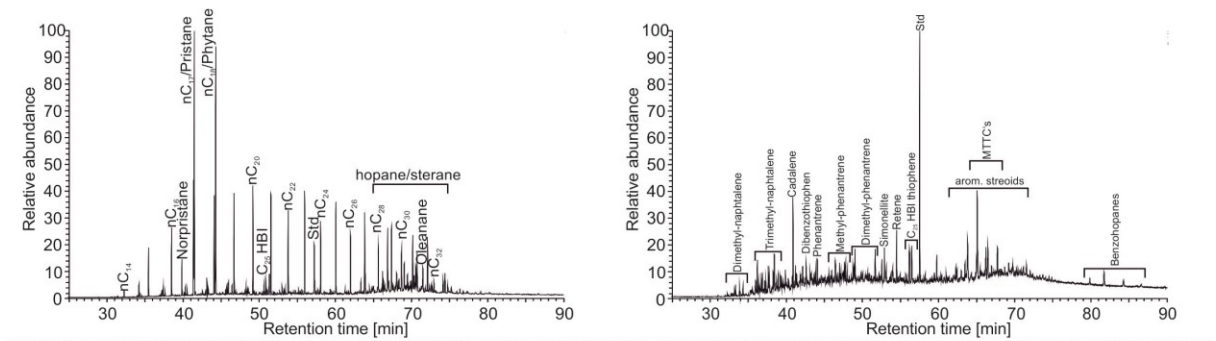
Menilite Formation/ Miocene/ Skyba nappe/ 928 m



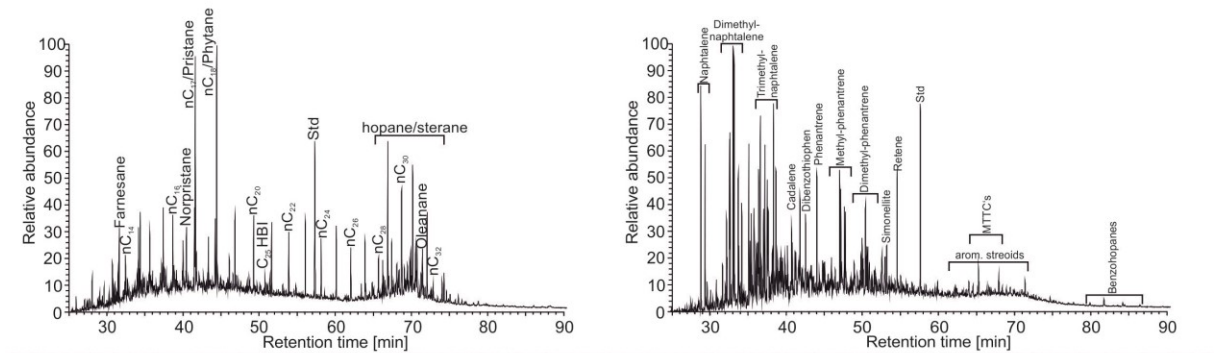
Menilite Formation/ Miocene/ Skyba nappe/ 985 m



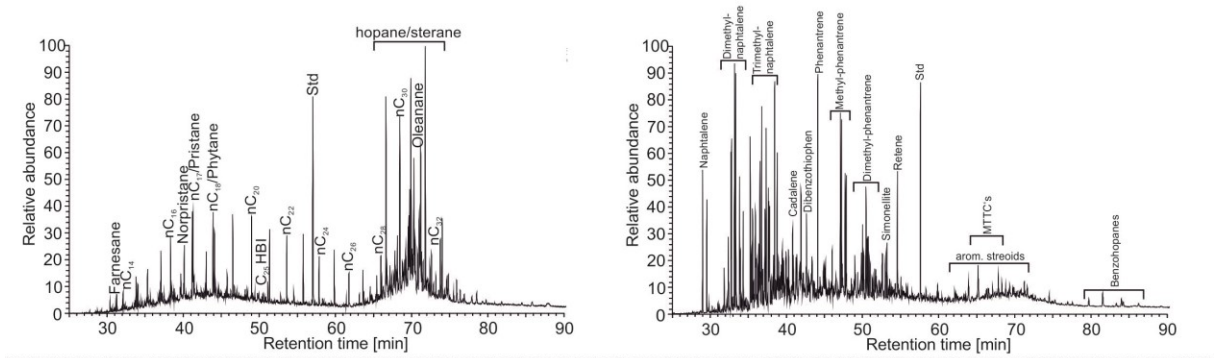
Menilite Formation/ Miocene/ Skyba nappe/ 1045.5 m



Menilite Formation/ Miocene/ Skyba nappe/ 1115.5 m



Menilite Formation/ Miocene/ Skyba nappe/ 1299 m



Menilite Formation/ Miocene/ Skyba nappe/ 1343 m

NP	Depth [m]	S ₁ [mgHC/gRock]	S ₂	T _{max} [°C]	TOC [%]	S [%]	TOC/S [-]	HI [mgHC/gTOC]	TIC [%]	Calc. Equiv. [%]	Isotopy δ13C δ18O		Biomarker
Lower Oligocene Lower Menilite Member													
24	0	0.04	1.21	419	0.83	0.97	0.86	145	2.55	21.25	-1.03	-6.00	
24	4	0.42	30.67	419	9.21	1.38	6.67	333	0.77	6.44	0.54	-9.95	x
24	8	0.01	0.10	420	5.80	1.40	4.16	314	4.91	40.94	4.92	1.45	
	11	0.20	14.24	421	4.08	1.01	4.04	349	0.43	3.57			
24	13	0.22	16.54	422	5.55	0.87	6.38	298	0.79	6.57	0.03	-4.58	
24	13.7	0.01	0.18	420	6.12	1.27	4.81	245	4.40	36.69	4.95	-0.05	
24	15	0.11	11.16	422	5.04	1.00	5.03	221	1.44	12.02	0.24	-4.22	
	17	0.95	47.38	421	11.58	2.35	4.92	409	0.07	0.56			x
24	19	0.09	4.56	421	3.41	1.18	2.89	134	2.59	21.59	-4.54	-9.51	
	21	0.85	37.15	419	10.18	2.40	4.24	365	0.09	0.71			
	24	1.00	49.96	416	11.94	4.28	2.79	419	0.13	1.10			
	26.5	1.09	48.02	418	12.66	3.00	4.22	379	0.19	1.60			
	28.5	0.76	34.67	417	9.51	4.60	2.07	365	0.13	1.08			
	30	0.89	47.99	414	13.08	6.03	2.17	367	0.00	0.02			x
	32	1.06	58.12	415	13.94	4.21	3.31	417	0.41	3.44			
24	35	0.50	14.79	421	3.77	1.11	3.39	392	2.53	21.05	-4.35	-9.12	
24	36	0.70	20.01	420	5.41	0.99	5.46	370	2.09	17.43	-4.30	-9.17	
24	38	0.75	20.41	418	5.34	1.23	4.32	382	2.03	16.93	-4.31	-9.45	
24	40	1.16	46.78	416	12.29	3.44	3.57	381	1.82	15.15	-0.14	-10.24	
	41.5	0.96	47.46	416	14.55	3.80	3.83	326	0.07	0.56			
	43	0.94	45.57	420	10.99	3.26	3.37	414	0.14	1.16			
24	45	0.99	51.64	418	10.86	2.56	4.24	475	0.59	4.91	-0.54	-10.45	
	46.5	1.00	46.86	417	10.79	2.52	4.28	434	0.11	0.94			
	48.5	1.64	60.12	416	16.09	4.66	3.45	374	0.03	0.23			x
24	50.5	0.97	49.73	415	12.26	5.00	2.45	406	0.51	4.22	-0.15	-10.27	
	52	0.64	28.74	421	7.59	2.90	2.61	378	0.19	1.55			
24	53	0.68	19.35	419	4.95	1.88	2.64	391	1.27	10.55	-0.24	-10.01	
	55	0.89	30.83	421	6.73	1.81	3.71	458	0.00	0.00			
24	56.5	0.66	26.51	420	6.42	2.53	2.54	413	1.18	9.82	-6.45	-10.45	
	58	1.01	49.69	420	10.74	2.61	4.12	463	0.06	0.48			
	59	1.10	61.61	417	13.97	3.20	4.36	441	0.00	0.01			x
	60	0.80	37.77	415	9.36	3.63	2.58	404	0.02	0.17			
	61	1.00	37.85	416	9.18	2.11	4.35	412	0.46	3.83			
	63	0.99	41.14	417	8.82	4.51	1.96	467	0.43	3.60			
	66	0.95	33.94	420	7.64	1.61	4.75	444	0.07	0.62			
24	68.5	0.64	26.51	418	7.07	2.30	3.07	375	0.66	5.47	-6.34	-5.65	
24	72	0.56	16.90	420	5.10	2.82	1.81	331	0.68	5.64	-11.56	-11.46	
	77	0.49	35.25	416	11.58	3.84	3.02	304	0.03	0.29			
	78.5	1.21	66.82	416	16.22	3.18	5.10	412	0.16	1.32			x
	82	1.27	57.84	419	12.62	2.39	5.28	458	0.13	1.08			
	84	1.15	55.31	416	15.00	3.45	4.35	369	0.03	0.26			
	85.5	0.41	34.20	419	10.14	1.89	5.35	337	0.00	0.00			
	87.4	1.15	50.96	417	13.27	2.68	4.96	384	0.00	0.00			

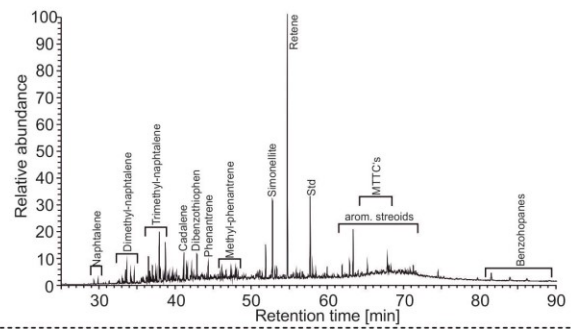
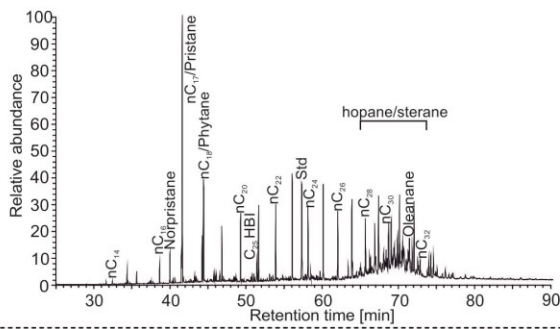
NP	Depth [m]	S ₁ [mgHC/gRock]	S ₂	T _{max} [°C]	TOC [%]	S [%]	TOC/S [-]	HI [mgHC/gTOC]	TIC [%]	Calc. Equiv. [%]	Isotopy δ13C δ18O		Biomarker
Lower Oligocene Lower Menilite Member													
	89.5	0.22	9.76	418	3.19	1.03	3.09	306	0.00	0.00			
	91	1.37	63.77	416	16.97	2.80	6.05	376	0.16	1.30			
	93	1.56	74.09	415	22.47	3.31	6.78	330	0.08	0.65			x
	94.5	0.93	58.53	417	16.57	2.97	5.57	353	0.09	0.78			
	97	1.41	60.33	414	18.44	4.53	4.07	327	0.39	3.21			
	99	1.00	49.11	414	15.36	2.51	6.11	320	0.07	0.59			
24	100.3	0.05	1.69	418	4.65	0.66	7.10	312	6.09	50.73	-8.42	-6.57	
24	101	1.38	67.74	412	19.42	4.00	4.85	349	0.97	8.10	-5.01	-10.66	
	102.5	1.18	61.98	414	15.57	2.64	5.89	398	0.40	3.31			
	105	1.18	57.52	416	14.29	4.44	3.22	402	0.58	4.81			
24	107	2.10	88.04	412	23.67	4.99	4.74	372	1.58	13.15	-11.34	-12.45	x
	109.5	1.09	47.88	415	10.87	5.34	2.03	440	0.20	1.67			
	111	0.08	3.05	416	1.99	0.55	3.63	153	0.04	0.29			
	112	1.20	67.95	415	16.25	4.74	3.43	418	0.47	3.92			
	114.5	1.07	55.48	415	12.44	3.00	4.15	446	0.46	3.80			
	116.5	1.20	85.04	414	24.25	3.74	6.49	351	0.29	2.42			x
24	118	0.32	20.88	415	5.58	4.83	1.15	374	0.91	7.55	-9.56	-8.55	
	119	0.83	62.69	416	15.11	2.86	5.28	415	0.00	0.00			
24	120.5	1.91	64.84	414	19.54	3.04	6.43	332	3.92	32.69	0.57	-11.45	
	122	0.65	54.12	416	17.21	2.36	7.30	314	0.00	0.00			
	124	0.51	26.07	415	7.10	2.34	3.03	367	0.03	0.24			
	125.5	0.74	43.32	415	12.19	2.30	5.30	355	0.17	1.43			x
	127	0.64	37.46	415	9.32	2.40	3.89	402	0.05	0.45			
	196	0.18	16.64	419	4.08	2.63	1.55	408	0.00	0.00			
	201	0.17	13.06	417	3.27	2.50	1.31	399	0.00	0.00			
	202	0.23	16.80	423	3.51	2.36	1.49	479	0.21	1.73			
	203	0.50	23.01	423	4.60	2.62	1.75	500	0.03	0.25			
	204	0.13	8.39	419	2.01	1.58	1.27	418	0.00	0.00			
	205	0.34	35.21	421	7.02	2.81	2.49	501	0.04	0.31			
	207	0.44	26.40	421	5.04	3.62	1.39	524	0.02	0.18			
	208	0.34	29.34	422	5.31	3.02	1.76	552	0.02	0.16			
	209	1.00	46.84	418	9.10	2.62	3.48	515	0.04	0.30			x
	210	0.94	2.46	421	0.72	0.34	2.15	341	0.16	1.36			
	212	0.16	8.88	420	2.31	0.73	3.14	385	0.07	0.56			
	215	0.71	31.20	421	7.46	3.29	2.27	418	0.08	0.68			x
	217	0.19	3.45	422	1.29	0.45	2.87	267	0.03	0.28			
	217.5	0.42	20.68	424	5.34	2.10	2.54	388	0.00	0.00			
	219	0.52	32.35	416	8.53	1.33	6.40	379	0.16	1.29			
	221	0.89	41.37	415	8.41	5.76	1.46	492	0.20	1.64			
	223	0.49	30.84	422	5.96	1.82	3.28	517	0.10	0.82			
	224	0.49	7.90	419	2.31	0.22	10.38	342	0.08	0.65			
	224.6	0.38	23.69	420	4.78	2.18	2.19	496	0.00	0.03			
	226	0.56	33.97	419	6.17	3.29	1.88	550	0.01	0.12			

NP	Depth [m]	S ₁ [mgHC/gRock]	S ₂	T _{max} [°C]	TOC [%]	S [%]	TOC/S [-]	HI [mgHC/gTOC]	TIC [%]	Calc. Equiv. [%]	Isotopy δ13C δ18O		Biomarker
Lower Oligocene Lower Menilite Member													
23	228	1.63	70.87	418	15.65	3.61	4.34	453	0.33	2.77			
	229	0.04	0.60	423	4.57	0.99	4.61	400	4.61	38.40	-7.12	-5.34	
	229.5	1.62	71.79	415	15.84	2.91	5.45	453	0.14	1.20			x
	231	0.46	22.55	419	4.60	2.15	2.14	490	0.51	4.24			
	233	0.32	15.84	422	3.80	3.10	1.23	417	0.00	0.00			
	234	0.58	33.87	420	6.77	2.68	2.53	500	0.01	0.07			
	235	0.57	34.89	418	6.82	3.30	2.07	512	0.04	0.34			
	236.5	0.80	43.24	423	6.59	2.34	2.81	656	0.17	1.44			
	238	0.82	41.64	421	7.18	3.07	2.34	580	0.05	0.46			
	240	1.06	55.22	421	8.83	2.44	3.62	625	0.14	1.18			x
	241.5	0.56	25.57	422	4.93	2.79	1.76	518	0.00	0.00			
	243.5	0.81	43.62	420	7.30	2.88	2.53	598	0.23	1.94			
	245	0.76	47.67	421	8.30	2.49	3.33	574	0.02	0.15			
	247	1.80	80.95	417	17.66	2.44	7.24	458	0.00	0.00			
	249	2.60	84.23	417	17.73	3.63	4.88	475	0.12	0.97			x
	253	0.02	0.25	421	0.86	0.37	2.31	29	0.00	0.00			
	254.5	0.75	1.78	422	7.71	2.97	2.59	23	0.06	0.46			
	256	0.02	0.25	421	0.39	0.13	3.08	64	0.00	0.00			
	257.4	0.50	24.68	422	5.01	3.67	1.37	492	0.00	0.00			
	258.5	0.03	0.23	420	0.22	0.58	0.38	104	0.02	0.15			
	260.5	1.05	37.80	418	7.90	5.54	1.43	479	0.00	0.00			x
	262	0.01	0.34	423	0.31	0.17	1.88	108	0.01	0.06			
	264	1.26	60.52	420	12.79	2.56	5.00	473	0.00	0.00			
266	0.01	0.07	422	0.10	0.21	0.47	70	0.00	0.00				
23	268	2.09	70.51	419	16.54	2.79	5.94	426	2.63	21.91	-1.10	-13.22	x
269.5	0.54	29.93	423	4.80	1.83	2.63	624	0.08	0.67				
271	0.33	27.18	423	4.29	2.04	2.11	634	0.00	0.00				
273	0.02	0.59	422	0.36	0.17	2.13	165	0.01	0.08				
275.2	2.31	80.89	417	21.94	3.43	6.40	369	0.10	0.81			x	
277.0	0.01	0.11	422	0.12	0.11	1.05	92	0.01	0.07				
278.5	0.40	38.21	419	6.80	3.39	2.01	562	0.00	0.00				
281.0	0.19	7.13	423	1.80	2.44	0.74	397	0.00	0.00				
282	0.01	0.08	424	0.12	0.21	0.59	65	0.02	0.14				
283.5	1.05	46.94	417	7.84	5.48	1.43	598	0.00	0.01			x	
285.5	0.01	0.14	417	0.14	0.23	0.59	101	0.02	0.17				
287	0.36	21.97	421	4.14	3.25	1.27	531	0.16	1.37				
288	0.01	0.30	423	0.30	0.28	1.05	99	0.00	0.00				
289.9	0.01	0.27	422	0.23	0.39	0.59	117	0.01	0.08				
291.5	0.06	2.19	427	0.65	0.71	0.92	335	0.06	0.47				
293	0.07	0.34	419	0.30	0.74	0.41	113	0.07	0.59				
294.5	0.29	14.04	426	2.84	2.24	1.27	494	0.00	0.12				
22	296	0.01	0.21	424	7.00	2.04	3.43	129	4.47	37.28	4.26	-2.38	

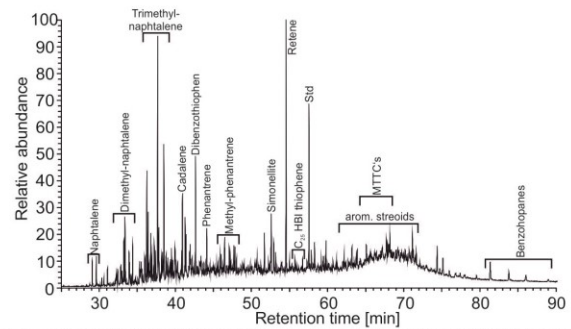
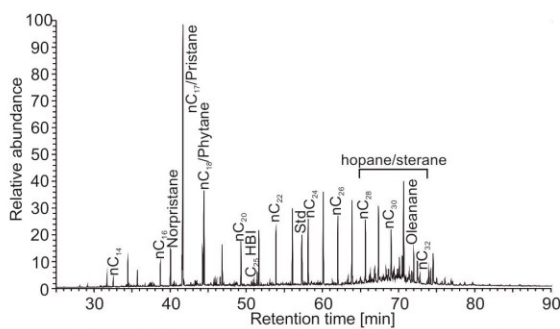
NP	Depth [m]	S ₁ [mgHC/gRock]	S ₂	T _{max} [°C]	TOC [%]	S [%]	TOC/S [-]	HI [mgHC/gTOC]	TIC [%]	Calc. Equiv. [%]	Isotopy δ13C δ18O		Biomarker
Lower Oligocene Lower Menilite Member													
	297.7	0.02	0.38	423	0.29	0.21	1.40	129	0.02	0.19			
	299.5	0.01	0.35	424	0.34	0.32	1.07	100	0.06	0.54			
	301	0.22	4.74	423	1.42	1.09	1.31	334	0.00	0.00			
	303	0.01	0.11	420	0.13	0.03	4.00	84	0.00	0.00			
	305	0.31	13.11	426	2.75	1.95	1.41	476	0.00	0.00			
	306.5	0.00	0.03	415	0.10	0.04	2.55	30	0.00	0.00			
	308	0.35	21.63	426	3.41	1.91	1.79	634	0.07	0.57			
	310	0.65	36.50	423	5.32	3.64	1.46	687	0.00	0.07			x
	311.5	0.29	18.86	422	3.34	3.41	0.98	565	0.01	0.10			
	312.7	0.38	37.51	424	5.26	3.73	1.41	713	0.00	0.00			
	314	0.29	18.62	420	3.11	3.17	0.98	598	0.10	0.80			
	315	0.29	29.58	418	5.05	4.70	1.07	586	0.02	0.19			
22	316	0.21	11.42	429	1.93	1.65	1.17	592	3.38	28.18	-2.12	-7.12	
	316.5	1.60	99.47	426	19.85	9.28	2.14	501	0.00	0.01			x
22	317	0.51	9.42	418	1.86	0.71	2.64	505	7.20	59.99	-2.86	-5.12	
22	317.5	0.38	5.16	419	1.12	0.42	2.64	459	4.45	37.05	-2.01	-4.77	
	318.8	1.77	122.54	425	21.11	4.73	4.46	581	0.00	0.01			x
22	320	0.10	4.96	432	0.82	0.65	1.26	605	0.65	5.42	0.65	-6.45	
22	321.5	0.76	76.28	421	11.21	1.66	6.76	680	2.55	21.26	4.76	-4.87	
	322.5	0.10	1.31	421	0.61	2.69	0.23	214	0.00	0.00			
	323.4	1.82	122.06	427	20.36	5.79	3.51	600	0.00	0.06			x
	325	0.04	3.14	421	0.85	0.97	0.88	368	0.03	0.22			
	326	0.05	7.57	425	1.22	0.54	2.26	621	0.05	0.41			
	327	0.12	21.55	433	2.69	1.57	1.72	801	0.05	0.42	Isotopy		
	329	0.04	6.45	433	1.04	0.53	1.96	620	0.09	0.73	δ13C	δ18O	
Upper Oligocene Middle Menilite Member													
NN2	0	0.03	0.66	423	0.86	0.6	1.54	77	3.04	25.36			
	0.7	0.68	26.67	425	7.86	0.9	8.49	339	0.50	4.20			
NN2	0.9	0.05	1.29	424	0.96	0.6	1.72	135	2.25	18.72			
	1.1	0.89	31.68	423	8.8	1	8.53	360	0.58	4.87			
NN2	7	0.04	0.92	423	0.8	0.5	1.76	115	2.86	23.86			
	7.5	0.36	9.94	427	3.19	0.5	5.81	311	0.41	3.42			
Eocene													
	0	0.11	5.67	429	1.32	1.2	1.11	428	1.74	14.48			
	~20	0.04	2.73	429	0.88	0.7	1.19	311	1.35	11.22			

Aliphatic fraction

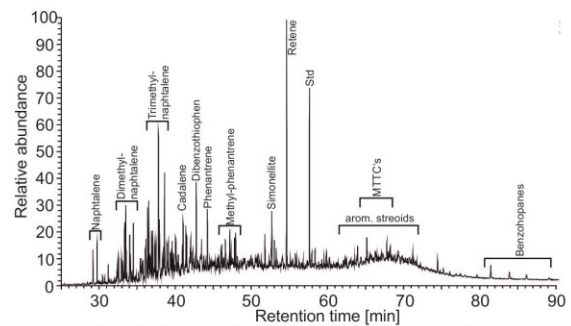
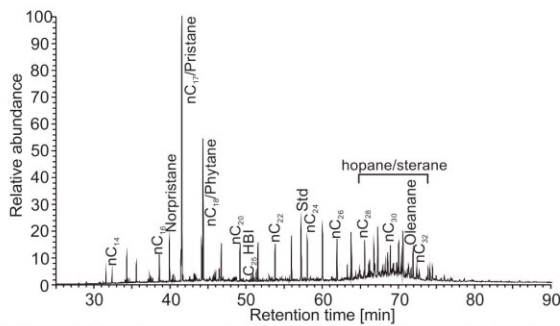
Aromatic fraction



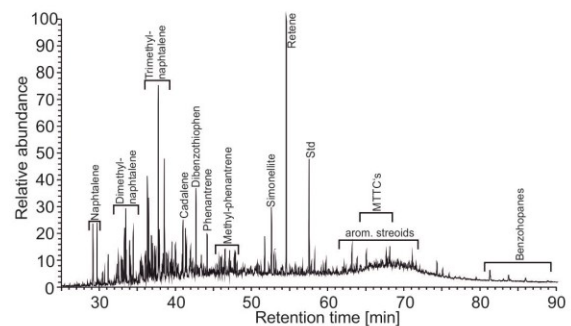
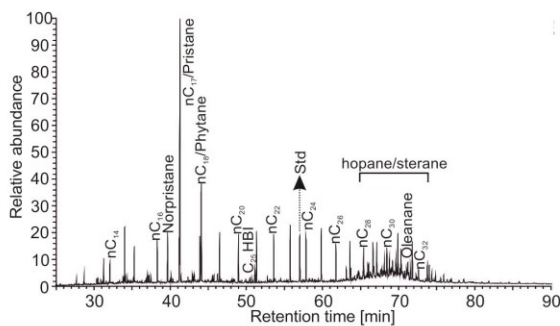
Menilite Formation/ Lower Oligocene/ Skyba nappe/ 4 m



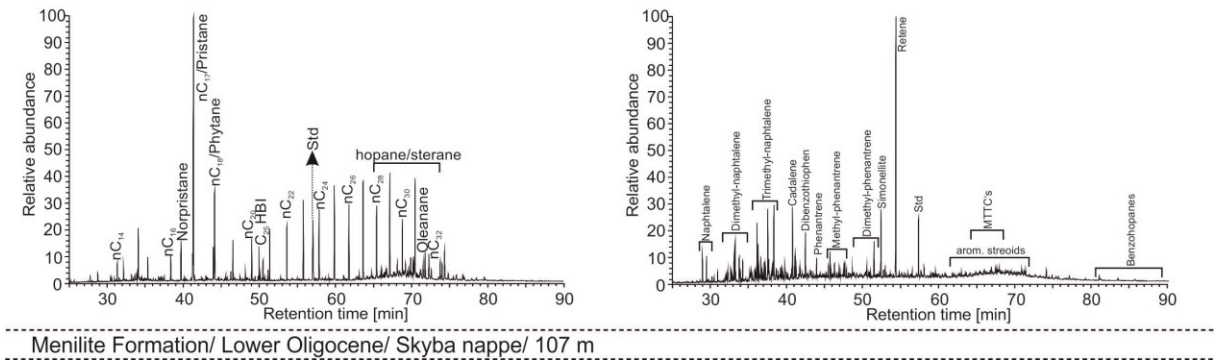
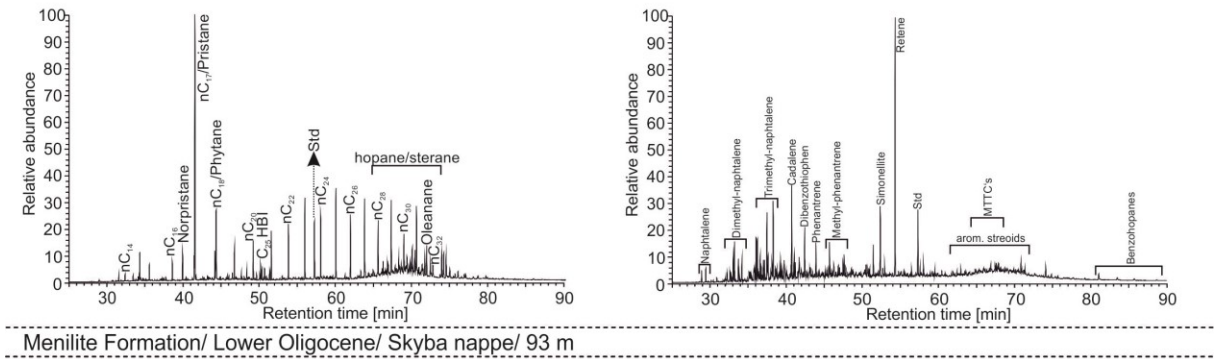
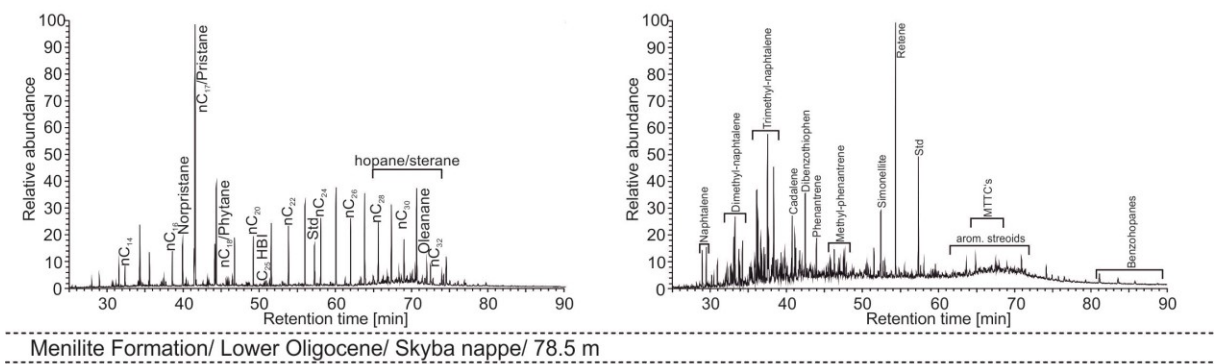
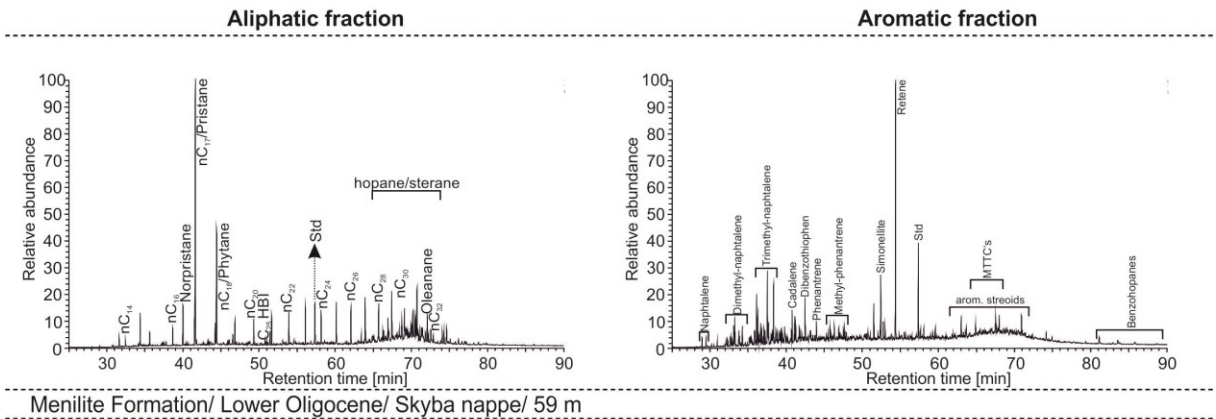
Menilite Formation/ Lower Oligocene/ Skyba nappe/ 17 m

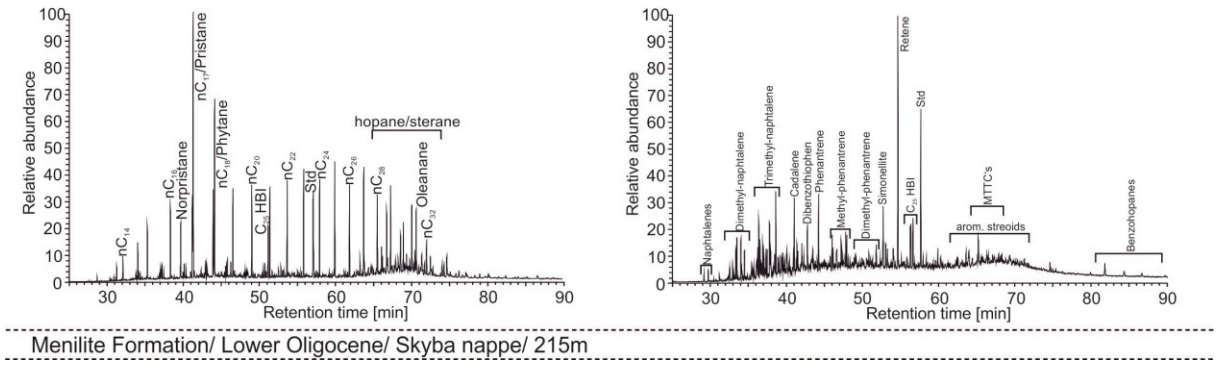
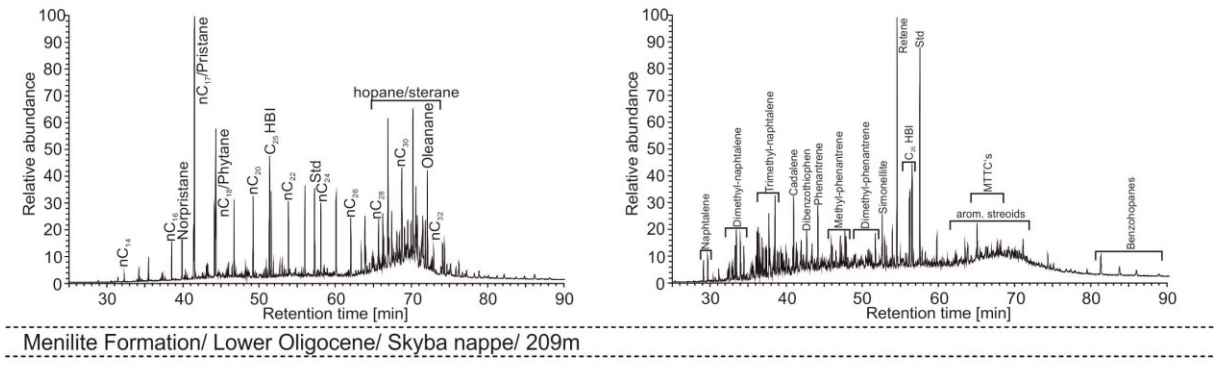
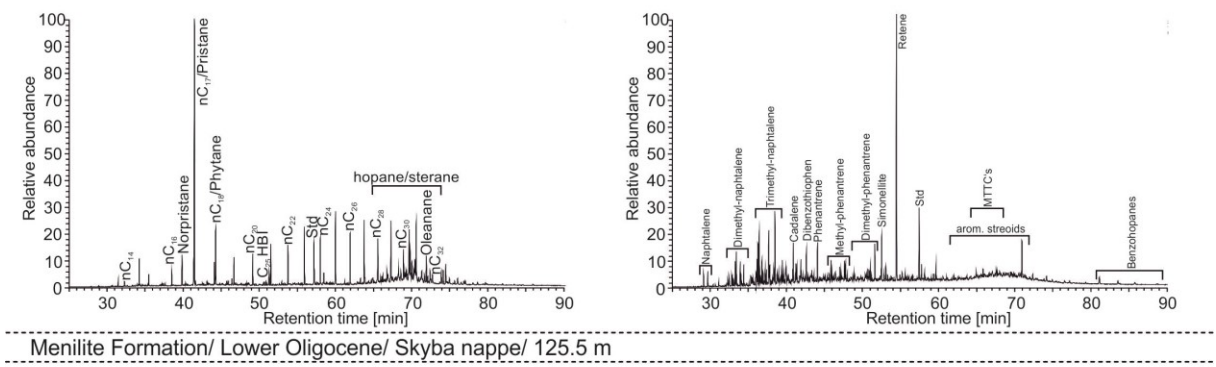
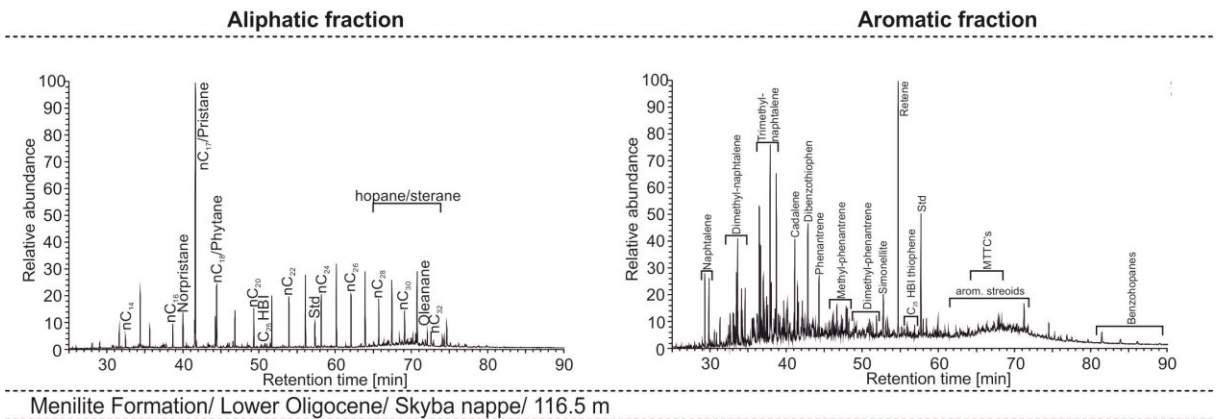


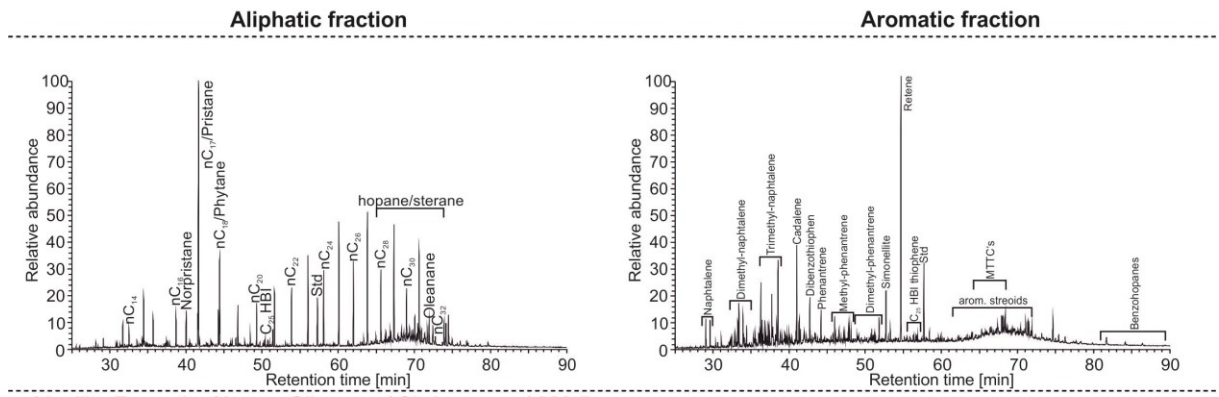
Menilite Formation/ Lower Oligocene/ Skyba nappe/ 30 m



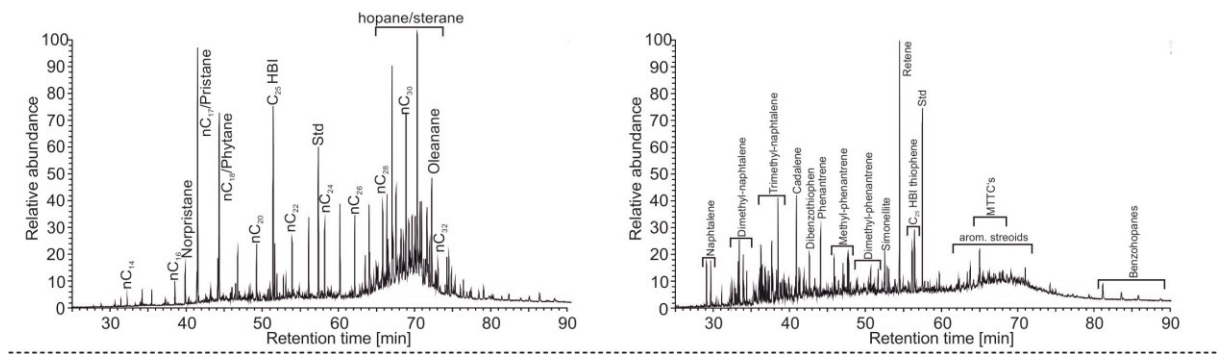
Menilite Formation/ Lower Oligocene/ Skyba nappe/ 48.5 m



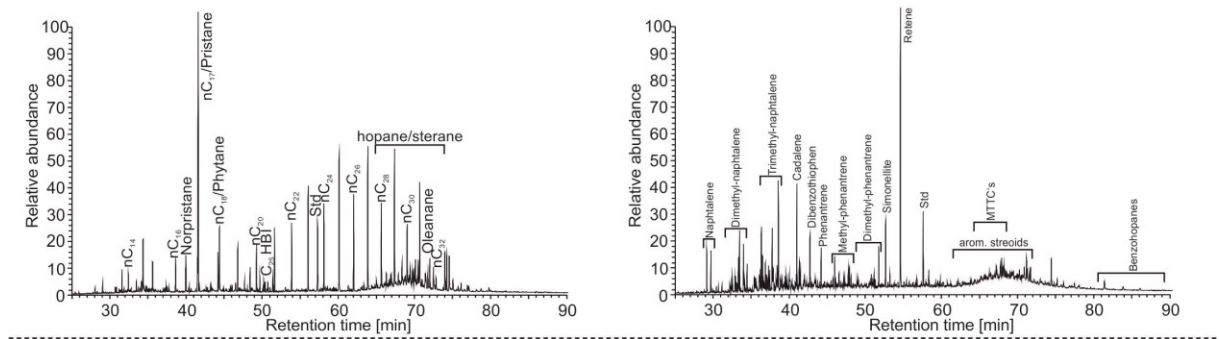




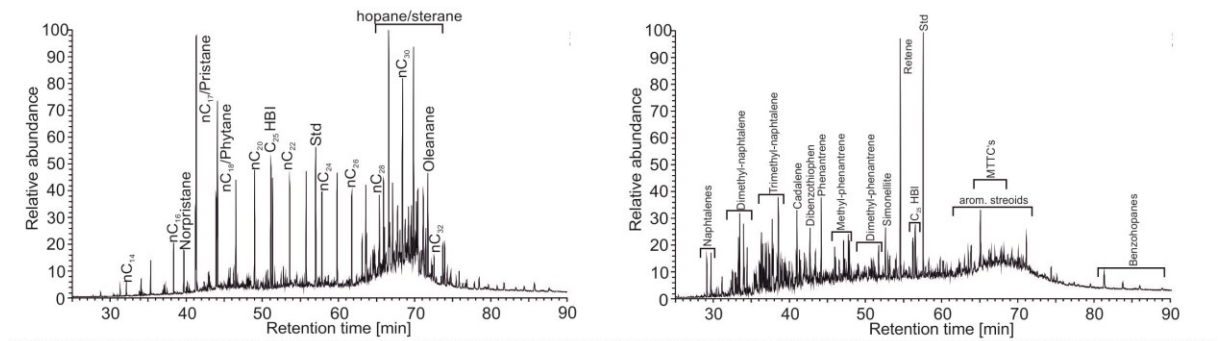
Menilite Formation/ Lower Oligocene/ Skyba nappe/ 229.5 m



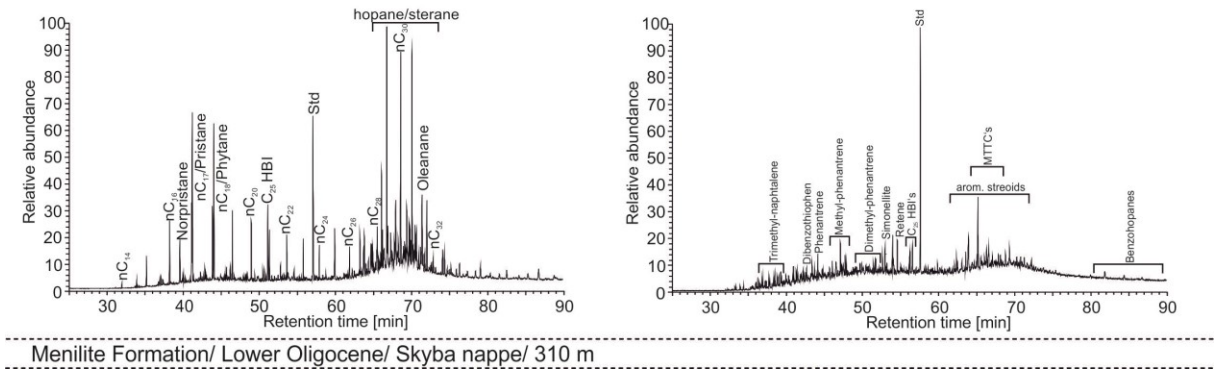
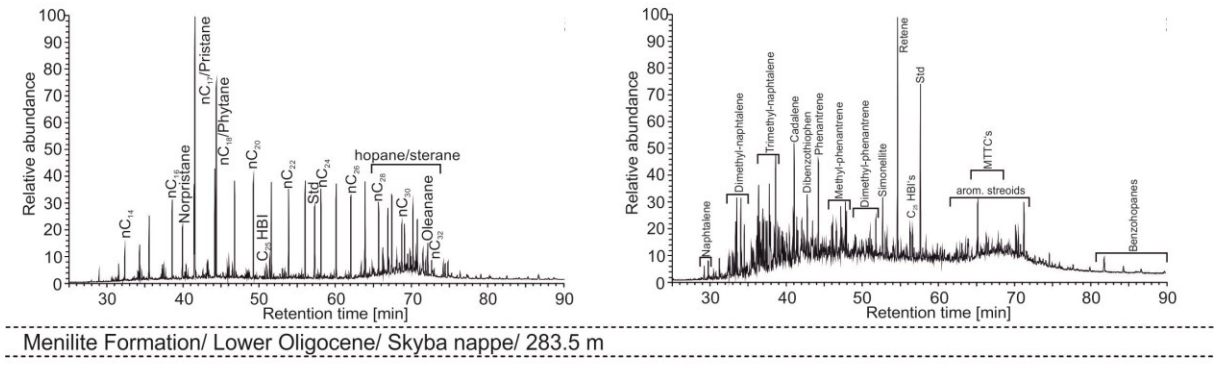
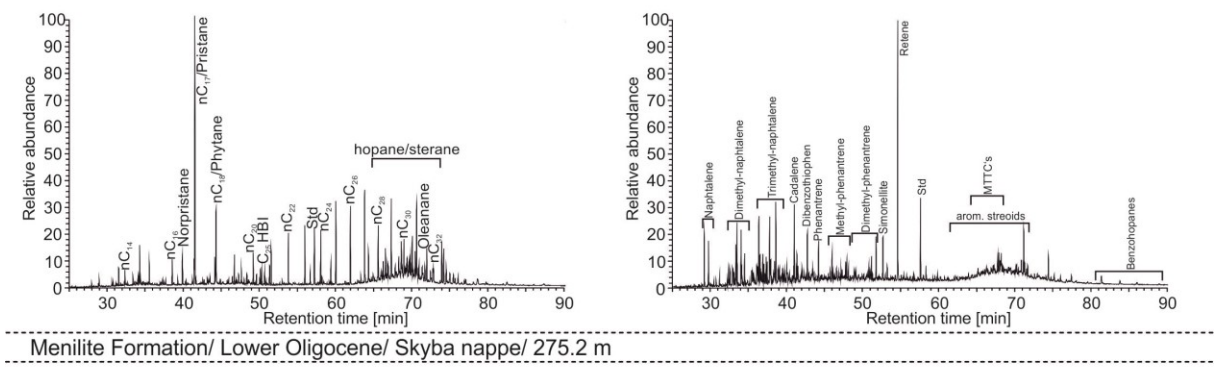
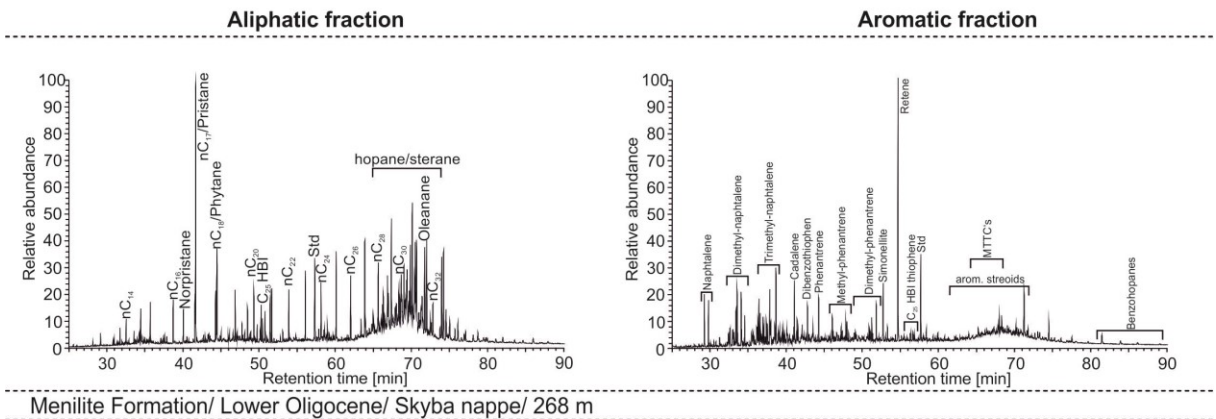
Menilite Formation/ Lower Oligocene/ Skyba nappe/ 240 m

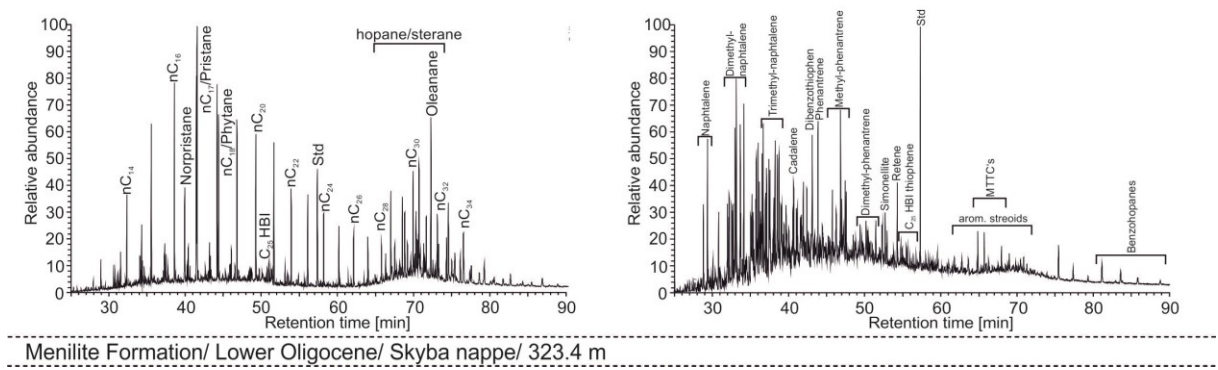
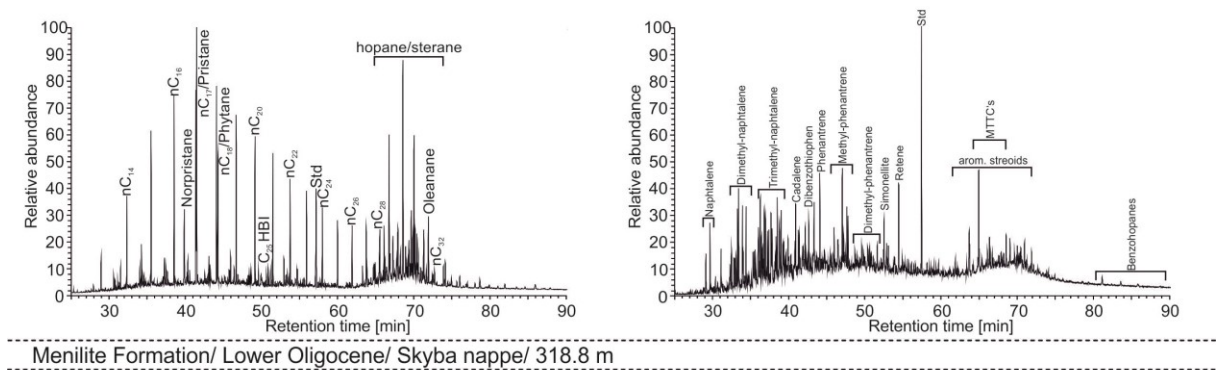
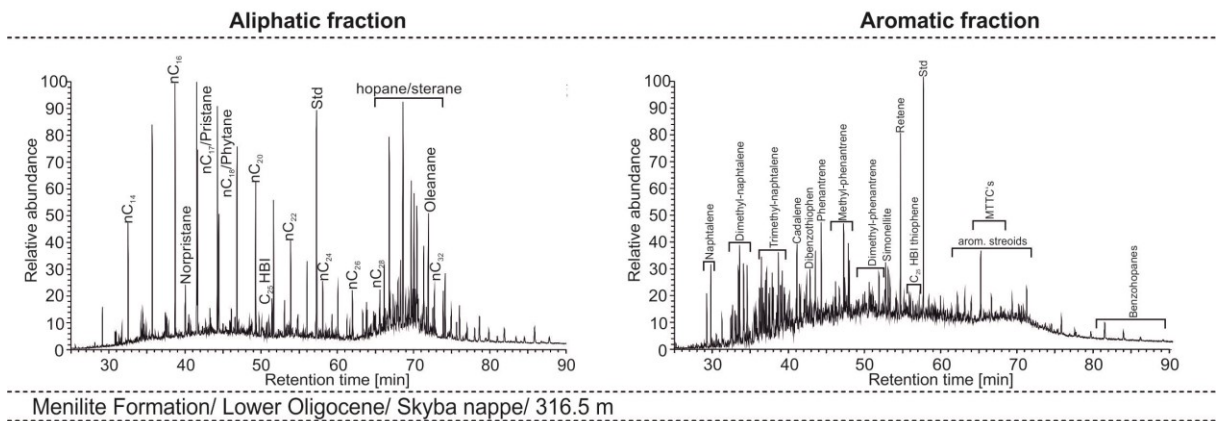


Menilite Formation/ Lower Oligocene/ Skyba nappe/ 249 m

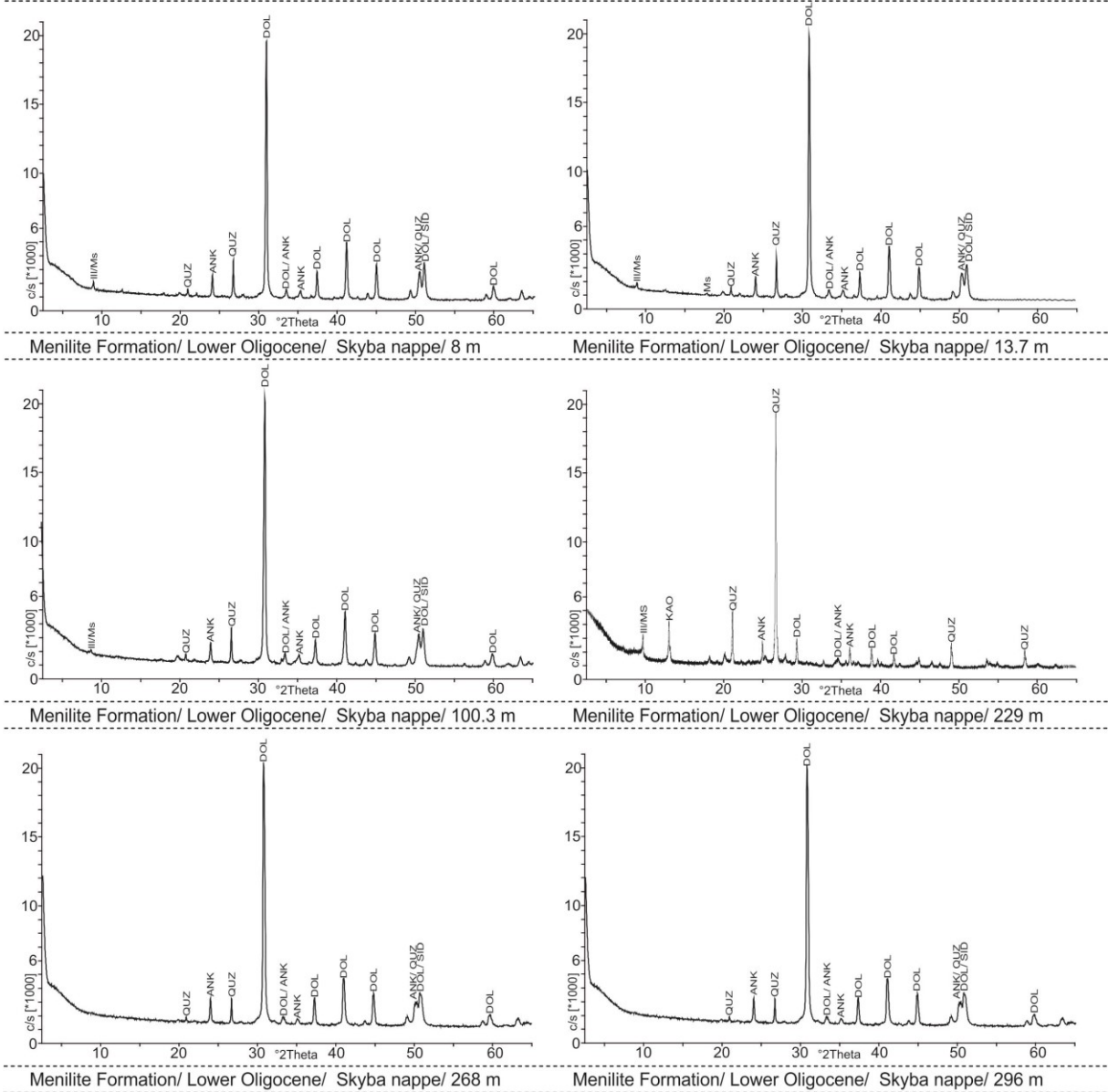


Menilite Formation/ Lower Oligocene/ Skyba nappe/ 260.5 m





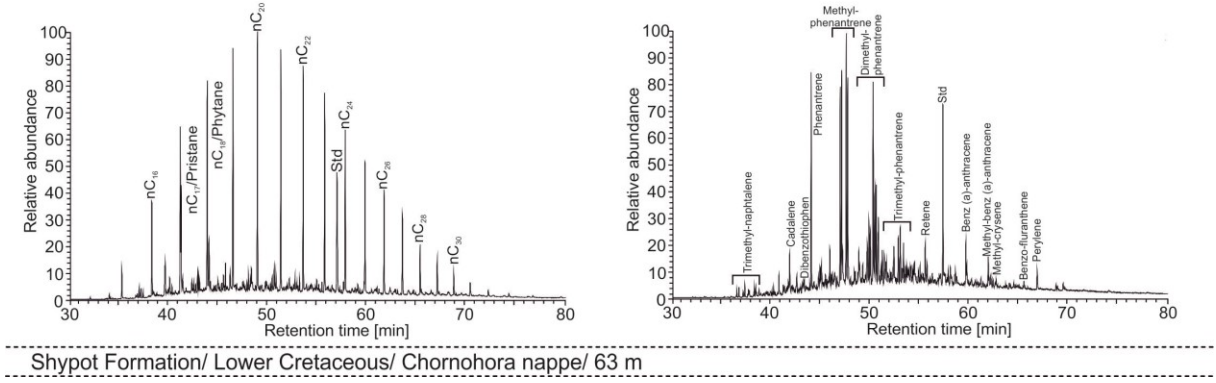
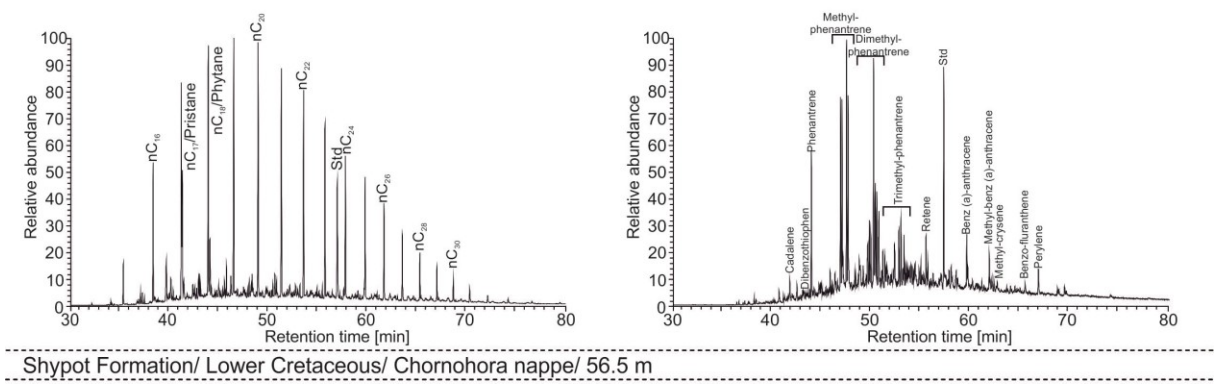
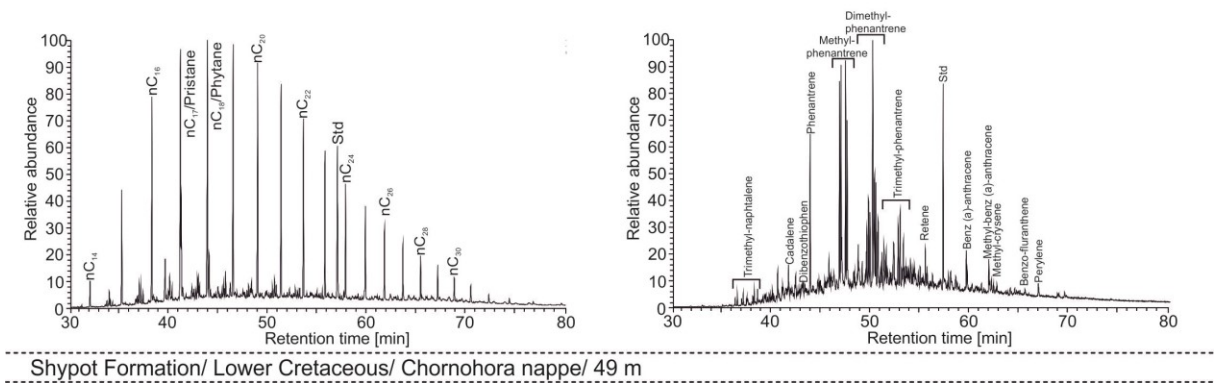
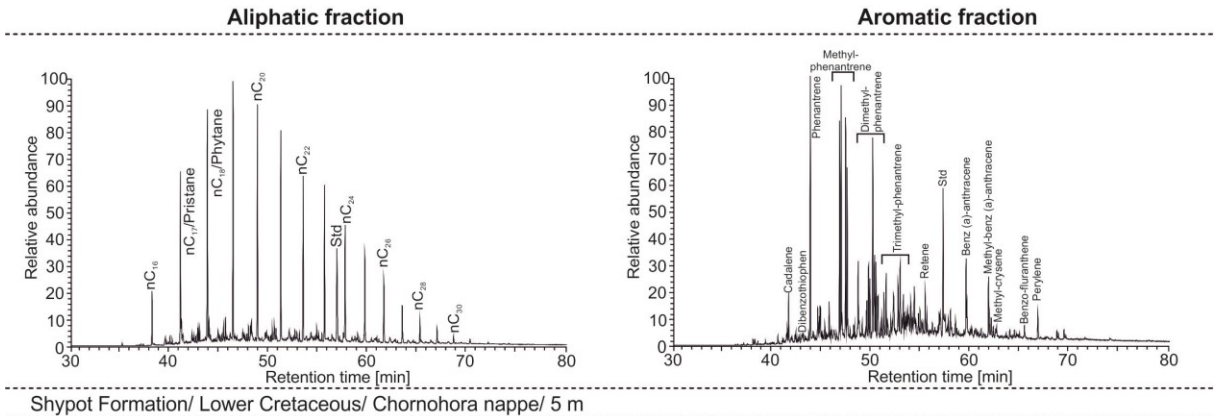
XRD-traces

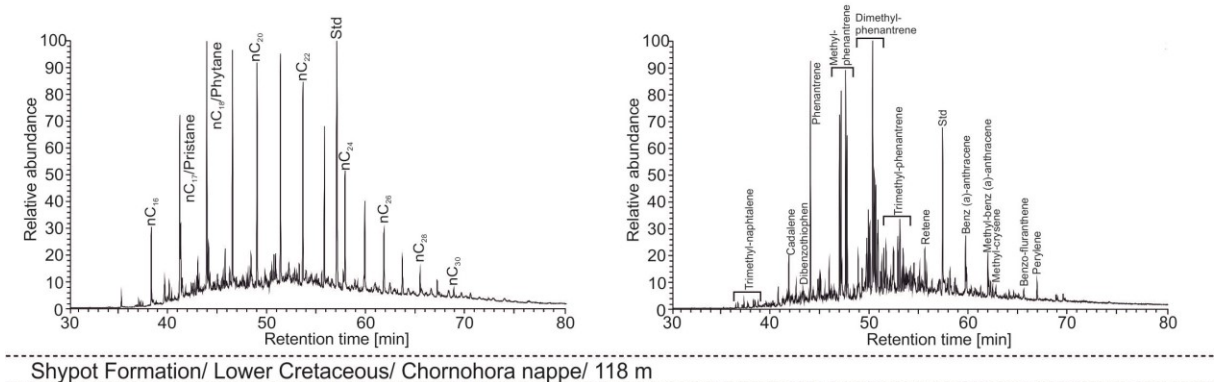
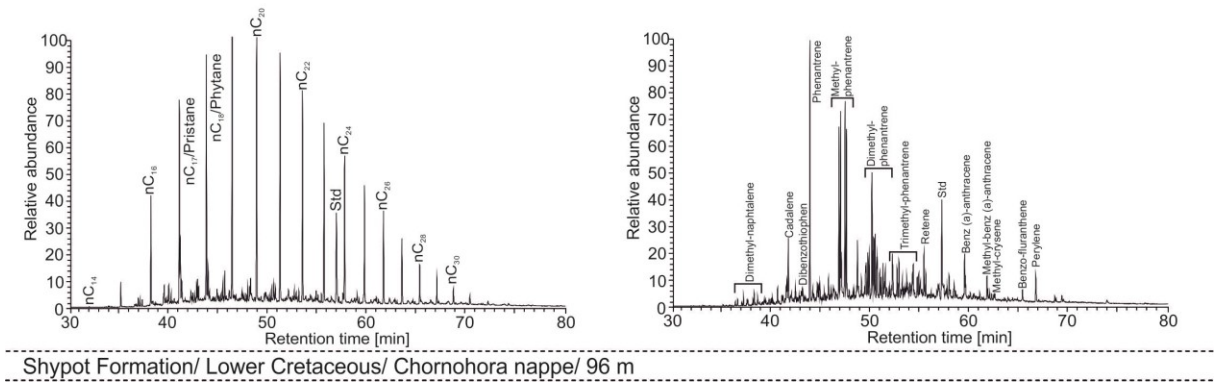
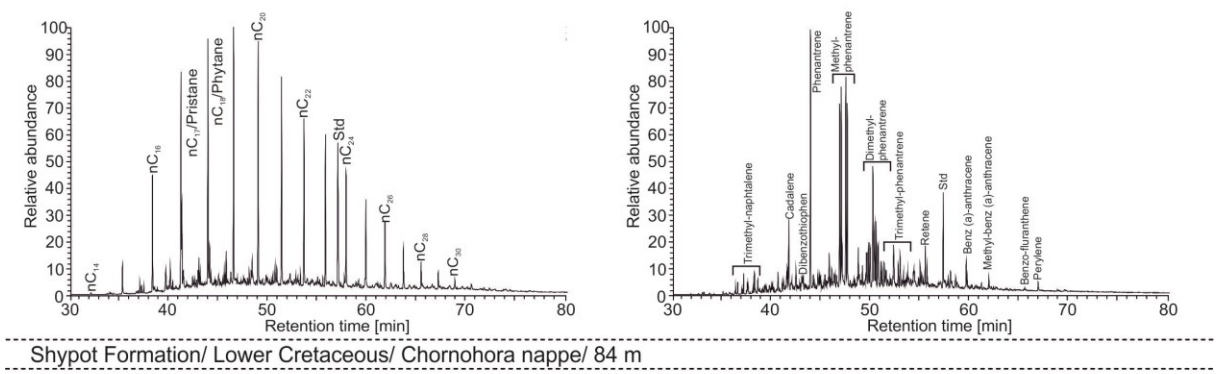
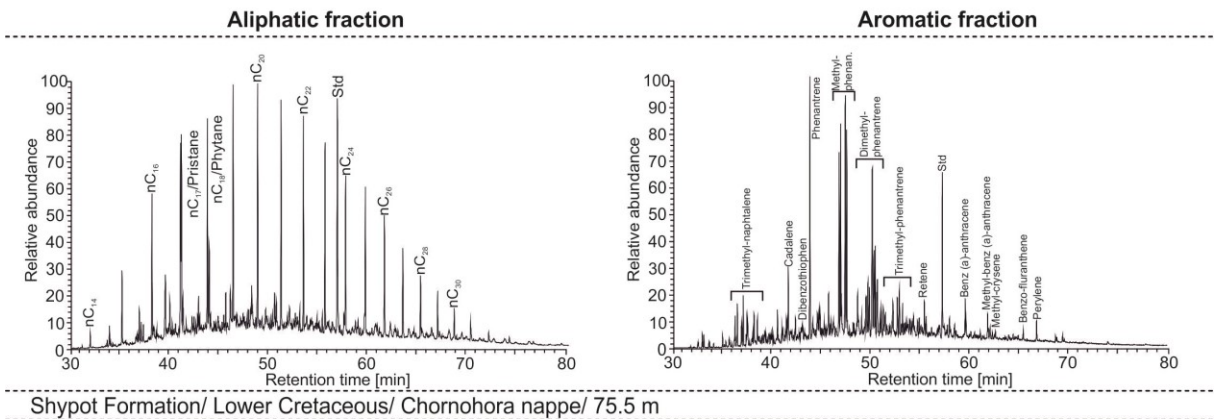


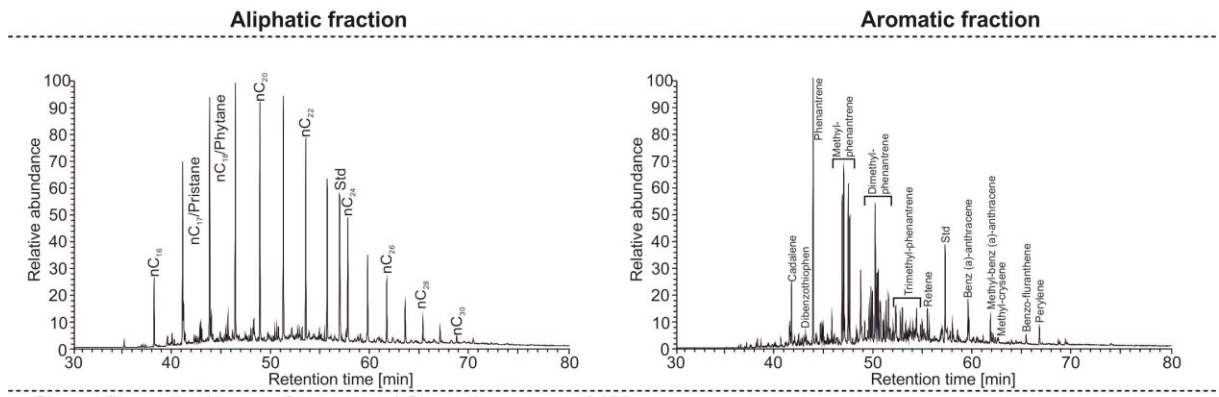
10.3 Appendix III - Lower Cretaceous (Barremian-Albian) Shypot Formation

Depth	S ₁	S ₂	T _{max}	TOC	S	TOC/S	HI	PI	TIC	Calc. Equiv.	Isotopy		Biomarker
[m]	[mgHC/gRock]		[°C]	[%]	[%]	[-]	[mgHC/gTOC]	[-]	[%]	[%]	δ13C	δ18O	
Lower Cretaceous Shypot Formation													
0	0.02	0.07	456	0.19	0.29	0.67	34	0.19	0.14	1.17			
5	0.34	2.31	461	3.08	1.73	1.78	75	0.13	0.53	4.38			x
49	0.43	2.76	450	1.94	0.80	2.41	143	0.13	0.31	2.60			x
50.5	0.22	1.66	453	1.44	0.59	2.45	115	0.11	0.07	0.62			
56.5	0.35	3.29	449	2.62	0.56	4.66	126	0.10	0.08	0.63			x
63	0.45	3.97	453	3.18	1.11	2.86	125	0.10	0.00	0.00			x
66	0.49	2.98	454	2.75	0.82	3.35	108	0.14	0.14	1.18			
69.5	0.57	7.17	448	3.93	1.10	3.56	182	0.07	0.87	7.24	-1.08	-11.83	
73	0.75	6.57	454	4.92	1.44	3.42	134	0.10	0.49	4.06			
75.5	0.78	9.85	451	5.33	1.50	3.56	185	0.07	0.46	3.86			x
77.5	0.53	7.70	451	4.53	1.36	3.33	170	0.06	0.70	5.83	-0.43	-10.77	
79.5	0.47	4.14	451	3.35	1.05	3.20	123	0.10	0.82	6.82	-2.42	-10.33	
82	0.33	2.17	450	2.18	0.57	3.83	99	0.13	1.17	9.78	-2.47	-10.45	
84	0.74	9.39	451	5.60	1.08	5.19	168	0.07	0.75	6.22	-0.58	-11.27	x
90	0.20	1.23	448	1.65	1.10	1.50	74	0.14	2.13	17.78	-2.34	-4.88	
92	0.40	2.73	449	2.90	0.91	3.17	94	0.13	0.91	7.62	-4.08	-10.90	
94	0.59	5.12	453	4.03	0.86	4.71	127	0.10	0.30	2.49			
96	0.65	7.02	447	4.45	1.44	3.09	158	0.08	0.84	6.97	-0.83	-9.62	x
114	0.22	2.42	451	2.14	0.73	2.95	113	0.08	1.22	10.13			
118	0.71	6.83	451	3.99	1.20	3.33	171	0.09	1.54	12.82	-1.20	-8.96	x
121	0.48	6.09	449	4.30	1.16	3.70	141	0.07	0.64	5.32	-0.13	-12.16	
127	0.16	0.96	455	1.31	0.85	1.54	73	0.14	0.29	2.44			
129	0.63	6.35	457	5.40	1.44	3.74	118	0.09	0.48	3.98			
131	0.46	4.57	456	4.37	1.33	3.27	105	0.09	0.48	3.96			
133	0.51	5.17	457	4.93	1.41	3.49	105	0.09	0.53	4.42			x
145	0.40	4.79	443	4.22	1.41	3.00	113	0.08	0.24	1.98			
157	0.25	1.44	452	1.66	0.90	1.84	87	0.15	1.46	12.14	-0.36	-5.67	
159	0.26	1.47	454	1.83	1.09	1.68	80	0.15	1.44	12.01			x
161	0.30	1.39	452	1.86	1.30	1.43	74	0.18	1.69	14.12			
163	0.26	1.51	453	1.60	1.46	1.09	94	0.14	2.24	18.66	-0.57	-7.12	
165	0.24	1.17	455	1.63	1.34	1.22	72	0.17	1.87	15.59			
168	0.02	0.10	455	0.26	0.61	0.43	36	0.17	0.09	0.78			
168.2	0.25	1.74	456	2.19	0.74	2.96	79	0.13	0.11	0.89			
170	0.39	2.51	457	3.07	1.00	3.06	81	0.13	0.68	5.68			x
173	0.27	2.05	454	2.61	1.52	1.72	78	0.12	0.68	5.67			
182	0.21	1.56	454	1.86	0.89	2.09	84	0.12	1.09	9.12	0.42	-6.14	
192	0.28	1.61	455	2.25	1.14	1.97	71	0.15	1.69	14.05	0.21	-6.79	
194	0.51	4.20	455	3.78	2.20	1.72	111	0.11	1.24	10.31	0.30	-9.03	x
196	0.49	3.56	457	3.67	2.41	1.52	97	0.12	0.69	5.79	-0.83	-11.44	
198	0.24	1.61	455	2.14	0.98	2.18	75	0.13	1.05	8.78	-1.31	-8.38	
228	0.36	1.59	457	1.77	1.10	1.60	90	0.18	2.54	21.15	0.70	-5.80	x
237	0.08	0.70	455	1.84	0.71	2.60	38	0.10	0.00	0.00			
246	0.24	1.00	456	1.46	0.72	2.05	68	0.19	1.95	16.24	-0.63	-7.71	
248	0.30	1.52	457	2.05	1.22	1.68	74	0.16	2.84	23.67	0.10	-7.75	x
250.5	0.43	1.98	459	2.42	1.33	1.82	82	0.18	2.26	18.80	0.53	-7.10	

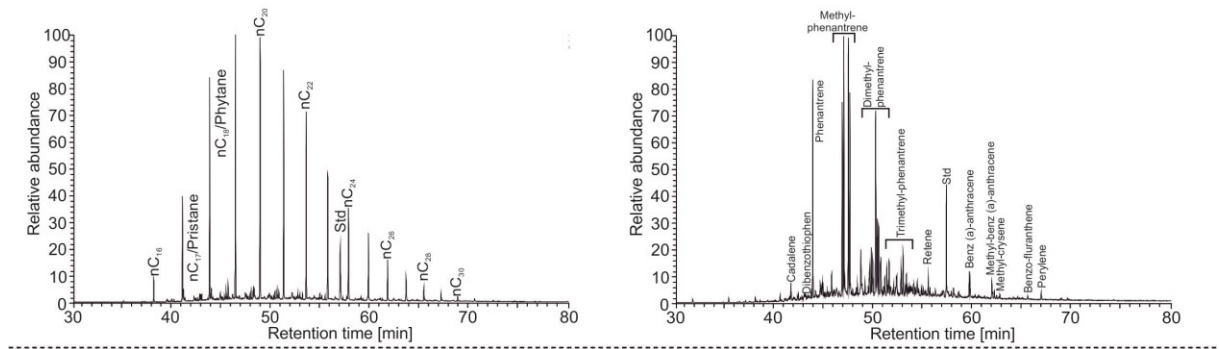
Depth	S ₁	S ₂	T _{max}	TOC	S	TOC/S	HI	PI	TIC	Calc. Equiv.	Isotopy		Biomarker
[m]	[mgHC/gRock]		[°C]	[%]	[%]	[-]	[mgHC/gTOC]	[-]	[%]	[%]	δ13C	δ18O	
Lower Cretaceous Shypot Formation													
252.5	0.02	0.07	454	0.15	1.33	0.11	46	0.18	0.02	0.17			
255	0.52	4.01	457	3.83	1.45	2.65	105	0.11	0.70	5.87			
257	0.64	3.35	458	3.77	1.88	2.01	89	0.16	1.36	11.31	0.27	-9.81	x
257.5	0.07	0.39	461	0.70	0.96	0.73	55	0.15	0.95	7.90	-2.00	-8.92	
279.5	0.10	0.73	461	1.62	2.05	0.79	45	0.12	0.00	0.00			
281	1.02	10.14	459	7.99	2.24	3.58	127	0.09	0.08	0.66			x
292.5	0.94	9.74	456	7.16	2.34	3.06	136	0.09	0.66	5.51	0.25	-12.64	
294	1.13	9.31	458	7.51	2.48	3.02	124	0.11	0.73	6.07	-0.11	-16.26	x
296	0.55	3.98	459	3.68	1.04	3.53	108	0.12	4.62	38.49	-1.71	-9.99	
298	0.62	3.77	461	3.95	1.43	2.76	95	0.14	0.65	5.41	-0.14	-10.11	
303	0.38	2.55	459	2.77	1.45	1.92	92	0.13	0.63	5.24	-0.26	-8.96	
305	0.35	2.11	457	2.60	1.93	1.35	81	0.14	1.67	13.95	0.10	-6.94	
313	1.23	12.76	459	8.15	2.34	3.48	157	0.09	0.68	5.64			x
323.8	1.21	11.60	459	9.39	2.27	4.14	124	0.09	0.46	3.80			x
324	0.04	0.27	460	0.52	0.34	1.49	51	0.13	0.01	0.06			
326	0.80	6.34	459	5.87	1.74	3.38	108	0.11	0.61	5.06	0.01	-12.06	
330	0.24	1.12	460	1.67	0.88	1.89	67	0.17	2.67	22.22	0.76	-6.55	
332	0.01	0.07	456	0.19	0.44	0.44	37	0.13	0.01	0.12			
332.5	0.17	1.22	460	1.81	1.24	1.45	67	0.12	0.98	8.18	0.38	-5.92	
334	0.12	0.98	458	1.76	0.67	2.62	56	0.11	0.77	6.46	0.86	-5.65	
350.5	0.39	2.79	458	4.04	1.22	3.30	69	0.12	0.00	0.00			x
352.5	0.23	1.18	457	1.94	1.06	1.82	61	0.16	0.53	4.39			
353.5	0.10	0.59	458	1.24	1.51	0.82	47	0.15	1.04	8.66	0.44	-2.43	
361	0.30	2.16	459	2.80	1.16	2.42	77	0.12	0.58	4.83			x
375	0.04	0.75	457	2.95	1.55	1.91	25	0.05	0.00	0.00			
377	0.29	1.90	457	2.50	1.55	1.61	76	0.13	2.14	17.80			
380	0.03	0.28	459	0.69	0.20	3.39	40	0.10	0.10	0.82			
382	0.64	3.91	461	3.56	1.99	1.79	110	0.14	1.76	14.65	0.11	-9.27	x
385	0.27	1.81	460	2.71	1.40	1.93	67	0.13	0.66	5.52	-0.41	-8.73	
386	0.14	0.98	448	1.48	0.76	1.95	66	0.12	0.77	6.42	-0.23	-7.39	
388	0.15	0.91	459	1.50	0.96	1.57	61	0.14	1.59	13.25	-0.90	-8.45	
389	0.11	0.63	463	1.10	1.06	1.04	57	0.14	0.81	6.76	-1.07	-8.32	
390	0.31	2.38	459	3.18	1.23	2.59	75	0.12	0.57	4.76			
391	0.34	2.14	461	2.79	1.10	2.54	76	0.14	0.01	0.08			
391.5	0.23	1.69	461	2.60	1.21	2.15	65	0.12	0.06	0.49			
393	0.16	1.05	462	1.64	0.87	1.89	64	0.13	1.16	9.68	-1.15	-9.32	
394	0.29	1.74	460	2.64	1.33	1.99	66	0.14	1.33	11.07	0.17	-7.51	x
395	0.20	1.00	459	2.00	0.95	2.10	50	0.16	2.44	20.34	-0.78	-6.48	
396	0.30	2.12	458	2.33	1.34	1.74	91	0.12	1.90	15.84	0.49	-6.77	
397.5	0.19	1.13	457	1.64	1.00	1.65	69	0.14	2.44	20.34	-0.47	-6.11	
399	0.01	0.04	455	0.13	1.69	0.08	31	0.20	0.01	0.07			
399.8	0.13	0.83	460	1.42	1.07	1.33	58	0.13	1.30	10.85	-0.51	-8.03	
400.5	0.29	2.21	459	3.10	1.98	1.57	71	0.12	0.68	5.68	0.71	-8.77	
401.3	0.05	0.24	458	0.56	1.01	0.56	42	0.16	1.41	11.77	-1.56	-6.50	
402.3	0.43	3.63	462	4.23	2.07	2.04	86	0.10	0.27	2.21			x
403.3	0.15	1.02	460	1.67	1.00	1.67	61	0.12	1.03	8.61	-0.83	-8.21	
404	0.15	0.92	459	1.45	1.08	1.34	63	0.14	1.31	10.95	-0.75	-6.76	
404.8	0.07	0.37	461	0.67	0.61	1.10	54	0.16	1.50	12.53	-1.51	-7.26	
405	0.39	2.56	463	3.44	1.23	2.80	74	0.13	0.49	4.12			



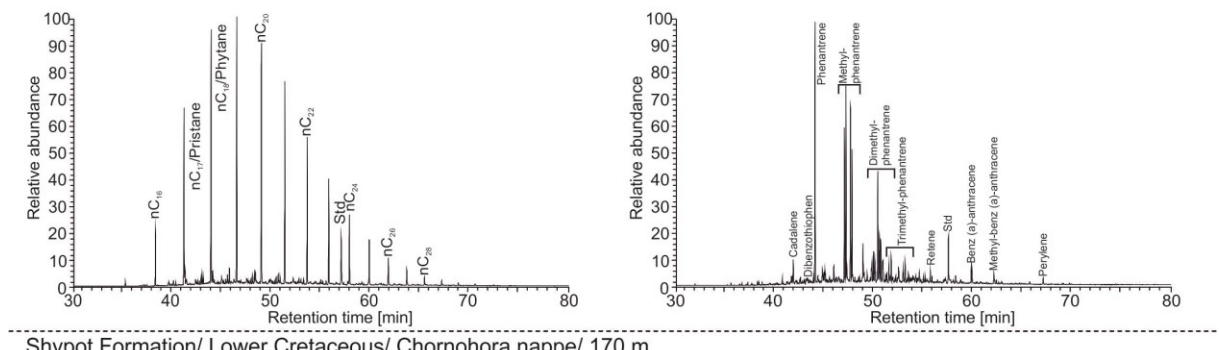




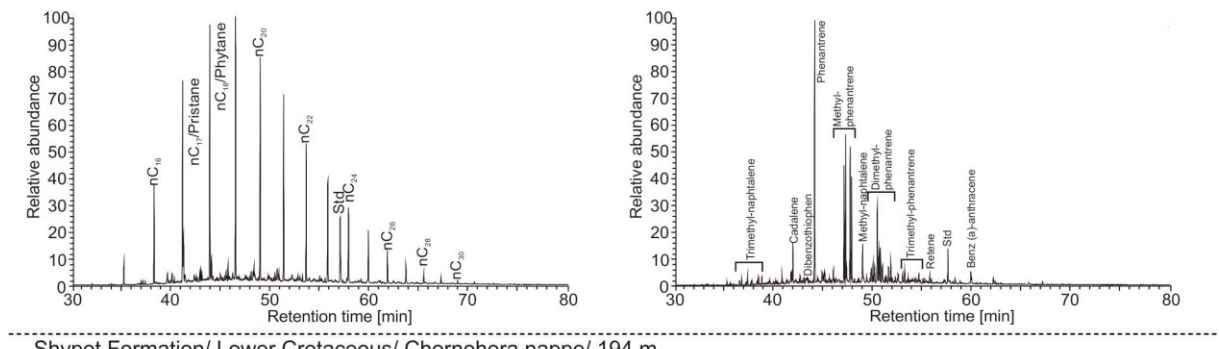
Shypot Formation/ Lower Cretaceous/ Chornohora nappe/ 133 m



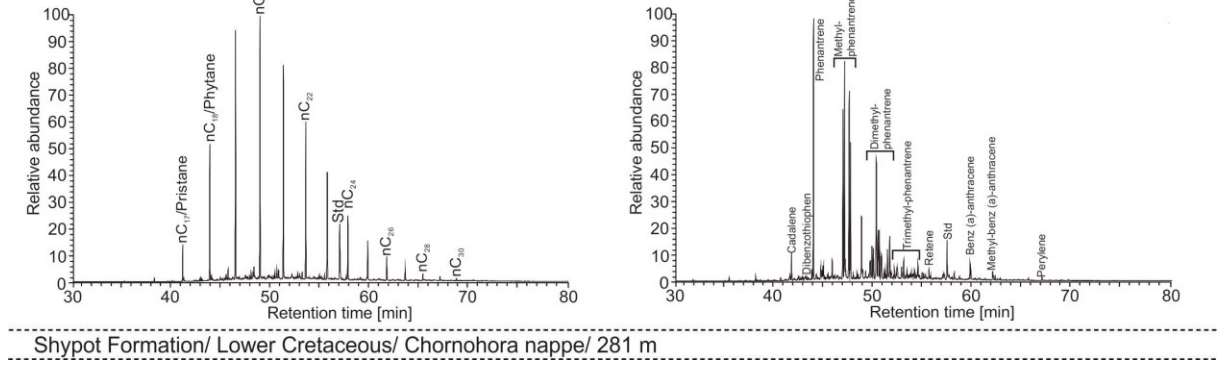
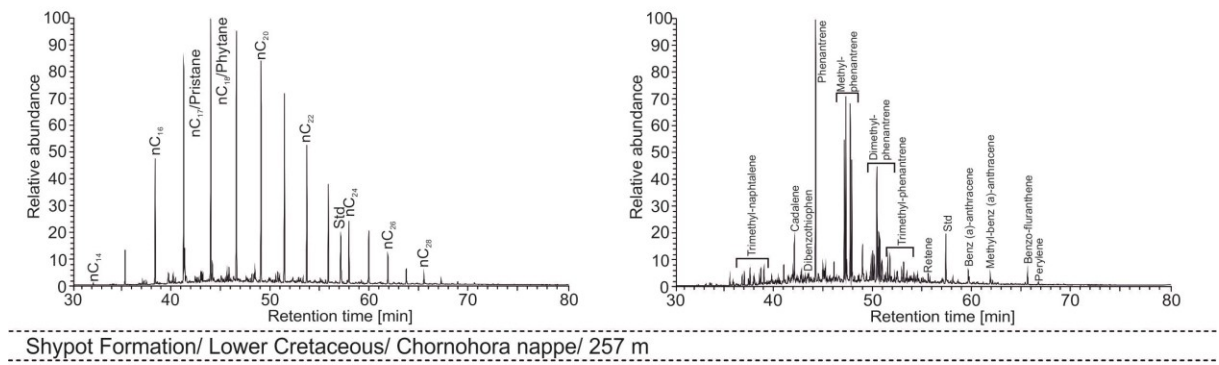
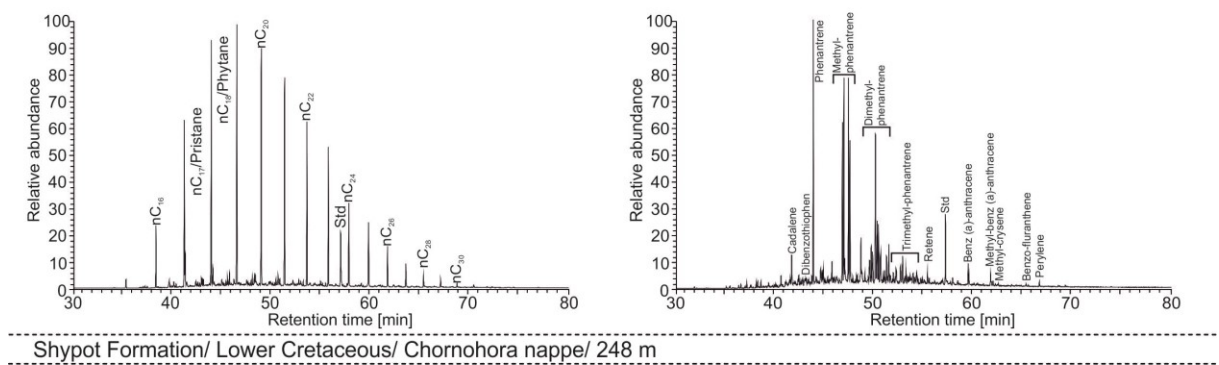
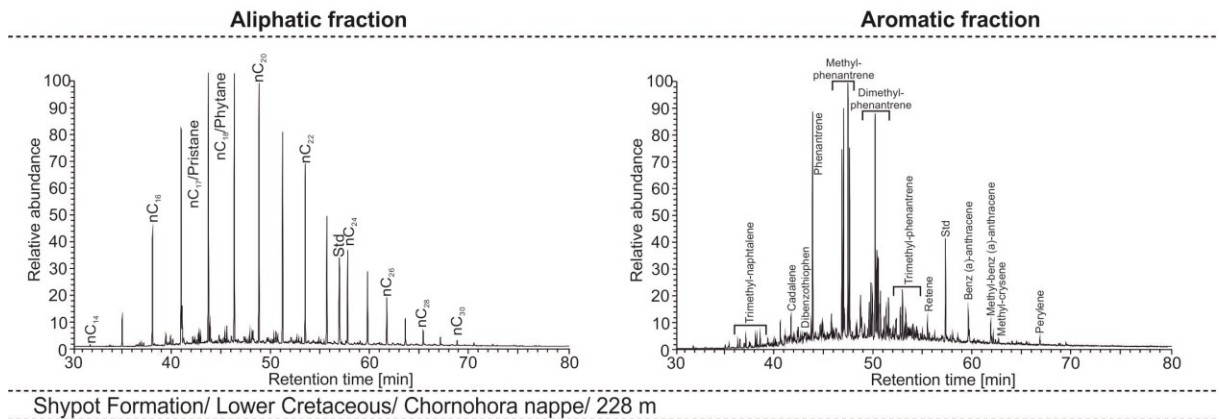
Shypot Formation/ Lower Cretaceous/ Chornohora nappe/ 159 m

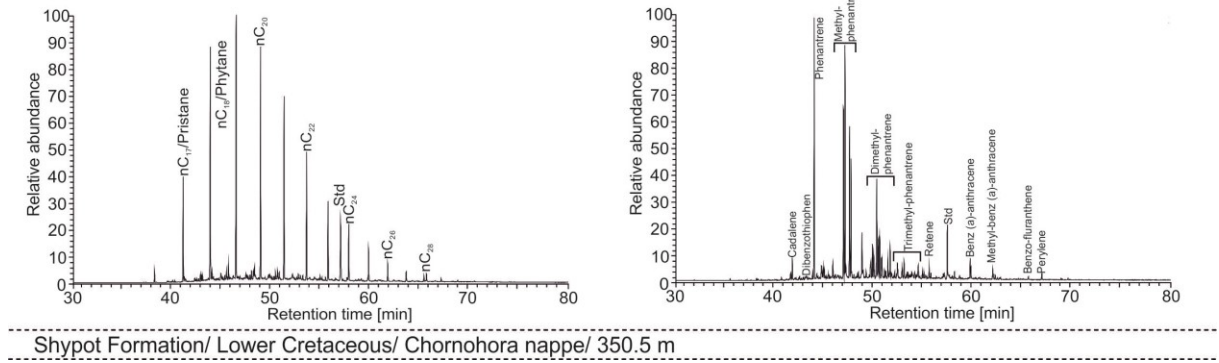
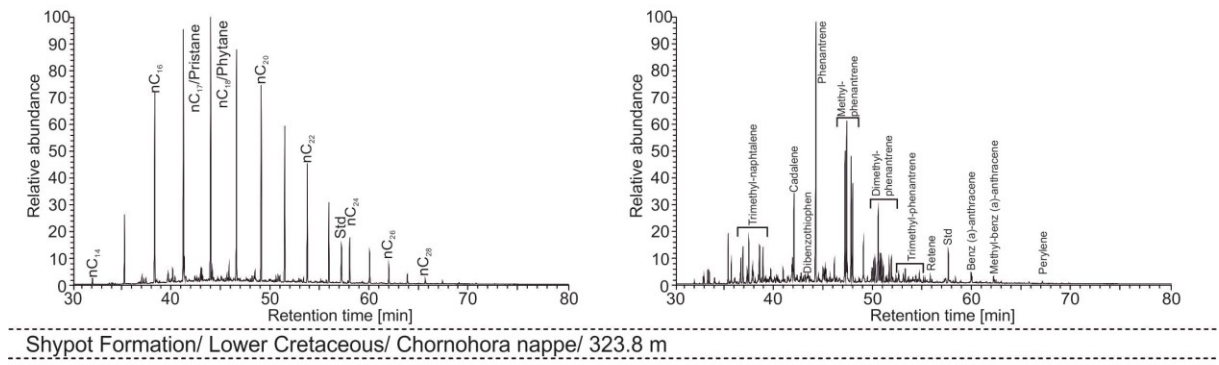
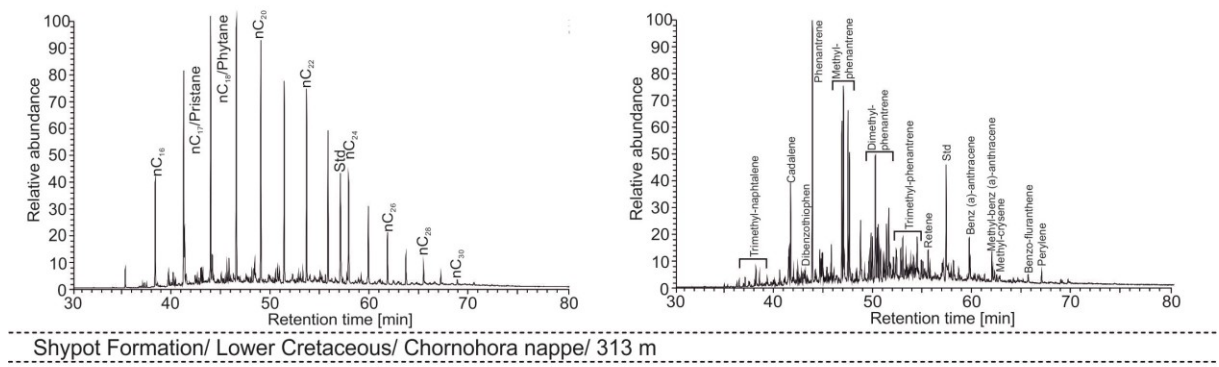
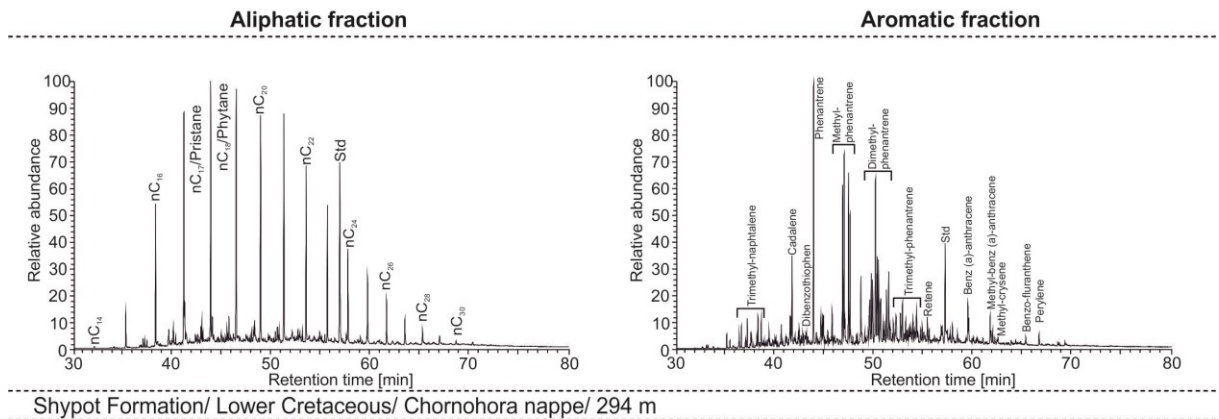


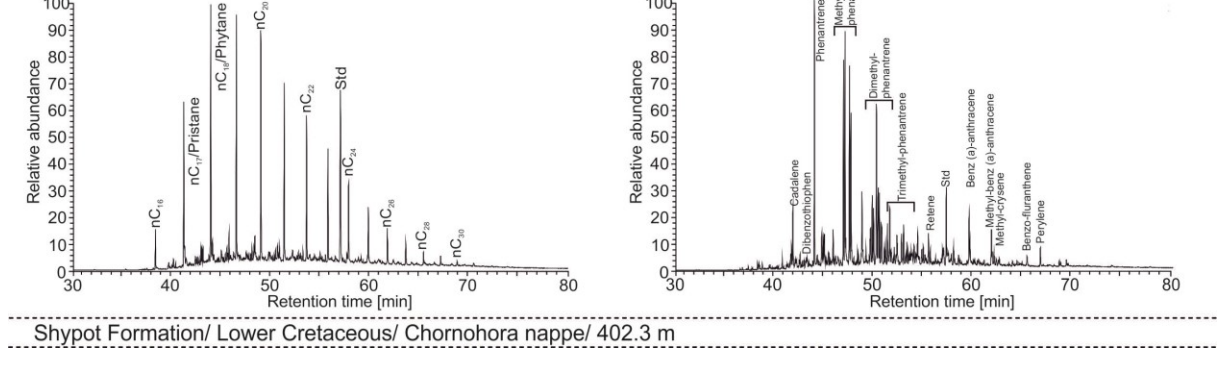
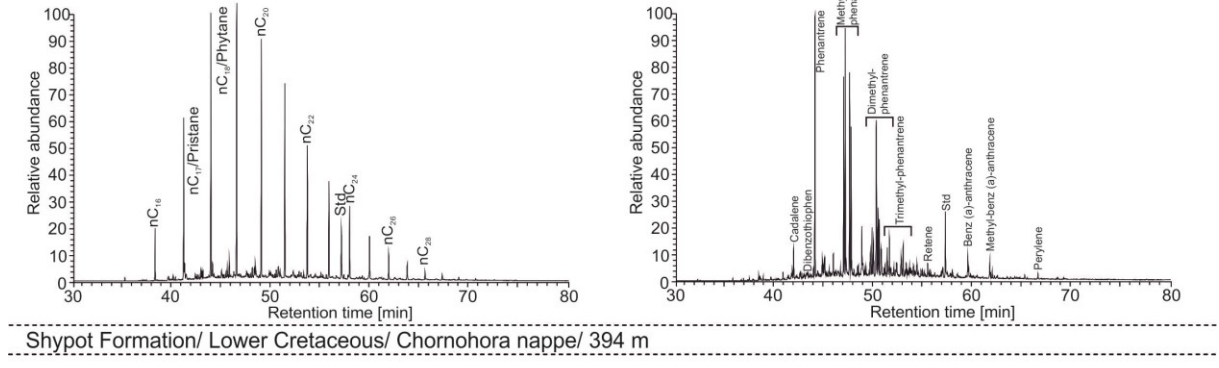
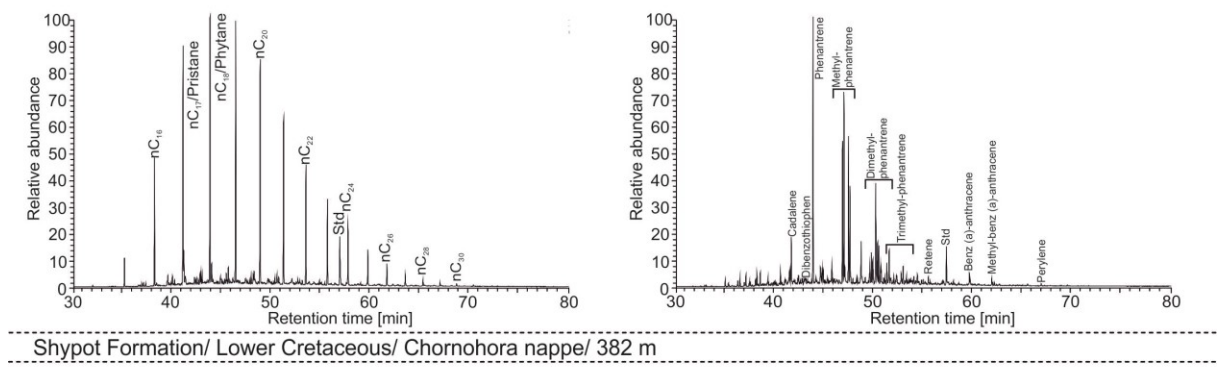
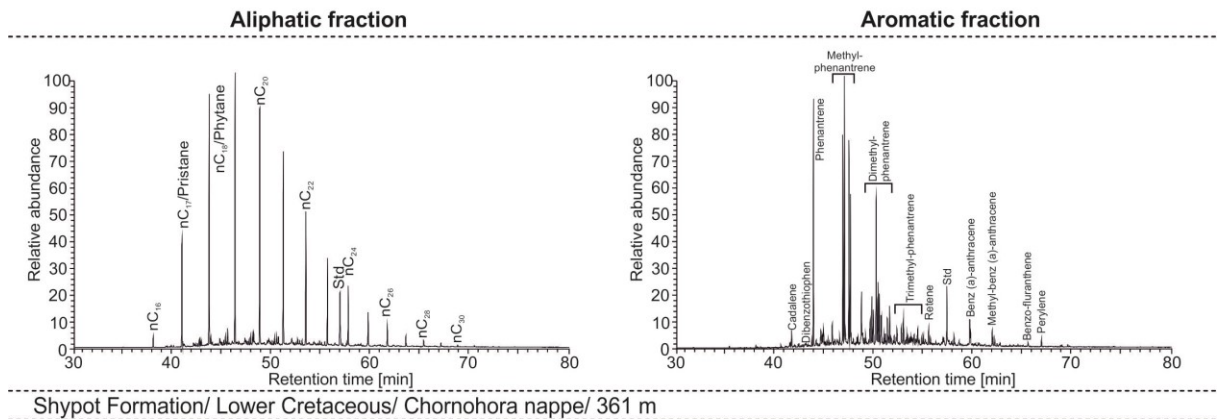
Shypot Formation/ Lower Cretaceous/ Chornohora nappe/ 170 m



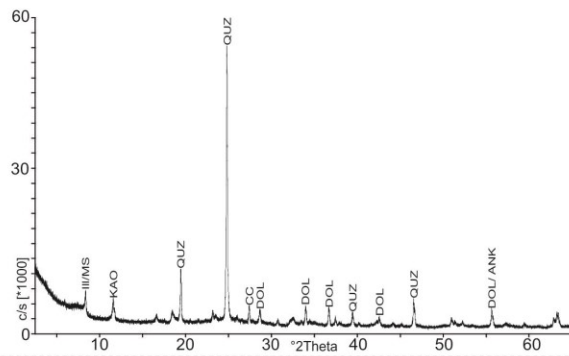
Shypot Formation/ Lower Cretaceous/ Chornohora nappe/ 194 m



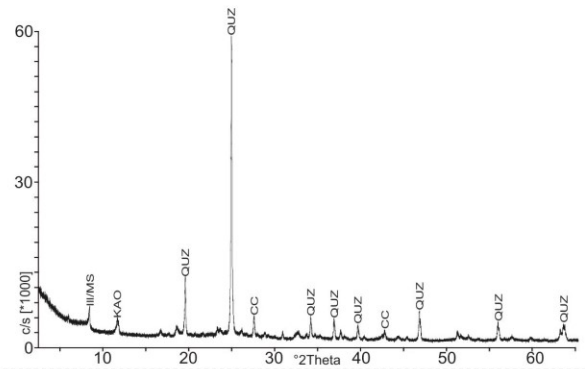




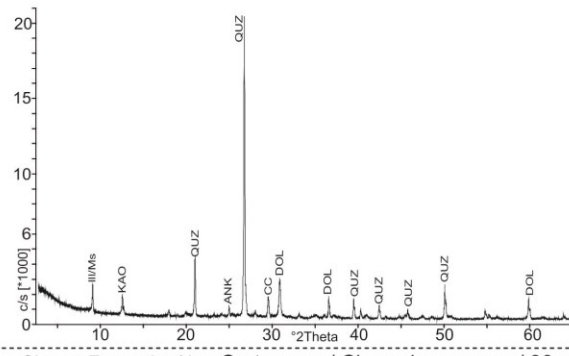
XRD-traces



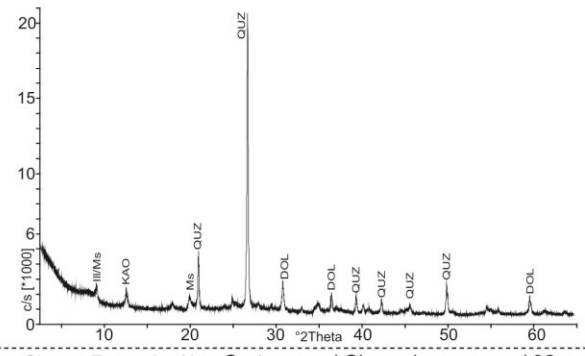
Shypot Formation/ Lo. Cretaceous/ Chornohora nappe/ 69.5 m



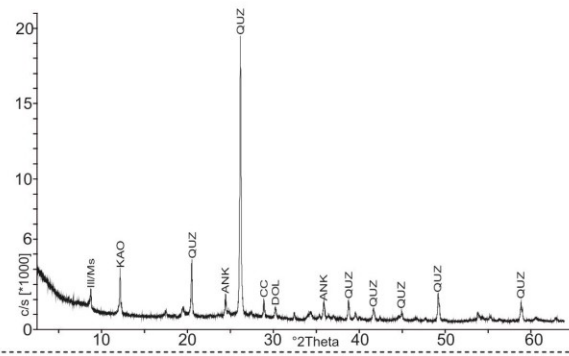
Shypot Formation/ Lo. Cretaceous/ Chornohora nappe/ 84 m



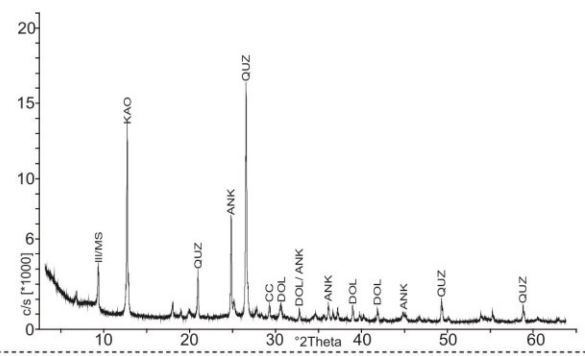
Shypot Formation/ Lo. Cretaceous/ Chornohora nappe/ 90 m



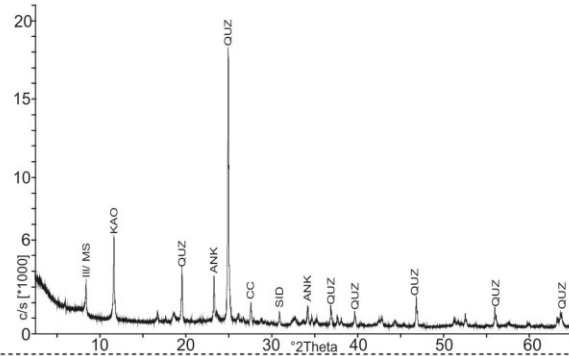
Shypot Formation/ Lo. Cretaceous/ Chornohora nappe/ 92 m



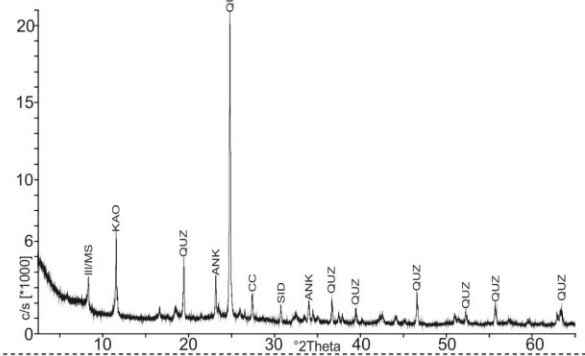
Shypot Formation/ Lo. Cretaceous/ Chornohora nappe/ 131 m



Shypot Formation/ Lo. Cretaceous/ Chornohora nappe/ 196 m

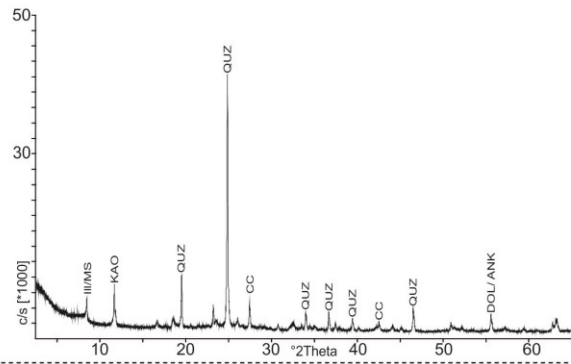


Shypot Formation/ Lo. Cretaceous/ Chornohora nappe/ 292.5 m

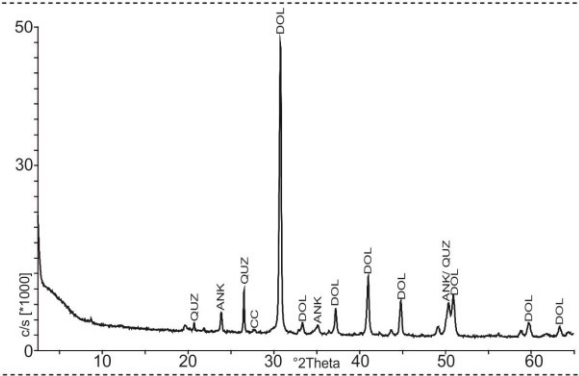


Shypot Formation/ Lo. Cretaceous/ Chornohora nappe/ 294 m

XRD-traces



Shypot Formation/ Lo. Cretaceous/ Chornohora nappe/ 298 m



Shypot Formation/ Lo. Cretaceous/ Chornohora nappe/ 326 m

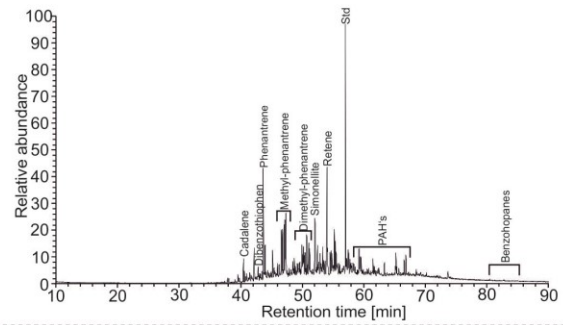
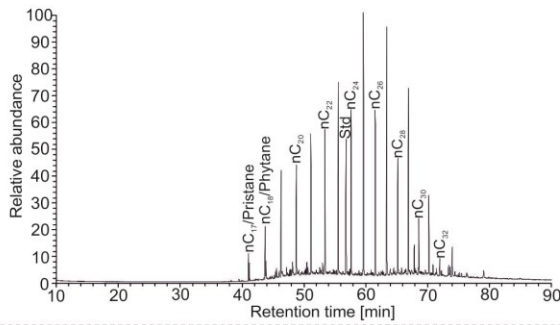
10.4 Appendix IV - Middle Jurassic strata

Depth [m]	S ₁ [mgHC/gRock]	S ₂	T _{max} [°C]	TOC [%]	S [%]	TOC/S [-]	HI [mgHC/gTOC]	PI [-]	TIC [%]	Calc. Equiv. [%]	Biomarker
Middle Jurassic											
Mosty-2											
2361	0.05	1.41	432	1.74	1.02	1.70	81	0.03	0.20	1.69	
2363	0.05	1.00	433	1.50	0.71	2.11	67	0.05	0.18	1.49	
2364	0.05	1.20	432	1.70	0.78	2.17	70	0.04	0.15	1.28	
2509	0.04	1.32	435	1.50	0.08	19.02	88	0.03	0.00	0.01	
2512	0.18	14.56	432	11.57	0.42	27.59	126	0.01	5.12	42.68	x
2513	0.06	4.40	431	3.97	0.31	12.65	111	0.01	4.69	39.06	
2516	0.09	10.11	436	6.07	0.18	33.21	167	0.01	0.06	0.51	
2518	0.14	19.78	433	8.17	0.14	59.50	242	0.01	0.02	0.00	x
2520	0.08	9.55	433	4.95	0.07	69.17	193	0.01	0.02	0.00	
2523	0.13	5.33	437	14.98	0.41	36.53	36	0.02	0.45	3.73	x
2524	0.08	3.15	440	7.28	0.18	40.38	43	0.02	0.87	7.28	
2525	0.06	7.19	437	3.25	0.09	34.51	221	0.01	0.01	0.07	x
2527	0.04	2.77	435	1.83	0.06	30.02	151	0.01	0.03	0.26	
2528	0.04	2.88	436	1.88	0.05	36.56	153	0.01	0.01	0.00	
2529	0.04	1.40	436	1.55	0.74	2.09	91	0.03	0.16	1.37	
2532	0.04	1.05	433	1.53	0.73	2.10	69	0.04	0.16	1.35	
2538	0.04	1.14	434	1.65	0.83	1.98	69	0.03	0.20	1.64	
2540	0.04	0.89	435	1.16	0.10	12.18	76	0.04	0.02	0.13	
2543	0.05	1.01	433	1.69	0.67	2.52	60	0.04	0.11	0.92	x
2552	0.07	4.43	434	2.69	0.24	11.10	165	0.01	0.03	0.00	
2560	0.07	1.56	434	1.82	0.83	2.18	86	0.04	0.22	1.82	
Korolyn-2											
3643	0.26	1.34	445	2.23	1.22	1.82	60	0.16	1.67	13.90	
3646	0.37	2.09	447	2.98	0.93	3.22	70	0.15	0.65	5.43	
3649	0.36	1.57	449	2.53	1.31	1.93	62	0.18	0.55	4.60	
3652	0.66	3.78	446	4.05	1.25	3.25	93	0.15	0.88	7.34	x
3696	0.59	2.17	448	3.01	2.13	1.41	72	0.21	0.53	4.45	
3697	0.28	1.22	449	2.20	1.04	2.12	56	0.19	0.66	5.53	
3698	0.40	2.22	449	3.00	1.47	2.04	74	0.15	0.48	4.03	
3699	0.32	1.56	449	2.51	0.97	2.58	62	0.17	0.31	2.56	
3700	0.30	1.41	449	2.25	1.22	1.84	63	0.17	0.39	3.23	
3701	0.32	1.50	449	2.44	1.33	1.83	62	0.18	0.55	4.62	
3702	0.34	1.46	450	2.36	1.28	1.85	62	0.19	0.34	2.82	
3703	0.35	1.18	449	2.13	1.40	1.52	55	0.23	0.29	2.39	
3708	0.31	1.52	450	2.48	1.30	1.91	61	0.17	0.41	3.41	x
3712	0.35	1.39	448	2.51	1.30	1.93	55	0.20	0.25	2.08	
3870	0.02	0.04	n.d	0.10	0.06	1.81	38	0.27	0.31	2.56	
3874	0.02	0.04	n.d	0.13	0.06	2.22	26	0.36	0.12	0.97	
3877	0.02	0.04	n.d	0.11	0.06	1.92	33	0.30	0.54	4.53	
3918	0.01	0.03	n.d	0.10	0.06	1.63	31	0.25	0.84	7.01	
3926	0.01	0.03	n.d	0.12	0.06	2.12	24	0.25	0.42	3.53	
3996	0.01	0.02	n.d	0.03	0.12	0.28	63	0.33	0.07	0.56	

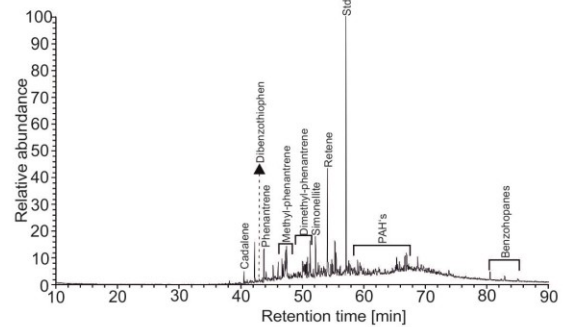
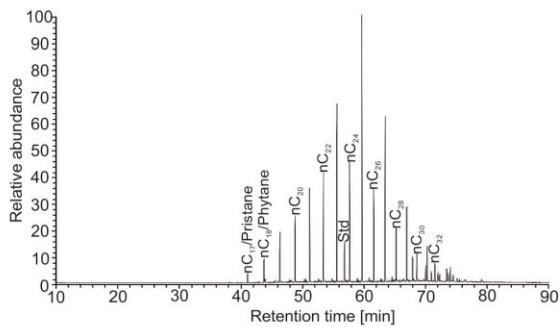
Depth [m]	S ₁ [mgHC/gRock]	S ₂	T _{max} [°C]	TOC [%]	S [%]	TOC/S [-]	HI [mgHC/gTOC]	PI [-]	TIC [%]	Calc. Equiv. [%]	Biomarker
Middle Jurassic											
Korolyn-6											
3418	0.22	3.18	439	3.67	1.32	2.78	87	0.06	1.34	11.13	
3419	0.26	3.97	440	3.89	0.68	5.71	102	0.06	0.74	6.18	
3420	0.29	4.28	442	4.04	0.93	4.32	106	0.06	0.80	6.68	
3421	0.29	4.93	441	4.39	0.66	6.63	112	0.06	0.97	8.05	
3422	0.28	3.19	440	3.36	0.84	4.01	95	0.08	1.41	11.73	
3423	0.32	4.26	441	3.81	1.81	2.11	112	0.07	1.25	10.40	
3424	0.29	4.47	445	4.39	1.95	2.25	102	0.06	0.74	6.19	
3425	0.25	4.46	445	4.30	1.06	4.05	104	0.05	0.92	7.63	
3426	0.21	4.15	444	4.13	1.04	3.97	100	0.05	0.65	5.41	
3427	0.24	4.07	442	3.90	0.59	6.56	104	0.06	0.89	7.39	
3428	0.40	4.73	440	4.07	0.63	6.48	116	0.08	0.89	7.40	x
3429	0.31	4.52	443	4.30	2.02	2.12	105	0.06	0.58	4.84	
3430	0.18	1.14	449	3.27	2.45	1.34	35	0.14	0.22	1.83	
3431	0.16	1.64	447	3.64	1.64	2.22	45	0.09	0.42	3.48	
3432	0.17	1.32	444	3.79	2.55	1.49	35	0.11	0.28	2.29	
3433	0.17	1.29	442	3.26	2.19	1.49	40	0.11	0.07	0.62	
3434	0.17	3.81	441	3.97	2.48	1.60	96	0.04	0.34	2.85	
3437	0.24	2.23	447	3.51	2.09	1.68	63	0.10	0.85	7.07	
3438	0.40	4.71	443	3.95	2.17	1.82	119	0.08	0.65	5.42	
3439	0.28	4.48	443	4.01	1.59	2.52	111	0.06	0.69	5.78	
3440	0.36	4.83	445	4.04	1.22	3.31	120	0.07	0.38	3.17	
3441	0.28	3.61	441	3.91	3.08	1.27	92	0.07	0.21	1.79	
3442	0.28	4.45	442	4.04	1.40	2.89	110	0.06	0.74	6.16	
3443	0.29	3.69	442	3.43	1.58	2.17	107	0.07	1.13	9.39	
3444	0.35	4.22	442	3.56	0.82	4.33	118	0.08	0.68	5.69	
3445	0.45	6.11	445	5.20	0.24	22.06	117	0.07	1.15	9.62	
3446	0.30	3.94	443	3.76	1.98	1.90	105	0.07	0.93	7.74	
3447	0.33	4.09	441	4.02	1.03	3.92	102	0.07	1.16	9.64	
3448	0.22	2.39	440	2.68	0.78	3.42	89	0.08	1.27	10.54	
3449	0.48	5.33	442	4.19	1.13	3.72	127	0.08	0.55	4.57	
3450	0.28	3.87	441	3.61	1.30	2.78	107	0.07	0.50	4.14	
3489	0.40	3.58	446	3.49	1.48	2.36	102	0.10	1.08	9.04	
3490	0.42	3.74	444	3.55	0.95	3.74	105	0.10	0.99	8.29	
3491	0.43	5.87	443	4.45	2.80	1.59	132	0.07	0.50	4.17	
3492	0.40	3.05	442	2.97	0.94	3.17	102	0.11	3.86	32.15	
3493	0.79	6.46	445	4.87	1.40	3.48	133	0.11	0.97	8.12	x
3496	0.59	6.18	444	5.12	0.91	5.60	121	0.09	0.83	6.91	
3497	0.60	7.67	445	5.74	1.71	3.35	134	0.07	0.87	7.22	
3498	0.57	6.67	446	5.01	1.65	3.05	133	0.08	1.16	9.71	
3499	0.53	6.58	445	5.20	0.44	11.84	127	0.07	1.20	9.99	
3500	0.50	6.24	444	4.91	0.35	13.94	127	0.07	1.27	10.56	
3518	0.50	6.54	444	5.25	0.94	5.58	125	0.07	0.71	5.89	
3519	0.54	5.82	444	4.43	1.06	4.17	131	0.08	0.93	7.75	
3520	0.46	5.32	444	4.84	1.52	3.18	110	0.08	1.85	15.40	
3521	0.74	8.09	445	5.75	0.20	29.38	141	0.08	0.75	6.23	x
3522	0.50	6.15	446	5.31	0.28	18.99	116	0.08	0.95	7.93	
3523	0.54	6.03	446	5.15	1.95	2.65	117	0.08	0.70	5.87	
3642	0.60	4.85	447	4.62	0.40	11.54	105	0.11	0.58	4.84	

Aliphatic fraction

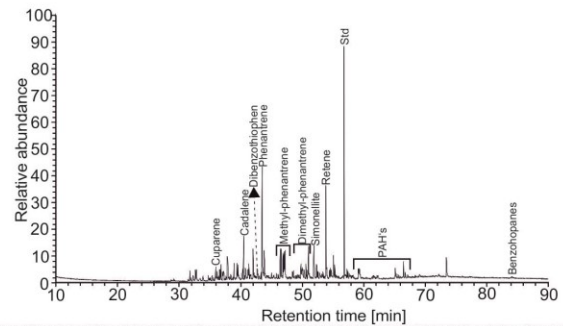
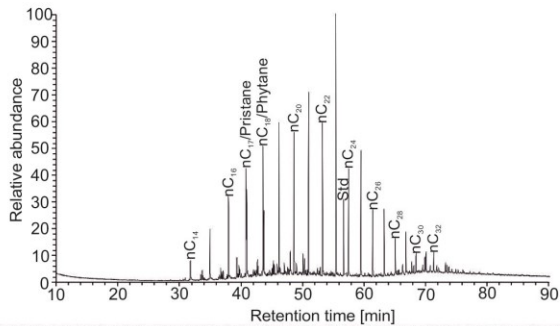
Aromatic fraction



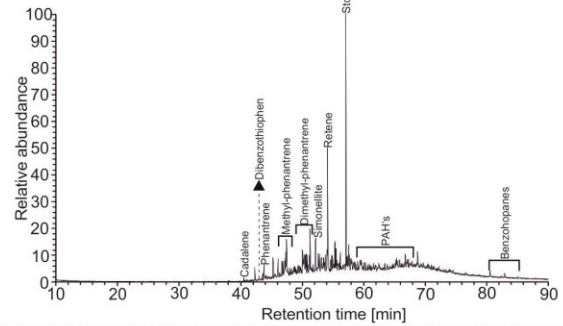
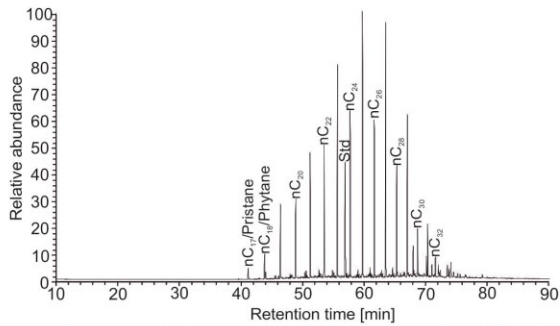
Middle Jurassic/ Mosty-2 borehole/ 2512 m



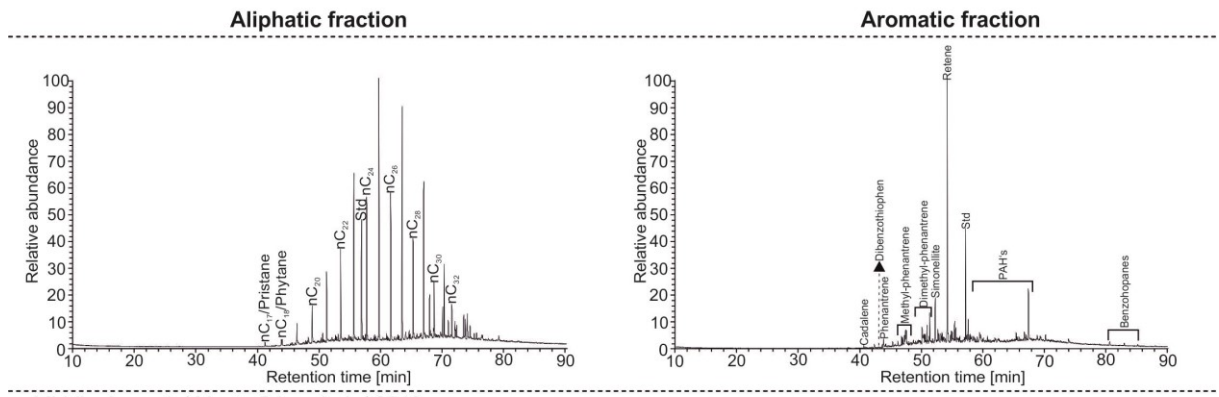
Middle Jurassic/ Mosty-2 borehole/ 2518 m



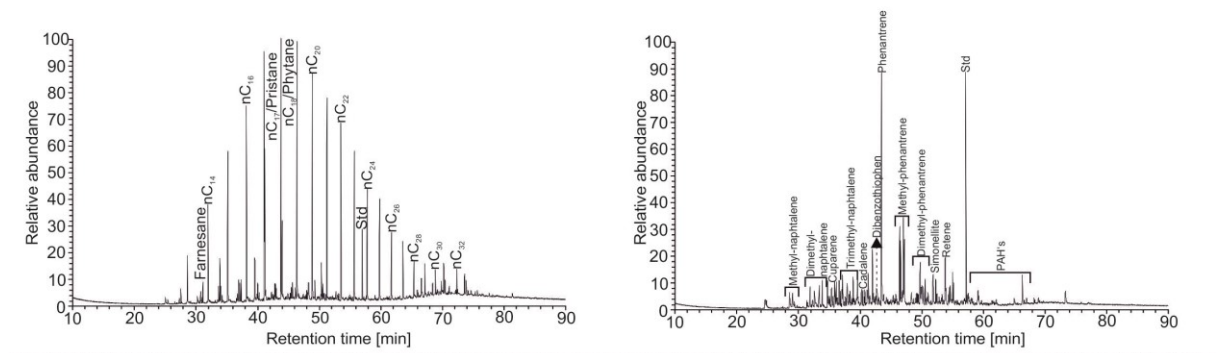
Middle Jurassic/ Mosty-2 borehole/ 2523 m



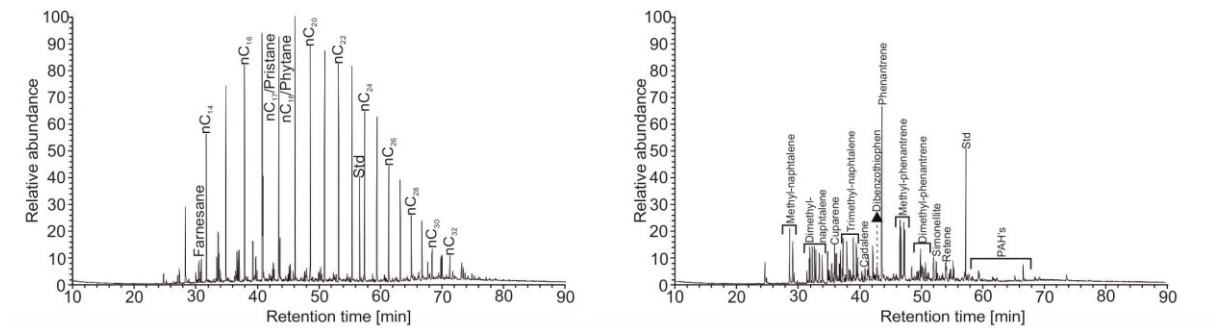
Middle Jurassic/ Mosty-2 borehole/ 2525 m



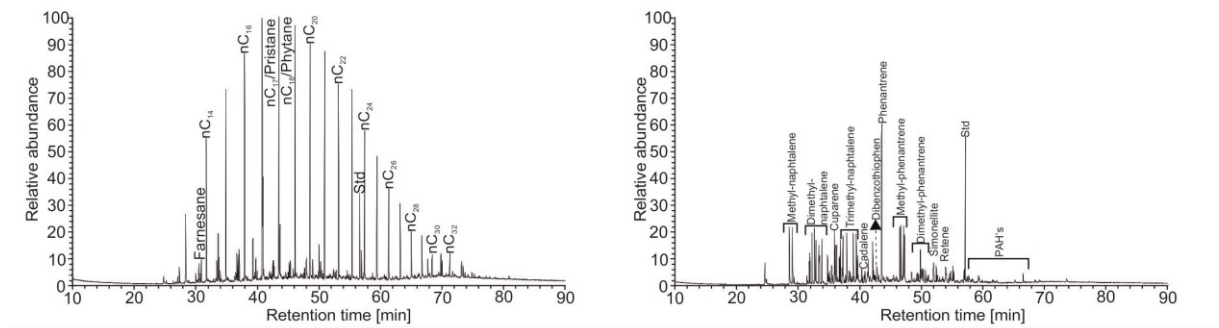
Middle Jurassic/ Mosty-2 borehole/ 2543 m



Middle Jurassic/ Korolyn-6 borehole/ 3428 m



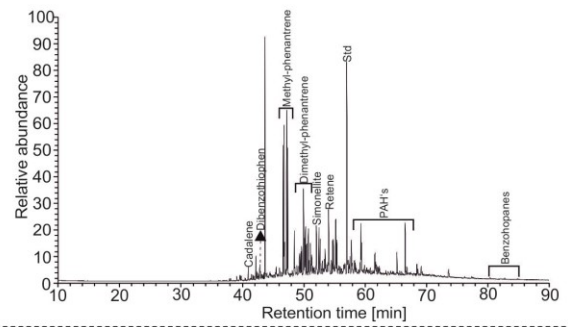
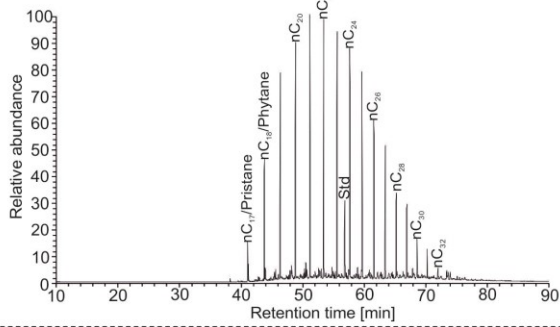
Middle Jurassic/ Korolyn-6 borehole/ 3493 m



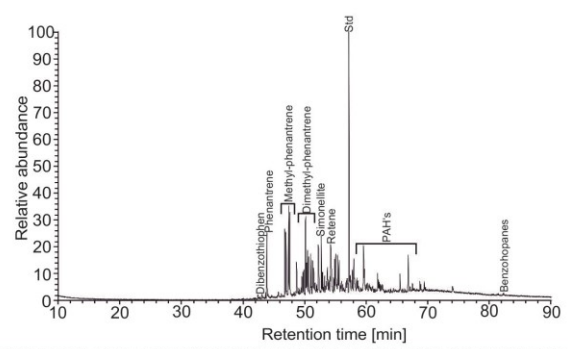
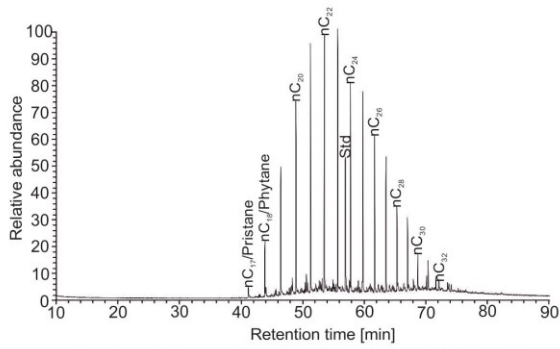
Middle Jurassic/ Korolyn-6 borehole/ 3521 m

Aliphatic fraction

Aromatic fraction



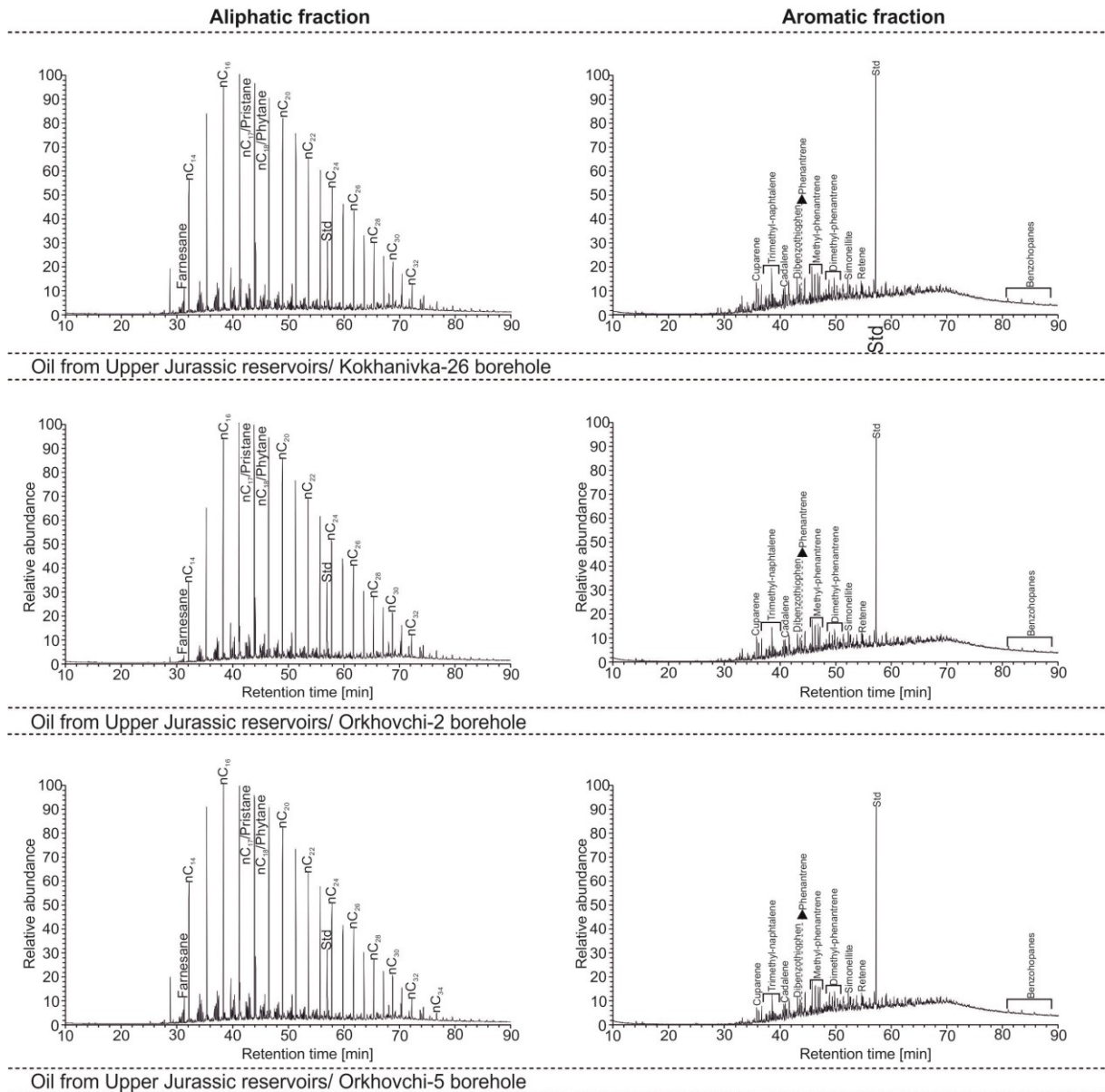
Middle Jurassic/ Korolyn-2 borehole/ 3652 m



Middle Jurassic/ Korolyn-2 borehole/ 3708 m


10.5 Appendix V – Oil samples from Upper Jurassic reservoirs

GCMS-traces




10.6 Appendix VI - Poster Presentations

AAPG/SEG International Conference and Exhibition (2017), London, UK.



Hydrocarbon potential of the Menilite Formation in western Ukraine



Rauball, J.F.¹⁾, Bechtel, A.¹⁾, Coric, S.²⁾, Gratzner, R.¹⁾, Sachsenhofer, R.F.¹⁾

¹⁾Department of Applied Geosciences and Geophysics, Montanuniversität Leoben, 8700 Leoben, Austria
²⁾Geological Survey of Austria, Neulinggasse 38, 1030 Vienna, Austria

1. Introduction

The Oligocene - Lower Miocene Menilite Fm. is the most important source rock in the Carpathians and has contributed to hydrocarbon accumulations across many parts of the Ukrainian Carpathians (Kotarba et al. 2007).

The main aim of the present study is to determine the hydrocarbon potential of the Menilite Fm. in the Ukrainian Carpathians, where detailed information on the vertical variation of the source potential is still missing.

The Menilite Fm. is traditionally subdivided into Lower (Lower Oligocene), Middle (Up. Oligocene) and Upper (Lower Miocene) members and comprises of alternating layers of claystone, mudstone and sandstone. The Lower Menilite Mb. (NP22-24) consists of alternating organic rich black shales and thick turbiditic sandstone beds. The Middle Menilite Mb. was not sampled as it is organic lean and not regarded as a potential source rock. The Upper Menilite Mb. (NN1-3) comprises primarily of black and grey shales (~85%).

2. Geological Overview

At the turn of the Eocene/Oligocene the Alpine Orogeny as well as a drop in sea level led to the formation of the epicontinental Paratethys Sea resulting in the deposition of organic rich sediments during the Oligocene and Early Miocene. The study area is situated within the Skyba Nappe, which is part of the eastern Carpathians.




Fig. 1: Geological map of the Ukrainian Carpathians (after Slaczka et al. 2006; Koltun et al. 1998). Sample locations are displayed on the map.

Western Ukraine is subdivided into the Carpathian Foreland, Outer Carpathians and the Transcarpathians (Fig. 1). The Outer Carpathians comprise a series of nappes which are thrust on top of each other. Each thrust sheet represents a separate or partly separate sedimentary sub-basin containing different lithostratigraphy and tectonic structures (Slaczka et al. 2006).

The study area is situated within the outer part of the Skyba nappe which forms a large portion of the eastern region of the N Carpathians as it stretches from Poland, through the Ukrainian Carpathians and into Romania.

Due to the complex geology of the outer Carpathians, the Menilite Fm. can be found within several nappes at depths ranging from the surface to over 6 km in the Boryslav-Pokutnya nappe and the outer part of the Skyba unit.

3. Methods

Total organic carbon (TOC), total inorganic carbon (TIC) and sulfur contents of 227 samples (153 samples from Lower Oligocene and 74 samples from Lower Miocene) were measured using an Eltra Instrument. Pyrolysis experiments were performed using a RockEval 6 analyzer.

A subset of the samples was used for biomarker and isotope analysis. Additionally, organic SiO₂ was determined using AAS.

4. Results & Discussion

The **Lower Oligocene succession**, 333 m thick, is marked by a chert horizon at its base which becomes progressively more shale rich. Organic rich black shales reach TOC contents of 24% in many parts of the succession (Fig. 2) and have an average TOC content of 9.8 wt.%. The Kliwa Sandstone, which acts as a reservoir in many parts of the Carpathians, is located towards the bottom half of the succession and is organically poor (average TOC: 0.3 wt.%). The upper part contains a thin coccolith limestone horizon (Jaslo Lmst.) and another chert horizon.

The **Lower Miocene strata**, approximately 1200 m thick, consist primarily of organic rich shales interbedded occasionally by sandstone beds. The base contains thin chert beds, whereas the upper part of the profile is marked by an ~70 m thick tuff horizon. Menilite shales contain average TOC content of 4.9 wt.%, whereas marl beds towards the top of the succession display an average TOC content of 1.4 wt.%.

Pristane/phytane (Pr/Ph) ratios indicate oxygen-depleted conditions for parts of the Lower Oligocene and for the entire Lower Miocene succession (Fig. 3). High Pr/Ph ratios in the Lower Oligocene succession are due to abundant landplant input.

High HI values prove the presence of prevailing type II kerogen (Fig. 4). Average HI for Lower Oligocene Menilite shales is 448 mgHC/TOC. Lower Miocene Menilite shales have an average HI of 364 mgHC/TOC.

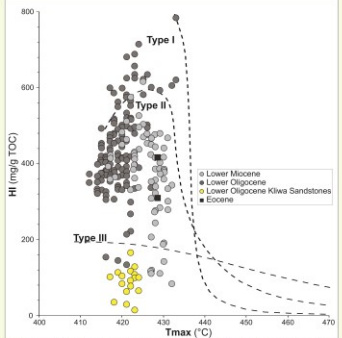


Fig. 4: Plot displaying the kerogen types of the Lower Miocene and Lower Oligocene Menilite Formation. Lower Oligocene Kliwa Sandstone samples are displayed separately.

Tmax measurements from Lower Oligocene and Lower Miocene strata indicate that organic matter is immature. Tmax values for the Lower Miocene strata are on average higher compared to values measured in the Lower Oligocene succession, which may be related to differences in facies.

5. Hydrocarbon potential

Plots of TOC versus the petroleum potential (S1+S2) are used to estimate the hydrocarbon potential of the Menilite Formation.

Fig. 5 shows that the petroleum potential of Lower Miocene and Lower Oligocene rocks in the Skyba unit is good to very good.

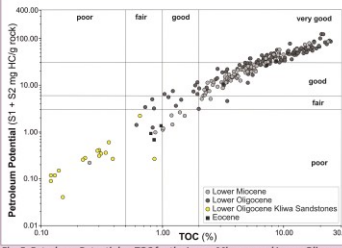


Fig. 5: Petroleum Potential vs. TOC for the Lower Miocene and Lower Oligocene Menilite Formation. Lower Oligocene Kliwa Sandstone samples are displayed separately.

The Source Potential Index (Demaison & Huizinger, 1991) of the Lower and Upper Menilite Mbs. is 16.6 and 57.9 tHC/m², respectively (Table 1). This shows that the Chechva profile contains a world-class source rock, which contains a higher source potential than any other profile in the Paratethys realm.

Age	Net thickness [m]	S1 + S2 [mg HC/g rock]	Density [g]	SPI [tHC/m ²]
L. Miocene	1225	22,52	2,1	57,9
L. Oligocene	190	41,7	2,1	16,6

Table 1: Source Potential Index (SPI) of Lower Miocene and Lower Oligocene rocks of the Chechva profile in the Skyba unit.

6. Conclusion

- The Lower Oligocene and Lower Miocene Menilite Mbs. of the Chechva profile possess a good to very good potential to generate oil.
- They are excellent source rocks and hold the highest source rock potential in the Paratethys realm.
- The Source Potential Index shows that they can generate 16.6 and 57.9 tons of hydrocarbons per m², respectively.

7. References

Andreeva-Grigorovich, A.S., Gassner, A.D., Ruffner, L.M., Sattler, S.E., 1988. Biostratigraphy: characteristics of the Menilite unit and correlation with the Eocene-Oligocene boundary.

Demaison, G., Huizinger, B.J., 1991. Genetic classification of petroleum systems. Am. Assoc. Pet. Geol. Bull. 75, 1626-1644.

Kotarba, J., Górecki, J., Górecki, M., Borek, J., Uliasz, M., Górecki, M., 1998. Petroleum generation in the Eocene-Oligocene Carpathians and the adjacent Silesia. Journal of Petroleum Geology, 21(3), 265-284.

Koltun, J., Górecki, J., Górecki, M., Uliasz, M., Górecki, M., 2007. Organic geochemistry study and genetic correlation of Eocene and Miocene source rocks in the Paratethys Sea (Poland and Ukraine). Journal of Petroleum Geology, 30, 1410-1419.

Slaczka, A., Kozłowski, T., Górecki, J., Górecki, M., 2006. Geology and Hydrocarbon Resources of the Outer Carpathians, Poland, Slovakia, and Ukraine. Geological Survey of Austria, Vienna, Austria, 1-220.

Fig. 2: Bulk geochemical data with nannoplankton zones (after Andreeva-Grigorovich et al.) for Lower Oligocene (below) and Lower Miocene (above) rocks in the Skyba unit.

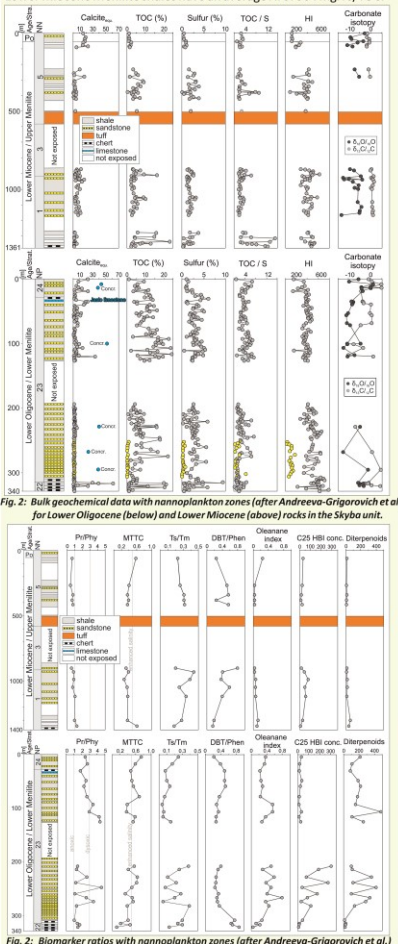
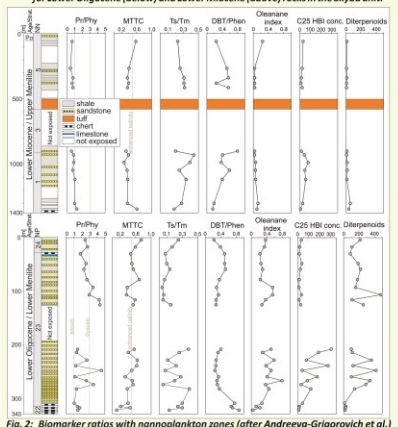


Fig. 3: Biomarker ratios with nannoplankton zones (after Andreeva-Grigorovich et al.) for Lower Oligocene (below) and Lower Miocene (above) rocks in the Skyba unit.



AAPG International Conference & Exhibition 2017, 15 October, London, UK

Acknowledgements
We thank Yury Koltun for organising our trips to the outcrops.

Contact: johannes.rauball@unileoben.ac.at
Chair of Petroleum Geology
http://erdolgeo.leoben.ac.at

78th EAGE Conference & Exhibition (2019), Vienna, Austria.



Hydrocarbon Potential of the Oligocene – Lower Miocene Menilite Formation and the Cretaceous Shyptot Formation in the Ukrainian Outer Carpathians



J.F. Rauball¹, R.F. Sachsenhofer¹, A. Bechtel¹, S. Coric², R. Gratzner¹

¹ Chair of Petroleum Geology, Montanuniversität Leoben, 8700 Leoben, Austria.
² Geological Survey of Austria, Neulinggasse 38, 1030 Vienna, Austria.

1. Introduction and Geological Overview

Two organic rich horizons are found within the Ukrainian Outer Carpathians: the Oligocene-Lower Miocene Menilite Fm. and the Lower Cretaceous Shyptot Fm.

The Outer Carpathians comprise a series of nappes thrust onto the southwestern margin of the East European Plate. Each thrust-sheet (Fig. 1b) represents a separate or partly separate sedimentary sub-basin containing different lithostratigraphy and tectonic structures. Flysch-type sediments in the Outer Carpathians range from Early Cretaceous to Early Miocene in age and may locally exceed thicknesses of up to 6 km (Slaczka et al., 2006).

The Menilite Fm., which is traditionally subdivided into Lower (Lower Oligocene), Middle (Up. Oligocene) and Upper (Lower Miocene) members, has a significantly higher petroleum potential than any other succession of the same age in the Paratethys region and, therefore, is of prime interest.

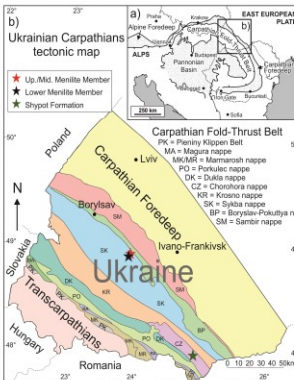


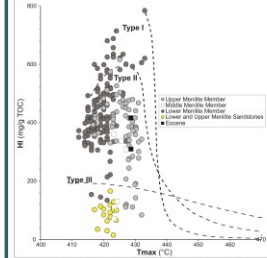
Fig. 1: a) Study area within the Carpathian Orogen, b) Tectonic map of Ukrainian Carpathians with sample locations for the Menilite Fm. and the Shyptot Fm.

2. Methods

Total organic carbon (TOC), total inorganic carbon (TIC) and sulfur contents of 227 samples as well as 94 Lower Cretaceous samples were measured using an Eltra instrument. Pyrolysis experiments were performed using a RockEval 6 analyzer. A subset of the samples from the Menilite Formation and the Shyptot Formation was used for biomarker and isotope analysis.

3. Results and Discussion

3.1 Menilite Formation



The Lower Miocene succession, 1300 m thick, comprises primarily of organic-rich Menilite shales interbedded occasionally by sandstone beds. TOC exceeds 20 wt.% only near its base and ranges from 1.5 to 23.1 wt.% (average: 5.2 wt.%; Fig. 3). Marl beds from the Polyanitsa Fm., towards the top of the succession, display an average TOC content of 1.4 wt.%. Average HI values for pelitic rocks is 364 mgHC/TOC.

Both successions are dominated by oil-prone type II kerogen (Fig. 2). Low Tmax values (average: 425°C) as well as vitrinite reflectance measurements (0.24-0.34 %Rr) indicate that organic-matter is immature.

Fig. 2: Plot displaying the kerogen types of Lower Oligocene and Lower Miocene rocks in the Skyba nappe.

The Lower Oligocene succession, 330 m thick, contains pelitic rocks that frequently exceed 20 wt.% in many parts of the succession and show an average TOC content of 9.8 wt.%. HI values typically range between 400 and 650 mgHC/gTOC in the lower part (max. 800 mgHC/gTOC) and from 300 and 450 mgHC/gTOC in the upper part (max. 475 mgHC/gTOC) of the succession (Fig. 3). Average HI for Menilite shales for all samples is 448 mgHC/gTOC.

The Upper Oligocene strata, which represents the Middle Menilite Member, was not studied in detail. TOC contents and HI values for 3 grey shale samples are low (0.80-0.96 wt.% TOC; 77-135 mgHC/gTOC) compared to 3 black shale samples (3.19-8.80 wt.%; 311-360 mgHC/gTOC).

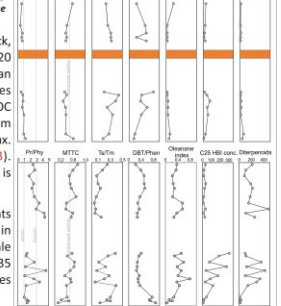
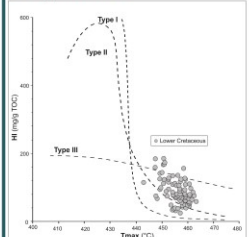


Fig. 3: Bulk geochemical data for Lower Oligocene and Lower Miocene rocks in the Skyba nappe.

3.2 Shyptot Formation



The Lower Cretaceous Shyptot Formation, approximately 405 m thick, contains pelitic rocks that reach a max. TOC content of 9.4 wt. % (average 2.83 wt.%). HI values increase slightly towards the top of the succession (max. 185 mgHC/gTOC; Fig. 6) and average 88 mgHC/gTOC for all samples.

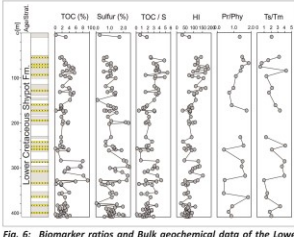


Fig. 6: Biomarker ratios and Bulk geochemical data of the Lower Cretaceous Shyptot Fm. in the Chorohora nappe.

An average Tmax value of 456°C for Lower Cretaceous rocks indicates that sediments in the Chorohora nappe are mature (Fig. 5).

Ts/Tm ratios are very irregular throughout the succession. High ratios reflect maturity.

Pr/Ph ratios range 0.39 - 1.84 and indicate O₂-depleted conditions throughout the entire succession.

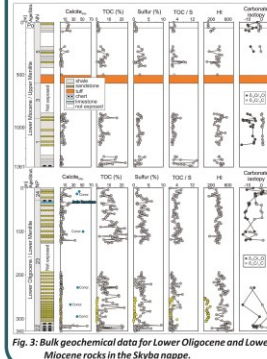


Fig. 4: Biomarker ratios with nannoplankton zones for Lower Oligocene and Lower Miocene rocks in the Skyba nappe.

Pristane/phytane (Pr/Ph) ratios indicate O₂-depleted conditions for parts of the Lower Member and for the entire Upper Member (Fig. 4). Higher ratios are due to landplant-input rather than redox conditions.

MTTC ratios for both Mbs. suggest normal marine conditions with minor salinity variations.

Ts/Tm ratios are low for both Mbs. indicating immaturity.

Moderately enhanced DBT/Phen ratios in the Lower Member and in the Upper Member suggests that low amounts of H₂S were available.

C25 HBIs, which may indicate that biomass derived from diatoms, as well as diterpenoids, which are gymnosperm-derived biomarkers, are elevated in the Lower Menilite Fm.

3.3. Hydrocarbon potential

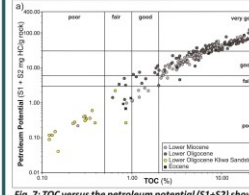


Fig. 7: TOC versus the petroleum potential (S1+S2) showing hydrocarbon potential of the Menilite Fm. (a) and Shyptot Fm. (b)

Age	Net thickness [m]	S1 + S2 [mg HC/g rock]	Density [ρ]	SPI [tHC/m ³]
L. Miocene	1225	22.5	2.1	57.9
L. Oligocene	190	41.7	2.1	16.6
L. Cretaceous	263	3.3	2.1	1.8

Table 1: Source Potential Index (SPI) of the Lower Oligocene - Lower Miocene Menilite Fm. and the Lower Cretaceous Shyptot Fm.

The Source Potential Index (Demaïson & Huizinga, 1991) of the Lower and Upper Menilite Mbs. as well as the Shyptot Fm. is 16.6, 57.9 and 1.8 tHC/m³, respectively. (Table 1). This shows that the Menilite Fm. contains a world-class source rock, with an excellent hydrocarbon potential (Fig. 7).

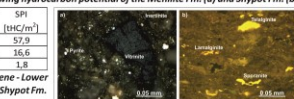


Fig. 8: Photomicrographs of the Shyptot Fm. in white light (a) and the Menilite Fm. in fluorescence mode (b). Maceral composition is characterized by a high presence of vitrinite in both the Shyptot Fm. and the Menilite Fm. (Fig. 8). Vitrinite appears to be the dominant maceral.

4. Conclusion

- The Lower Oligocene and Lower Miocene Menilite members in the Skyba nappe possess a good to very good potential to generate oil.
- The Shyptot Fm. is mature and has a varied hydrocarbon potential and ranges from fair to good.
- The Lower Oligocene and Lower Miocene Menilite members are slightly immature whereas the Shyptot Fm. is over-mature.
- The Menilite Formation is an excellent source rock and holds the highest source rock potential in the Paratethys realm.
- The Source Potential Index for the Lower Oligocene and Lower Miocene Menilite members as well as for the Shyptot Formation is 16.6, 57.9 and 1.8 tHC/m³, respectively.

References

Demaïson, G., Huizinga, B.J., 1991. Genetic classification of petroleum systems. Am Assoc Pet Geol Bull 75, 1626-1643.
 Slaczka, A., Kruglov, S., Golonka, J., Oszyrko, N., Popadyuk, I., 2006. Geology and Hydrocarbon Resources of the Outer Carpathians, Poland, Slovakia, and Ukraine: General Geology. In: Golonka, J., Picha, F.J. (eds.) AAPG Memoir, 84, 221-258.

Contact: johannes.rauball@stud.unileoben.ac.at